



From Lipophilic to Hydrophilic: A Library of Soluble Polyaziridines

Master Thesis

Zum Erlangen des akademischen Grades

Master of Science

Fachbereich 09 des Fachbereiches Chemie, Pharmazie und
Geowissenschaften (FB 09)

der Johannes-Gutenberg-Universität Mainz

vorgelegt von

Thomas Kuckhoff

geboren in Koblenz

Mainz, Januar 2019

Erstgutachter: Herr Dr. Frederik Wurm

Zweitgutachter: Herr Prof. Dr. Holger Frey

*So I will pave this road 'till glory sets our broken spirit free
From every cross-soaked nail pours endless rain with tears no eye should see
But they could fill our highest ocean and the rivers in between
With every blade that flowers must grow then drown with love, our cruelest sea*
With a Wonder and a Wild Desire
Flogging Molly

Danksagung

Ich möchte mich zunächst bei Frau Prof. Dr. Katharina Landfester für die Möglichkeit bedanken, in ihrem Arbeitskreis meine Masterarbeit durchführen zu können.

Ein großer Dank gilt Herrn Dr. Frederik Wurm, für das bereit gestellte Thema die hilfreichen Anmerkungen und interessanten Diskussionen, sowie die Fahrt zu Evonik Industries in Darmstadt.

Ein weiterer Dank gilt Herrn Prof. Dr. Holger Frey, für die dankenswerte Übernahme des Zweitgutachters.

Für die Einweisung und Einarbeitung in die Welt der anionischen Polymerisation von Aziridinen und Ethylenoxid, sowie zahllose Diskussionen und Erläuterungen habe ich besonders Tassilo Gleede zu danken.

Bei Frau Dr. Klein von Evonik Industries in Darmstadt möchte ich mich für den interessanten Betriebsbesuch und die freundliche Zusammenarbeit bedanken.

Auch möchte ich mich natürlich beim Team der Polymer Analytik bedanken. Für die GPC-Messungen bedanke ich mich daher bei Sandra Seywald, Ute Heinz, Christine Rosenauer, Monika Schmelzer und Regina Holm. Weiter danke ich Petra Räder für die DSC- und TGA-Messungen und Elke Muth für die IR-Messungen und die Oberflächenspannungsmessungen.

Für die durchgeführten ^1H NMR Kinetik-Messungen, sowie die 2D-NMR danke ich Dr. Manfred Wagner und Stefan Spang. Jens Markwart danke ich für die Auswertung der ^1H NMR Kinetik.

Für die angenehme Arbeitsatmosphäre möchte ich mich vielmals bei der ganzen Arbeitsgruppe bedanken. Bei Tassilo Gleede, Jens Markwart, Sebastian Beckers und Sabrina Brand bedanke ich mich darüber hinaus noch für die großartige Zeit im Labor. Der größte Dank gilt meiner Familie ohne deren Hilfe ich nie so weit gekommen wäre. Ich danke meiner Mutter für ihre grenzenlose Unterstützung und meinem Vater dafür, dass er mir zeigte worin die Schönheit der Arbeit liegt.

List of content

Danksagung	4
List of content	5
List of Abbreviations	8
1. Abstract	11
1. Zusammenfassung	12
2. Introduction	13
3. Motivation	15
3.1 Project 1: lipophilic Poly(sulfonyl aziridine)s	15
3.2 Project 2: hydrophilic Poly(sulfonyl aziridine)s	16
4. Theory	18
4.1 Anionic ring-opening polymerization	18
4.2 Polymerization of activated and non-activated aziridines	22
4.3 Characteristics of activated polyaziridines <i>via</i> AROP	26
4.3.1 Kinetics	26
4.3.2 Temperature	26
4.3.3 Solvent influence and counter ion influence	26
4.3.5 Substituent influence	27
4.4 Copolymerization/ functionalization	29
5. Analytics	31
5.1 ¹ H NMR Kinetic	33
5.2 Gel permeation chromatography	34
5.3 Surface tension and spinning drop	36
5.4 Contact angle measurement	37
6. Results and discussion	39
6.1 Project 1: Synthesis of lipophilic polyaziridines	39

List of content

6.1.1 Synthesis of lipophilic <i>N</i> -sulfonylaziridines monomers	40
6.2 Polymerization	49
6.2.1 Initiator synthesis.....	49
6.2.2 Polymerizations	51
6.3 Copolymerization	60
6.4 ¹ H NMR kinetics	65
6.5 Solubility assay	71
6.6 Contact angle measurements	72
6.7 Spinning drop	80
7.0 Project 2: hydrophilic Poly(sulfonyl aziridine)s	82
7.1 Synthesis route: Grafting- <i>from</i>	83
7.2 One-pot synthesis of Poly(TsEtOHaz)- <i>graft</i> -PEG	92
8. Outlook.....	96
9. Experimental Part.....	98
9.1 Materials and methods of characterization.....	98
9.2 Synthesis of Monomers and Initiator	101
9.3 Polymer synthesis	121
9.3.1 Poly(2-Methyl- <i>N</i> -octasylaziridin) (Poly(OsMAz)).....	122
9.3.2 Poly-2-Methyl- <i>N</i> -octasylaziridin (Poly(OsMAz)).....	126
9.3.3 Poly-2-Methyl- <i>N</i> -dodesylaziridin (Poly(DDsMAz))	128
9.3.5 Poly(2-Cyclohexanemethyl- <i>N</i> -Mesylaziridin) (Poly(MsCyhexAz))	135
9.4 Copolymers.....	138
9.4.1 Poly(OsMAz)- <i>co</i> -(MsMAz)	138
9.4.1 Poly(MsCyhexAz)- <i>co</i> -(MsMAz).....	141
9.5 Project 2: Synthesis of Poly(TsEtOHaz)- <i>graft</i> -PEG	143
9.5.1 Poly{2-(2-Ethylethoxy)-Ethanol- <i>N</i> -Tosylaziridine}.....	143

List of content

9.5.1 Poly(2-Ethanol- <i>N</i> -Tosylaziridine)	145
9.5.1 Poly(TsEtOHaz)- <i>graft</i> -PEO	148
9.5.1 Poly(TsEtOHaz)- <i>graft</i> -PEO	150
10. Index.....	153
10.1 Scheme index	153
10.2 Table index	155
11. References	164
12. Appendix.....	168
12.1 Contact angle measurement	169
12.2 Layer thickness measurement	172
12.4 Spinning drop measurement	201
12.5 ¹ H NMR-Kinetic	207

List of Abbreviations

A-AROP	Aza anionic ring opening polymerization
ACN	acetonitrile
AcOH	Acetic acid
AG	Activation group
AROP	anionic ring opening polymerization
BnNHMs	benzyl- <i>N</i> -methylsulfonamide
4- ^t b-BnNHMs	4-tert-butylbenzyl- <i>N</i> -mesylsulfonamid
COSY	correlation spectroscopy
CROP	Cationic ring opening polymerization
\bar{D}	Molecular dispersity
DCM	dichloromethane
DDsMAz	2-methy- <i>N</i> -dodesylaziridine
DMF	<i>N,N</i> -Dimethylformamide
DMSO	Dimethylsulfoxide
DOSY	Diffusion ordered spectroscopy
EO	Ethylene oxide
GPC	Gel permeation chromatography
<i>hb</i>	hyperbranched
HDsMAz	2-methy- <i>N</i> -hexadecasyaziridine
Hz	Hertz
J	coupling constant
k_{ct}	Chain transfer rate
kDA	Kilodalton
KHMDS	Potassium bis(trimethylsilyl)amide
K_i	Initiation rate
K_p	Propagation rate
K_t	Termination rate

List of Abbreviations

MeOH	methanol
MgSO ₄	Magnesium sulfate
MHz	Megahertz
mL	milliliter
M_n	The number average molar mass
mN/m	millinewton per meter
MsCyhexAz	(2-cyclohexylmethyl)- <i>N</i> -mesylaziridine
MsMAz	2-methylmesylaziridine
NaHCO ₃	Sodium hydrogencarbonate
NaOH	Sodium hydroxide
Nuc	nucleophile
NEt ₃	triethylamine
nm	nanometer
NMR	Nuclear magnetic resonance
OsMAz	2-methyl- <i>N</i> -octasylaziridine
PAz	Poly(aziridine)
PEG	Poly(ethylene glycol)
PEI	Poly(ethylene imine)
Poly(DDsMAz)	Poly(2-methyl- <i>N</i> -Dodesylaziridine)
Poly(HDsMAz)	Poly(2-methyl- <i>N</i> -Hexadecasyaziridine)
Poly(MsCyhexAz)	Poly(2-(cyclohexylmethyl)- <i>N</i> -mesylaziridine)
Poly(OsMAz)	Poly(2-methyl- <i>N</i> -octasylaziridine)
Poly(TsEEEtAz)	Poly{ 2-((1-Ethoxyethoxy)ethyl)- <i>N</i> -Tosylaziridine}
Poly(TsEtOHAz)	Poly(2-Ethanol- <i>N</i> -Tosylaziridine)
ppm	Parts per million
PpTs	Pyridinium <i>p</i> -toluenesulfonate
Ps	Poly(styrol)
Rf	Retention value
RT	Room temperature

List of Abbreviations

THF	tetrahydrofuran
TsEtOHaz	2-Ethanol- <i>N</i> -Tosylayiridine
TsMAz	2-methyl- <i>N</i> -Tosylayiridine
TMPAB	Trimethylphenylammonium tribromide
w.t%	Weight percentage
X _n	Degree of polymerization

1. **Abstract**

The solubility of Poly(sulfonyl aziridine)s in non-polar solvent was studied. Therefore, novel monomers with increasingly lipophilic side chains were synthesized and polymerized. A variety of *homo*- and copolymers were polymerized, and the influence of the new activating group and side groups were studied by calculating the copolymerization parameters *via* ^1H NMR kinetic. Further a solvation assay in cyclohexane and dodecane was conducted. The polymers were used for spin coating of microscopy slides and contact angle measurements of water droplets were conducted to study the properties of the hydrophobic polyaziridine coatings, in dependence of concentration, X_n and side chain length. Further, surface activity of the polymer was analyzed by measuring the interfacial tension of a cyclohexane/water system *via* spinning drop.

In a second project the first Poly(sulfonyl aziridine)-*graft*-PEG polymers were synthesized and analyzed through diffusion ordered spectroscopy (DOSY). The synthesis of Poly(sulfonyl aziridine)-*graft*-PEG polymer was achieved *via* a *grafting-from* polymerization as well as a one-pot copolymerization of Poly(sulfonyl aziridine) and ethylene oxide.

1. Zusammenfassung

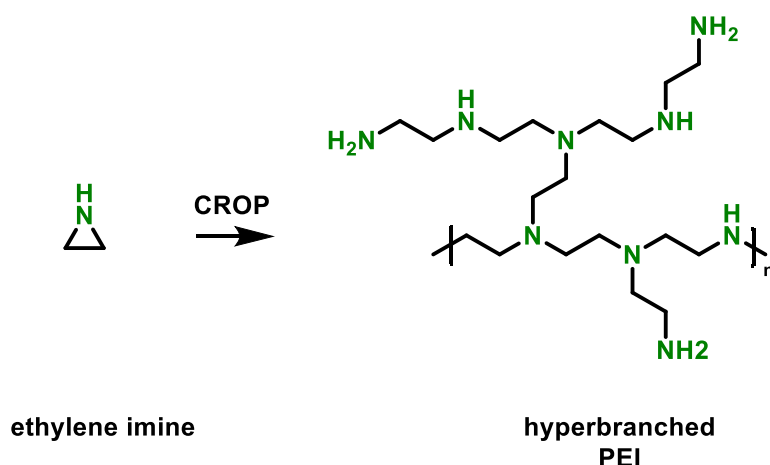
Die Löslichkeit von Poly(sulfonyl aziridine)en in nicht polaren Lösungsmitteln wurde untersucht. Vier neue Monomer mit zunehmend lipophilen Seitenketten wurden synthetisiert und polymerisiert. Der Einfluss der neuen Aktivierungsgruppen und Seitenketten wurde durch Berechnung der Copolymerisationsparameter *via* ^1H NMR Kinetik bestimmt. Die Löslichkeit der hergestellten Polymere wurde in Cyclohexan und Dodecan getestet. Die Polymere wurden weiter für die Beschichtung von Objektträgern *via* spin coating verwendet. Durch Kontaktwinkelmessungen von Wassertropfen, wurden daraufhin die Eigenschaften der hydrophoben Poly(sulfonylaziridine)-oberflächen, in Abhängigkeit von X_n , Seitenkettenlänge und Konzentration der verwendeten Poly(sulfonylaziridine)lösung gemessen. Durch Messung der Oberflächenspannung eines Cyclohexan/Wasser-Probe *via* Spinning drop, wurde die Oberflächenaktivität der Polymere untersucht.

In einem zweiten Projekt wurden die ersten Poly(sulfonyl aziridine)-graft-PEG polymere hergestellt und über diffusion ordered spectroscopy (DOSY) analysiert. Die Synthese wurde über eine graft-*from* Polymerisation, sowie durch eine One-pot Copolymerisation von Poly(sulfonyl aziridine) und Ethylenoxid erzielt.

2. Introduction

Aziridines are three-membered rings with nitrogen as heteroatom in the ring; therefore, they are closely related to ethylene oxide and their derivatives. Ethylene imine was first discovered and synthesized by Gabriel in 1888.¹ Since then different and more efficient synthesis routs were developed like the Down process.² The most known processes with industrial use are the Nippon and the Wenker Process, which use 2-aminoethanol as starting compound.³ Today the yearly production of ethylene imide and propylene imide is mainly produced by BASF and Nippon Shokubai with a production capacity of an estimated 9.000 t **per year** ([retrieved 2006](#)).³

Although aziridines have many uses for synthetic purposes in academia, the main industrial use is the polymerization to polyethyleneimine (PEI) (Scheme 1).



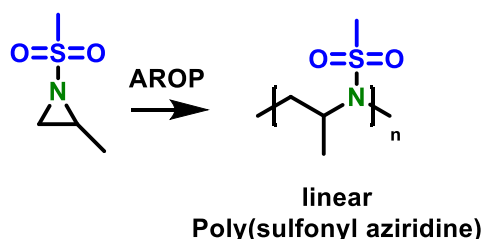
Scheme 1: Cationic ring opening polymerization of aziridines leads to hyperbranched (*hb*PEI).

This is achieved through the cationic ring opening polymerization (CROP) of ethylene imine, which produces hyperbranched (*hb*), i.e. statistically branched, PEI. This procedure can only empirically control molar masses, dispersities and branching density.⁴

In 2005 Stewart *et al.* described the anionic ring opening polymerization (AROP) of sulfonyl aziridines towards Poly(sulfonyl aziridines).⁵ (**Scheme 2**) With this approach, it was possible to combine the benefits of a living anionic polymerization (LAP) with the unique properties of polyaziridines (PAz). The anionic polymerization allowed

Introduction

synthesizing polyaziridine derivatives, with precise control over molar mass, dispersities and enabled quantitative end group modification by choosing an appropriate initiator or termination species. Furthermore, PAz-monomers tolerate a widespread of modifications to adjust polymer properties.



Scheme 2: Anionic ring opening polymerization of activated *N*-sulfonylaziridines.

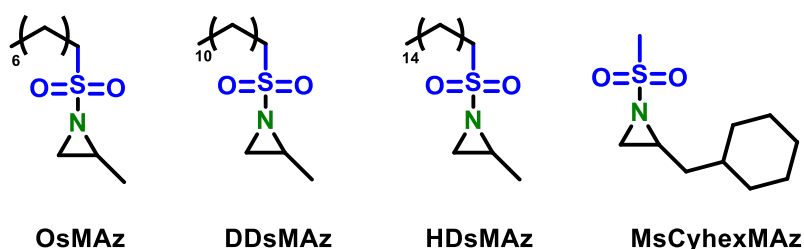
As the main use of PEI caused by its chelating ability and the enveloping of highly polar or charged molecules.^{6,7} *hb*PEI is mainly used as additive in the papermaking process, in detergents, adhesives, and as flocculating agent. These applications are based on chelating ability and its positive charges.^{8,9,10} In the research field of bio applications and gene delivery, PEI is one of the most important non-viral transfection agents to be studied.^{6,7,11,12} PEI main point of interest is therefore its polar backbone and high electron density, which allows an easy enveloping of particles and its use as surfactant. Therefore, enveloping of particles, nucleotides and proteins is the key feature of PEI. Nevertheless, PEI has an undefined hyperbranched structure and is restricted to polar solvents. Through A-AROP it is possible to synthesize linear Poly(sulfonyl aziridine)s with specific molecular weights and low dispersity, while modifying the solubility through different side chains.

3. Motivation

This master thesis involves a synthetic approach to modify the solubility of Poly(sulfonyl aziridine)s, which are known as being only soluble in a few polar solvents such as DMSO, DMF, DCM, CHCl_3 . Therefore, two projects were undertaken to modify the solubility characteristics and properties of PAz to enable a solubility in non-polar solvent such as cyclohexane, dodecane and oil as well as water without modifying the highly polar Poly(sulfonyl aziridine) backbone.

3.1 Project 1: lipophilic Poly(sulfonyl aziridine)s

The first project of this master thesis is a synthetic approach to introduce new PAz with modified hydrophobic side chains to improve solubility in non-polar solvents. Therefore, four different hydrophobic monomers were synthesized and polymerized (**Scheme 15**). In this regard, PAz could be a completely new alternative for the introduction as dispersant in non-polar solvent. Through A-AROP it is possible to synthesize Poly(sulfonyl aziridine)s with specific molecular weights and low dispersity while also introducing non-polar side chain in the monomer reducing necessary synthesis steps and rise the ratio of polar head to non-polar side chain. Through its brush like structure a use as coating, material could be favorable. Through its long non-polar side, chains it could shield coated surfaces from wear or metal from oxidation through moisture.



Scheme 3: Different synthesized hydrophobic monomers

To further study, the hydrophobic properties and surface activity of the synthesized polymers, were analyzed by spinning drop measurement in cyclohexane/water and used as coating on a prepared silica slide to measure the contact angles on a water droplet. Furthermore, real time ^1H NMR spectroscopy was used to measure the kinetic properties and calculate the reactivity ratios for Poly(OsMAz-co-MsMAz), Poly(OsMAz-co-TsMAz) and Poly(MsMCyhexAz-co-MsMAz).

3.2 Project 2: hydrophilic Poly(sulfonyl aziridine)s

The use of AAROP for the synthesis of well-defined PAz has many benefits over the CROP of ethylene imine but reduce the water solubility of the polymers due to the activation group. As most usages of PEI are conducted in the presence of water the introduction of hydrophilic groups, which allow a water solubility are of a key interest. As the modification of sidechains enable the altering of solubility it could also be used to enable the water-solubility of Poly(sulfonyl aziridine)s through introduction of PEG side chains, while also negating a downside of PEI as gen transfer agent. PEI is due to its full protonation cationic form under neutral condition (pH 7.3) can attach to negatively charged substances like nucleotides or proteins. Although these so called polyplexes show high transfection efficiency and stability in the blood cycle, PEI is regarded as cytotoxic.^{11,12}

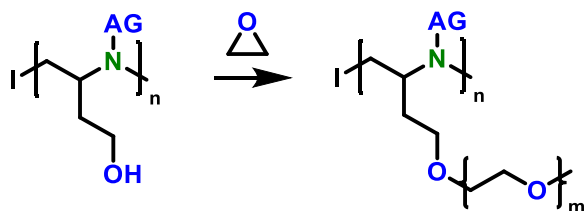
Many modifications have been made to negate its cytotoxicity while increasing its biocompatibility.¹² A promising possibility are copolymers consisting of PEG units. Homopolymerized PEG has a very low immunogenic, is nontoxic and approved by the FDA for internal consumption.¹³⁻¹⁵ Further PEGylation of nucleotides leads to a higher solubility in water, lower degradation and increased cell transport.^{16,17,18}

The copolymerization of ethylene oxide and activated aziridines was recently introduced by Gleede *et al.*¹⁹ It was shown that the copolymerization of both monomers leaded to block like copolymers with sharp gradients. Further two protocols for the synthesis of linear Poly(sulfonyl aziridine)s with active hydroxide side chains are known.^{20,21}

A new approach could be the introduction of PAz-*graft*-PEG-polymers. Through AROP of aziridines, highly controlled linear PAz with hydroxide-functionalized groups can be

Motivation

synthesized without use of protective groups and could be copolymerized with ethylene oxide to gain excesses to this new Polymer (Scheme 4).



Scheme 4: Synthesis of PEI-graft-PEG-polymers

4. Theory

4.1 Anionic ring-opening polymerization

Since the discovery of the living anionic polymerization (LAP) by Szwarc in 1956,²² the LAP was established as the method with best control over molar mass and molar mass distribution for various polymer architectures.^{23,24} Furthermore, with the LAP the synthesis of block copolymers and telechelics is possible. As the propagating anions can be sensitive towards impurities or water and CO₂, LAP requires strict purification of reagents and solvents and the use of special reaction conditions. Therefore, purification of monomer, dry solvents, as well as use of inert gas and standard Schlenck conditions is indispensable.

As monomer, vinyl derivatives or lactones and epoxides can be used. Vinyl monomers benefit from a –I/-M-effect in a substituent, which stabilizes the active chain end and increases the monomer reactivity towards a nucleophilic attack.²⁵ In cyclic monomers, the released ring strain is the driving force behind the polymerization.²⁵

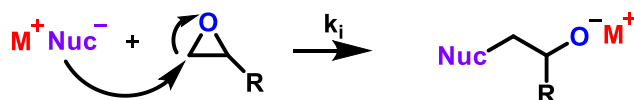
Initiation can be achieved through different methods, a classic base addition like butyl lithium or alkali hydroxides are the most common initiation method and need to be chosen according to the monomer structure. Otherwise, an electron transfer through a reductant is possible; a frequent example is the use of a naphthalene-sodium solution.²⁵

Epoxide monomers hold a key position in industrial and commercial use with a production scale of more than 33 million tons per year.²⁶ Poly(ethylene oxide) or Poly(ethylene glycol) (PEO/PEG) is the standard for biocompatible water-soluble polymers and have favorable features like low toxicity and antigenicity, a high solubility in water. Although ethylene oxide can be polymerized through various methods, PEG is mostly prepared by a living oxyanionic ring-opening polymerization.²⁶ (**Scheme 5**) As initiators, strong nucleophiles like deprotonated alcohols or diphenylmethyl potassium (DPMK) can be used, while the industrial production uses alkali hydroxides due to its simplicity and low costs. Initiation occurs through the nucleophilic attack on the oxirane. The ring opening leads to an oxyanion, which again leads a nucleophilic attack on an

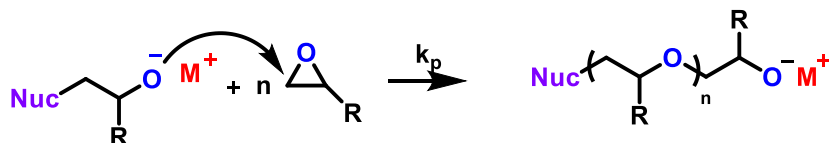
Theory

epoxide and therefore the chain propagation occurs. It has to be mentioned that for an initiation of epoxide monomers a partly deprotonation is often sufficient caused by a rapid proton exchange which allows a simultaneous chain growth.²⁶ Termination can occur through either an electrophilic terminating agent or impurities.²⁶

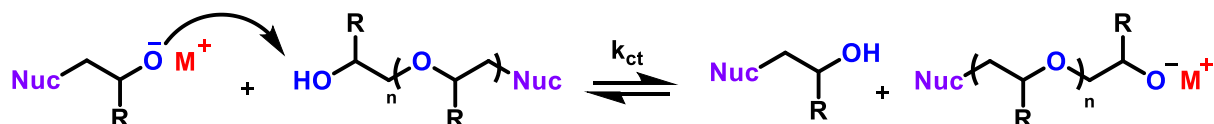
Initiation:



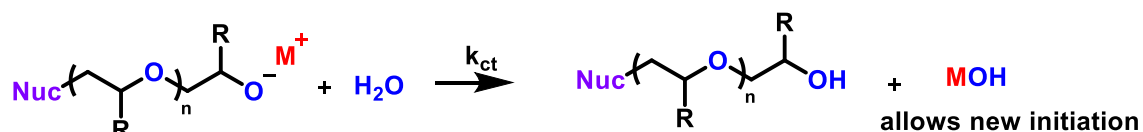
Propagation:



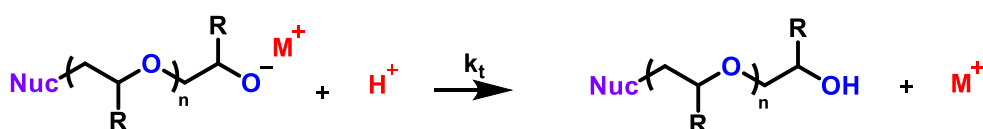
chain transfer



chain transfer due to impurities



termination



M = Counter ion Cs⁺ or K⁺

R = H, alkyl, alkenyl, alkynyl, aryl

Nuc = nucleophile

k_i = initiation rate

k_p = propagation rate

k_t = termination rate

k_{ct} = chain transfer rate

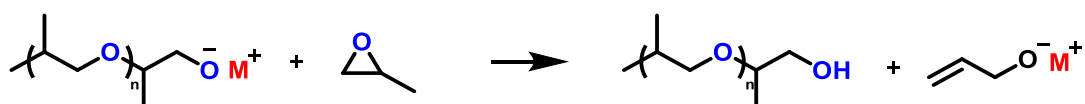
Scheme 5: Anionic ring opening polymerization explained on the example of ethylene oxide derivatives

To be counted as an anionic living polymerization (LAP), the chain end must remain active, termination does not occur, the initiation must be faster than the propagation to

Theory

ensure a simultaneously start of all chains and lastly the propagation must be independent from the chain length to ensure a linear growth over time.²⁷

Consequently, in contrary to the polymerization of ethylene oxide, propylene oxide cannot be categorized as LAP as deprotonation of the monomers' methyl group leads to chain transfer. (**Scheme 6**)²⁶



Scheme 6: Chain transfer to propylene oxide monomer due to deprotonation at the methyl group.

Through a linear propagation, no termination and a simultaneous start of all chains the degree of polymerization (X_n) can be estimated through the ratio of monomer to initiator (eq. 1). After the same time span, a higher initiator concentration leads therefore to a lower X_n .

$$\frac{[M_0]}{[I_0]} = \bar{X}_n \quad (1)$$

with: $[M_0]$: Monomer concentration $[I_0]$: Initiator concentration

The simultaneous growth enables also a sharp and distinct polymer dispersion (\mathcal{D}), where the number average molar mass (M_n) and mass average molar mass (M_w) have similar values and yields $\mathcal{D} \approx 1$ (close to 1) (eq. 2).

$$\frac{[M_w]}{[M_n]} = D \approx 1 \quad (2)$$

The polymerization starts with the initiation. The amount of created active chain ends ($[P^-]$) over time, corresponds to the concentration of used initiator $[I^-]$.

$$[I^-] = [P^-] \quad (3)$$

The speed of the initiation (k_i) must be much faster than the following propagation rate (k_p) to ensure a simultaneous chain propagation.

$$k_i \gg k_p \quad (4)$$

Theory

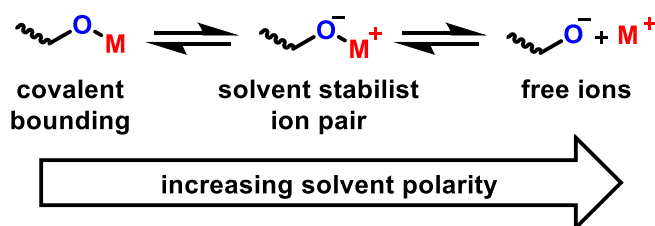
Consequently, the propagation rate (k_p) can be described by the linear decline of monomer over time.

$$-\frac{d[M]}{dt} = k_p[P^-][M] = k_p[I^-][M] \quad (5)$$

Through integration of equation (5) and the known initiator concentration, the rate of propagation can be determined through equation (6) which can be used for the analysis of ^1H NMR kinetic studies (see chapter 5.1 and 6.4)

$$\ln\left(\frac{[M_0]}{[M_t]}\right) = k_p[I^-]t \quad (6)$$

Ionic polymerization is influenced strongly by the polarity of solvents.²⁸ Through the solvent, the interaction between the active chain end and its counter ion is determined. In solvents with low polarity the bounding can be described as covalent and the distance between the ions is low therefore the chain end is shielded through the counter ion and the propagation is slower. In polar solvents on the other hand the ions are dissolved through a hydration shell and ions behave like a solvent stabilized ion pair if the polarity is high enough the ions can be completely separated and behave like free ions (Scheme 7). Consequently, polar solvents can increase the speed of the propagation drastically.



Scheme 7: Influence of solvent polarity on chain end/ counter ion interactions.




The influence of counter ions can be explained through the Pearson and HSAB concept.^{29, 30} This concept divides acids and bases through their ratio of charge and ion radius in soft and hard acids/bases. In theory ion pairs, which are, both hard or soft form bounds, which are more stable than those of different Pearson-strength. The effect can be shown through the AROP of ethylene oxide were potassium or cesium

are common counter ions because lithium coordinates strongly with the hard oxide chain end.^{26, 27} Consequently, in the AROP of epoxides polar and aprotic solvents such as tetrahydrofuran (THF), dioxane, or dimethyl sulfoxide (DMSO) are often used.

4.2 Polymerization of activated and non-activated aziridines

The main similarity between aziridines and ethylene oxide is the ring strain of 111 kJ mol⁻¹ for ethylene imine and 114 kJ mol⁻¹ for ethylene oxide and in both cases, the released ring strain is the driving force for the polymerization. However, in contrary to ethylene oxide, which can be polymerized through an AROP, ethylene imine cannot undergo an anionic polymerization due to the acidic N-H bond (Scheme 8) and only through an activation group, an AROP with aziridines is possible.²⁶

Table 1: Comparison of ethylene oxide and ethylene imine derivatives.

	Properties of rings		
			
Strain energy	114 kJ/mol	111 kJ/mol	
AROP	✓	✗	✓
CROP	✓	✓	?

Consequently, the most common kind of polymerization for aziridines is the cationic ring opening polymerization (CROP) which leads to the hyperbranched PEI. (Scheme 9)

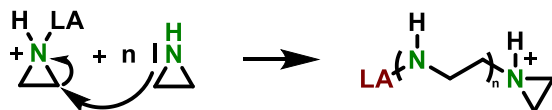
The polymerization uses a Lewis acid or halogen alkane as initiator and is conducted at elevated temperatures. The resulting *hb*PEI has a ratio of 1:2:1 for primary, secondary and tertiary amine groups.³ In contrast to linear PEI, the branched structure of *hb*PEI prevents crystallization and is therefore amorphous.¹⁰

Theory

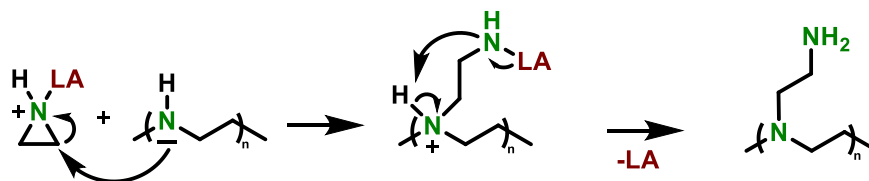
Initiation:



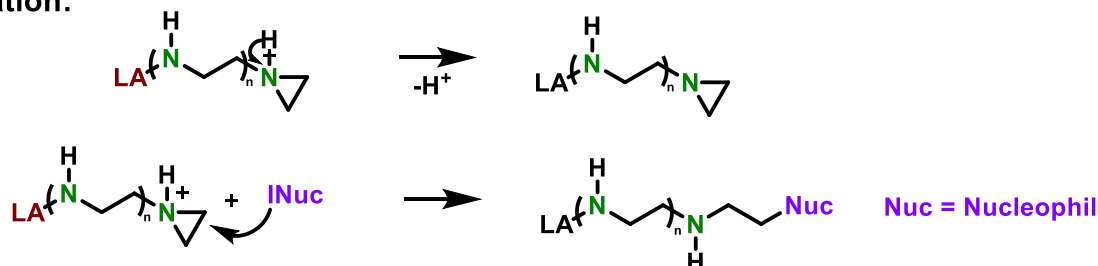
Propagation:



Branching:

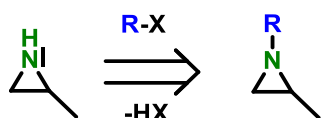


Termination:



Scheme 8: Mechanism of cationic ring opening polymerization of aziridines.

While the ring strain for epoxide and aziridines are nearly the same the unique properties of aziridine are caused by a lower electron negativity of the nitrogen as well as its free electron pair and protic N-H bond. Due to its free electron pair the nitrogen can react in a nucleophilic substitution reaction effectively substituting the N-H bond (Scheme 10).³¹




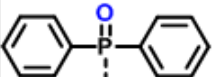
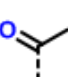
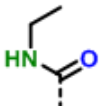
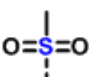
Scheme 9: Possible reactions by substituting the N-H bond

Since the mid-1960 aziridines are therefore categorized in an activated and none-activated form.³² Activated aziridines are substituted at the nitrogen, by electron withdrawing groups (-I-effect) such as sulfonyl, phosphoryl or carbonyl there by the polarity of the ring is increased and the aziridine can be ring opened by nucleophiles.

Theory

Although different substituents can be used for synthetic purposes only sulfonyl groups seem to be suitable for the AROP.⁵ Other activating groups which were tested did not produce the desired molecular weights and low dispersity.⁵(Table 2)

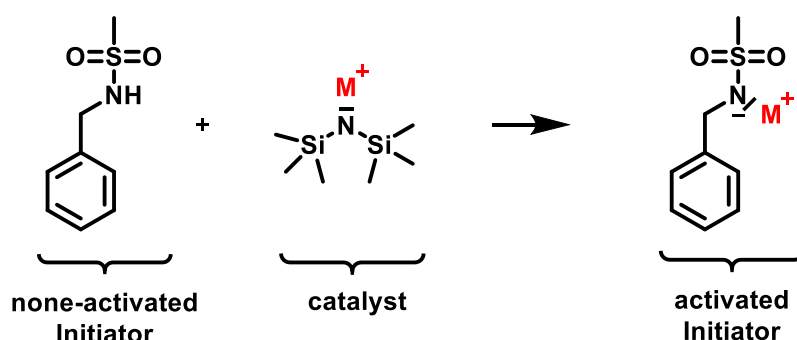
Table 2: Investigated activation group for aza-anionic ring opening polymerization by Stewart: diphenylphosphinyl-, acetyl- and ethylcarbamoyl-.⁵

				
Activation group				
Synthesis	✓	✓	✓	✓
AROP	✗	✗	✗	✓

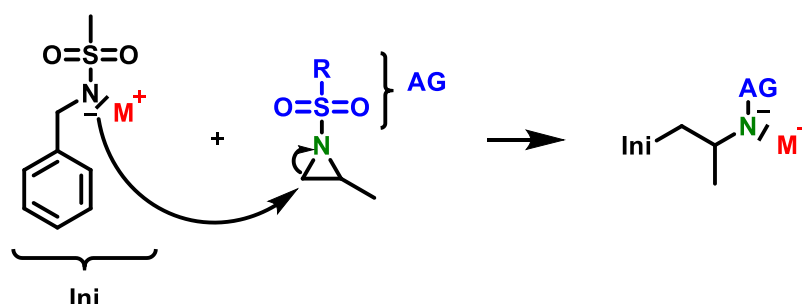
The produced polymers are poly(ethylene imine) derivatives with substituted nitrogen's in the polymer backbone. Therefore, we name them polyaziridine (PAz) or Poly(sulfonyl aziridine)s. In contrast to the CROP a linear PAz backbone growth is achieved without branching. Furthermore, PAz show a narrow molecular weight distribution, linear propagation rates and a degree of polymerization, which is dependent on the ratio of monomer to initiator. The cleavage of the S-N bond is possible through the usage of a microwave reactor or modified sulfonyl groups like para-cyanobenzenesulfonyl.^{31,33}

The polymerization mechanism uses a two-component initiator system, consisting of an Initiator *N*-benzylmesylsulfonamid (BnNHMs) and a base in form of potassium bis(trimethylsilyl)amide (KHMDs) is used. (Scheme 12) Through deprotonation, the inactive initiator is deprotonated (BnNKMs). Caused by the high ring strain and its activation the propagation accurs through ring opening after a nucleophilic attack at the unsubstituted carbon-atom.

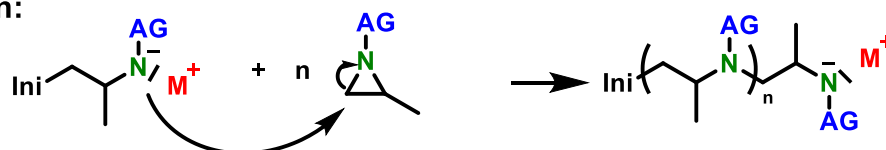
Initiator activation:



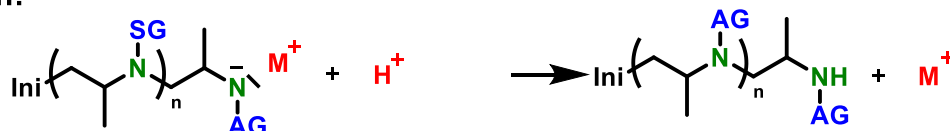
Initiation:



Propagation:



Termination:



Scheme 10: Mechanism of aza-anionic ring opening polymerization (AAROP) of activated *N*-sulfonylaziridines.

4.3 Characteristics of activated polyaziridines via AROP

4.3.1 Kinetics

The anionic polymerization aziridines follow the same kinetics as other anionic polymerizations.³⁴ With a very fast initiation and $k_i \gg k_p$ a linear propagation following eq. (5) occurs. This behavior allows an indebt study of the influence of various factors on the polymerization and like temperature, counter ions, solvent, and used sulfonyl derivatives. In a study conducted by Rieger *et.al.* 2-methylmesylaziridine (MsMAz) and 2-methyltosylaziridine (TsMAz) were polymerized *via* AROP. Using eq. (6) and measuring the monomer conversion over time through real time ¹H NMR spectroscopy allows a direct insight of various effects on k_p .^{34,35}

4.3.2 Temperature

Following the Arrhenius equation (7) the temperature has a direct influence on the speed of propagation.

$$k = A * \exp\left(\frac{-E_A}{RT}\right) \quad (7)$$

In the kinetic study AROP were conducted by 20, 50, 100 °C in DMF-*d*₇ and it was shown that a temperature of 50 °C is necessary to conclude a polymerization in 8 hours, while under 100 °C a complete conversion was achieved in only 30 minutes. In all cases, the chain end remained living and co-polymerization could be achieved.

4.3.3 Solvent influence and counter ion influence

The Solvent influence is also seen in the AAROP were only DMSO & DMF are suitable solvents and lead to a total conversion over an acceptable time period. Interestingly THF is not polar enough to sustain a polymerization of aziridines.

Unlike the oxy-anionic ROP for ethylene oxide, lithium is an acceptable counter ion. Lithium forms with the oxy-anion a covalent bond and does not act as nucleophile

Theory

anymore. For aza-anionic ROP all counter ions are adequate and do not influence the polymerization kinetic as hard as for the oxy-anionic ROP, with tosyl-substituents the propagation speed follows the line $\text{Cs} > \text{Li} > \text{Na} > \text{K}$. (Figure 1).

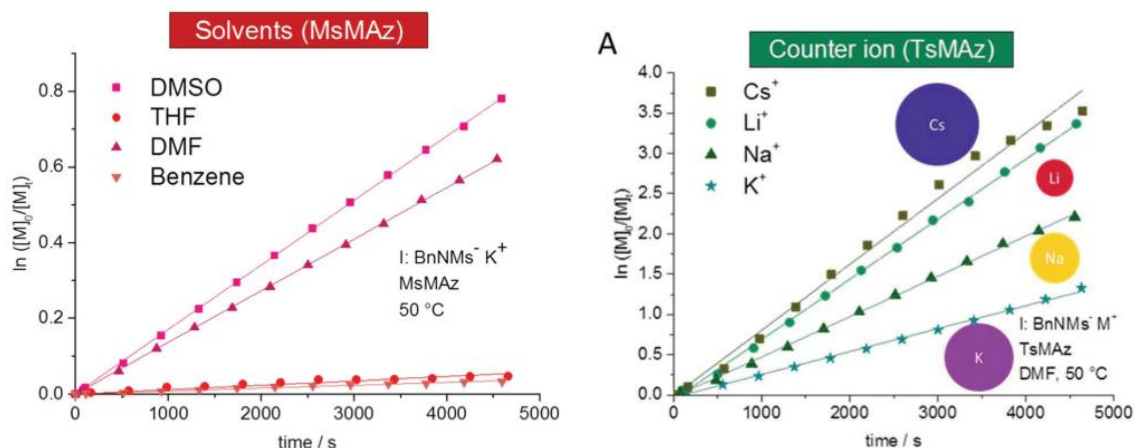


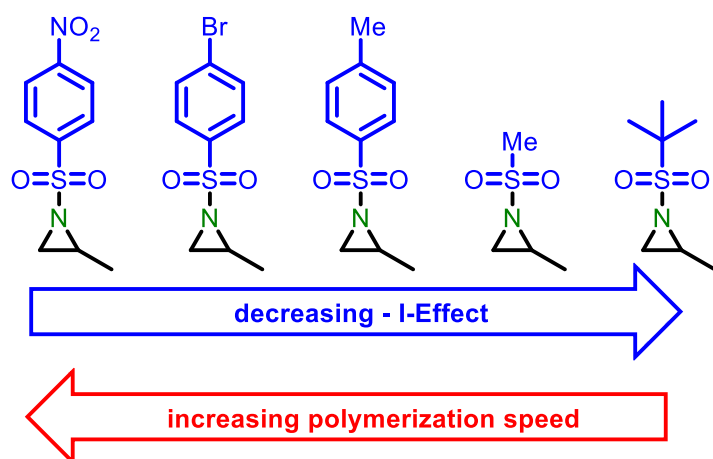
Figure 1: Left; propagation rate of MsMAz by 50 °C and potassium as counter ion in different solvents to visualize the influence of solvent polarity on the propagation rate. Right; propagation rate of TsMAz by 50 °C in DMF with different counter ions. By Riegler *et al.*³⁴

4.3.5 Substituent influence

The influence of modified sulfonyl substituents on the speed of propagation were studied and published by Rieger *et al.* in 2016.³⁵ In the study, a sequence-controlled copolymerization in one-pot was presented. The speed of polymerization is directly dependent on the electron withdrawing effect of the substitute, which activates the ring (Scheme 11). Through this $-I$ -effect the C-N bond is polarized.

If different monomers are used a gradient depending on k_p is achieved. If the speed of propagation is vastly different, a sharp gradient can occur which leads to block like microstructures, which can change or modify properties. In contrast, the influence of sidechains on the aziridines doesn't have a high impact as a comparison of 2-methylmesylaziridin and 2-decylmesylaziridin showed no significant impact on the speed of polymerization. Further, it was shown that different substitutes have a high impact on the tolerance of impurities. While mesyl- and tosyl- protected aziridines have a high resilience against impurities like water or alcohols it was reported that aziridines with a *o*-nitrosulfonyl group undergo spontaneous polymerization in the presents of low

amounts of impurities, which is due to the strong activation of the ring.³⁶ The influence of the activation group on the aziridine ring is far greater than on the active chain end. (Figure 2) While different activation groups (AG) have a small effect on the HOMO of the anion, the LUMO of the aziridine rings varies strongly depending on the $-I$ -effect of AG.²⁰



Scheme 11: Indication of substituent influence on the rate of propagation. Through increasing $-I$ -effect the reactivity of the monomer is increased drastically, while the influence on the chain end is insignificant in comparison. (compare Fig. 2)

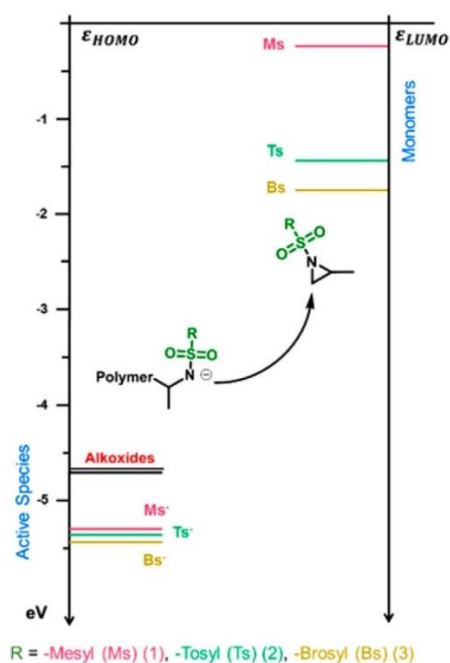
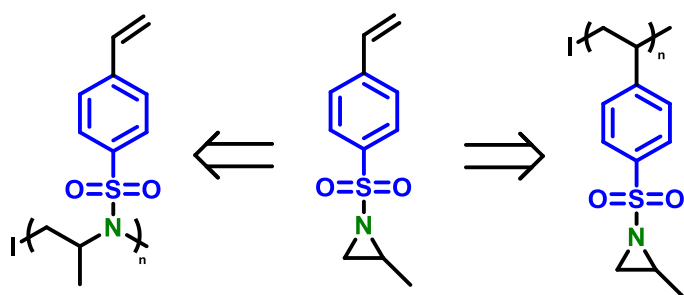


Figure 2: HOMO/LUMO Diagram in eV. Right: Influence of different substitutes on the LUMO of aziridine. Left: Influence of different substitutes on the HOMO of the active chain end compared to alkoxides By Gleede *et al.*²⁰

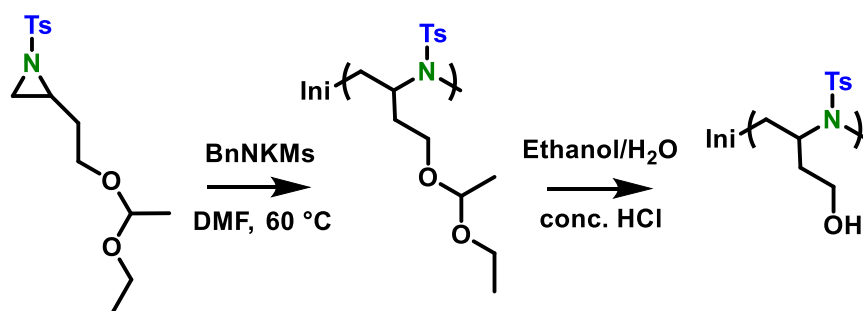
4.4 Copolymerization/ functionalization

Due to low basicity of the active chain end and the high reactivity of the stretched aziridine ring block-co-polymerization and polymerization of monomers with functional groups like alkenes are possible. The first successful polymerization of functionalized aziridine was done by Thomi and Wurm in 2015.³⁷ A mesylated aziridine with an alkene side chain was successfully synthesized from the ethylene oxide derivative and polymerized. To prove the activity of the alkene side chain a functionalization through a thiol-ene reaction was carried out. In the same regard 4-Styrenesulfonyl-(2-methyl)-aziridine was synthesized and proved to be the first bivalent aziridine monomer (Scheme 14).³⁸



Scheme 12: 4-Styrenesulfonyl-(2-methyl)-aziridine can be used as a bivalent monomer and either be polymerized through radical or anionic polymerization.

It is further possible to introduce hydroxide groups in the side chain (Scheme 15). A polymerization was first conducted under the use of an ethyl vinyl ether protection to ensure no interference through the alcohol group.²¹ However a protection is not necessary and polymerization can be carried out without it.²⁰



Scheme 13: First synthesis of PAz with a functionalized hydroxide side chain.²¹

Theory

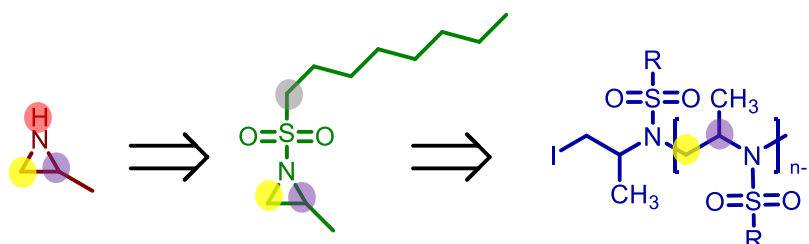
As aziridines and ethylene oxide are close relatives, recent focus lays on the study of copolymerization behavior. Caused by the electron withdrawing effect of the sulfonamide of the aziridine the propagation rate is higher than for ethylene oxides. As a result, copolymers are reported with sharp gradients. Real time ^1H NMR spectroscopy proved that a crossover from aza- to oxy-anionic takes place after nearly all aziridine monomer is consumed. Due to this aziridine/ ethylene oxide copolymerization possess the highest reactivity ratio for anionic polymerizations.¹⁹ As a cationic polymerization of activated aziridines and ethylene oxide was unsuccessfully³⁹ and AROP gives excess to the first block-co-polymers. A statistically or alternating copolymer has not been synthesized by now.

5. Analytics

To verify the successful synthesis and polymerization as well as to determine existing properties various analytic technique were used. Polymers were analyzed via ^1H NMR GPC and TGA/DSC, while for the copolymerization a kinetic study was conducted to analyse the copolymerization parameter. Further the successfully synthesized polymers were analyzed for their surface activity *via* spinning drop & contact angle measurement.

Characterization of all monomers and polymers is conducted through ^1H NMR spectroscopy and GPC. Activated aziridines as well as PAz show specific behavior which enables a clear characterization and precise analysis. In ^1H NMR aziridines have a unique signal pattern consisting of two doublets (●) with different coupling constants from the hydrogen atoms at the unsubstituted carbon atoms and one multiplet from the hydrogen atom at the substituted C-atom (●). Through the masking of the N-H bond, the singlet caused by N-H (●) vanishes after substitution. Due to the nature of the activation group, the chemical shift for these peaks varies but stays consistent as a pattern. (Scheme 14, Figure 3)

Following the polymerization, the aziridine rings build the polymer backbone. Therefore, the aziridine pattern vanishes and is replaced through a backbone pattern, which is formed by three broad peaks between 2.75-4 ppm. Although broad and sometimes overlapping an assignment and integration is easily possible. The first signal in the downfield can be again assigned to the hydrogen at the substituted carbon (●). Followed by the backbone signal of the two hydrogen atoms on the unsubstituted carbon (●). The last peak is caused by the two hydrogens at the α -C-atom of the sulfonyl group (●).



Scheme 14: highlighted reaction schema for assignment of classic ^1H -NMR patterns

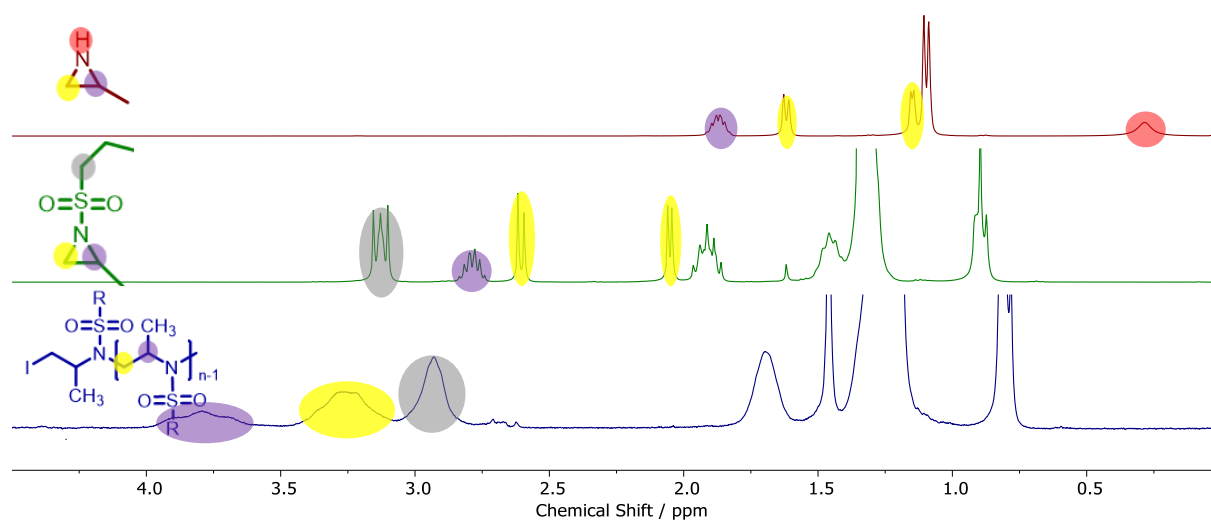


Figure 3: ^1H NMR spectra of 2-methylaziridine, substituted 2methyl-N-octasyaziridine and poly-(OsMAz). Highlighted areas show the classic patterns of aziridines and its polymers

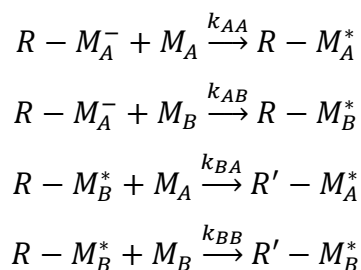
If an initiator with an aromatic group is used it can serve as an integration standard. With the known ratio of the backbone peaks of 1:2:2. The degree of polymerization (X_n) as well as the real M_n can be calculated (eq. 8).

$$M_n = m(I) + \sum(m(M)) + m(TG) \quad (8)$$

The use as integration standard is possible, if non-aromatic monomers are used, due to the otherwise overlapping aromatic peaks. In these cases, other aromatic initiators like *N*-pyrenylmesylamide (PyNHMs) need to be used.

5.1 ¹H NMR Kinetic

A ¹H NMR kinetic measurement can give access to the incorporation rate of the individual monomers as well as the propagation rate. In a copolymerization the active chain end ($R - M^-$) has four different reaction routes depending on the last incorporated monomer (M).



Through division of the propagations rates (k) the copolymerization parameter (r) are determined (eq 9).

$$\frac{k_{AA}}{k_{AB}} = r_1 \quad \frac{k_{BB}}{k_{BA}} = r_2 \quad (9)$$

These r-parameter are only relevant for the corresponding copolymerization and display the probability of the active chain end to incorporate the same monomer. A high r-value indicates that the chain end will likely incorporate the same monomer again, while a low r-value imply that the chain end tends to incorporate not the same monomer again. For copolymerization different ratios of r-values can be obtained, which leads to four different types of incorporation.

Table 3

Ideal azeotrope copolymer	$r_A = r_B = 1$
Statistics (ideal) non-azeotrope copolymer	$r_A > 1 ; r_B < 1 \text{ and } r_A = \frac{1}{r_B}$
Statistics (non-ideal) azeotrope copolymer	$r_A < 1 ; r_B < 1$
alternating copolymer	$r_A \approx 1 ; r_B \approx 1$

The use of ^1H NMR real time spectroscopy allows the determination of monomer decline over time which in combination with the extended copolymerization equation (10) can be used to determinate the r-parameters.

$$F_A = \frac{r_A f_A^2 + f_A f_B}{r_A f_A^2 + 2f_A f_B + r_B f_B^2} \quad (10)$$

F_A incorporated mole fraction of monomer in the copolymer

f_A mole fraction of monomer in solution

Many different mathematical approaches can be taken to calculate the r parameter on basis of the copolymerization equation with the most known being Mayo-Lewis and Fineman-Ross. Further possibilities are after Meyer-Lowery⁴⁰ and Jaacks⁴¹, which were used in this work (Appendix ^1H NMR Kinetic).

5.2 Gel permeation chromatography

The gel permeation chromatography is one of the most common and important relative analytic methods for polymers. A polymer is dissolved in the mobile phase flows through the column, which is filled with a stationary phase consisting of porous beads. In an ideal scenario a polymer does not interact with the stationary phase. This stands in the contrast to other chromatographic methods and the separation is therefore based on size exclusion and the hydrodynamic radius of the polymers. Due to the fact that the beads are porous and small particles can enter into them while big particles can't, explains the fact that smaller particles have a longer retention time than larger particles.

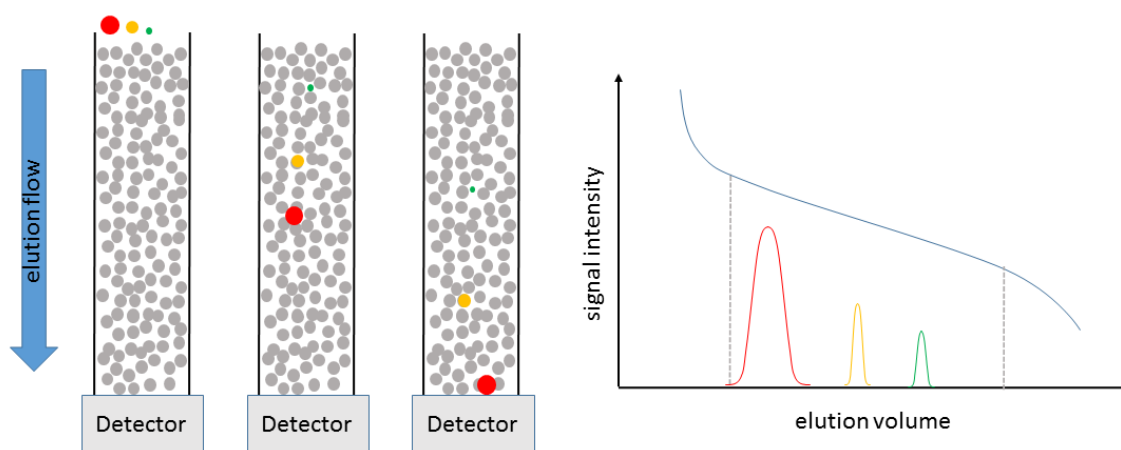


Figure 4: Left: depiction model of a size exclusion chromatography. Molecules of different hydrodynamic radius (pictured through colored shapes) are fractionated through different retention times. Right: depiction of a GPC diagram by plotting elution volume against the signal intensity. Blue line indicates high and low exclusion limited through calibration standard.

While ^1H NMR or light scattering are absolute methods, GPC needs a standard for calibration purposes and all calculated molar masses are correlated to the used standard. As a standard for PAz, PEO in DMF or PS in THF are used. As the standard does not reflect the hydrodynamic radius of PAz perfectly the calculated molar masses are 2-3 times smaller than the actual M_n measured through ^1H NMR. Nevertheless, the GPC gives valuable information about the dispersity of the polymer probe and is essential for its analysis.

Due to the fact that the AAROP has a very low dispersity the values gained by GPC and ^1H NMR could be used to calculate a new better fitting calibration curve. On the other hand, aziridines can be easily modified through the sulfonyl group, side chain or co polymerization therefore a new calibration curve would most likely only fit for a specific form of PAz with comparable hydrodynamic behavior.

5.3 Surface tension and spinning drop

In a system of two insoluble species like water/cyclohexane a phase separation occurs, and a surface area is formed, which possesses a specific interface tension. Surfactants are known for their behavior to reduce the surface tension of such systems due to their structure, which consist of a hydrophobic and hydrophilic part. Due to this, surfactants align on the surface area, mediate between the insoluble phases and reduce the surface tension.

In a liquid, all molecules are pulled equally in every direction due to intrinsic cohesive forces. On the surface located molecules on the other hand are pulled towards their counter parts, which results in the contraction of the surface area to minimize its energy (Figure 5).

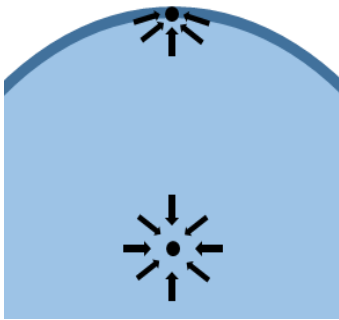


Figure 5: intrinsic forces affecting molecules of a liquid

The work (ω) necessary to increase the surface area (σ) is proportional to it and the proportional coefficient (γ) is the surface tension given in J/m² or N/m.

$$d\omega = \gamma * d\sigma \quad (11)$$

At constant volume and temperature, eq. can be transferred into the Helmholtz free energy (**A**)

$$dA = \gamma * d\sigma \quad (12)$$

Therefore, the decrease in surface area lowers the free energy, which explains that two insoluble species phase-separate as well as the formation of droplets, as spheres have the lowest ratio between volume and surface.

In a spinning drop measurement, the interfacial tension (γ) can be determined by the deformation of a droplet under centrifugal forces. In a test tube, a two-phase system is prepared. Therefore, a solvent droplet of lesser density is played inside a second fluid ($\Delta\delta$). (Figure 6) Through rotary around its axis (ω) the droplet experiences a centrifugal force and deforms. The change in radius (r) can be used to determine the interfacial tension, which is given by the Vonnegut's equation (eq 13).⁴⁴

$$\gamma = \frac{\Delta\delta\omega^2}{4} r^3 \quad (13)$$

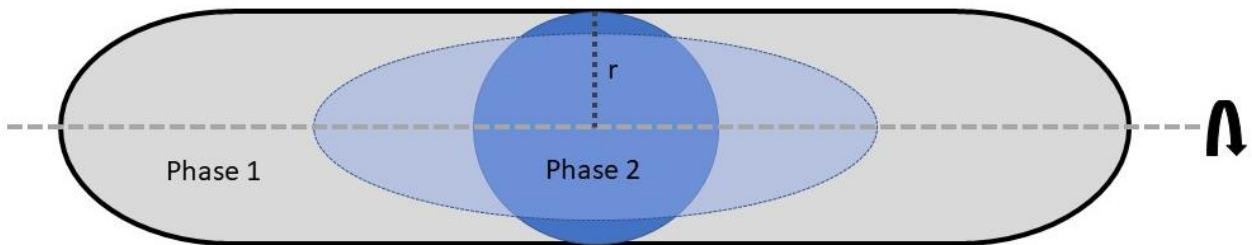


Figure 6: Depiction of a spinning drop measurement. The second phase (deep blue) deforms (light blue) through centrifugal force.

5.4 Contact angle measurement

To quantify the wetting ability of a surface the contact angle between a surface and a droplet can be measured. (Figure 7)

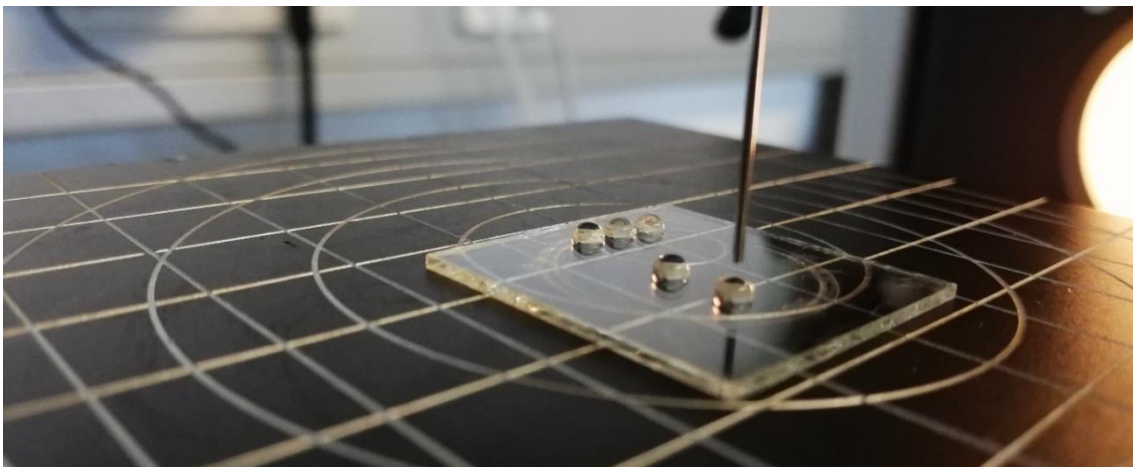
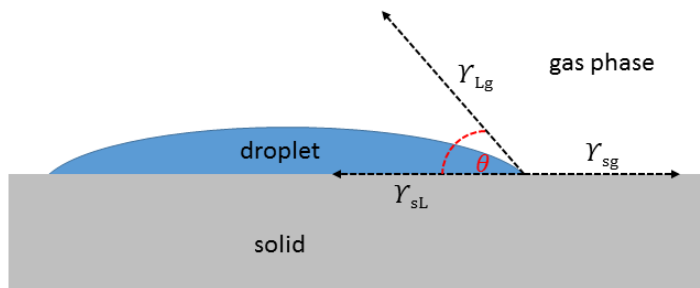


Figure 7: Depiction of the measurement process. A 100 μL syringe is used to create 5 μL droplets on the coated microscope slide.

As the droplet interacts with the solid, the shape of the droplet is determined by adhesive and cohesive forces. If a droplet expands on a surface, the contact angle decreases and an interaction with the surface is favorable. If on the other hand a water droplet is in contact with a hydrophobic surface, the solid-liquid interface is decreased while the surface tension of the droplet increases. Therefore, it can be concluded that a hydrophobic surface leads to high contact angles while hydrophilic surfaces tend to low contact angles if a water droplet interacts with the solid.

To measure the contact angle a droplet of specific volume is applied on a surface, aligned to the surface a camera is adjusted to measure the left and right angle between droplet and surface.

The contact angle itself was defined by Thomas Young in 1805 as the angle on the phase boundary of gas, liquid and solid. (Figure 8, eq. 15)



$$Y_{sg} = Y_{sL} + Y_{Lg} * \cos\theta \quad (14)$$

$$\cos\theta = \frac{Y_{sg} - Y_{sL}}{Y_{Lg}} \quad (15)$$

Figure 8: Definition of the contact angle after Thomas Young

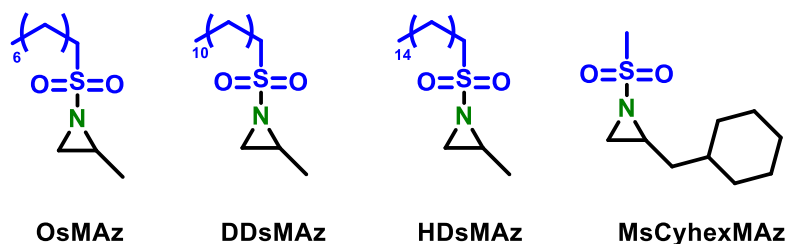
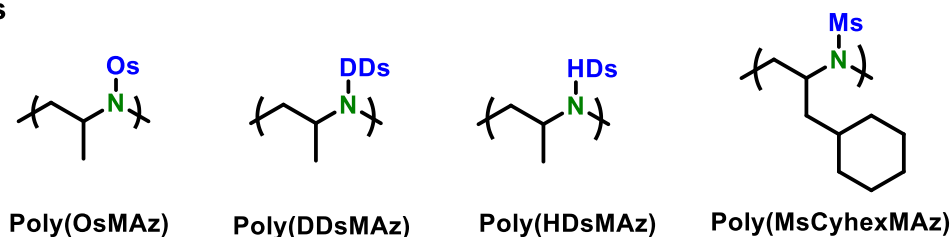
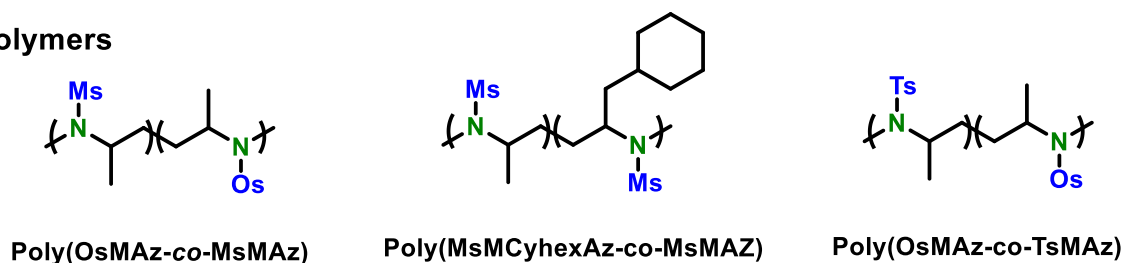
6. Results and discussion

As this master thesis covers the synthetic approach of novel lipophilic and hydrophilic Poly(sulfonyl aziridine)s in two projects, each is addressed individually. In the following the first project about the synthesis of lipophilic Poly(sulfonyl aziridines) will be discussed. Therefore, a short overview is given followed by the monomer synthesis and the polymerization. Afterwards the conducted analytic measurements and results are shown and discussed.

Afterwards in the second project the first Poly(sulfonyl aziridine)-*graft*-Poly(ethylene oxide) (PAz-*graft*-PEO) are then introduced. Therefore, two different synthetic approaches are described, and the successful synthesis discussed.

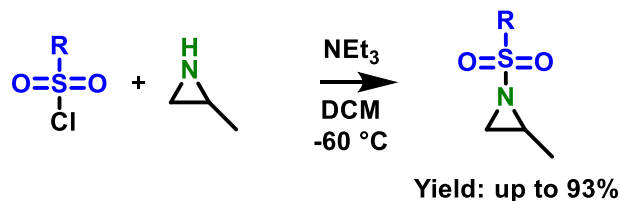
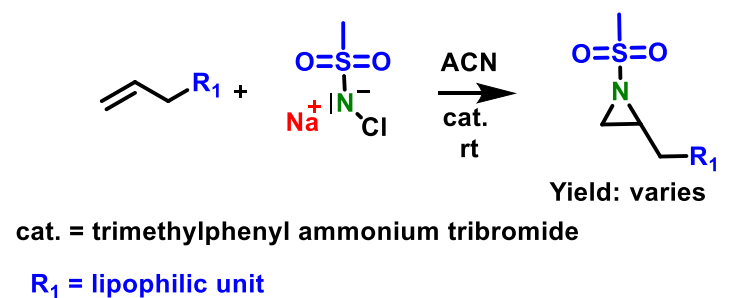
6.1 Project 1: Synthesis of lipophilic polyaziridines

As the major aim of this thesis, the solubility of Poly(sulfonyl aziridine)s in non-polar solvent was studied. Therefore, four novel monomers with different hydrophobic side chains were synthesized and polymerized. A variety of *homo*- and copolymers with increasing X_n and in different monomer ratios were polymerized. (Scheme **15**) To study the influence of the new activating group and the prone side groups of the monomers the copolymerization parameters calculated. Solvation assays in different solvents were performed and the obtained polymers were used as coatings to study their material properties as a novel hydrophobic coating. Contact angles of water droplets as well as the layer thickness of polyaziridine coatings were measured in dependence of concentration, X_n and side chain length. Further, the polymers were used as a surfactant and the impact on the surface tension was analyzed *via* spinning drop of a cyclohexane/water probe.

Monomers**Polymers****Copolymers****Scheme 15:** Synthesized lipophilic monomers, Polymers and Copolymers**6.1.1 Synthesis of lipophilic *N*-sulfonylaziridines monomers**

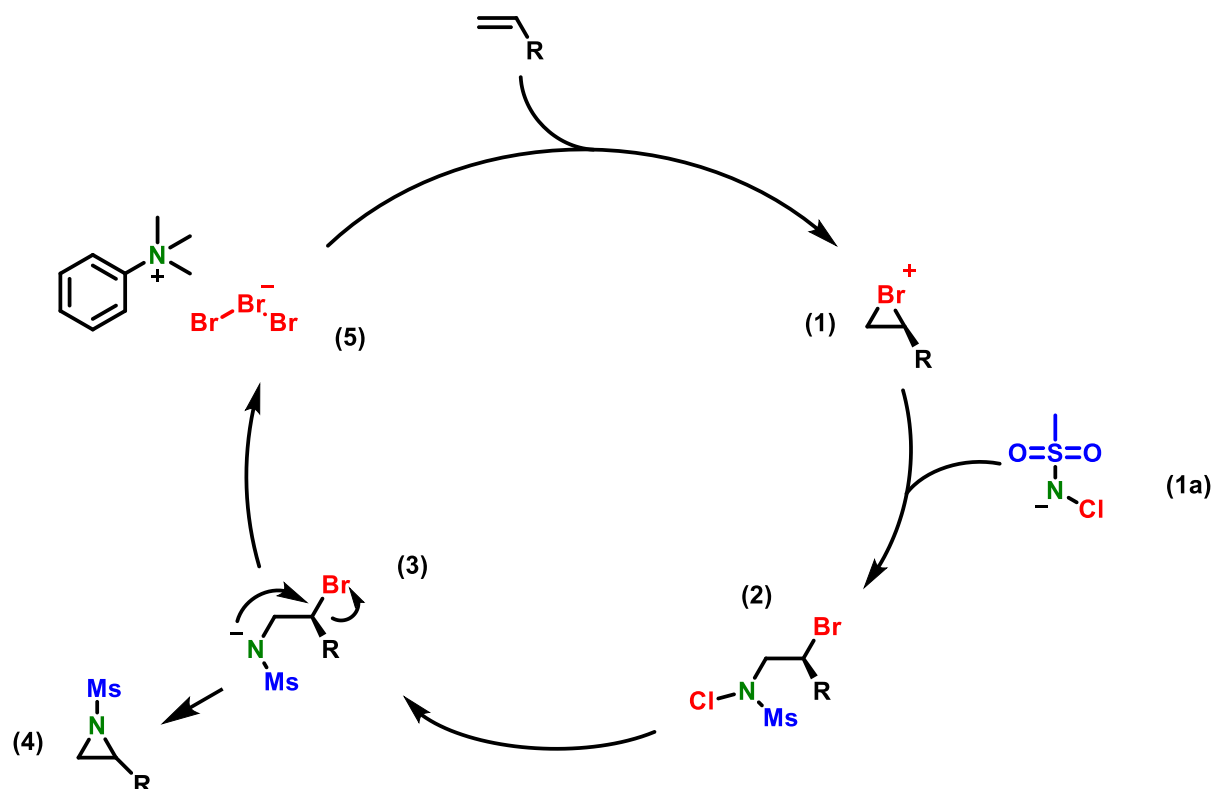
The modification of aziridine monomers for the AAROP can be done through multiple synthesis strategies, the two most established of them were used, due to their high yield and one-step synthesis. The used synthetic approaches after Sharpless⁴² and through amidation of sulfonyl chlorides⁵ allow a modification of the yielded *N*-sulfonylaziridine monomers in two different positions. (Scheme 16)

Results and discussion



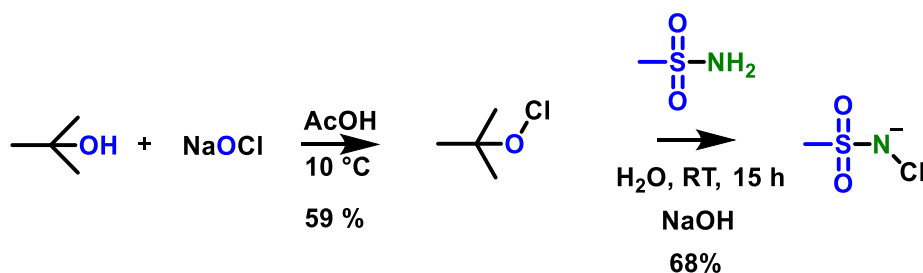
Scheme 16: Synthesis routes of activated *N*-sulfonylaziridines after Sharpless⁴² and through amidation of sulfonyl chlorides

The bromine-catalyzed aziridination after Sharpless uses terminal olefin and various Chloramine-derivatives like Chloramine-M (sodium *N*-chloro-(methylsulfonylamide)) as starting material. While the terminal olefins are commercially available, the used Chloramine-M is easily synthesized. As organic catalyst trimethylphenyl ammonium tribromide (TMPAB) was found to be effective. The by Sharpless proposed catalytic mechanism (Scheme 17) starts by the formation of a bromonium ion (**1**) which is nucleophilic attacked by the used Chloramine-M and forms a sulfonamide (**2**) after ring opening. A following nucleophilic attack of a bromide or another chloramine cleaves the N-CL bound of the intermediate (**2**) leads to the corresponding anion (**3**). Through expulsion of Br⁻ from anion (**3**) product (**4**) is generated while TMPAB is regenerated.



Scheme 17: bromine-catalyzed aziridination after Sharpless of a terminal olefin through trimethylphenylammonium tribromide

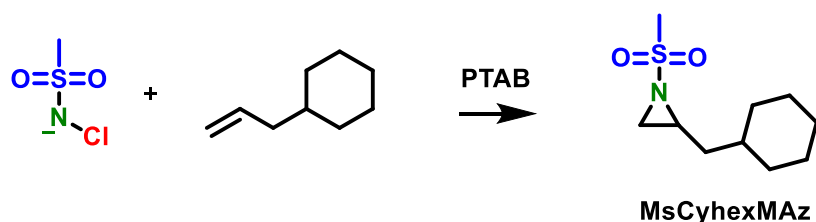
As the synthesis after Sharpless needs a nitrogen source in form of chloramine-M, it was synthesized following a known synthesis process.³⁵ (Scheme 18) In the first step, tert-butanol was converted to tert-butyl hypochlorite, through chlorination with sodium hypochlorite solution (14 % in H₂O) in the absence of light (yield 59 %). The chlorination agent was used directly for the synthesis of chloramine-M. For this methanesulfonamide was dissolved in water deprotonated with NaOH, mixed with tert. butyl hypochlorite and stirred for one day (yield 68%).



Scheme 18: Preparation of chloramine-M under exclusion of light

Results and discussion

The synthesis *via* Sharpless was used to synthesis 2-(cyclohexylmethyl)-*N*-mesylaziridine. (MsCyhexAz).(Scheme 19) For that, the starting materials are dried and dissolved in dry acetonitrile and a catalytic amount of trimethylphenyl ammonium tribromide was added. The solution was stirred for two days at room temperature and purified *via* silica column.



Scheme 19: synthesis 2-(cyclohexylmethyl)-*N*-mesylaziridine *via* Sharpless.

In the ^1H NMR the peaks of the aziridine ring can only be partly assigned 2.64 – 2.56 ppm (m, **c**), 2.29 ppm (d, $J = 7.0$ Hz, **b**), **b** and **b'** separated in two duplets with different coupling constants but **b'** is overlaying with the equatorial hydrogen peaks of the cyclohexane ring (**f,f',g,g',h (eq.)** 1.64 – 1.48 ppm (m, 6H)) The CH_3 -group of the mesyl-group is clearly visible at 2.64 – 2.56 ppm (**a**) (Figure 9).

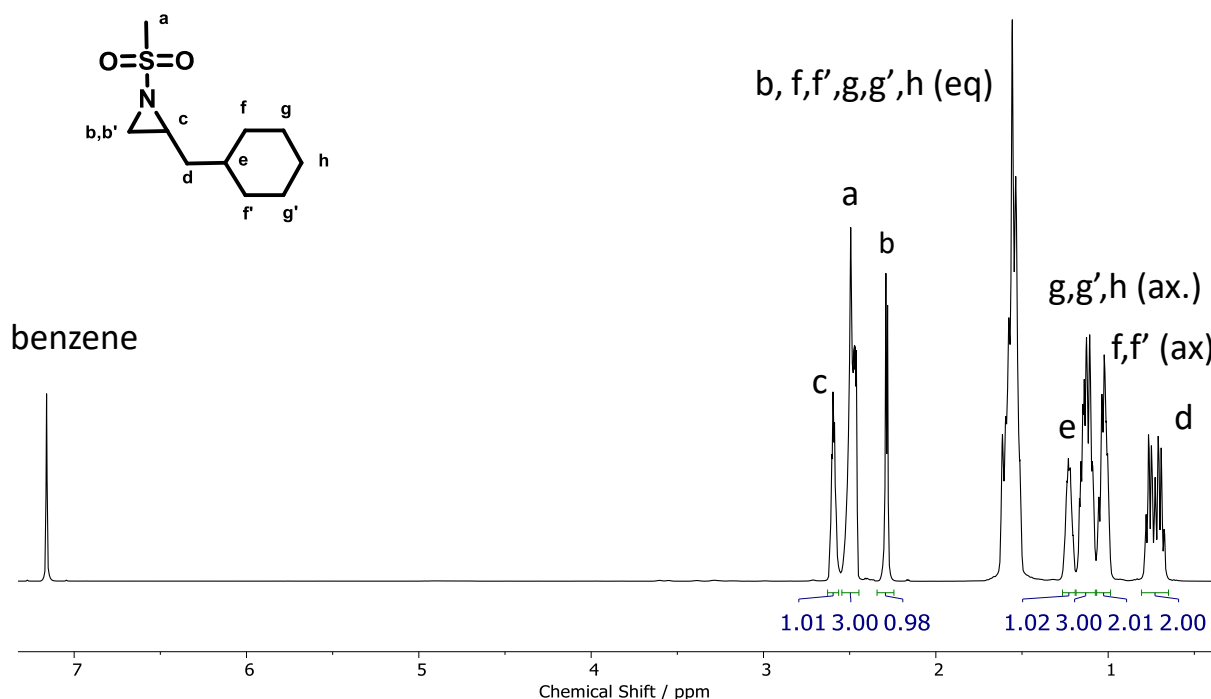
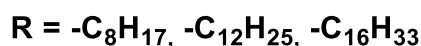


Figure 9: ^1H NMR (700 MHz, benzene- d_6) of 2-(Cyclohexylmethyl)-*N*-mesylaziridin (MsCyhexAz).

Results and discussion

The reaction had a low yield of 48 % although a reaction control *via* ^1H NMR indicated a full double bonds conversion of the starting material. Although the reaction has a low yield and is more time consuming than its alternative approach it has the possibility to use various activation groups which could increase the solubility or the introduction of other hydrophobic groups. Further it is possible to remove of the sulfonamide groups after polymerization which could have an impact on solubility of the polymers.

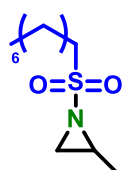
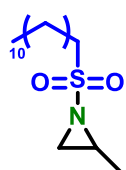
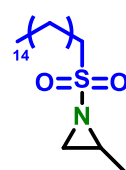
The second synthesis approach is to tune the aziridine properties and the solubility behavior of the polymers by introduces lipophilic activation group through amidation of sulfonyl chloride derivatives with varying alkyl chain lengths $-(\text{CH}_2)_x\text{CH}_3$ $x=7, 11, 15$).



Scheme 20: Synthesis of activated N-sulfonylaziridines after Stewart.⁵

These sulfonyl chlorides with increasing lipophilic alkyl chains were used to obtain three novel monomers 2-methyl-N-octasylaziridine (OsMAz) as well as dodesyl- and hexadesyl-aziridine derivatives. (Scheme 20) The amidation of sulfonyl chloride derivatives can use various non-activated aziridines and was performed with propylene imine (2-methylaziridine) due to its lower toxicity compared to ethylene imine. The reaction follows an $\text{S}_{\text{N}}2$ -mechanism and was executed with an excess of TEA at -30°C in DCM due to its exothermic behavior. Beneficial for this strategy are the easy and strait forward synthesis strategy with high yields of up to 93 % and a single purification step *via* column chromatography, which allowed monomer synthesis of up to 20 g scales to be performed and maintaining high yields. (Scheme 21)

Results and discussion

			
OsMAz	DDsMAz	HDsMAz	isolated yield
78 %	69%	73%	after purification
93%	--	--	without purification

Scheme 21: Yield of synthesized *N*-sulfonylaziridines with lipophilic activation group before and after purification.

After a reaction time of 12 h, the reaction was neutralized with a NaHCO_3 solution. Workup was achieved, by washing the organic phase with water. After evaporation, the monomers were obtained as colorless oily liquid (OsMAz) or colorless solid, which usually needed to be purified by column chromatography. OsMAz could be polymerized directly after the crude workup and demanded no purification through silica chromatography resulting in the high yield of up to 93%.

It is known, that the LAP of sulfonyl aziridines is comparably robust and can tolerate a certain amount of impurities. Therefore column chromatography was not required. Potential remaining impurities, which were not noticed by the ^1H NMR could only be the alkyl sulfonic acid which did not interfere with the polymerization.

Characterization of 2-Methyl-*N*-Octasulfonylaziridine (OsMAz)

In the ^1H NMR the hydrogen of the aziridine ring can be assigned to a multiplet at 2.84–2.69 ppm (**b**) and two duplets with different coupling constants at 2.59 ppm ($J = 7.0$ Hz, **c**) and 2.03 ppm ($J = 4.6$ Hz, **c**). Due to the $-I$ effect of the sulfonyl group the hydrogens of the α - and β -C atom are shifted towards the low field at 3.17–3.06 ppm and 1.97–1.80 ppm (**d, e**). (Figure 10)

Results and discussion

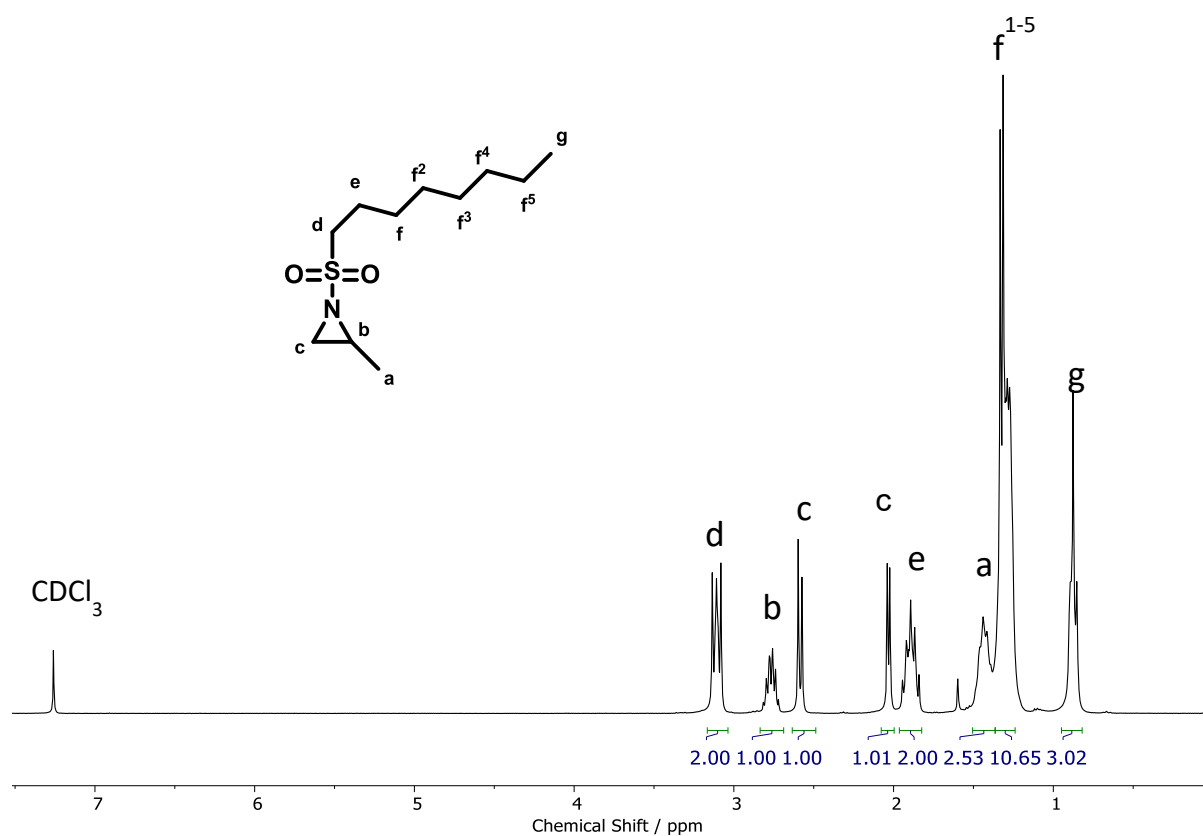


Figure 10: ¹H NMR (300 MHz, Chloroform-*d*) of 2-Methyl-*N*-Octasylaziridin (OsMAz).

Characterization of 2-Methyl-*N*-Dodesylaziridin (DDsMAz)

The ^1H NMR of DDsMAz is comparable to the ^1H NMR of OsMAz due to the same chemical structure. (Figure 11, compare Figure 10) The aziridine pattern is visible with the multiplet at 2.81 – 2.62 ppm (m, **b**) and two duplets with different coupling constants at 2.53 ppm ($J = 7.0$ Hz, **c**) and 2.02 ppm ($J = 4.7$ Hz, **c**). Due to the $-I$ effect of the sulfonyl group the hydrogens at the α - and β -C-atom are shifted towards the low field at 3.16 – 2.99 and 1.93 – 1.75 ppm (**d**, **e**). The alkyl side chain is clearly visible 1.37 – 1.19 (**f**¹⁻⁹) (Figure 11)

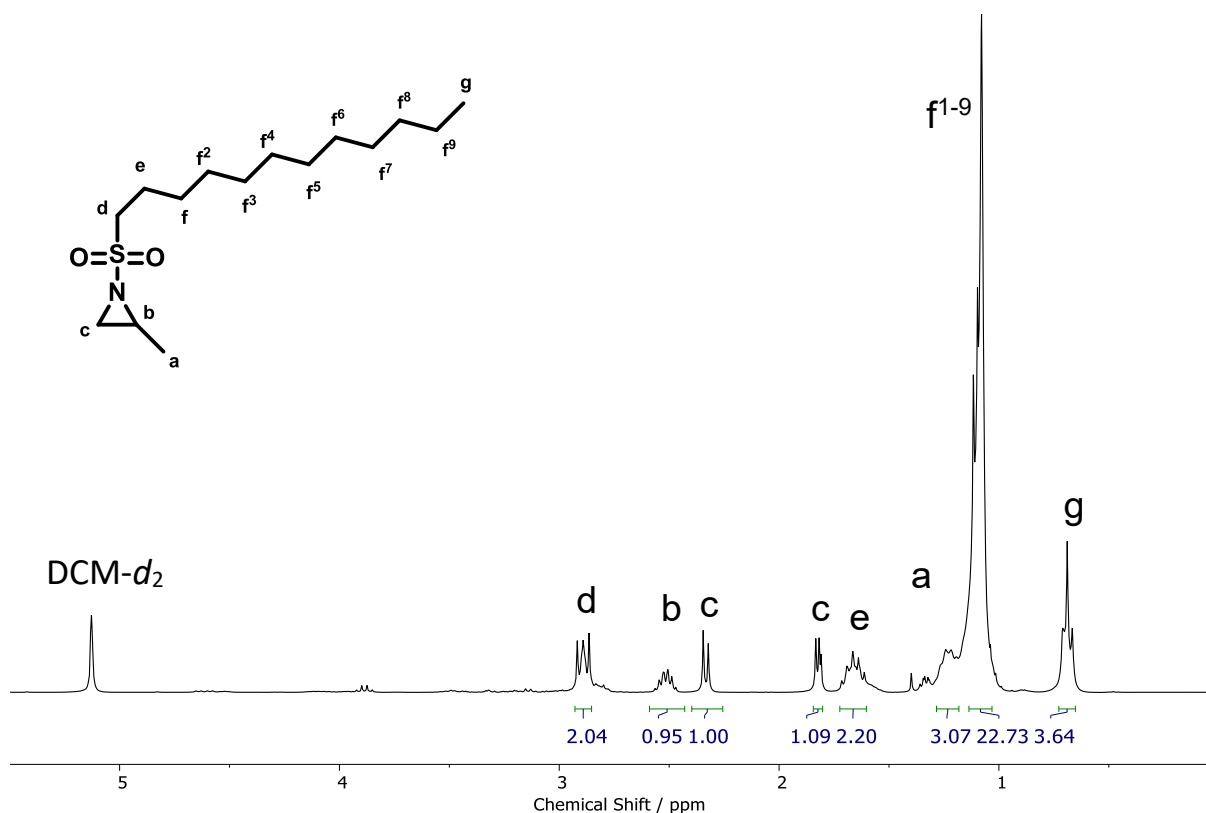


Figure 11: ^1H NMR (300 MHz, Methylene Chloride- d_2) of 2-Methyl-*N*-Dodesylaziridin (DDsMAz).

Characterization of 2-Methyl-*N*-Hexadecylaziridin (HDsMAz)

Again the ^1H NMR of HDsMAz is comparable to DDsMAz and OsMAz due to the same chemical structure. The only significant change is the ratio due to the increasing alkyl chain. The aziridine pattern is visible with the multiplet by 2.70 – 2.56 ppm (**b**) and two duplets with different coupling constants 2.47 ppm ($J = 7.0$ Hz, **c**) and 1.96 ppm ($J=4.7$ Hz, **c**). (Figure 12) Due to the $-I$ effect of the sulfonyl group the hydrogens at the α - and β -C-atom are shifted towards the low field by 3.08 – 2.93 and 1.87 – 1.68 ppm (**d**, **e**). The alkyl side chain is the broadest peak by far by 1.30 – 1.05 (**f¹⁻¹³**)

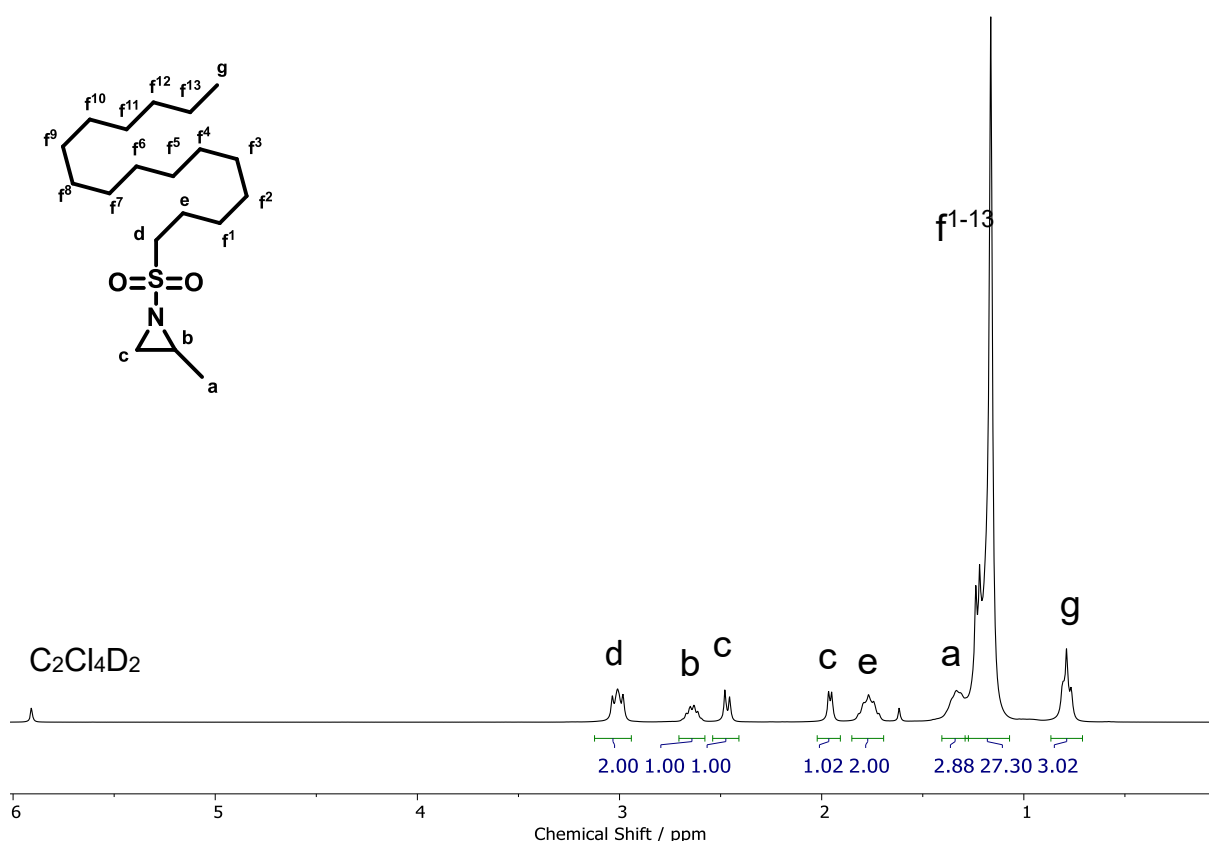
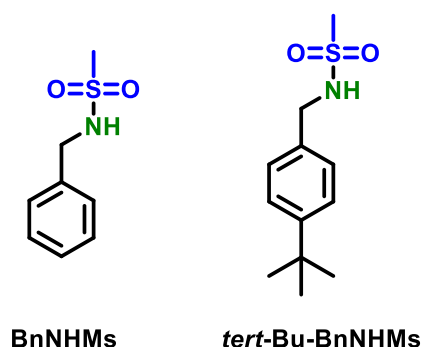


Figure 12: ^1H NMR (300 MHz, Tetrachloroethane- d_2) of 2-methyl-*N*-hexadecylaziridine (HDsMAz).

6.2 Polymerization

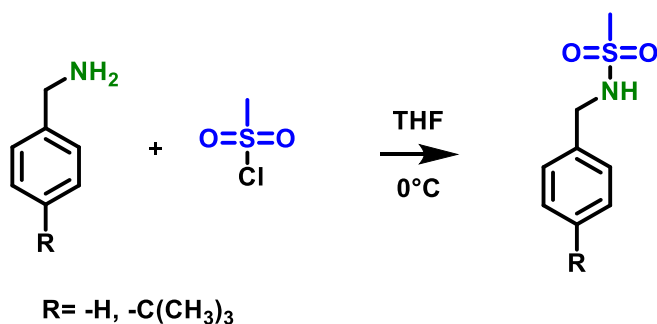
6.2.1 Initiator synthesis

For the initiation of the polymer synthesis, the two-component initiator consisting of *N*-benzylmesylsulfonamide (BnNHMs) and potassium bis(trimethylsilyl)amide (KHMDs) was used (compare Section 5.1). In addition, BnNKMs can be used, as an integration standard in ^1H NMR analysis.



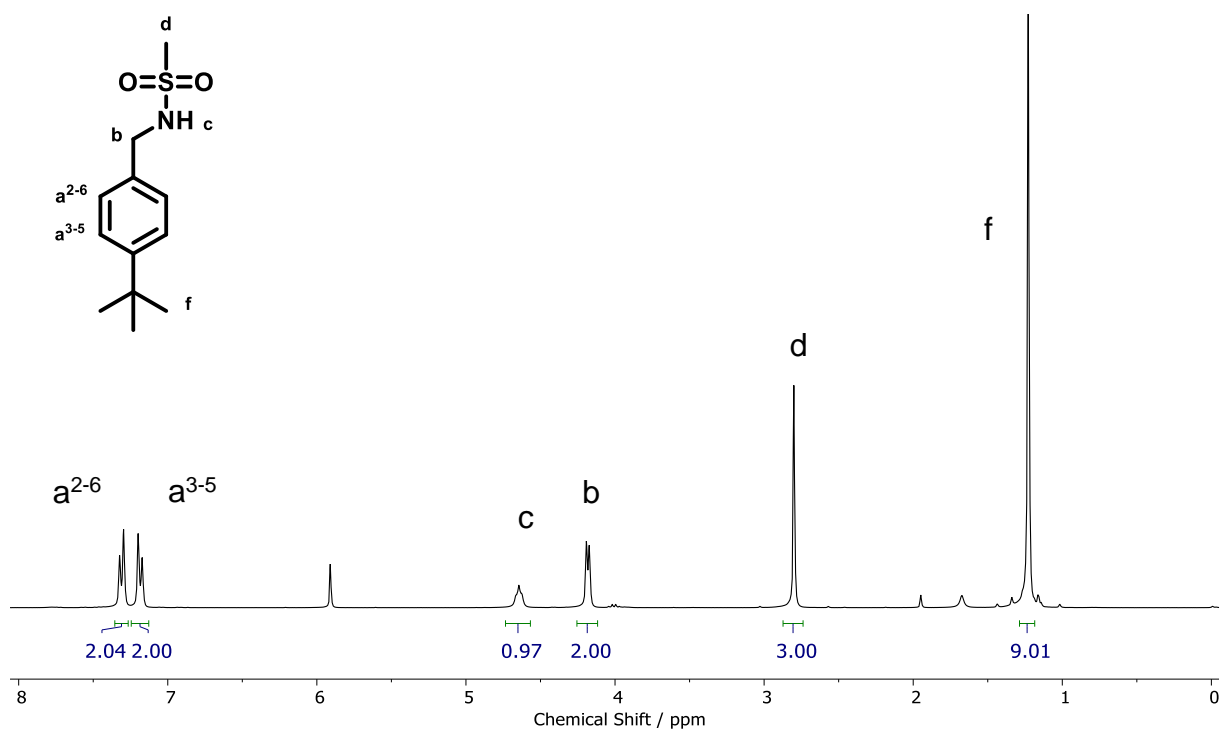
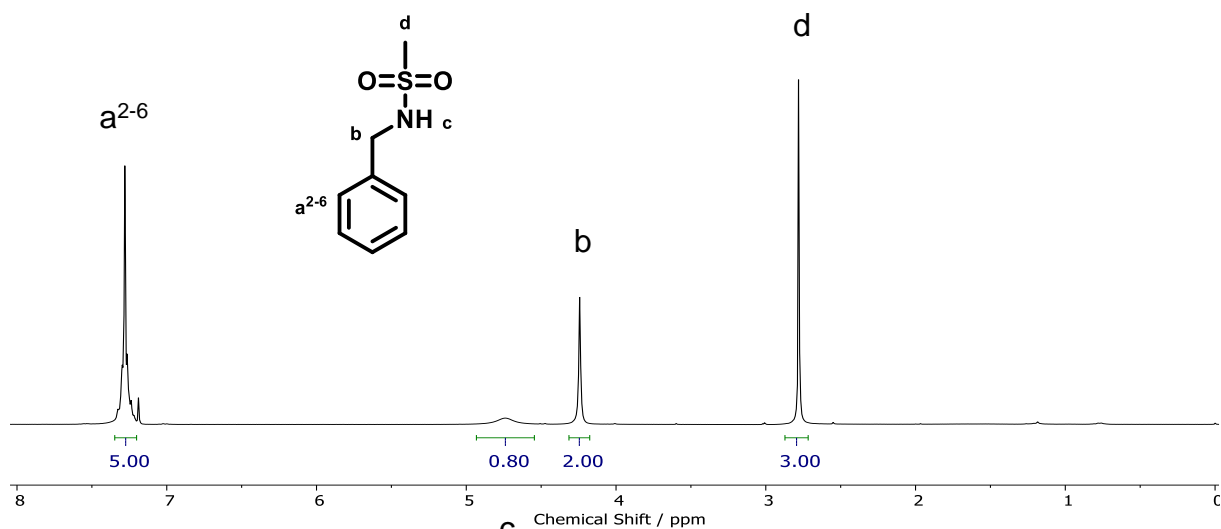
Scheme 22: Initiators for the anionic ROP of sulfonyl aziridines.

Besides BnNHMs, the novel 4-*tert*-Butylbenzylmesylsulfonamid was synthesized to further increase solubility in non-polar solvents. (Scheme 22) Both syntheses followed a known literature procedure and are one-step synthesis and yield the corresponding product as colorless crystals, which can be used without further purification. (BnNHMs yield 85%, 4-*tb*-BnNHMs yield 99%).⁴³



Scheme 23: Synthesis of BnNHMS and 4-*tb*-BnNHMS.

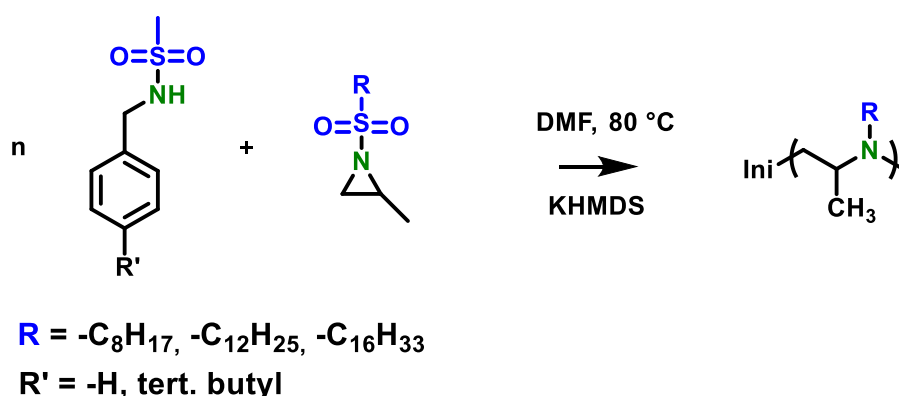
Results and discussion



The ^1H NMR of BnNHMs (Figure 13) and 4- t -b-BnNHMs (Figure 14) are comparable. In both cases, the mesyl-group is clearly visible as a singlet 2.85 resp. 2.80 ppm (s, **d**), as well as the hydrogen of the sulfonylamine -NH-group (**c**). Distinctions can be made through the -C(CH₃)₃ peak 1.23 ppm (s, **f**) and the separation of the aromatic peaks for 4- t -b-BnNHMs at 7.31 ppm (d, $J=8.0$ Hz, **a**^{2,6}) and 7.18 ppm (d, $J=7.9$ Hz, **a**^{3,5})

6.2.2 Polymerizations

Reactions were carried out in flame-dried Schlenk tubes, while all starting materials were dried with benzene at reduced pressure, with the only exception being KHMDS, which was dried overnight at reduced pressure. The dried monomers were dissolved in dry *N,N*-dimethylformamide (DMF), while the Initiator (BnNHMS) was dissolved in DMF and added to the solid KHMDS. After 1 minute, the activated Initiator was transferred into the monomer solution, which was stirred in a preheated oil bath (60-80 °C) for 12-24 h. (Scheme 24) The reaction progress was followed by ¹H NMR analysis and the polymerization terminated, when full monomer conversion was achieved; the polymer was precipitated into methanol or deionized water. As M_n and the degree of polymerization cannot be determined by GPC, the integration of the resonances of BnNHMS was used to determine DP (multiplet, **h**). As the backbone peaks are separated from each other, the real molecular weight and X_n can be calculated (eq.8).



Scheme 25: Homopolymerization.

Poly(2-methyl-*N*-octasylaziridine)

Poly(OsMAz) was the first successful synthesized polymer with a lipophilic side chain and was conducted at 80 °C overnight. The polymerization proved to be highly durable and polymers with up to 116 repeating units were achieved, while maintaining a low molecular dispersity. The yielded polymers were soluble in cyclohexane at room temperature, proving that through the modification of the activation group the solubility in non-polar solvent can be improved. Regardless of various tests, altering the degree of polymerization and the used initiator a solubility in hexane or dodecane could not be achieved at any temperature. Therefore, monomers with increasing alkyl-side chain length were synthesized and polymerized in the form of Poly(DDsMAz) and Poly(HDsMAz).

Table 4: Overview of Poly(OsMAz). M_n (NMR) given by eq. (8); M_n (GPC) and \bar{D} in DMF/PEG-standard

sample	X_n	Initiator	M_n (NMR) g/mol	M_n (GPC) g/mol	\bar{D}
P(OsMAz)	31	BnNHMs	7400	3200	1.15
P(OsMAz)	32	BnNHMs	7600	6900*	1.14
P(OsMAz)	58	BnNHMs	13700	5500	1.16
P(OsMAz)	116	BnNHMs	27100	8500	1.21
P(OsMAz)	12	^t b-BnNHMs	3000	1600	1,22
P(OsMAz)	13	^t b-BnNHMs	3500	1600	1.21

The ^1H NMR spectra of Poly(OsMAz), shows no remaining monomer signals. The polymer backbone forms in the ratio of 1:2:2 and lays around 2.84–4.24 ppm (multiplets, **e,g,d**) depending on the X_n . Further the aromatic peaks of the used initiator are seen at 7.50 –7.30 (m, **h**). (Figure 15)

The GPC traces of various Poly(OsMAz) samples with different degree of polymerization ranging from X_n 31 to X_n 116. (Figure 16) As expected, the elution volume decreases with increasing molecular weight and the GPC traces show a narrow and monomodal distribution which is reflected in the low dispersity ranging from 1.14 to 1.21, which shows a detection to higher elution volume.

Results and discussion

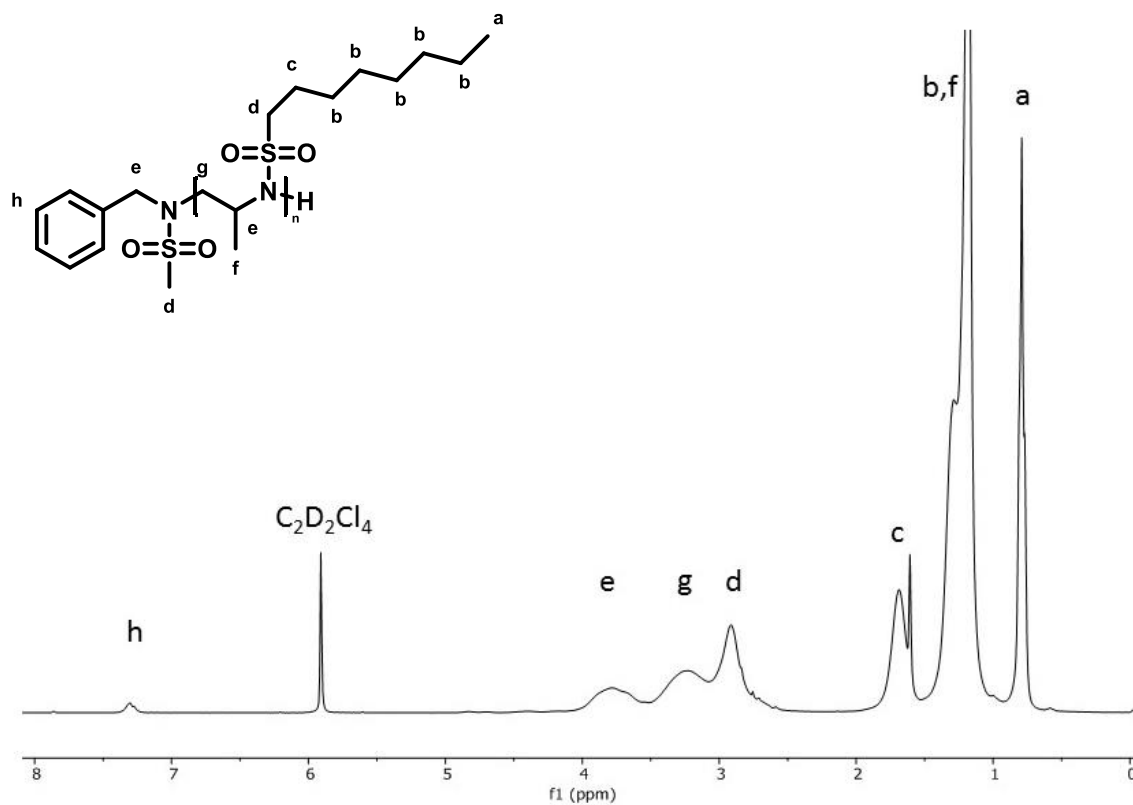


Figure 15: ^1H NMR (300 MHz, tetrachloroethane- d_2) of Poly(2-methyl-*N*-octasylaziridine).

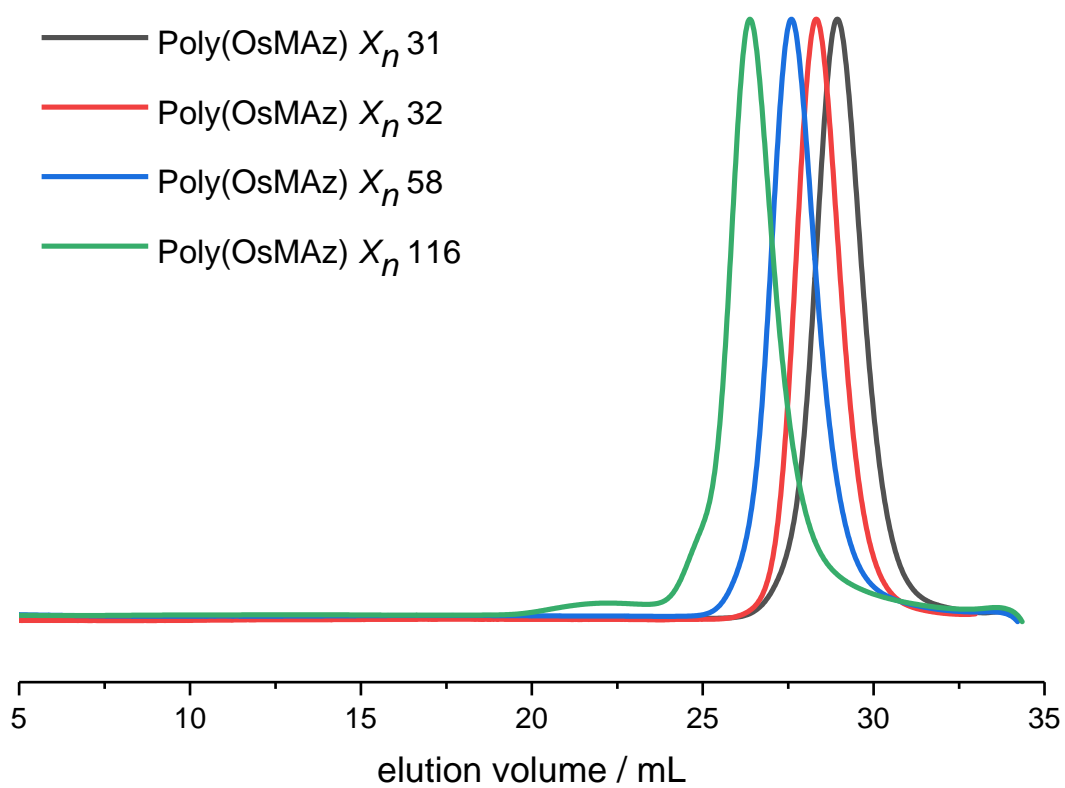


Figure 16: GPC traces (RI detection) of Poly(2-methyl-*N*-octasylaziridine) in DMF.

Poly(2-methyl-*N*-dodesylaziridine) and Poly(2-methyl-*N*-hexadecasyaziridine)

Following the successful polymerization of Poly(OsMAz), Poly(DDsMAz) and Poly(HDsMAz) was synthesized. It was observed that in both polymerizations after initiation a turbidity of the solution occurred and that the corresponding monomer DDsMAz and HDsMAz only dissolved in DMF over time. As mentioned before DMF or DMSO are highly polar solvents and in the case of AAROP necessary for a successful polymerization but stand in contrast to the increasingly non-polar monomer and polymer alkyl-side chains. While OsMAz and its product Poly(OsMAz) were still soluble in DMF, DDsMAz and HDsMAz only dissolved over time and after initiation a rapid turbidity of the solution was observed which led to the formation of a suspension. Nevertheless, the chain end was still active and full monomer conversions were achieved. It can be argued that in relation to a surfactant, the non-polar sidechain aligns towards each other, while the polar sulfonyl amine backbone remained in contact with the polar solvent and consequently enabled a polymerization.

Regardless the polymerizations were successful leading to a full conversion and low molecular dispersity. The solubility was further increased due to the fact that contrary to Poly(OsMAz), Poly(DDsMAz) and Poly(HDsMAz) were soluble in non-polar dodecane under heating but precipitates under cooling again.

Table 5: Overview of successful polymerized Poly(2-methyl-*N*-dodesylaziridine) (DDsMAz). M_n (NMR) given by eq. (8); M_n (GPC) and \bar{D} in THF/PS-standard

sample	sample number	X_n	Initiator	M_n (NMR) g/mol	M_n (GPC) g/mol	\bar{D}
P(DDsMAz)	TK100	48	BnNHMs	14000	8600	1.10
P(DDsMAz)	TK102	102	BnNHMs	29700	14400	1.12

Results and discussion

Table 6: Overview of successful polymerized Poly(2-methyl-*N*-hexadecasylaziridine) Poly(HDsMAz). M_n (NMR) given by eq. (8); M_n (GPC) and \mathcal{D} in THF/PS-standard

sample	X_n	Initiator	M_n (NMR) g/mol	M_n (GPC) g/mol	\mathcal{D}
P(HDsMAz)	12	BnNHMs	4332	3762	1,15
P(HDsMAz)	15	BnNHMs	5369	4620	1.15
P(HDsMAz)	32	BnNHMs	11244	7485	1,26
P(HDsMAz)	35	BnNHMs	12281	-	-

The ^1H NMR spectra of Poly(DDsMAz) and Poly(HDsMAz) are comparable to Poly(OsMAz), the polymers have nearly identical shifts due to their comparable structure and follow the before explained pattern. While the aziridine signals of the monomer decreases the polymer backbone forms in the ratio of 1:2:2 (multiplets, **e,g,d**) and lays around 2.8 –4.3 ppm depending on the X_n . (Figure 17, 18) The only significant difference lays in the peak ratio between the polymer backbone (multiplets, **e,g,d**) and the alkyl side chain 1.47–1.02 ppm (multiplet **b,f**), which decreases due to the increasing alkyl chain length.

The GPC traces of Poly(DDsMAz) for two samples with different degree of polymerization X_n 48 and X_n 102 are shown and have a very narrow monomodal distribution, which is reflected in the low dispersity with 1.10 (X_n 48) and 1.12 (X_n 102). (Figure 19)

The GPC traces Poly(HDsMAz) shows three different samples with various degree of polymerization ranging from X_n 12 to X_n 32. (Figure 20) The GPC traces show a monomodal distribution, dispersity ranging from 1.15 (X_n 12) to 1.26 (X_n 32). The polymerization of X_n 32 was a batch synthesis of over 10 grams showing the possible upscaling of the polymerization.

Results and discussion

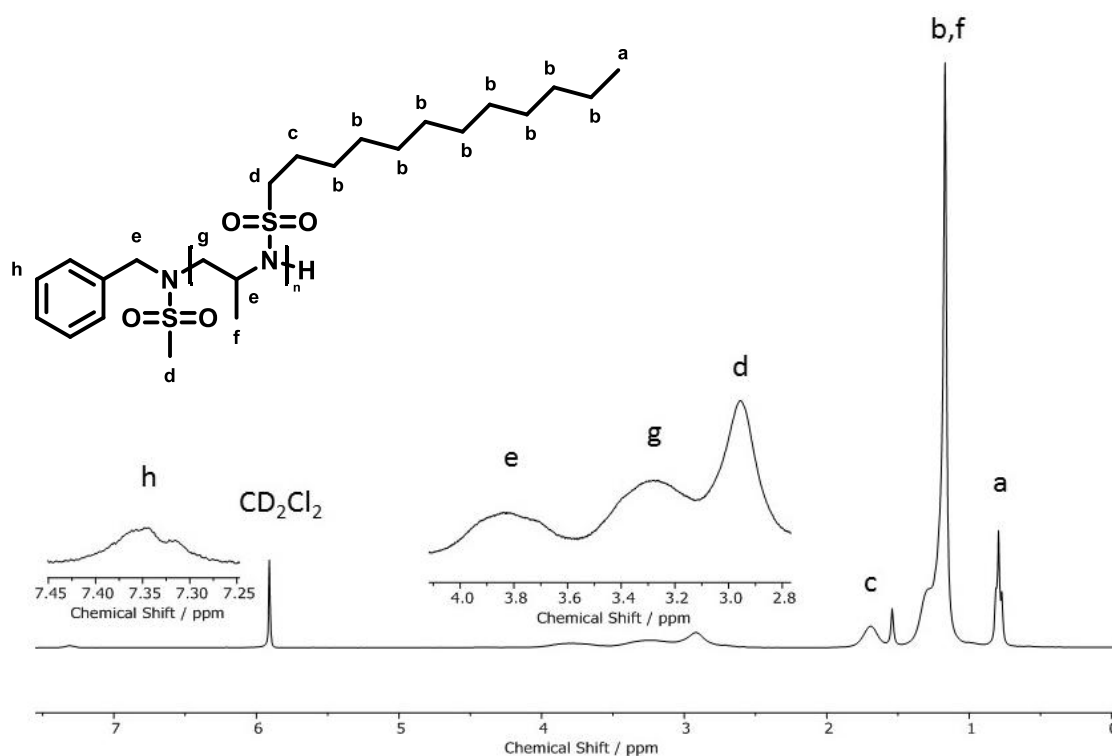


Figure 17: ^1H NMR (300 MHz, tetrachloroethane- d_2) of Poly(2-methyl-N-dodecylaziridine) Poly(DDsMAz).

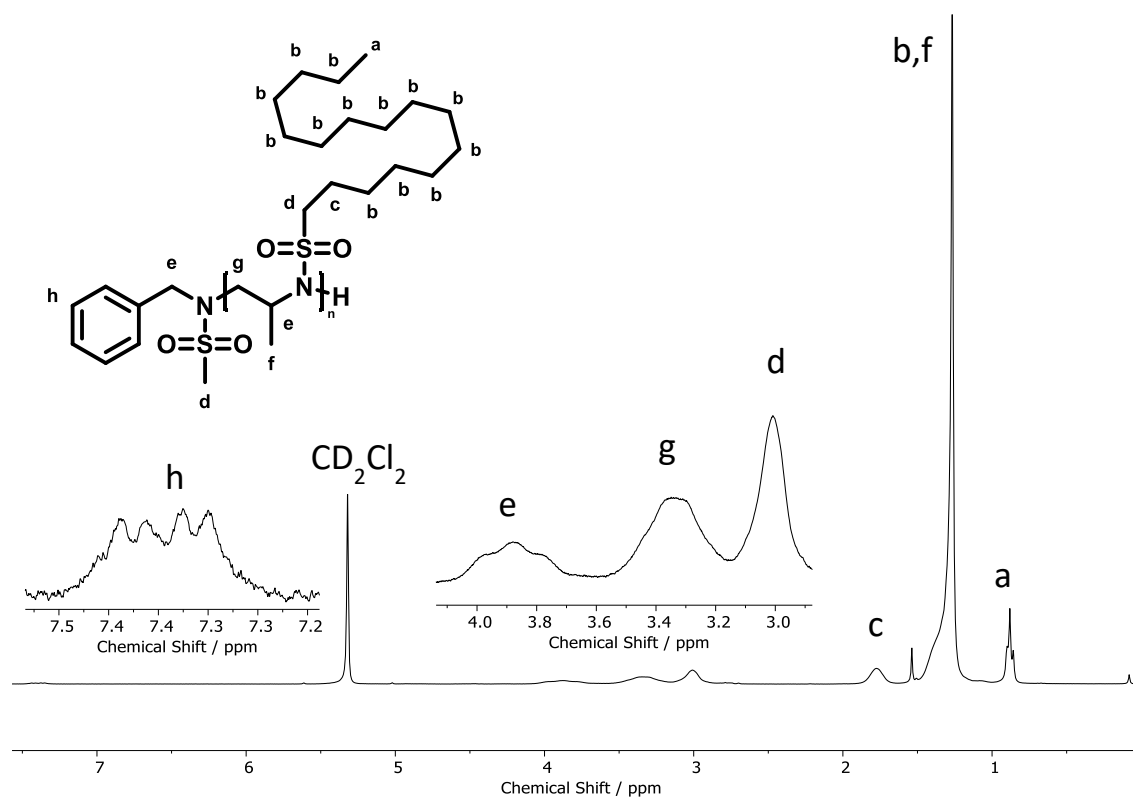


Figure 18: ^1H NMR (300 MHz, Methylene Chloride- d_2) of Poly(2-methyl-N-hexadecylaziridine) Poly(HDsMAz).

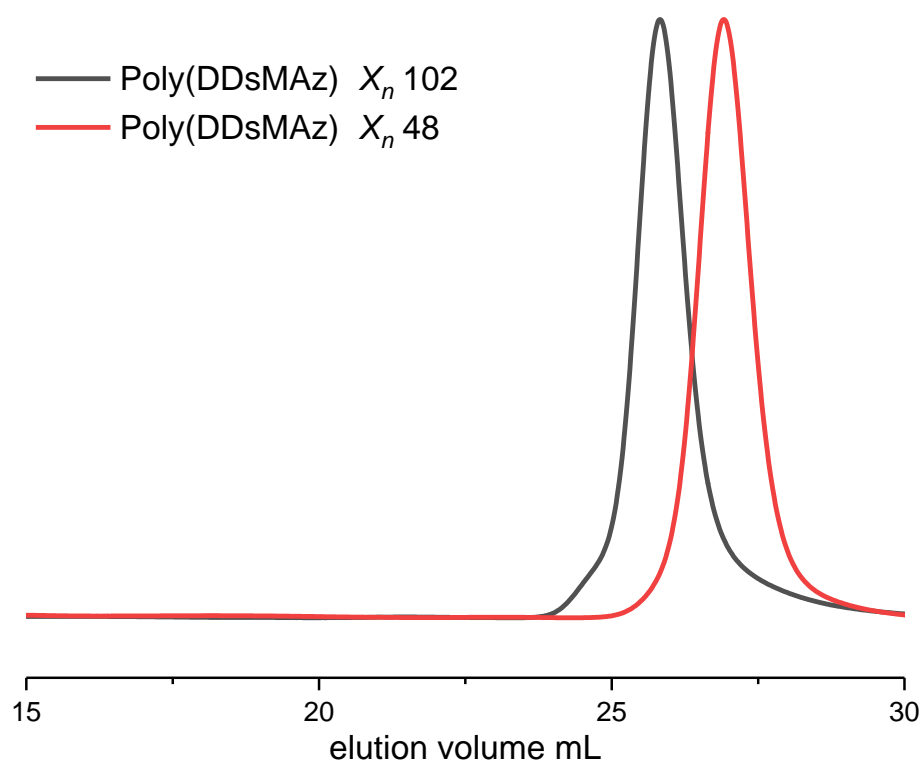


Figure 19: GPC traces (RI detection) of Poly(2-methyl-*N*-dodecylaziridine) (Poly(DDsMAz)) in THF.

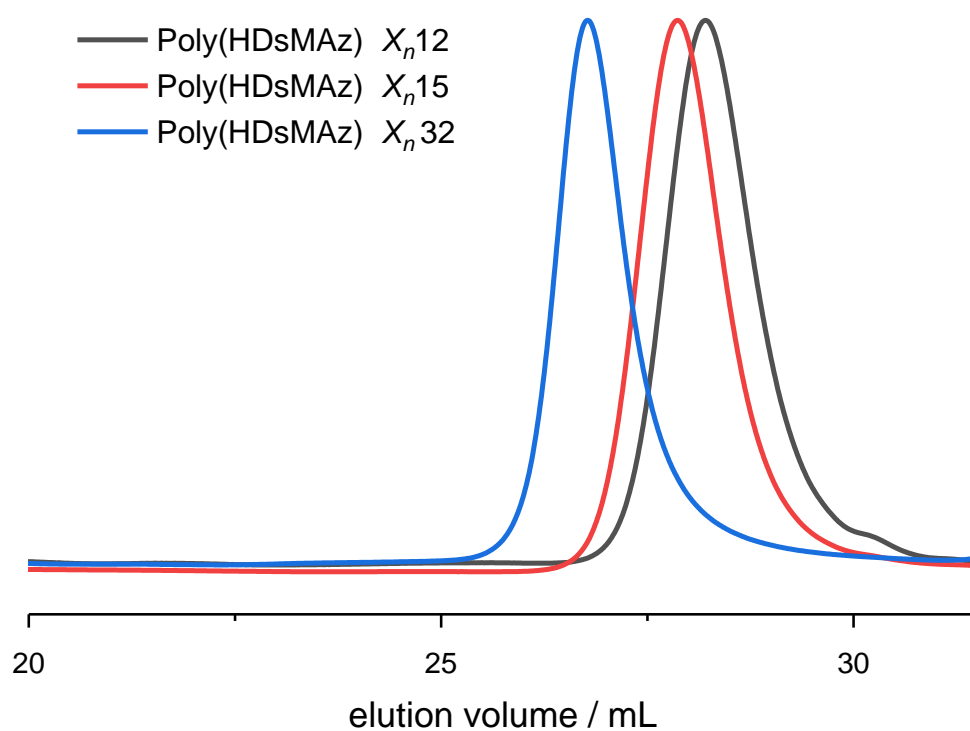


Figure 20: GPC traces (RI detection) of Poly(2-methyl-*N*-hexadecylaziridine) (Poly(HDsMAz)) in THF.

Poly((2-(cyclohexylmethyl)-N-mesylaziridine))

Table 7: Overview of successful polymerized Poly(2-(cyclohexylmethyl)-N-mesylaziridine) Poly(MsCyhexAz). M_n (NMR) given by eq. (8); M_n (GPC) and \bar{D} in DMF/PEG-standard

sample	X_n	Initiator	M_n (NMR) g/mol	M_n (GPC) g/mol	\bar{D}
P(MsCyhexAz)	26	BnNHMs	5800	1800	1.15

The ^1H NMR of Poly(MsCyhexAz) shows an increased backbone ratio to 1:2:3 due to the CH_3 -mesyl group (multiplets **e,g,d**). Furthermore, the sterically demanding cyclohexylmethyl-group peaks overlap between 1.34–0.69 ppm (**multiplet, b**). (Figure 21) The polymerization itself was conducted over 4 days as a first ^1H NMR indicated a not completed conversion.

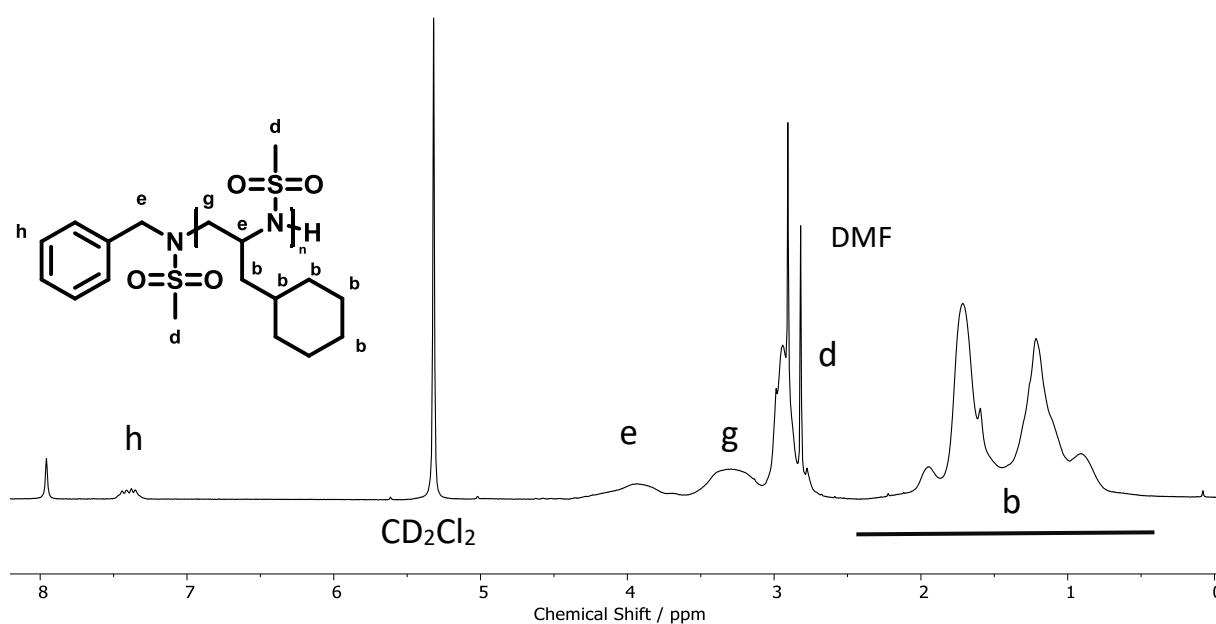


Figure 22: ^1H NMR (300 MHz, Methylene Chloride- d_2) Poly(2-(Cyclohexylmethyl)-N-mesylaziridine) Poly(MsCyhexAz).

The GPC trace of Poly(MsCyhexAz) has a monomodal distribution. The GPC traces shows a detection an around 20 mL. (Figure 23)

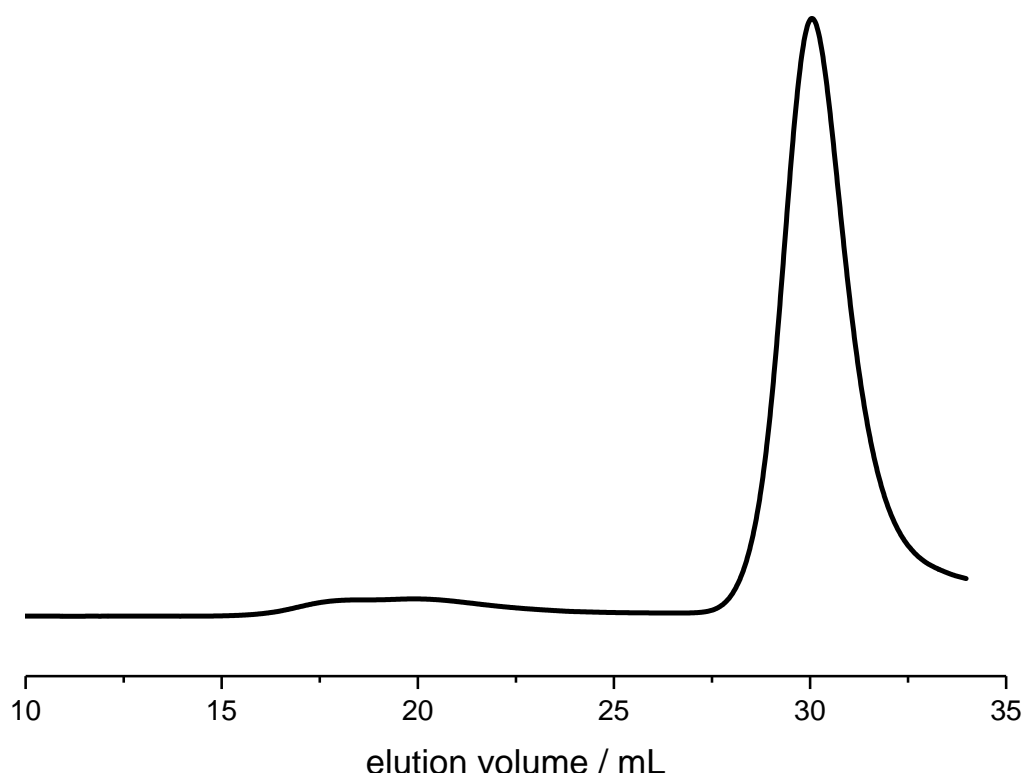


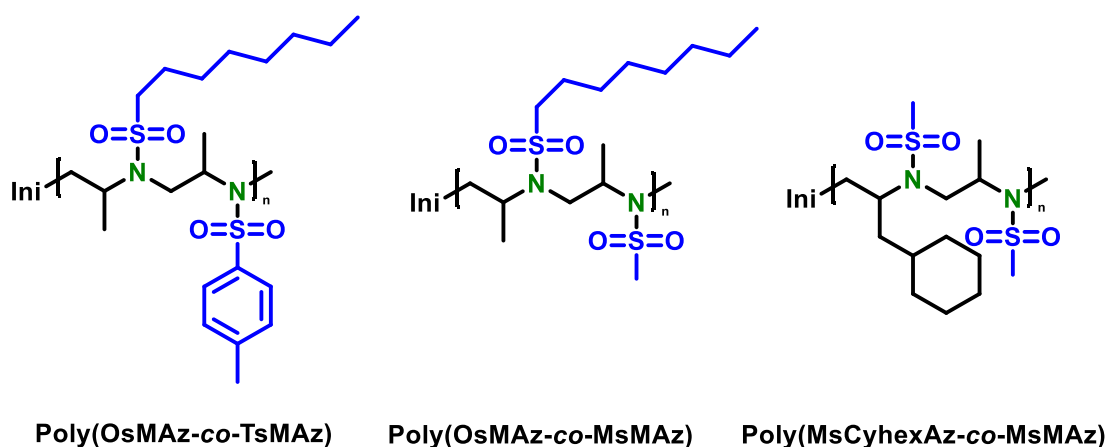
Figure 23: GPC traces (RI detection) of Poly(2-(cyclohexylmethyl)-*N*-mesylaziridine) Poly(MsCyhexAz) in DMF.

To Summarize, ^1H NMR and GPC analysis prove that the synthesis of Poly(sulfonyl aziridines) with lipophilic side chains were successful. Through ^1H NMR a full conversion after 12 hours could be confirmed even in the presence of hexadecasy-side chains without termination. The GPC furthermore proves a monomodal distribution and therefore a simultaneous chain growth. Through the use of lipophilic AG a solubility in cyclohexane was achieved for all 3 polymers, while Poly(DDsMAz) and Poly(HDsMAz) were soluble in dodecane under heating. Poly(MsCyhexAz) in contrary was insoluble in non-polar solvent. It can be assumed that due to the polar sulfonyl aziridine backbone the polymer starts to aggregate to minimize contact between solvent and the polymer backbone. The lipophilic sidechains improve the solubility but cannot negate the effect of the polymer backbone.

6.3 Copolymerization

As Poly(OsMAz) was soluble in cyclohexane at room temperature various copolymers were synthesized to analyze if the incorporation of OsMAz in copolymers still enables a solubility in non-polar solvent. As expected, the copolymerization of OsMAz with MsMAz decreased solubility, although Poly(OsMAz-co-MsMAz) in a ratio of 3:1 was soluble in cyclohexane (10 mg/mL). Further a copolymer of MsCyhexAz and MsMAz was synthesized as it was suspected that the steric hindrance of the cyclohexylmethyl-group lowered the propagation rate and solubility

Therefore, a real time ^1H NMR analysis was used to conduct a kinetic study of Poly(OsMAz-co-MsMAz), Poly(OsMAz-co-TsMAz), Poly(MsCyhexAz-co-MsMAz). The resulting copolymerization diagram, copolymerization parameter and gradient are shown below.



Scheme 26: Synthesized Copolymers.

All polymerization followed the same execution as used for the homopolymerization, i.e. the polymerizations were conducted at 80 °C under Schlenk conditions in DMF with BnNHMs/KHMDs as the initiator system. The monomers were weighed and dissolved separately in benzene but combined before freeze-drying.

Results and discussion

Table 8: Overview of all synthesized copolymers and their ratios. M_n (NMR) given by eq. (8); M_n (GPC) and \mathcal{D} in DMF/PEG-standard

sample	ratio	X_n	M_n (NMR) g/mol	M_n (GPC) g/mol	\mathcal{D}
P(OsMAz-co-MsMAz)	1:1	30	5700	3000	1.15
P(OsMAz-co-MsMAz)	3:1	33	7100	3800	1.11
P(OsMAz-co-MsMAz)	1:3	20	3500	2000	1.14
P(MsCyhexAz-co-MsMAz)	1:1	25	4600	2100	1.22

Poly(OsMAz-co-MsMAz)

Poly(OsMAz-co-MsMAz) was synthesized in three different ratios.(Table 8) In the ^1H NMR the aromatic peaks are visible at 7.55-7.23 ppm (multiplet, **h**). The only visible difference to the *homo*-polymer of Poly(OsMAz) lays in the third polymer backbone peak, at 3.13-2.86 ppm (multiplet, **d**) shows two slightly separated peaks for the CH_3 -mesyl group and the CH_2 -octasyl group. (Figure 24)

The GPC have a very narrow monomodal distribution and the dispersity lays below $\mathcal{D} \leq 1.15$. As to be expected, the ratio of monomer has an impact on the elution volume. A high amount of OsMAz in the polymer, shifts elution to a lower volume due to its increasing hydrodynamic radius. (Figure 25)

Results and discussion

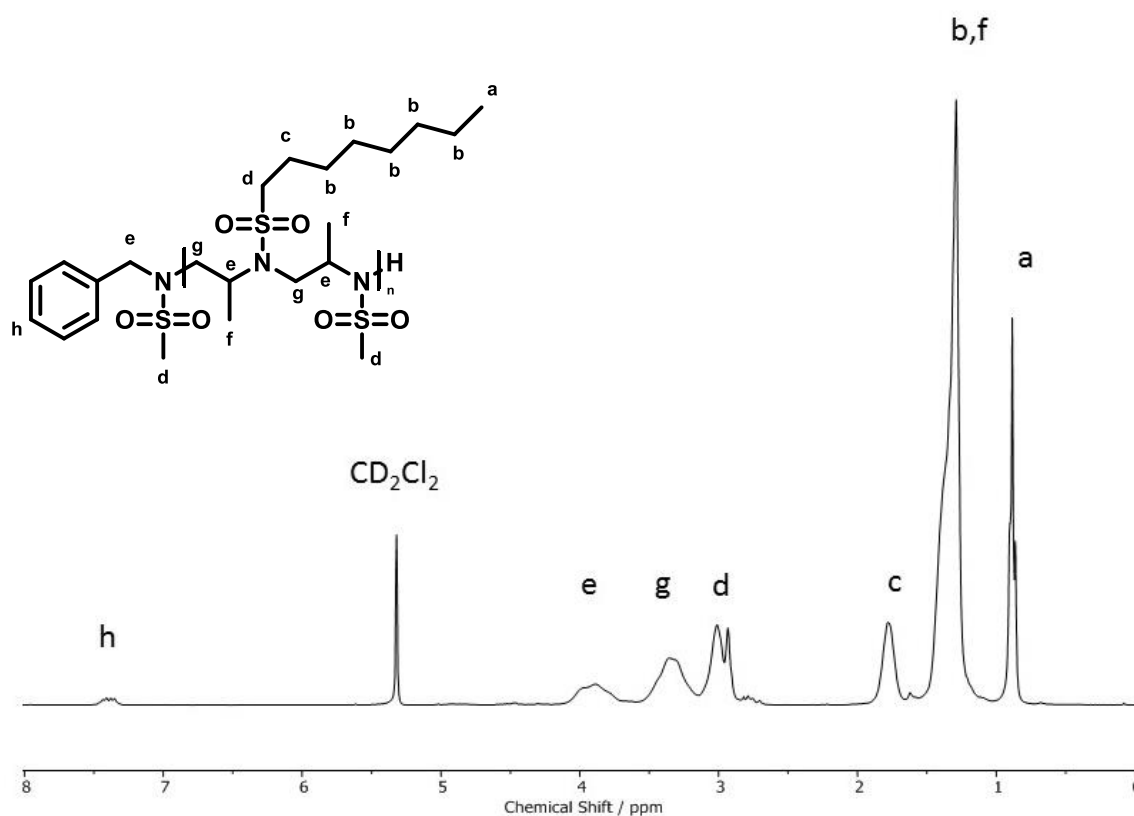


Figure 24 ^1H NMR (300 MHz, Methylene Chloride- d_2) of Poly(OsMAz-co-MsMAz).

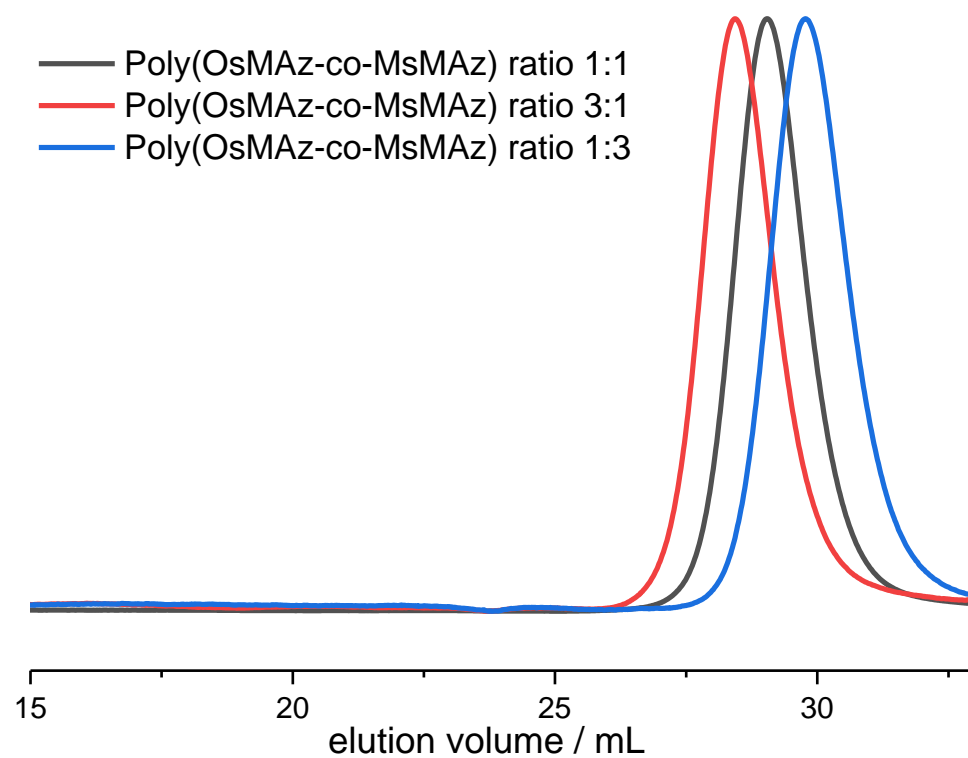


Figure 25: GPC-traces (RI detection) of Poly(OsMAz-co-MsMAz) in different ratios in DMF.

Poly(Cyhex-co-MsMAz)

In the ^1H NMR of Poly(OsMAz-co-MsMAz) the sterically demanding cyclohexylmethyl-side chain overlays between 1.98 – 0.72 ppm and overlays with the methyl group (f) of the MsMAz monomer (multiplet, **b,f**). Further the polymer backbone follows the ratio 1:2:3 due to the CH_3 -mesyl group (multiplets **e,g,d**). (Figure 26)

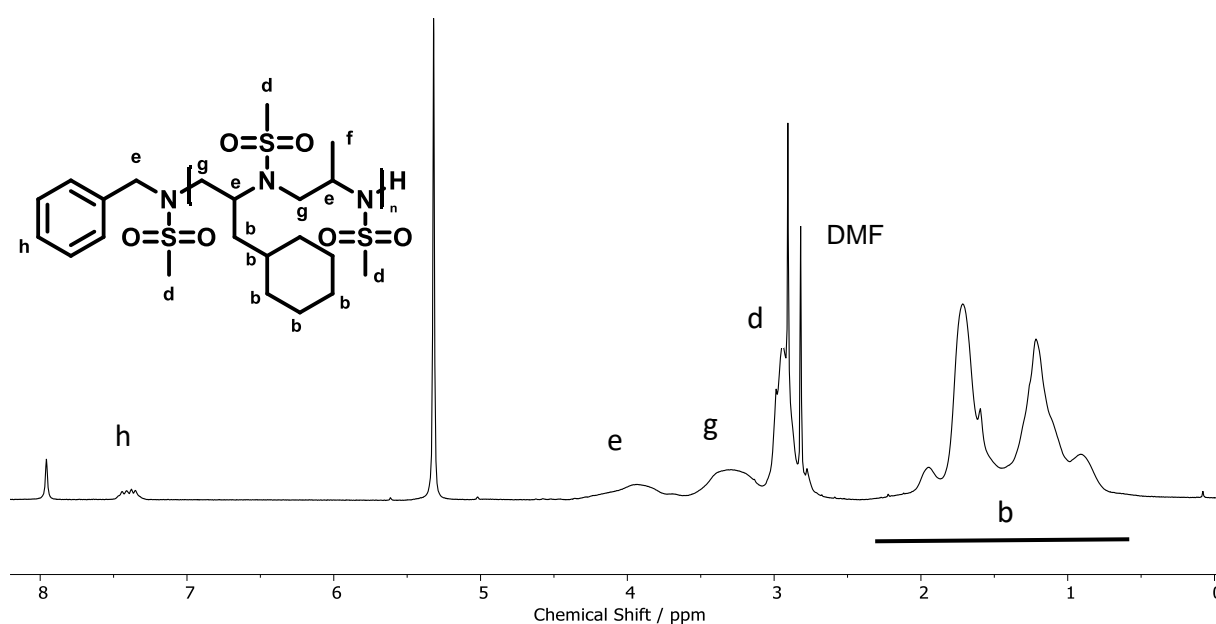


Figure 26: ^1H NMR (300 MHz, $\text{DCM}-d_2$) of Poly(Cyhex-co-MsMAz).

In the GPC-traces of Poly(Cyhex-co-MsMAz) shows a monomodal distribution with a \bar{D} of 1.22. (Figure 27) Further, the GPC shows no sign of a second peak or shoulders therefore a successful co-polymerization can be assumed.

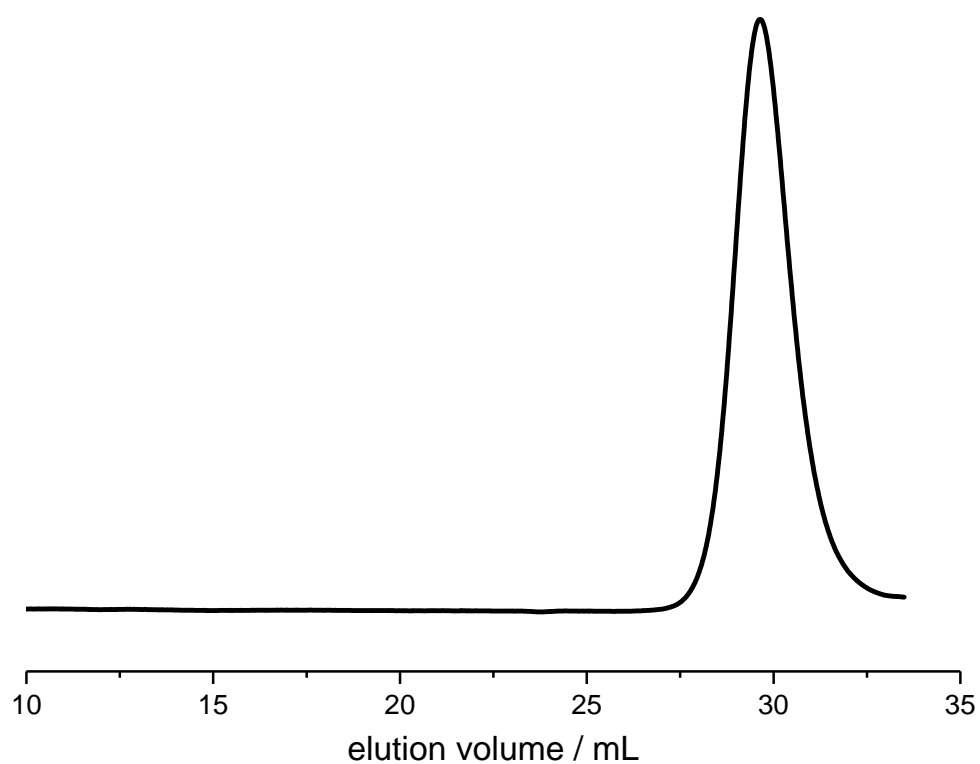


Figure 27: GPC-traces (RI-detection) of Poly(MsCyhexAz-co-MsMAz).

6.4 ^1H NMR kinetics

As shown by Rieger *et al.*³⁵, the kinetic behavior and speed of propagation is, in the case of activated aziridines highly dependent on the $-I$ -effect of the activation group and with the synthesis of novel alkyl chain activation groups, an expansion of the aziridine monomer family was achieved. Monomers with a strong electron withdrawing effect like a tosyl-group have a faster propagation rate. In the case of a copolymerization the different AG determine the copolymerization parameter and the monomer distribution in the synthesized copolymer. By choosing, a combination of different AG the copolymer microstructure is adjustable with soft or hard gradient depending directly on the difference of the EWD-effect.

For the execution the polymerization was conducted in a flame-dried NMR-tube. All educts as well as BnNHMs were dissolved in benzene and dried for at least 3 hours. After drying of all components, the monomers were dissolved in 0.5 ml deuterated DMF- d_7 and transferred into the prepared NMR-tube and sealed under argon with a septum. Before initiation with 0.1 ml BnNHMs/KHMDS DMF- d_7 solution, a ^1H NMR was measured to show the monomer composition. After initiation, of the reaction mixture a series of NMR experiments (real-time ^1H NMR spectroscopy) were taken at 50 °C, 200 experiments, with 16 scans each at 700 MHz (Appendix 12.5 ^1H NMR Kinetik). After polymerization, additional GPC was used to analyze the copolymers.

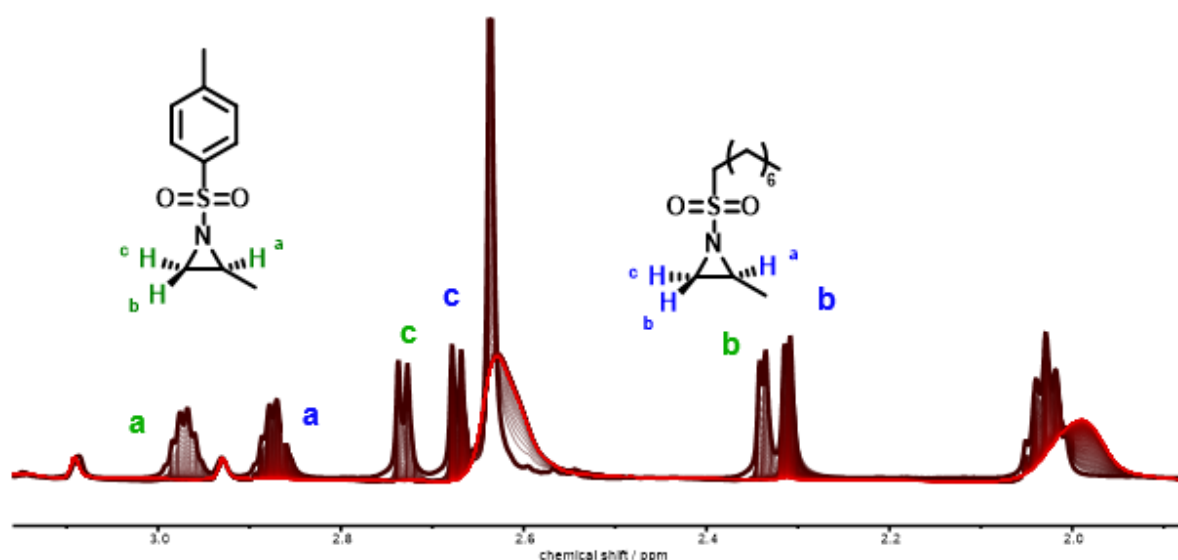


Figure 28 ^1H NMR (700 MHz, DMF- d_7) of Poly(OsMAz-co-TsMAz).

Figure **28** shows all ^1H NMR of Poly(OsMAz-co-TsMAz) after initiation and the significant ring protons as they decrease over time. In the shown ^1H NMR the typical aziridine pattern can be assigned to the corresponding monomers. The pattern consists of a multiplet (**a**) and two duplets (**b,c**). These peaks possess different shifts for each monomer, due to different side chains and activation groups. As the ratio is known, the peaks can be integrated. Through the aza-AROP the aziridine monomer peaks decrease after initiation by time and can be evaluated through peak integration over all ^1H NMRs.

This process was repeated for the copolymerization of Poly(MsCyhexAz-co-MsMAz). In both cases, the data were used to not only plot the monomer conversion but also calculate the copolymerization parameters by the methods Jaacks and Meyer-Lowry.^{40,41} A kinetic study of Poly(OsMAz-co-MsMAz) was not possible due to overlapping peaks of the different ring protons.

Poly(OsMAz-co-TsMAz)

Through the introduction of novel lipophilic activation groups, the reactivity can be ranged in with the reactivity's of other aziridine monomers. As the reactivity is a result of the -I effect of sulfonyl group the novel activation groups possessing a long alkyl chain have a very low propagation rate and have therefore stronger gradients in copolymerization's. Further due to the length of the alkyl chains lipophilic activation groups could have the lowest incorporation rates of all know sulfonyl aziridine monomers. Therefore, a kinetic study of Poly(OsMAz-co-MsMAz) was conducted but could not be analyzed as the peaks, contrary to Poly(OsMAz-co-TsMAz) perfectly overlapped (Appendix **12.5** ^1H NMR Kinetik, Figure **138**) and an integration of the peaks decline was not possible. Consequently, a kinetic study of the polymerization Poly(OsMAz-co-TsMAz) was conducted.

Results and discussion

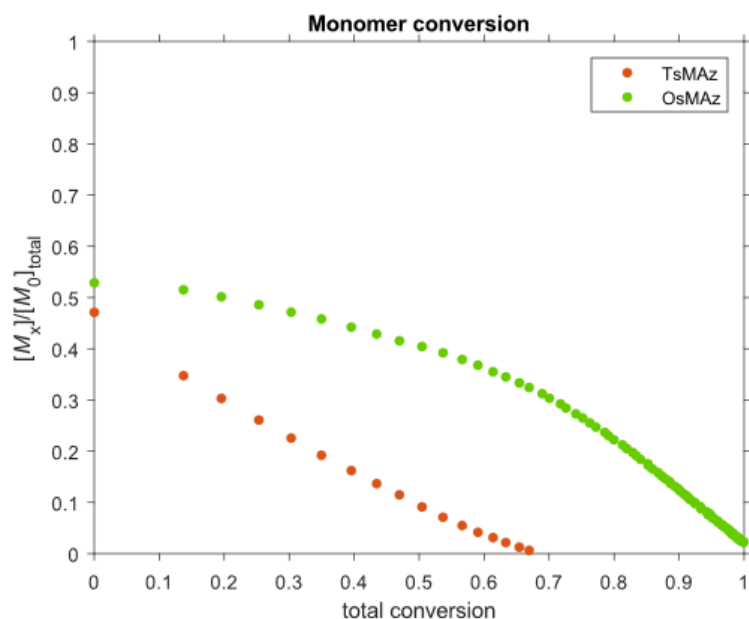


Figure 29: Monomer conversion of OsMAz (orange) and TsMAz (green) vs the total conversion.

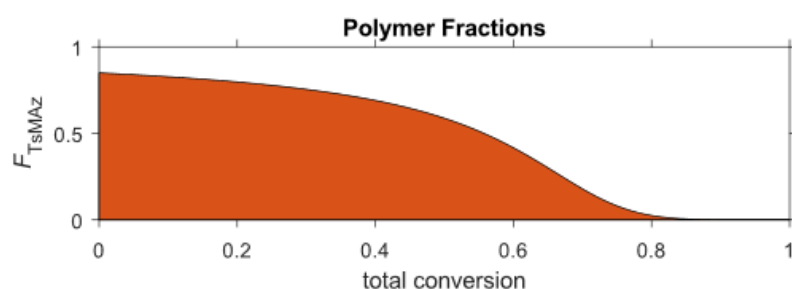


Figure 30: mole fraction of the incorporated TsMAz (orange) vs the total conversion.

TsMAz is incorporation faster into the polymer than OsMAz. (Figure 29) This was to be expected, due to the stronger electron withdrawing effect of the tosyl-AG. The TsMAz incorporation in the polymer lays by over 80 % in the beginning of the polymerization and slowly decreases, after a conversion of around 80% the polymer starts to consist of a pure OsMAz backbone. (Figure 30) This can also be seen as the slope of OsMAz increases due to *homo*-polymerization. (Figure 29) The copolymerization diagram is shown, and the copolymerization parameters are calculated (Table 9; Figure 31). As the copolymerization parameter are given by the division of the propagation rate of the homopolymerization through the propagation rate for the incorporation of a co-monomer.

Results and discussion

A high r -parameter indicates that the active chain end will likely react with a monomer of the same species, while a low r -parameter smaller than one, shows a high probability to incorporate a different monomer.

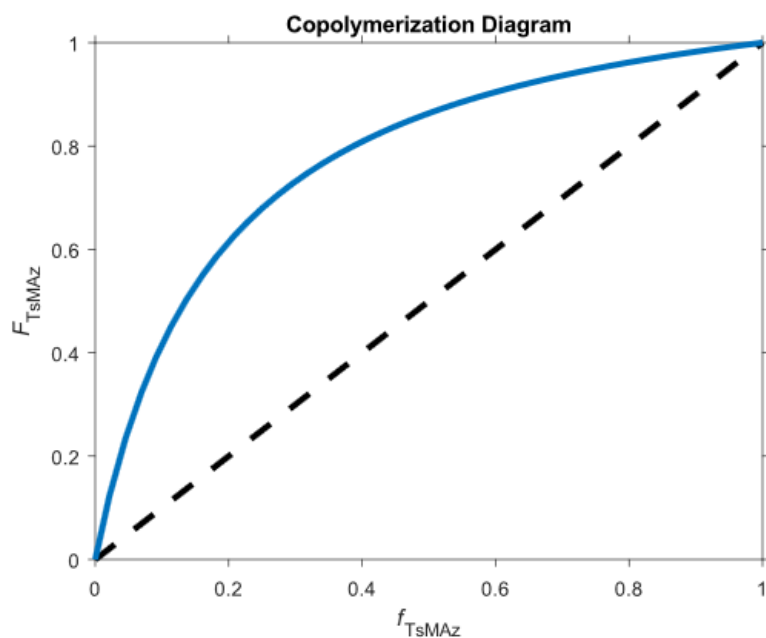


Figure 31: Copolymerization diagram of Poly(OsMAz-co-TsMAz).

Table 9: Calculated r -parameter for the copolymerization of Poly(OsMAz-co-TsMAz).

Methods	r_{TsMAz}	r_{OsMAz}	$r_{\text{TsMAz}} * r_{\text{OsMAz}}$
Meyer-Lowry	6.31	0.15	0.97
Jaacks	6.18	0.16	0.99

Poly(MsCyhexAz-co-MsMAz)

Although MsCyhexAz does not possess a new AG, a kinetic study was conducted as it was observed that the propagation of the homopolymerization was much slower than the copolymerization with MsMAz. As the used AGs for both monomers are the same, the incorporation is only defined by the substituent. Therefore, the kinetic measurement was conducted as it was hoped to gain excess to a more alternating structure in which the incorporation is determinate by the steric hindrance of the cyclohexylmethyl-group.

The monomer conversion for the copolymerization of Poly(MsCyhexAz-co-MsMAz) deviation from the polymerization of Poly(OsMAz-co-TsMAz). (Figure 32)

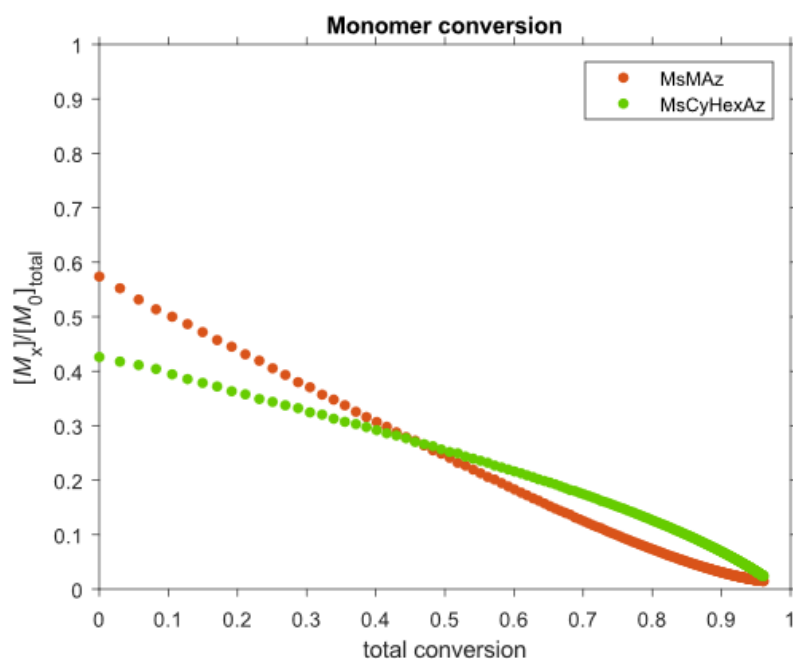


Figure 32: Monomer conversion of MsMAz and MsCyhexAz vs the total conversion.

The MsMAz is incorporated faster but in a significantly lower rate than for the copolymerization of Poly(OsMAz-co-TsMAz). As the Monomer conversion and polymer incorporation (Figure 32/33) as well as the copolymerization diagram (Figure 34) show the copolymerization is close to a statistic copolymerization. Therefore, it can be concluded that the sterically hindrance of the MsCyhexAz has only a slight effect on the copolymerization and the polymers micro structure.

Results and discussion

The copolymerization of OsMAz or HDsMAz with MsCyhexAz would be an interesting possibility, as the homopolymerization of OsMAz/HDsMAz is slower than for MsMAz and therefore allows a more ideal statistic copolymerization.

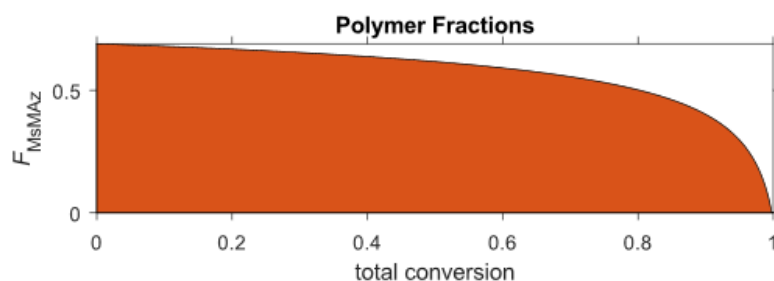


Figure 33: mol-fraction of the incorporated MsMAz vs the total conversion.

Table 10: calculated r-parameter for the co-polymerization of poly-(MsCyhexAz-co-MsMAz).

Methods	r_{MsMAz}	$r_{\text{MsCyHexAz}}$	$r_{\text{MsMAz}} * r_{\text{MsCyHexAz}}$
Meyer-Lowry	1.52	0.50	0.76
Jaacks	1.70	0.59	1.00

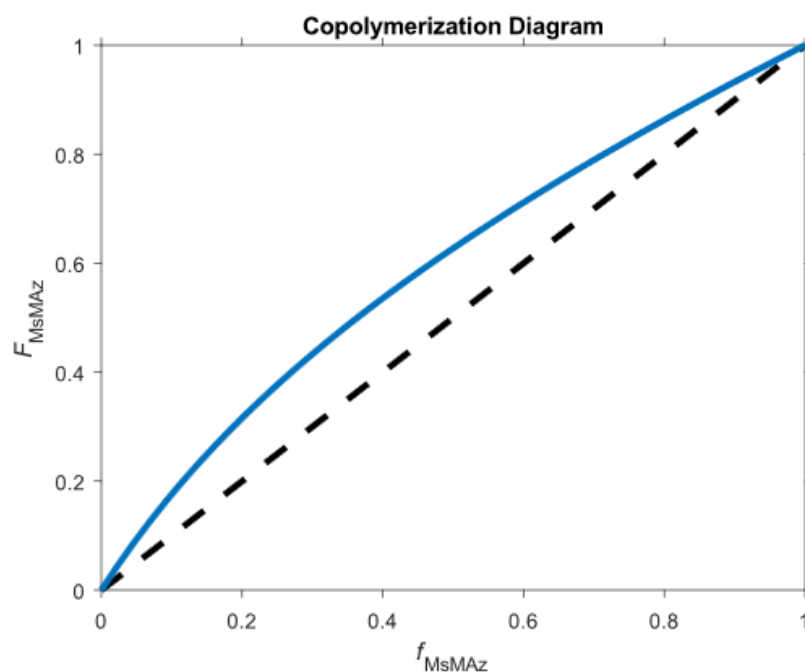


Figure 34: Copolymerization diagram of Poly(MsCyhexAz-co-MsMAz).

6.5 Solubility assay

To quantify the solubility of the synthesized lipophilic polymers a solubility assay in cyclohexane and dodecane was conducted. Therefore 10 mg of each polymer were diluted in 1 mL of solvent.

The polymer was considered to be dissolved if the solution remained transparent after mixture and no turbidity or precipitation occurred over time.

The first polymerized OsMAz was easily dissolved in cyclohexane at room temperature and was seen as a first success as no turbidity occurred over time. But a following test in dodecane was not successful even at higher temperature. Therefore, the length lipophilic side chain was increased in the form of Poly(DDsMAz) and Poly(HDsMAz). In both cases the polymers were soluble in cyclohexane and could be dissolved in dodecane under heating ($\Delta T \approx 80\text{ }^{\circ}\text{C}$) but started to precipitate after a short period of time leading to a turbidity solution. Through the increased lipophilic side chains the solubility in non-polar solvent was increased from Poly(OsMAz) over Poly(DDsMAz) to Poly(HDsMAz) but no stable solubility in dodecane was achieved. (Table 11)

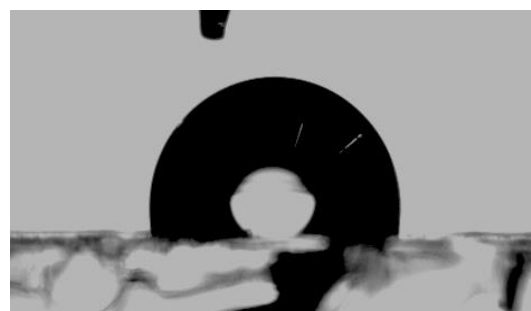
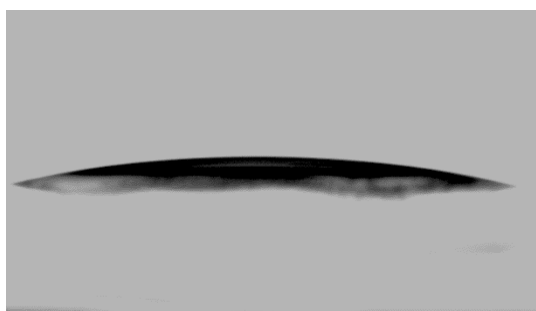
Further tested polymers included the copolymer Poly(OsMAz-co-MsMAz), which was soluble in cyclohexane at a ratio of 3:1 and Poly(MsCyhexAz) as well as Poly(MsCyhexAz-co-MsMAz) which both were insoluble in non-polar solvent.

Table 11: Solubility assay of synthesized Polymers with (10mg/mL)

Polymer	cyclohexane (π)	Dodecane (ΔT)
Poly(OsMAz)	✓	—
Poly(DDsMAz)	✓	✓
Poly(HDsMAz)	✓	✓
Poly(OsMAz-co-MsMAz)	✓	—
Poly(MsCyhexAz)	—	—
Poly(MsCyhexAz-co-MsMAz)	—	—

6.6 Contact angle measurements

To quantify the hydrophobicity of the synthesized Poly(sulfonyl aziridine)s a contact angle measurement series on glass microscopy slides was conducted. Therefore, the slide was coated with the polymers and the contact angles of a water droplet were measured. On an uncoated hydrophilic glass surface, a water droplet expands on the surface, leading to a small contact angle, (Figure 35) while the coated surface (PolyHDsMAz X_n 30, 1.0 wt. %) is hydrophobic and the contact area between droplet and coating is less favorable, leading to a minimizing of the surface area. (Figure 36)



To prepare the coated microscope slide, the slides were cleaned and ionized through argon-plasma. Due to the ionization the glass surface becomes hydrophilic and the adhesion of the Poly(sulfonyl aziridine)s backbone is increased.

To measure the influence of concentration, X_n and the different polymers on the contact angle eight different polymer solutions were prepared as coatings in 1 mL DCM (Table 12). The prepared polymer solutions did not visibly differ in their viscosity. The coating was conducted *via* spin coating. After the spin-coating process, the glass slides remained colorless and transparent. The black markings are artificial for location purpose under the microscope. (Figure 38) The contact angles were measured 5 times for each sample with water droplets (5 μ L) on varying positions and both angles (left and right) were recorded. (Appendix Contact angle measurement 12.1)

Table 12: Overview over used polymer solutions in DCM for spin coating.

Name	Concentration	X_n	Layer thickness <i>nm</i>
HDsMAz	0.5 wt. %	30	39±2
HDsMAz	1.0 wt. %	30	127±2
HDsMAz	2.0 wt. %	30	252±14
HDsMAz	1.0 wt. %	15	77±1
HDsMAz	1.0 wt. %	60	127±2
DDsMAz	1.0 wt. %	30	106±5
OsMAz	1.0 wt. %	30	105±5
MsMAz	1.0 wt. %	30	118±3

To prove the formation of a homogeneous film, the layer thickness was measured with a profile stepper. Therefore, the coating was partly removed from the microscope slide and the depth measured with a cantilever along one axis (Figure 37). The average values of three traces-sections were used to calculate the coating thickness.

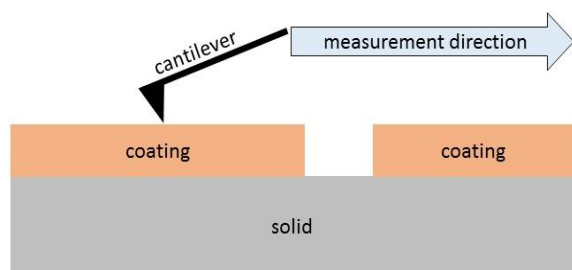


Figure 37: illustration of a layer thickness measurement through a cantilever.

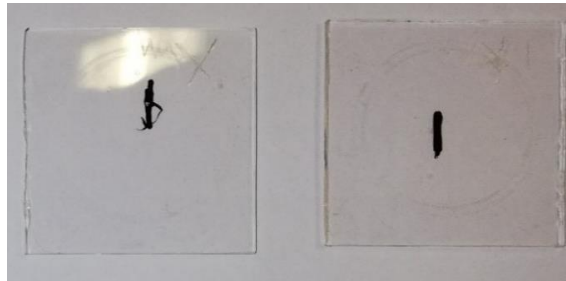


Figure 38: coated microscope slides on white paper. Black line for location purpose under the microscope.

In the measured surface profile of Poly(HDsMAz) X_n 60 it can be seen that the surface is homogeneous, while the coating is partly removed. (Figure 39) As the layer thickness was measured after the contact angle measurements, some coated surfaces show deposits on the surface and are therefore inhomogeneous.

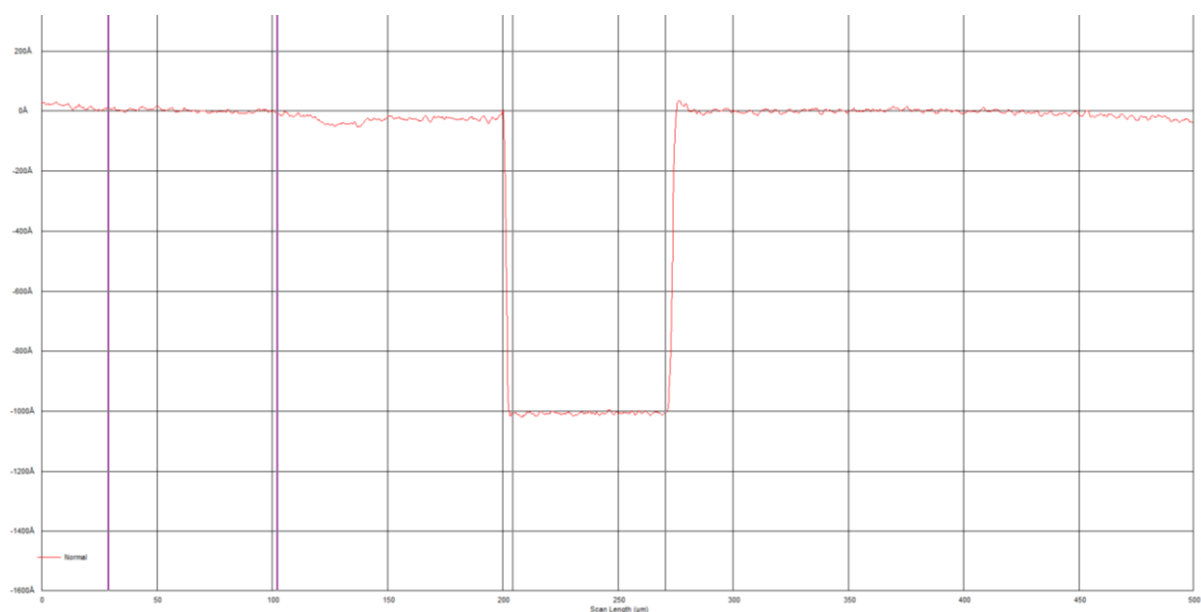


Figure 39: Obtained surface profile of a spin coated microscopy slide. Sharp peak is caused by the removal of the polymer layer Poly(HDsMAz) X_n 60 measurement 2.

Influence of concentration

The influence of different Poly(HDsMAz) concentrations on the contact angles were studied. Therefore, three microscopy slides were coated with 0.5, 1.0 and 2.0 wt.% DCM-solution. The coating layer increased with increased concentration from 39 ± 2 nm (0.5 wt.%) over 127 ± 2 nm (1.0 wt.%) to 252 ± 14 nm (2.0 wt.%), while the microscopy slides remained transparent. For the coating Poly(HDsMAz) was used as it was expected to possess the highest hydrophobicity. The influence of the concentration would therefore be observable, while excluding other effects as thresholds. The calculated left and right contact angles are shown, including the standard deviation from five measurements, (Figure 40) as well as the layer thickness including the standard deviation from three measurements (Table 13 and Appendix, Layer thickness measurement 12.2). With an increasing layer thickness of the polymer film the measured contact angles reach a plateau. (Figure 40) From the 0.5 wt.% to the 1.0 wt.% solution the contact angles increase from around 99 degrees to approximately 104 degrees, while the layer thickness more than 3 folds from 39 ± 2 nm to 127 ± 2 nm. Interestingly from 1.0 wt.% to 2.0 wt.% a doubling of the layer thickness can be noticed while the contact angles increase only slightly from around 104 degrees to 105 degrees.

Results and discussion

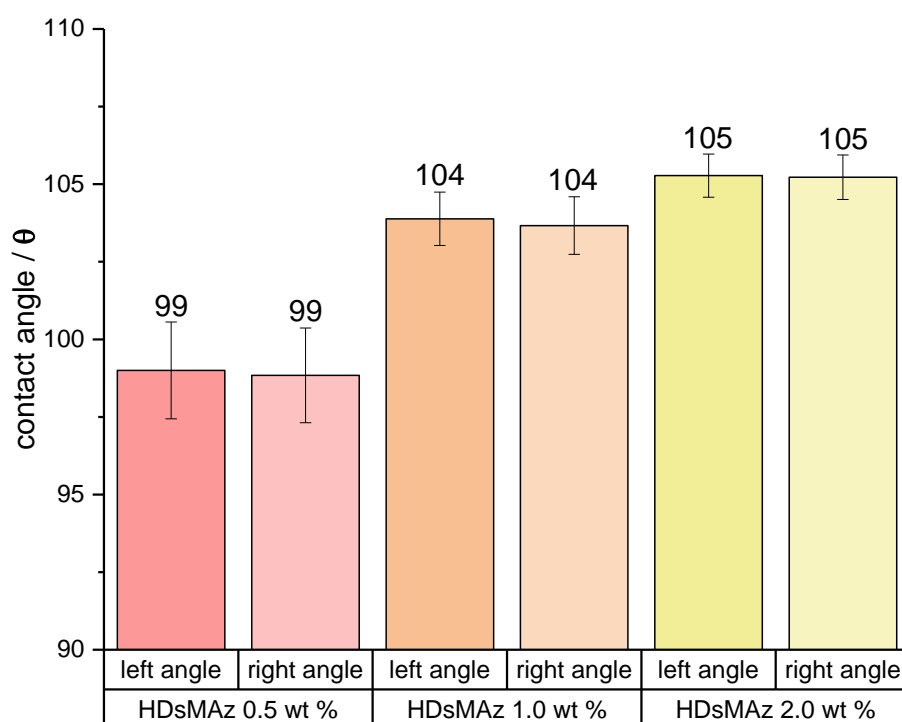


Figure 40: Contact angles for coated glass slides vs polymer concentration.

Table 13: Average values and standard deviation for left and right contact angle as well as layer thickness in dependence to the concentration.

Name	contact angle left (θ)	Contact angle right (θ)	Layer thickness (nm)
HDsMAz 0.5 wt. %	99 \pm 2	99 \pm 2	39 \pm 2
HDsMAz 1.0 wt. %	104 \pm 1	104 \pm 1	127 \pm 2
HDsMAz 2.0 wt. %	106 \pm 1	105 \pm 1	252 \pm 14

Showing no increase in the contact angle and the correlating degree of hydrophobicity, as well as proving a homogeneous formation of the polymer film all following measurements were conducted with a 1.0 wt.% polymer solution in DCM and the beforehand explained spin coating protocol.

Influence of side chain length

To study the influence of the alkyl chain length of the polymers, on the hydrophobicity, four polymers with different side chain length were used. (Figure 41, Table 14) To evaluate the actual impact of the hydrophobic alkyl chains Poly(MsMAz) was included in the measurements. It is clearly visible that by introducing long alkyl side chains the hydrophobicity of the coated slides increases drastically. The contact angles increase from around 63 degrees to up to 104 degrees. From Poly(OsMAz) over Poly(DDsMAz) to Poly(HDsMAz) the alkyl chain length increases from C₈ to C₁₂ and C₁₆, while the angles increase from 97 to 104 degrees. (Figure 41) Although the angle is clearly increasing with increasing chain length, the hydrophobic character reaches a plateau and increasing length does not further increase the hydrophobic character of the polymer films. The contact angle increases from Poly(OsMAz) to Poly(DDsMAz) by around four degrees and from Poly(DDsMAz) to Poly(HDsMAz) by two degrees. The creation of a plateau could be explained through a sufficient coating and shielding of the hydrophilic surface and an increase of alkyl chain length does not increase the shielding of the surface. This means for the use as oil additive, that Poly(OsMAz) should be an appropriate candidate if the lipophilic character is singularly necessary for the solubility, longer alkyl chains do not impact the degree of hydrophobicity.

Results and discussion

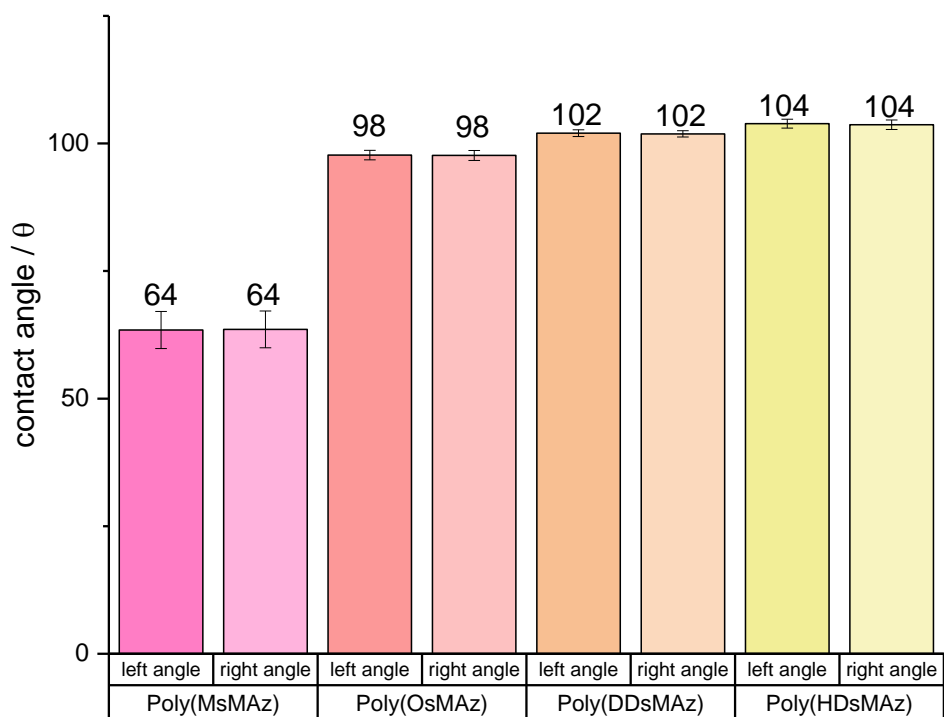


Figure 41: Contact angle of various polymers with different side chain lengths.

Table 14: Average values and standard deviation for left and right contact angle as well as layer thickness in dependence to the side chain length.

Name	Contact angle left (θ)	Contact angle right (θ)	Layer thickness (nm)
Poly(MsMAz)	64±4	64±4	118±3
Poly(OsMAz)	98±1	98±1	105±5
Poly(DDsMAz)	102±1	102±1	106±5
Poly(HDsMAz)	104±1	104±1	127±2

Influence of degree of polymerization

To study the impact of X_n towards the hydrophilic character of the polymer films, three coatings of Poly(HDsMAz) with X_n of 15, 30, 60 and a concentration of 1.0 wt. % were studied.

The impact between X_n 15 and 30 on the contact angle is negligible and less pronounced compared to the influence of side chain length. This is understandable due to the fact that the hydrophobic behavior of the polymers are caused by the side chain length and length of the polymer should have only a small effect *after* the coating was successful. The major difference, between X_n 15 and 30 are the measured layer thicknesses with 77 ± 1 nm (X_n 15) and 127 ± 2 (X_n 30), which shows that the polymer length has an impact on the coating process itself. The values for X_n 60 are also visible and include inconsistent measurement values with a standard deviation of more than 17% for the contact angles (θ), (Figure 42, Table 15) while the layer thickness again decreases from 127 ± 2 (X_n 30) to 98 ± 3 (X_n 60). It can be concluded that the coating for (X_n 60), was not successful. This can have various reasons like an inconsistent solution or a slow arrangement on the glass surface leading to a removal of the polymer through the centrifugal forces. Nevertheless, it seems that the polymer length has an impact on the coating process and it is therefore challenging to obtain a comparable layer thickness.

Table 15: average values and standard deviation for left and right contact angle as well as layer thickness in dependence to the degree of polymerization.

Name	Contact angle left (θ)	Contact angle right (θ)	Layer thickness (nm)
HDsMAz X_n 15	103 ± 2	103 ± 2	77 ± 1
HDsMAz X_n 30	104 ± 1	104 ± 1	127 ± 2
HDsMAz X_n 60	69 ± 12	75 ± 10	98 ± 3

Results and discussion

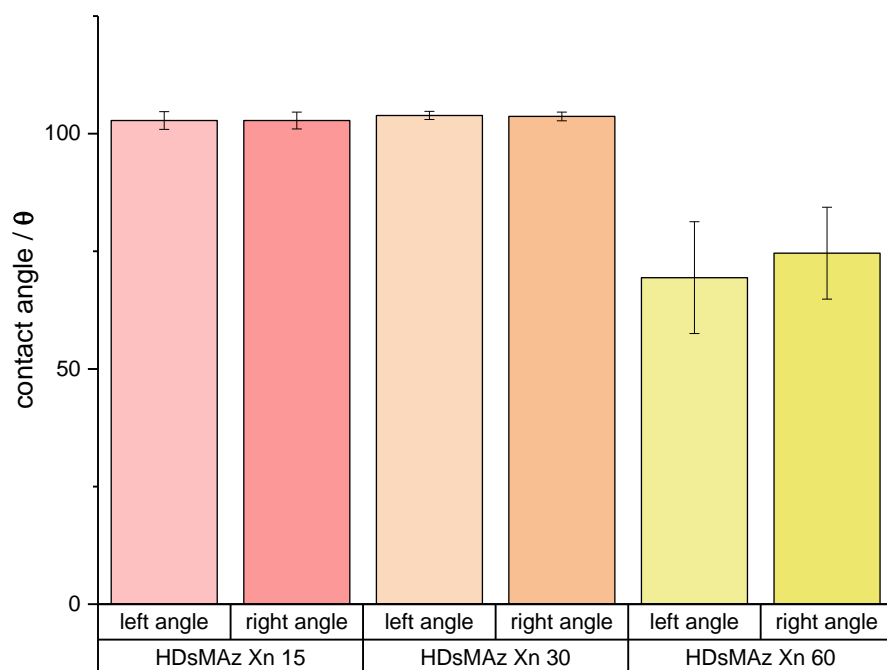


Figure 42: Contact angle of Poly(HDsMAz) with X_n 15, 30, 60

6.7 Spinning drop

In a spinning drop measurement series after Vonnegut the interface tension of a cyclohexane water system is used to study the surfactant behavior of three synthesized Polymers.⁴⁴

Therefore 1.0 wt.% of Poly(OsMAz), Poly(DDsMAz) and Poly(HDsMAz) (X_n 30) were dissolved in 1 mL cyclohexane. These three solutions as well as a blank sample of cyclohexane were measured *via* spinning drop. Each sample was measured twice with 100 measurements at 10000 rpm (Appendix 12.4 Spinning drop measurement). The surface tension was calculated after Vonnegut and the average value as well as the standard deviation. (Figure 43, Table 16)

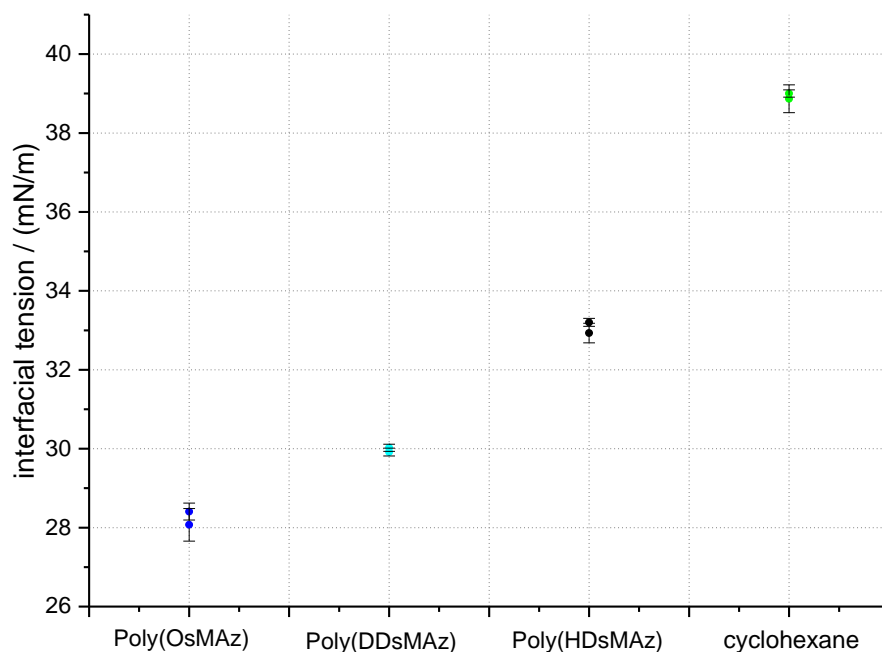


Figure 43: average interfacial tension for a 1wt.% polymer cyclohexane solution.

Through dissolving 7.8 mg (1wt.%) of polymer in 1 ml of cyclohexane it is possible to reduce the interface tension by 28% from 39 mN/m to 28.1mN/m (Poly(OsMAz)). It shows that hydrophobic Poly(sulfonyl aziridine)s can be used as surface active materials and have corresponding effect by aligning at the surface area. The highest effect is achieved by the use of Poly(OsMAz), due to a higher ratio of polar to unpolar groups, with longer the alkyl chains are the smaller the measured effect is.

Results and discussion

Table 16: average interface tension for a 1wt.% polymer cyclohexane solution.

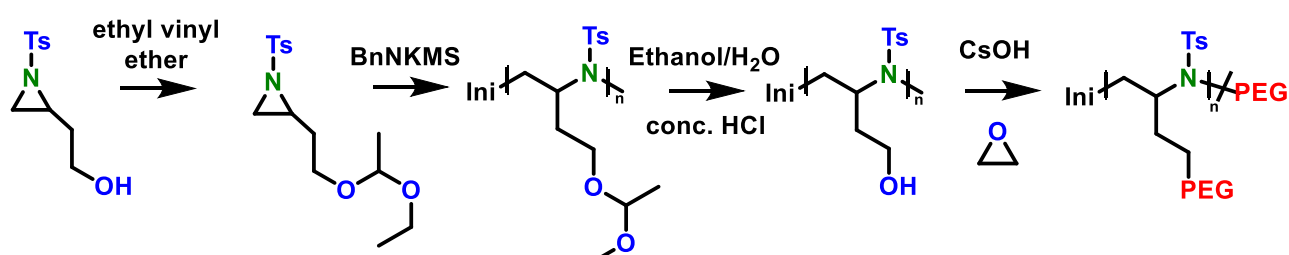
Sample	surface tension / (mN/m)	standard divination (mN/m)
Cyclohexane	39.0	0.1
Cyclohexane	38.9	0.4
Poly(OsMAz)	28.1	0.4
Poly(OsMAz)	28.4	0.2
Poly(DDsMAz)	29.9	0.1
Poly(DDsMAz)	30.0	0.1
Poly(HDsMAz)	32.9	0.2
Poly(HDsMAz)	33.2	0.1

7.0 Project 2: hydrophilic Poly(sulfonyl aziridine)s

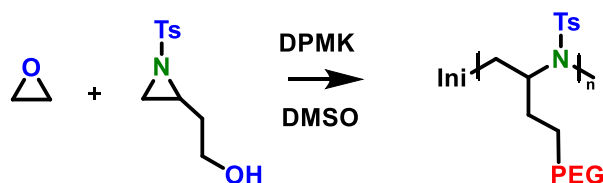
As the second project of this thesis the first Poly(sulfonyl aziridine)-*graft*-PEG polymers were synthesized and analyzed through diffusion ordered spectroscopy (DOSY). In line to the first project, the second project introduces hydrophilic PEG side chains to Poly(sulfonyl aziridine)s to achieve solubility in water, without compromising the Poly(sulfonyl aziridine) backbone, which could reduce the enveloping properties of the polymer.

The synthesis of Poly(sulfonyl aziridine)-*graft*-PEG polymer was achieved by two different synthesis routes. The first synthesis is a grafting-*from* process starting with the synthesis of Poly(2-ethanol-*N*-tosylaziridine) (Poly(TsEtOHaz)), while the second synthesis is a one-pot copolymerization of TsEtOHaz with ethylene oxide. (Scheme 26) In case of the one-pot synthesis various initiations can occur, which can lead to a branching of the polymer and is discussed further in fitting section.

Synthesis route: grafting-*from*



Synthesis route for one-pot copolymerization



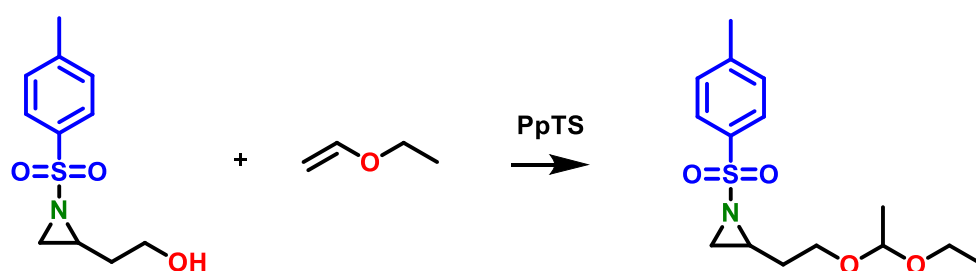
Scheme 27: Synthesis overview of both conducted synthesis routes.

7.1 Synthesis route: Grafting-*from*

To synthesis a novel PAz-*graft*-PEG polymer it was assumed that a grafting-*from* polymerization would be the easiest method to achieve well-defined polymers. As mentioned before the synthesis of Poly(TsEtOHaz) was previous achieved by Riegler *et al.* by first protecting TsEtOHaz with ethyl vinyl ether and after polymerization deprotecting the hydroxide group with acid in ethanol.²¹ Later Gleede *et al.* proved that the protection can be neglected and a propagation without branching can be achieved. Nevertheless, a protection group was used in the synthesis to ensure linearity of the polymer as well as to exclude a source for errors.

2-((1-Ethylethoxy)ethyl)-*N*-Tosylaziridine

The first synthesis route started with the protection of the hydroxide group of TsEtOHaz with ethyl vinyl ether. (Scheme 27) TsEtOHaz was kindly provided by T. Gleede. For the protection of the alcohol, ethyl vinyl ether was cryo-distillated and used in high excess of 15 eq. Both educts were transferred into a flame dried flask and pyridinium *p*-toluenesulfonate (PpTs) was added in catalytic amount. The reaction was stirred over night at -10 °C and after evaporation of the ethyl vinyl ether, the product was purified over column chromatography (yield: 85%).



Scheme 28: Protection of TsEtOHaz through ethyl vinyl ether.

As the reaction is known in literature²¹ the product was singularly analyzed *via* ¹H NMR showing a successful protection of the hydroxyl group. The typical aziridine peaks are visible through the pattern shown by 2.86–2.74 ppm (m, 1H, **f**), 2.60 (dd, *J*=7.1, 5.4 Hz, **g**), 2.11ppm (t, *J*=4.4 Hz, **g'**). (Figure 44) Furthermore, the tosyl-group can by

Results and discussion

identified through the two doublets 7.79 (d, $J=8.2$ Hz, **i**), 7.36 (d, $J=8.0$ Hz, **j**) and the singlet of the $-CH_3$ -group 2.44 ppm (s, **k**). The protective group can be seen through the diastereomeric hydrogen 4.58 ppm (q, $J=5.3$ Hz, **c**), 4.47 ppm (q, $J=5.3$ Hz, **c**) and the two terminal $-CH_3$ groups 1.25 – 1.09 ppm (m, **a**).

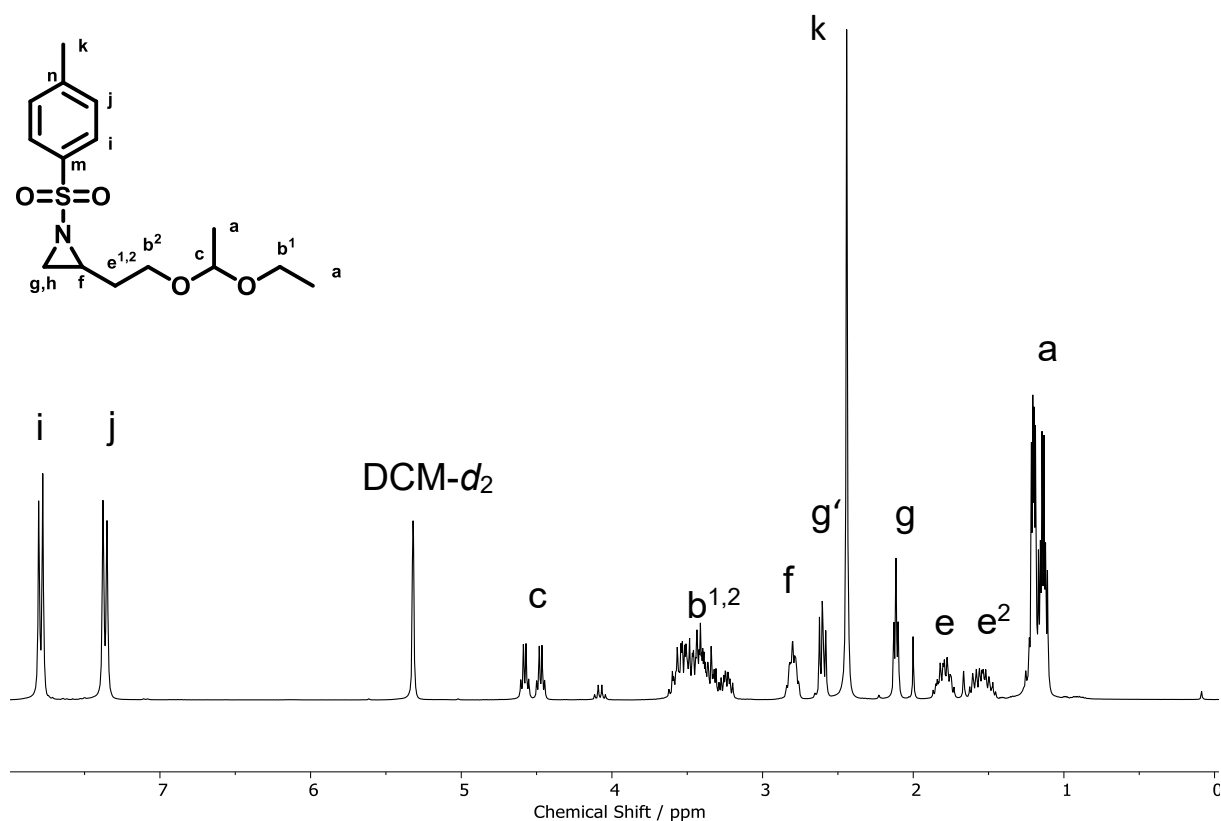
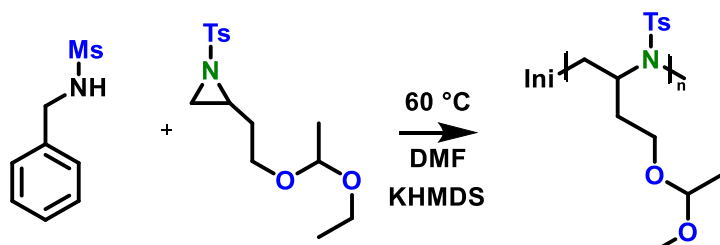


Figure 44: ^1H NMR (300 MHz, $\text{DCM}-d_2$) 2-((1-Ethylethoxy)ethyl)-N-Tosylaziridine.

Poly{2-(2-Ethylethoxy)-Ethanol-*N*-Tosylaziridine} Poly(TsEEEEAz)

As initiator system BnNHMs/KHMDS was used and the polymerization, the monomer and initiator were dried in benzene overnight and the polymerization was conducted at 60 °C under Schlenk condition in dry DMF. (Scheme 28, Table 11)



Scheme 29: Homopolymerization of TsEEEEAz

Table 17 Overview of synthesized Polymers. M_n (GPC) and \bar{D} in DMF/PEG-standard

sample	X_n	M_n (GPC) g/mol	\bar{D}
Poly(TsEEEEAz)	50	3838	1,2
Poly(TsEEEEAz)	50	4770	1,19

The polymer was analyzed *via* GPC and ^1H NMR. The GPC shows a monomodal distribution and low \bar{D} . (Figure 46) The assignment of the ^1H NMR is difficult as most peaks are not separated and most hydrogens in the backbone and side chain cannot be assigned 4.73 – 2.50 ppm (m, **c**). (Figure 45) What can be assigned are again the tosyl-AG group consisting of the aromatic peaks 8.20–7.51 ppm (m, **i**), 7.53 – 6.98 ppm (m, **h**) as well as the CH_3 -group 2.44–2.22 ppm (m, **d**). Furthermore, the CH_3 -groups of the protection group are seen 1.27 – 0.81 ppm (m, **a**).

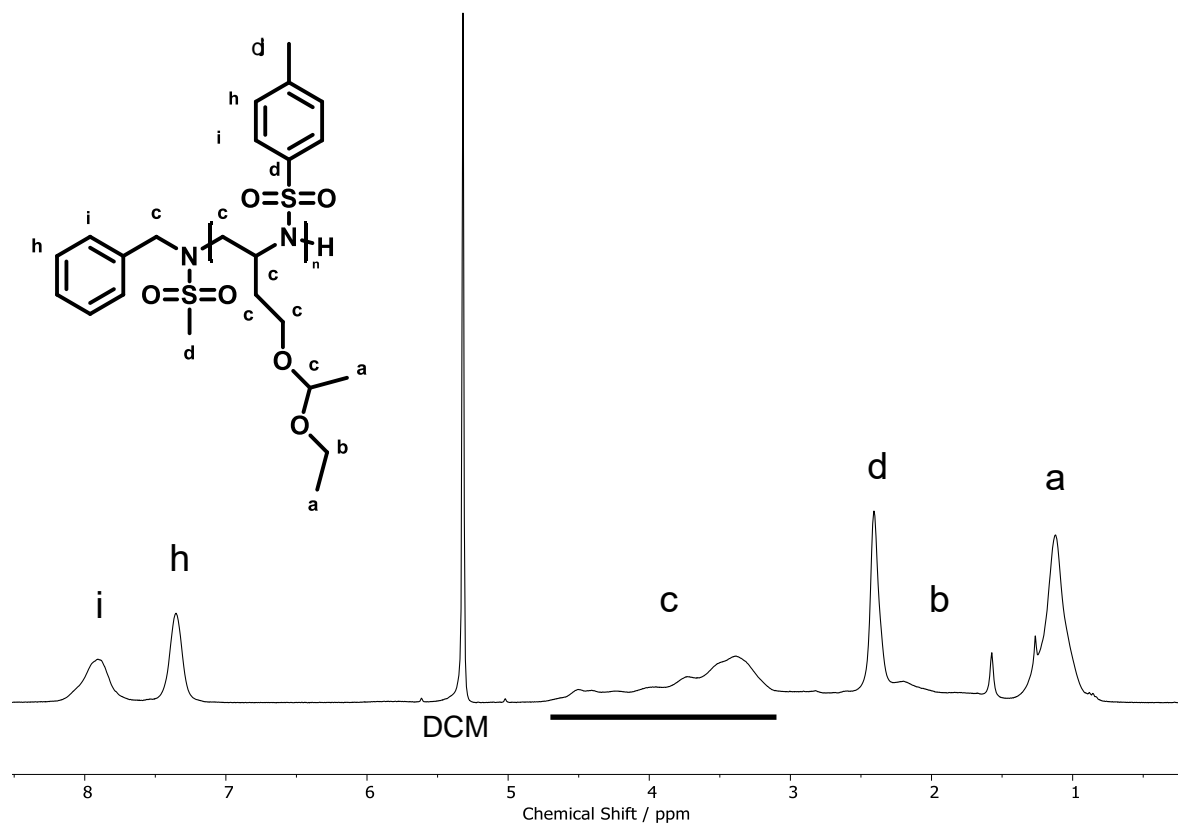


Figure 45: ¹H NMR (300 MHz, DCM-d₂) of Poly(TsEEEAz).

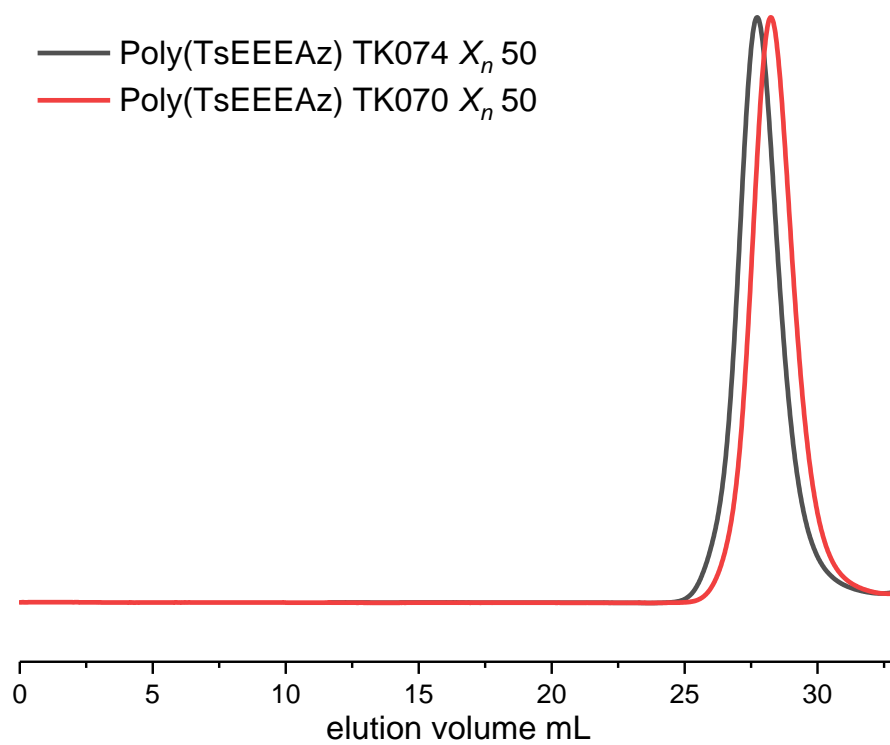


Figure 46: GPC traces (RI-detection) of Poly(TsEEEAz).

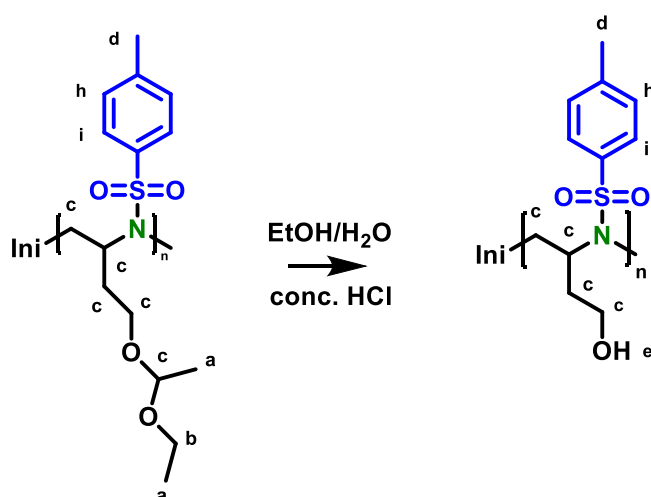
Hydrolysis of acetal groups

The hydrolysis of the acetal group was conducted after the protocol of Rieger *et al.*²¹ (Scheme 29) The starting material was taken up in an ethanol and concentrated HCl was added. The solution was then stirred overnight by 70 °C and reduced at the rotary evaporator.

Yielding a brown solid, which was insoluble in DCM or non-polar solvent. For the synthesis of *graft*-polymers all traces of acid needed to be removed and the product was dialyzed in THF (2000 g/mol, regenerated cellulose).

Table 18 Overview of synthesized Poly(TsEtOHAz); M_n (GPC) and \bar{D} in DMF/PEG-standard

sample	X_n	M_n (GPC) g/mol	\bar{D}
P(TsEtOHAz)	50	3474	1.37
P(TsEtOHAz)	50	4567	1.13



Scheme 30: Deprotection of Poly(TsEEEEAz) through hydrolysis of the acetal group.

Like for the used starting material Poly(TsEEEEAz) the assignment of the hydrogen peaks in the ¹H NMR is difficult due to an overlapping of various peaks. Therefore, a stacked ¹H NMR of Poly(TsEEEEAz) and the product Poly(TsEtOH) is shown. (Figure 47) Again, the Tosyl-AG can easily be assigned through its aromatic peaks (h,i) and the -CH₃-group (d). Through the stacking of starting material and product, two mayor differences can be seen. First the disappearance of the -CH₃-groups of the

Results and discussion

protection group are seen (**a**), as well as a new peak by 3.67–3.5 (m, **e**) which belongs to the now free hydroxide group.

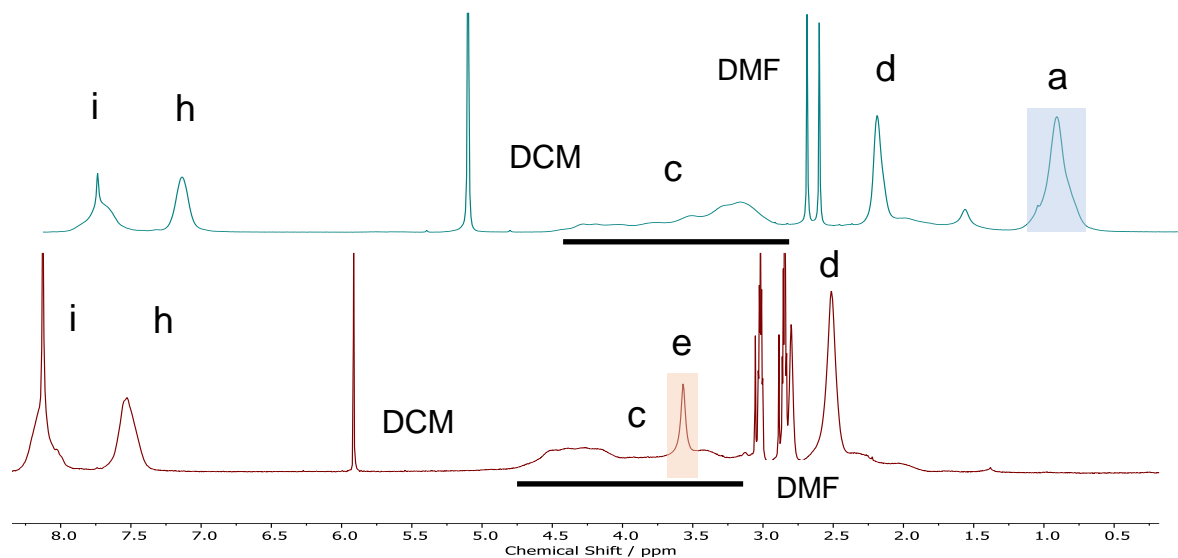


Figure 47: Stacked ¹H NMR of starting material Poly(TsEEEEAz) (blue) and product Poly(TsEtOHAz) (red).

In two GPC traces of Poly(TsEtOHAz) are shown, which both possess a monomodal, nearly symmetrical traces. (Figure 48) Both possess a molecular dispersity and molecular weight, which is close to their educts. Therefore it can be assumed that no backbone cleavage occurred and the X_n did not change.

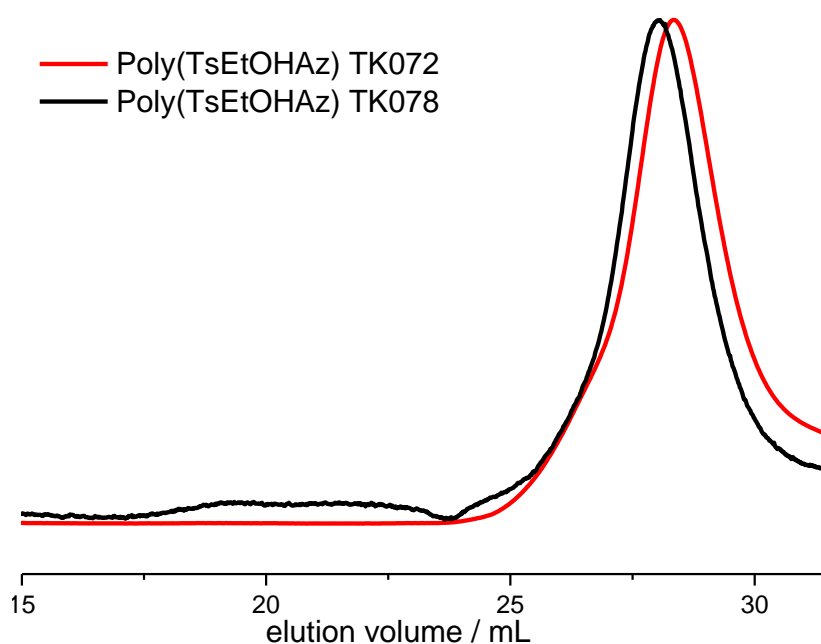
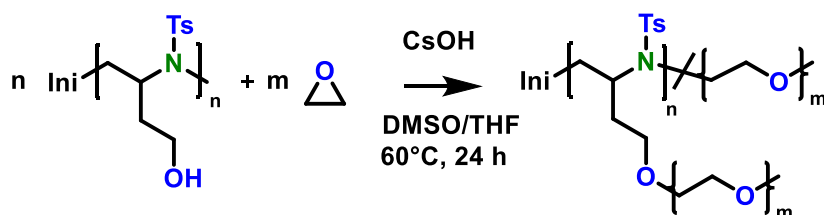


Figure 48: GPC traces (RI-detection) of Poly(TsEtOHAz).

Poly-(TsEtOHAz)-graft-PEG**Scheme 31:** Synthesis scheme of Poly(TsEtOHAz)-graft-PEG synthesis route one.

The reaction was carried out in a flame-dried Schlenk flask under Argon atmosphere. Poly-(TsEtOHAz) was transferred into the Schlenk flask, CsOH·H₂O (0.2-0.5 eq.) was added, heated in benzene (60°C) for at least 3 h and dried under reduced pressure. The deprotonated macroinitiator was dissolved in pre-dried THF and anhydrous DMSO. Ethylene oxide was cryo-transferred into the reaction flask from a graduated ampule. The reaction mixture was heated in an oil bath (60°C) for 12 h. (Scheme 30) Subsequently the polymer was precipitated in Et₂O (30-40 ml), centrifuged and dried *in vacuo*.

In the GPC traces are shown including an overlay of the starting material to illustrate the products trace shifts to higher or lower elution volume. (Figure 49) The GPC trace of the crude product (black trace) shows two peaks, one at a lower elution volume than the starting material and one at higher elution volume. The peak at higher elution volume shows that a homo-polymerization of ethylene oxide took place as a side polymerization, while the peak with lower elution volume belongs to the successfully synthesized graft polymer. Dialysis was conducted to separate the graft polymer from the homo polymerized PEG (blue and green trace). Both were conducted in water (first: 3.5kDA regen. Cellulose, second: 6-8 kDA regen. Cellulose). Through the use of the dialysis the amount homo polymerized PEG was removed. The molecular dispersity is with 2.3 comparably broad for an AROP.

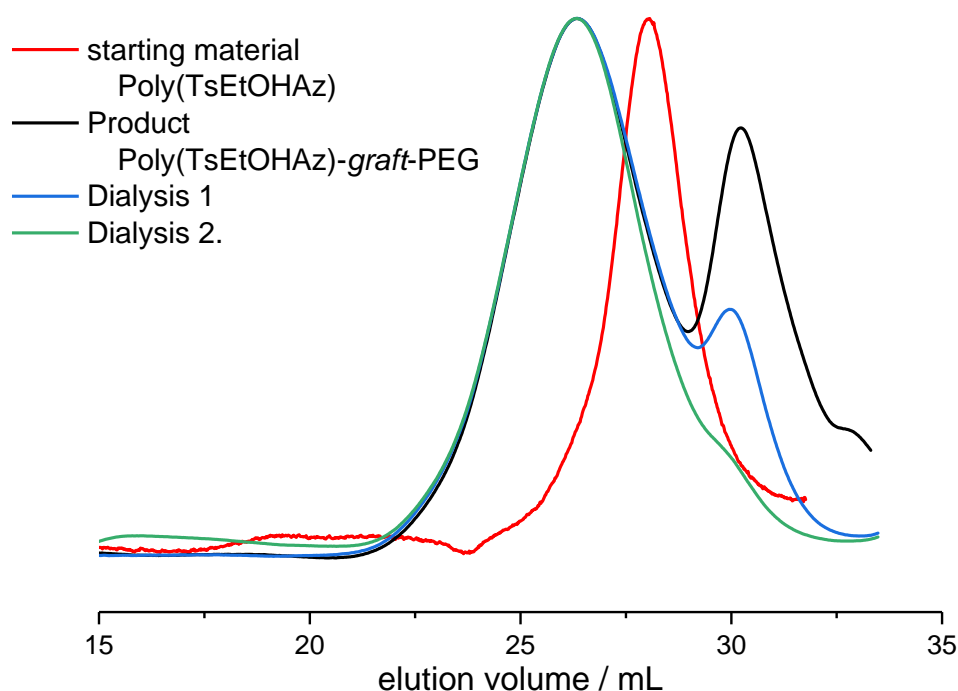


Figure 49: GPC traces (RI detection) of Poly(TsEtOHaz)-*graft*-PEG.

In the measured ^1H NMR is depicted and shows next to the assignable tosyl-AG groups 7.99–7.57 ppm (m, **i**) 7.53 – 7.26 ppm (m, **h**) and 2.44 – 2.32 ppm (m, **d**) a strong ethylene oxide peak 3.57 – 3.42 ppm (m, **a**). (Figure 50) Further, a peak at 4.63 – 4.51 ppm can be assigned to a hydroxide-group (**e**). The integration of **i**, **h**, **d** and **e** gives a ratio of 2:2:3:1 showing that for every tosyl-AG a hydroxide group exist. This ratio and the increased elution volume indicate a successful synthesis of a graft polymer.

To have additional proof for the successful synthesis of a graft-copolymer a diffusion ordered spectroscopy (DOSY) was measured and the chemical shift was plotted against the diffusion coefficient ($\log(\text{m}^2/\text{s})$). (Figure 51) In the spectra a black line is plotted indicating the same diffusion coefficient for the aziridine backbone visible through the tosyl-AG (**h**, **i**, **d**) and the PEG peak (**a**) as well as the hydroxide group. Below the line, two clearly separated peaks show the diffusion coefficient of the deuterated solvent DMSO- d_6 as well as water. Taking into account that the product has a higher elution volume than the starting material, a clear assignment of all peaks is possible and the alignment in the ^1H DOSY leads to the conclusion that the synthesis of a Poly(TsEtOHaz)-*graft*-PEG was successful.

Results and discussion

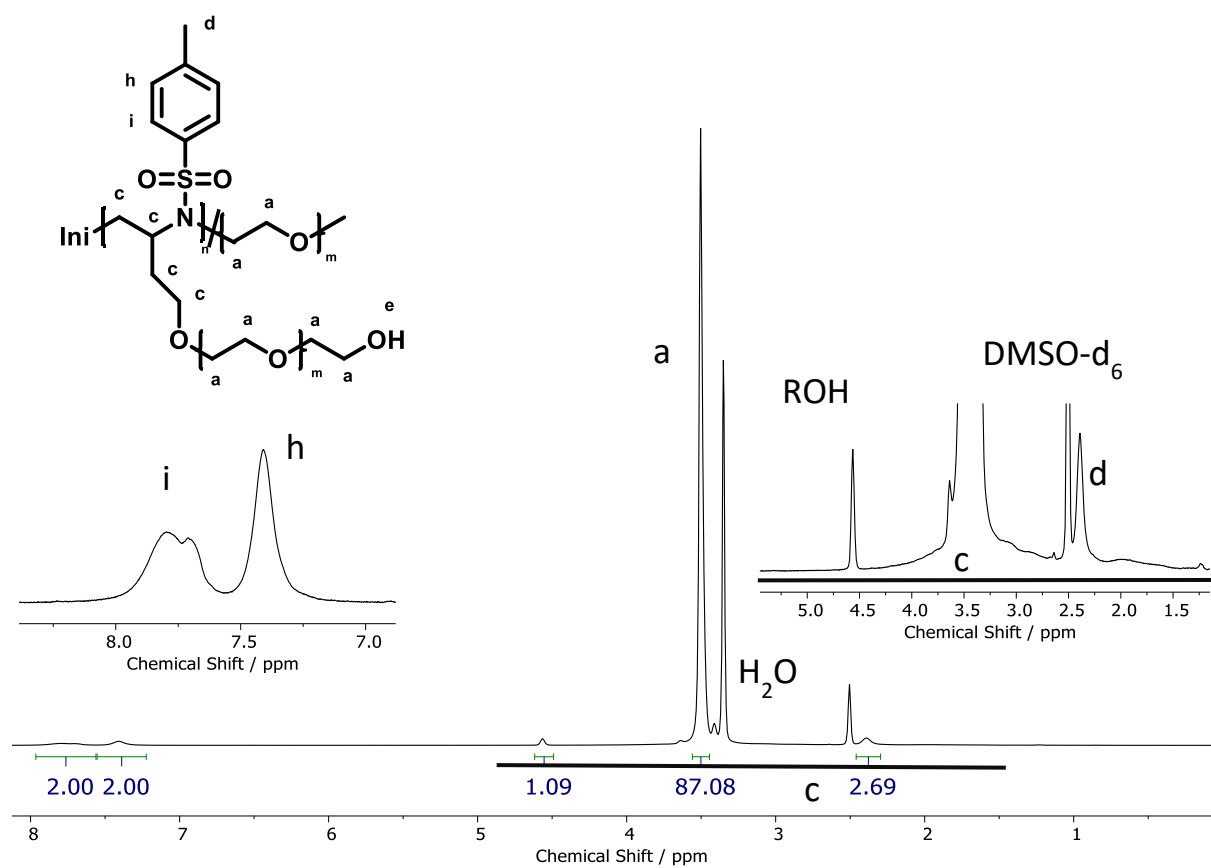


Figure 50: ¹H NMR (500 MHz, DMSO-*d*₆) of Poly(TsEtOHAz)-graft-PEG.

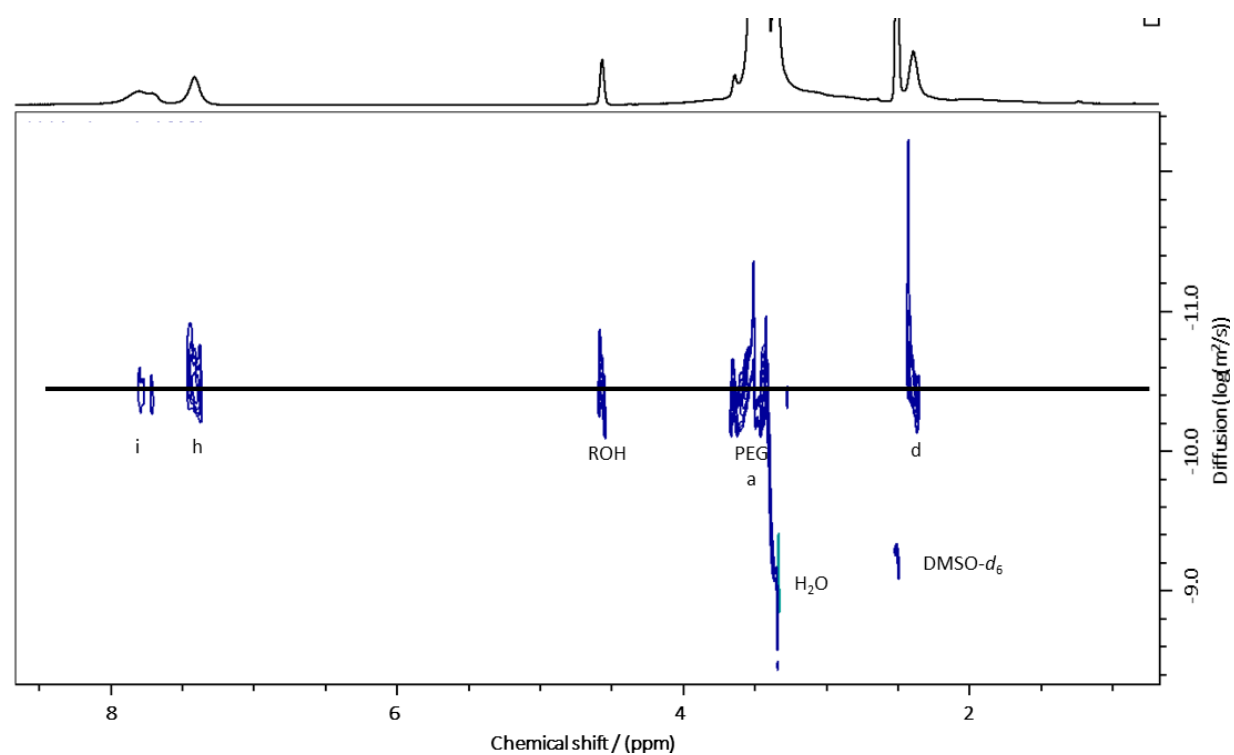
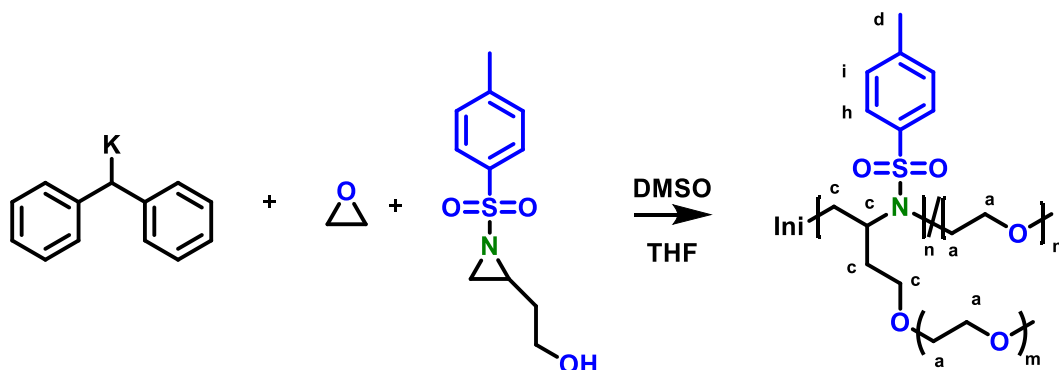


Figure 51: ¹H DOSY (DMSO-*d*₆, 700MHz, 298 K) of Poly(TsEtOHAz)-graft-PEG.

7.2 One-pot synthesis of Poly(TsEtOHaz)-*graft*-PEG

After the grafting-*from* synthesis was successful but proved to be more challenging than expected, due to necessary purification of starting material and product. A direct one-pot synthesis of TsEtOH and ethylene oxide was conducted. As mentioned before Gleede *et al.* succeeded in the copolymerization of ethylene oxide and sulfonyl aziridine, which leads to block like copolymers with sharp gradients in which the activated aziridine monomers were incorporated before the ethylene oxide.¹⁹ Further he proved that the polymerization of TsEtOH without a protection group still leads to linear polymer, with active hydroxide groups.²⁰ Combining these observations, an one-pot synthesis should lead to the polymerization of graft-polymers. First the AAROP occurs leading to Poly(TsEtOHaz), after depletion of the aziridine monomer the polymerization continuous by incorporation of ethylene oxide. Due to the rapid proton exchange of the hydroxide groups a regular incorporation of ethylene oxide at all free hydroxide groups should occur.



Scheme 32: One-pot synthesis of Poly(TsEtOHaz)-*graft*-PEG.

In the polymerization DPMK was used as initiator due to its easy handling, which needed no separated preparation. Because DPMK has a stronger basicity as BnNHMs branching can occur due to different initiation steps.

The ring opening of activated aziridines is favored over the ring opening of ethylene oxide and should therefore be the dominant initiation step. In both cases the active chain end will start with the incorporation of TsEtOHaz monomer and no branching occurs.

A different initiation can occur due to an acid-base reaction of DPMK with a hydroxide group. In this case the now active species starts an AROP by incorporating TsEtOHaz. In this case branching or backbiting can occur. The degree of branching could be estimated using the hydroxide end groups. In an unbranched polymer each Poly(sulfonyl aziridine) repeating unit possesses a hydroxide group, through branching the amount of free hydroxide groups is reduced and which can be determinate either through titration or integration of the corresponding ^1H NMR peaks

The synthetic approach to the one pot synthesis of Poly(TsEtOHaz)-*graft*-PEG followed the same execution as for the homo polymerization of PEG with DPMK. The reaction was carried out in a flame-dried Schlenk flask under argon atmosphere. TsEtOHaz was dried with benzene overnight and dried THF and 1 ml DMSO were added to the flask and the solution frozen with liquid N_2 . Ethylene oxide was cryo-transferred into the flask. DPMK (1.1 M in THF, 1 equiv.) was added to the reaction mixture, which was then heated in an oil bath (60°C) for 12 h. (Scheme 31) Subsequently the polymer was precipitated in Et_2O (30-40 ml), centrifuged and dried *in vacuo*.

Table 19: Overview of one-pot synthesis of Poly(TsEtOHaz)-*graft*-PEG,; M_n (GPC) and \bar{D} in DMF/PEG-standard

sample	M_n (GPC) g/mol	\bar{D}
P(TsEtOHaz) - <i>graft</i> -PEO	2222	1.87

The GPC trace of the one-pot synthesis shows a molecular dispersity of 1.87, which is lower than for the *graft-from* polymerization. (Figure 52, compare Figure 49) Further, the GPC trace does not show a second peak corresponding to PEG homopolymer like in the *graft-from* polymerization occurred. In the ^1H NMR, the tosyl-AG can be assigned to the peaks (**i**, **h** and **d**), while a PEG signal (**a**) as well as a ROH-peak (**e**) are visible. (Figure 53) The one-pot synthesis was further analyzed via a ^1H DOSY (Figure 54) confirming the copolymerization of TsEtOHaz and ethylene oxide. In ^1H DOSY the chemical shift is plotted against the diffusion coefficient ($\log(\text{m}^2/\text{s})$) and a black line indicates the same coefficient for the aziridine backbone, visible through the tosyl-AG (**h**, **i**, **d**), and the PEG peak (**a**) between 10.3 and 10.8 $\log(\text{m}^2/\text{s})$. Below the line, two separated peaks show the diffusion coefficient of the deuterated solvent $\text{DMSO}-d_6$ and water.

Results and discussion

As the GPC shows no indication of two separated homopolymerizations and an alignment in the ^1H DOSY is seen the conclusion can be drawn that the synthesis of a Poly(TsEtOHaz)-*graft*-PEG is considered to be successful.

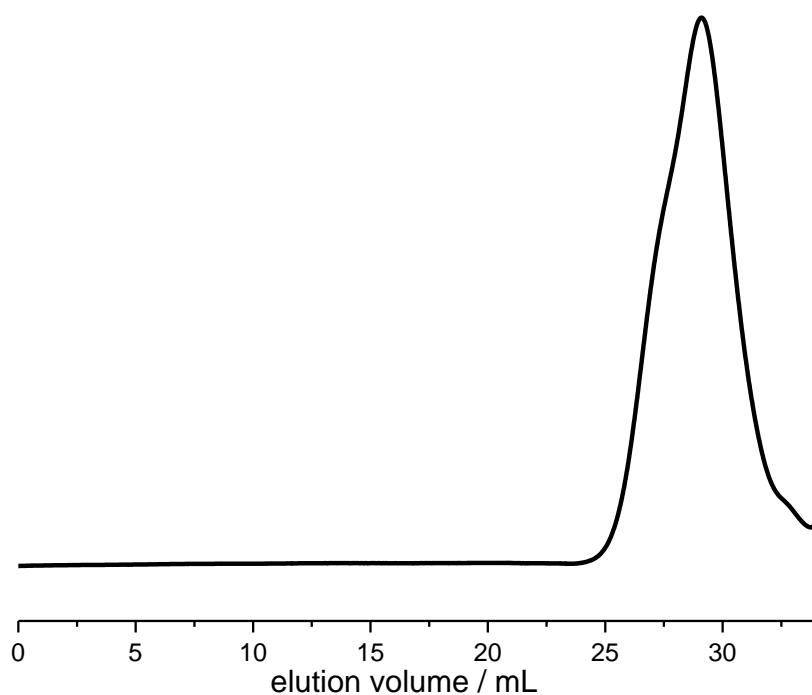


Figure 52: GPC trace (RI detection) of Poly(TsEtOHaz)-*graft*-PEG one-pot synthesis.

Results and discussion

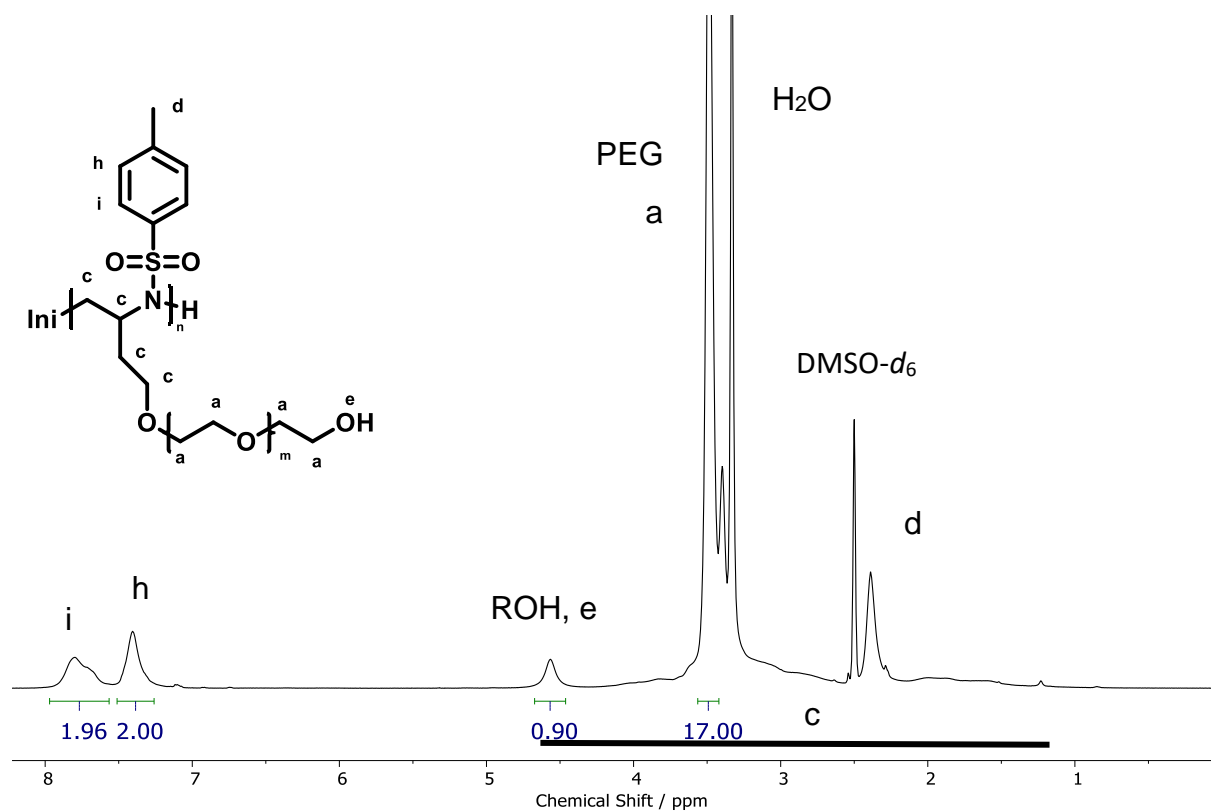


Figure 53: ^1H NMR (500 MHz, $\text{DMSO}-d_6$) of Poly(TsEtOHaz)-*graft*-PEG one-pot synthesis.

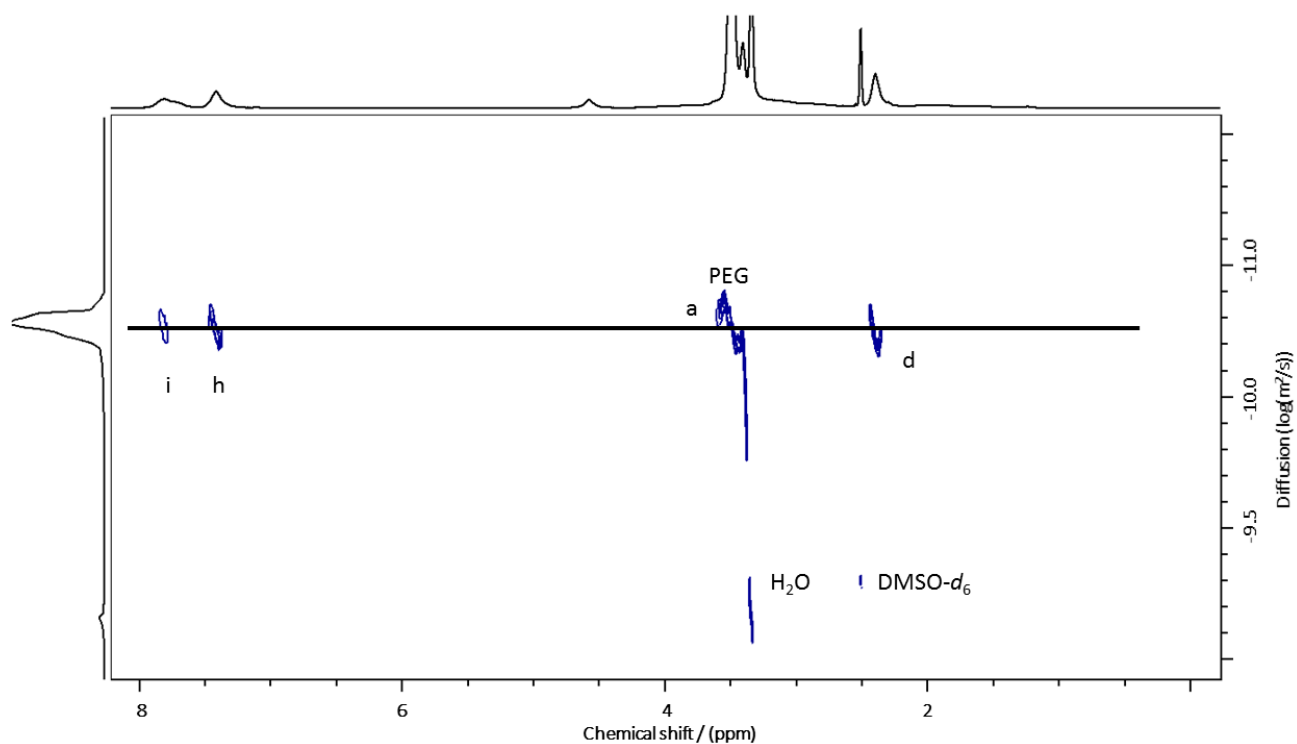


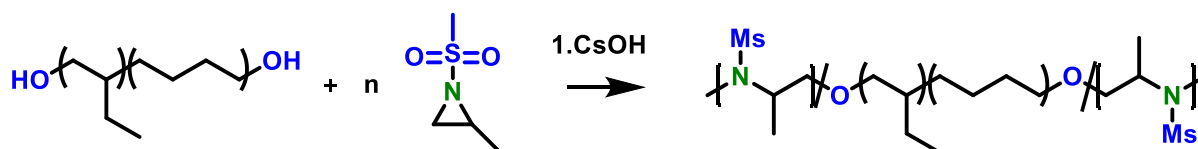
Figure 54: ^1H DOSY ($\text{DMSO}-d_6$, 700 MHz, 298 K) of Poly(TsEtOHaz)-*graft*-PEG one-pot synthesis.

8. Outlook

Over the last 6 months, significant progress was made to improve the solubility of polar Poly(sulfonyl aziridine)s. In two projects, the polymer backbone was left unchanged while through the modification of side chains a solubility in non-polar solvents as well as in water was achieved.

In the first project, four new monomers and various homo- and copolymers were synthesized. Although Poly(MsMAz) is normally only soluble in polar org. solvents like DMF, DMSO or DCM a solubility in cyclohexane at room temperature, as well as in dodecane and hexadecane at high temperatures were achieved. Further the use of these new polymers as surfactants was analyzed *via* contact angle measurement and spinning drop. In both cases, it was found that the polymers were surface active, either as a coating or in solution.

A possibility to further increase the solubility in non-polar solvents would be the introduction of a new initiator system or the modification through a termination agent. The use of initiators with long alkyl chains would be an easy task. Also, the synthesis of block-co-polymers is possible, in a first attempt the synthesis of a triblock-co-polymer was undertaken but could not be completed successfully. A triblock-copolymerization was attempted with a lipophilic polybutadiene block (commercial purchased Kraton ($X_n=45$)) and two hydrophilic short MsMAz blocks ($X_n=10$). (Scheme 32) However, the formation of an elastic solid was confirmed, which was insoluble in most solvents and GPC measurement showed no detection of any kind as the product was neither soluble in THF nor Toluene. Nevertheless a $^1\text{H-NMR}$ in CDCl_3 showed a formation of a Poly(sulfonyl aziridine) backbone.



Scheme 33: Polymerization of a tri-block-copolymer.

Outlook

In the second project novel Poly(TsEtOHaz)-*graft*-PEO were introduced. As was shown by Gleede *et al.* the one pot synthesis of ethylene oxide and activated-aziridines allows access to block like structures.¹⁹ A one-pot synthesis of *graft*-polymers is therefore a valid progression in the new field of ethylene oxide and aziridine copolymerization. To confirm the ¹H DOSY measurements a solution of homopolymers could be measured to compare the yielded data. Further the synthesis of Poly(TsEtOHaz) was undertaken with a protective group, which was counterproductive as a strong acid was used for the following deprotection and needed to be removed completely to not interfere with the following graft polymerization. It would therefore be easier to refrain from using a protective group, which could simplify the following graft polymerization. A next step needs to be the determination of material properties which were not conducted due to a lack of time.

9. Experimental Part

9.1 Materials and methods of characterization

Materials

All chemicals were purchased from common suppliers (Sigma-Aldrich, Acros, Roth, Fisher Scientific, Fluka, TCI Europe) and used without further purification. Deuterated solvents were supplied by Deutero GmbH (Kastellaun, Germany). All dry solvents were stored under argon and molecular sieve. 2-Methylaziridine and 2- ω -propanol-*N*-tosylaziridine, were kindly provided by T. Gleede.

Nuclear magnetic resonance

Nuclear magnetic resonance (NMR) measurements were conducted on Bruker AVANCE 250, 300, 500, 700 spectrometers operating with 250, 300, 500, 700 MHz frequencies at 298 K and were analyzed *via* MestReNova 12 from Mestrelab Research S.L. ^1H DOSY (Diffusion ordered spectroscopy) was measured on a Bruker 500 at 298 K and analyzed *via* TopSpin 3.5 from Bruker. Real-time ^1H NMR spectroscopy) were taken at 50 °C, 200 experiments, with 16 scans each at 700 MHz using a Bruker AVANCE 700 spectrometer. Chemical shifts are given in ppm

Size-Exclusion Chromatography

SEC measurements were conducted using DMF as eluent and a Poly(ethylene oxide) standard at 60 °C at a flow rate of 1ml/min. The measurements were performed with a PSS SECurity (Agilent Technologies 1260 Infinity) equipment including three Gram (PSS) columns (1000, 1000, 100) and a PSS SECurity (RID, UV 270 nm).

Experimental Part

Further SEC measurements were conducted using THF as eluent and a Polystyrol standard at 30 °C and a flow rate of 1ml/min. In this case three SDV (PSS) columns (10^6 , 10^4 , 500 Å) and a PSS SECcurity (RID, UV 254 nm) were used.

Contact angle measurements

The contact angles were measured on a Krüss DSA 1. As droplet 5 µL of demineralized water were used. For the manufacture of the polymer coatings microscopy slides were cut into 2.5*2.5 cm squares and cleaned *via* water and soap, distilled water and acetone. Afterwards they were further treated, in an *iso*-propanol bath, with ultra-sound for 10-15 minutes and ionized through argon-plasma by 0.25 mbar/ 270 W for 10 minutes.

Eight different polymer solutions were prepared as coatings in 1 mL DCM (table 20).

Table 20: Overview over used polymer solutions in DCM for spin coating

Name	Concentration	X_n	Layer thickness nm
HDsMAz	0.5 wt. %	30	39±2
HDsMAz	1.0 wt. %	30	127±2
HDsMAz	2.0 wt. %	30	252±14
HDsMAz	1.0 wt. %	15	77±1
HDsMAz	1.0 wt. %	60	127±2
DDsMAz	1.0 wt. %	30	106±5
OsMAz	1.0 wt. %	30	105±5
MsMAz	1.0 wt. %	30	xxx

The coating was conducted by putting the freshly ionized slides on a spin coater, applying 0.5 mL polymer solution and spinning after 5 seconds with 3000 rpm for 20 seconds. The solvent is removed through the centrifugal force and leaves a polymer film on the microscopy slide. The coated microscopy slides were heated for 5 minutes at 100 °C to remove all remaining solvent.

Tensometry

Spinning drop measurements were conducted on a Dataphysics SVT 20N, spinning drop tensiometer by 10000 rpm at 22 °C.

Differential scanning calorimetry

Differential scanning calorimetry (DSC) was measured on a Mettler Toledo DSC 823 calorimeter. Two, three or five scanning cycles of heating and cooling were performed with 10 mg of sample and a heating rate of 10 °C /min.

Thermogravimetric analysis

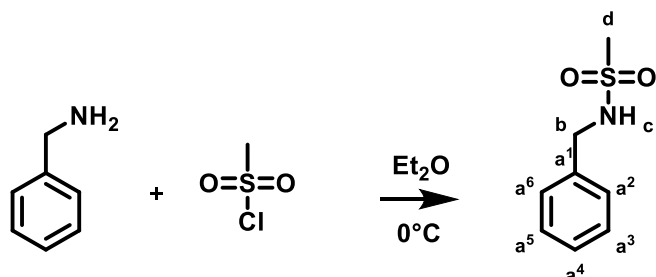
Thermogravimetric analysis (TGA) was measured on a Mettler Toledo TGA 851, with 10 mg of sample under nitrogen from 25 °C to 900 °C, with a heating rate of 10 °C/min.

Mass spectroscopy

Mass spectroscopy was measured on an Advion CMS-L using CMS-1917-0726. Evaluation was conducted *via* Advion data express version 5.1.0.2.

9.2 Synthesis of Monomers and Initiator

benzyl-N-methylsulfonamide (BnNHMs)



Scheme 34 synthesis of benzyl-N-methylsulfonamide (BnNHMs)

The synthesis followed a known literature procedures.⁴³ In a flame-dried flask benzyl amine (15.0 g, 139 mmol) were dissolved in dried THF (200 ml). Mesylchloride (5.38 ml, 69.5 mmol) was added dropwise under heavy stirring at 0 °C and then stirred for another 3 hours at room temperature. The solvent was evaporated under reduced pressure and the crude solid was dissolved in ethyl acetate. The solution was washed with 2 M HCl and brine. The organic phase was dried over MgSO₄ and reduced at the rotary evaporator, yielding the product as colorless crystals.

Yield: 11.06 g, 59.71 mmol 85%

¹H NMR (300 MHz, Chloroform-*d*) δ 7.42 – 7.29 (m, 5H, a²⁻⁶), 4.81 (s, 1H b), 4.31 (s, 2H, c), 2.85 (s, 3H, d).

¹³C NMR (300 MHz, Chloroform-*d*) δ 136.80 (a¹), 129.04 (a^{2, 6}), 128.24 (a⁴), 128.04 (a^{3, 5}), 47.32 (b), 41.23 (d).

Experimental Part

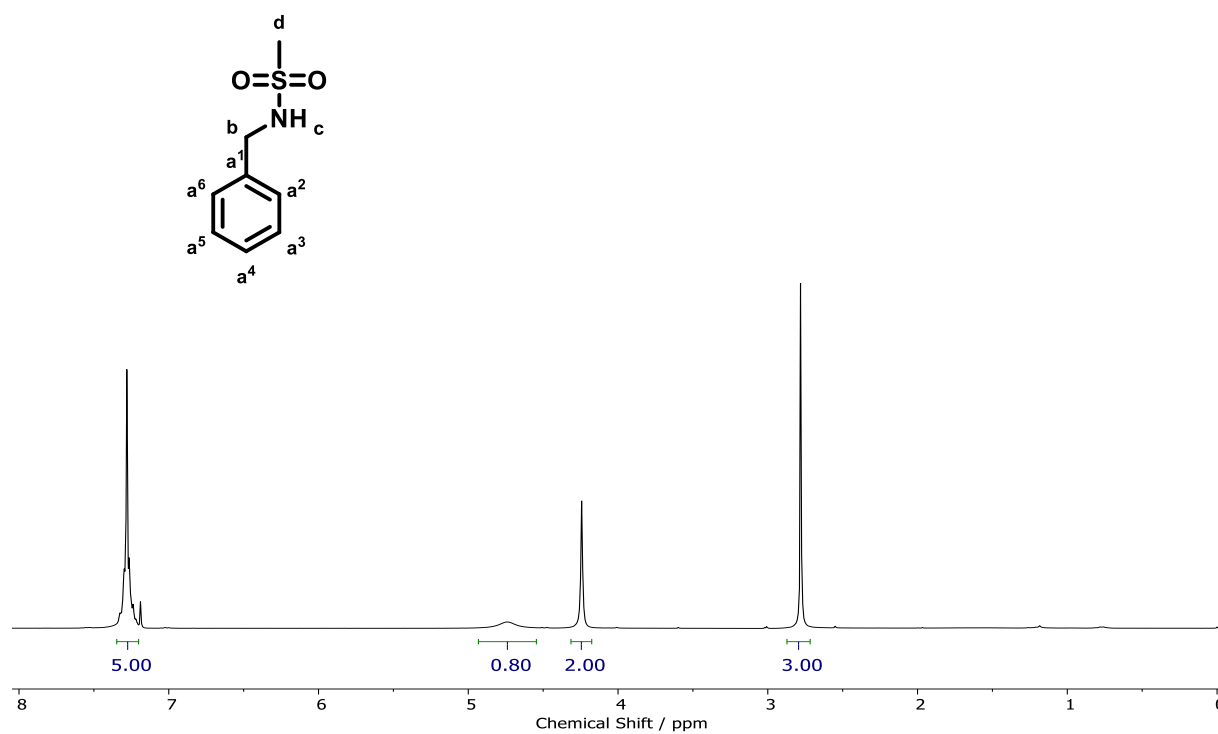


Figure 55: ¹H NMR (300 MHz, Chloroform-*d*) of benzyl-*N*-methylsulfonamide

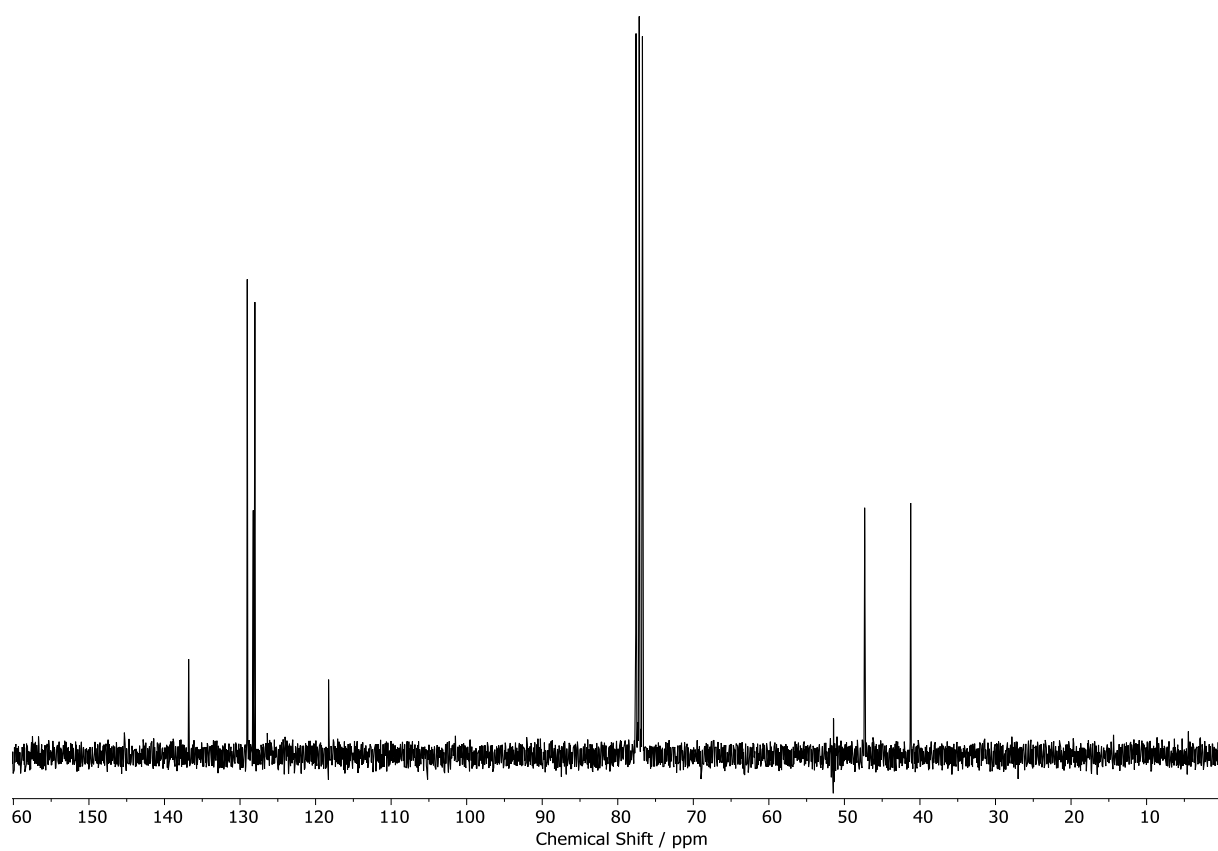
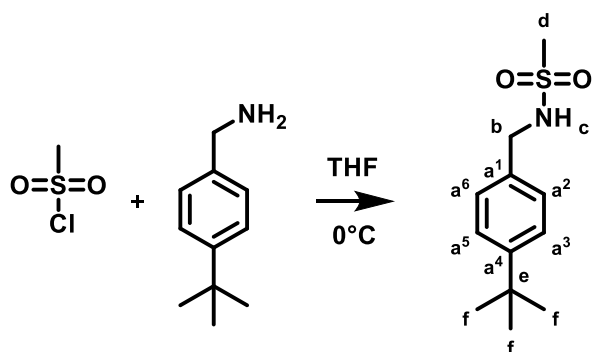


Figure 56: ¹³C NMR (300 MHz, Chloroform-*d*) of benzyl-*N*-methylsulfonamide

4-tert-Butylbenzylmesylsulfonamid (^tb-BnNHMs)**Scheme 35:** Synthesis of (^tb-BnNHMs)

The synthesis followed a known literature procedures.⁴³ In a flame-dried flask 4-tert-butylbenzylamine (5.0 g, 30.63 mmol) were dissolved in dried THF (200 ml). Mesylchloride (1.75 g, 15.3 mmol) was added dropwise under heavy stirring at 0 °C and then stirred for another 3 hours at room temperature. The solvent was evaporated under reduced pressure and the crude solid was dissolved in ethyl acetate. The solution was washed with 2 M HCl and brine. The organic phase was dried over MgSO₄ and reduced at the rotary evaporator, yielding the product as yellowish crystals.

The product was recrystallized in ethyl acetate.

Yield: 3.66 g, 15.16 mmol 99%

¹H NMR (300 MHz, tetrachloroethane-*d*₂) δ 7.31 (d, *J* = 8.0 Hz, 2H, a^{2,6}), 7.18 (d, *J* = 7.9 Hz, 2H a³⁻⁵), 4.65 (t, *J* = 6.2 Hz, 1H, c), 4.18 (d, *J* = 5.8 Hz, 2H, b), 2.80 (s, 3H, d), 1.23 (s, 9H, f).

¹³C NMR (300 MHz, tetrachloroethane-*d*₂) δ 151.10 (a⁴), 133.25 (a¹), 127.44 (a^{2,6}), 125.72 (a^{3,5}), 46.72 (b), 40.82 (d), 34.36 (e), 31.18

Experimental Part

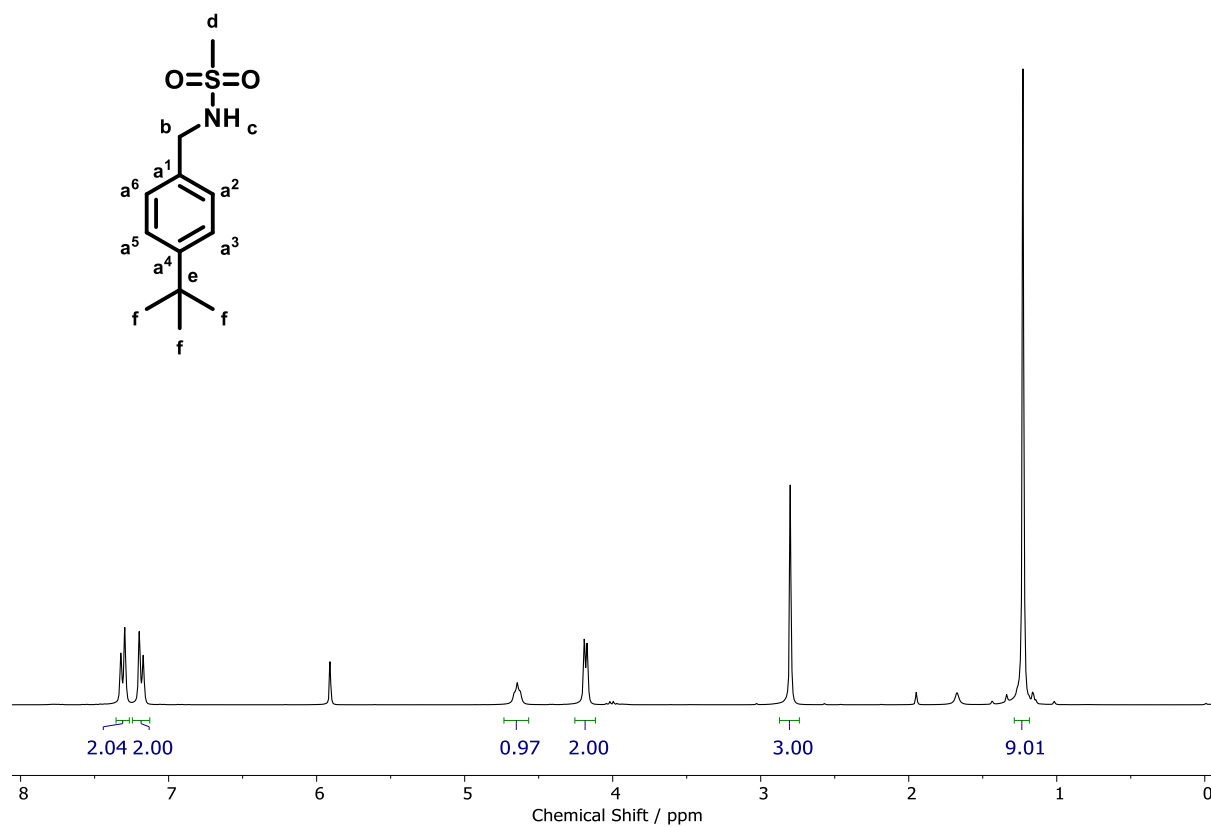


Figure 57: ¹H NMR (300 MHz, tetrachloroethane-*d*₂) of (b-BnNHMs)

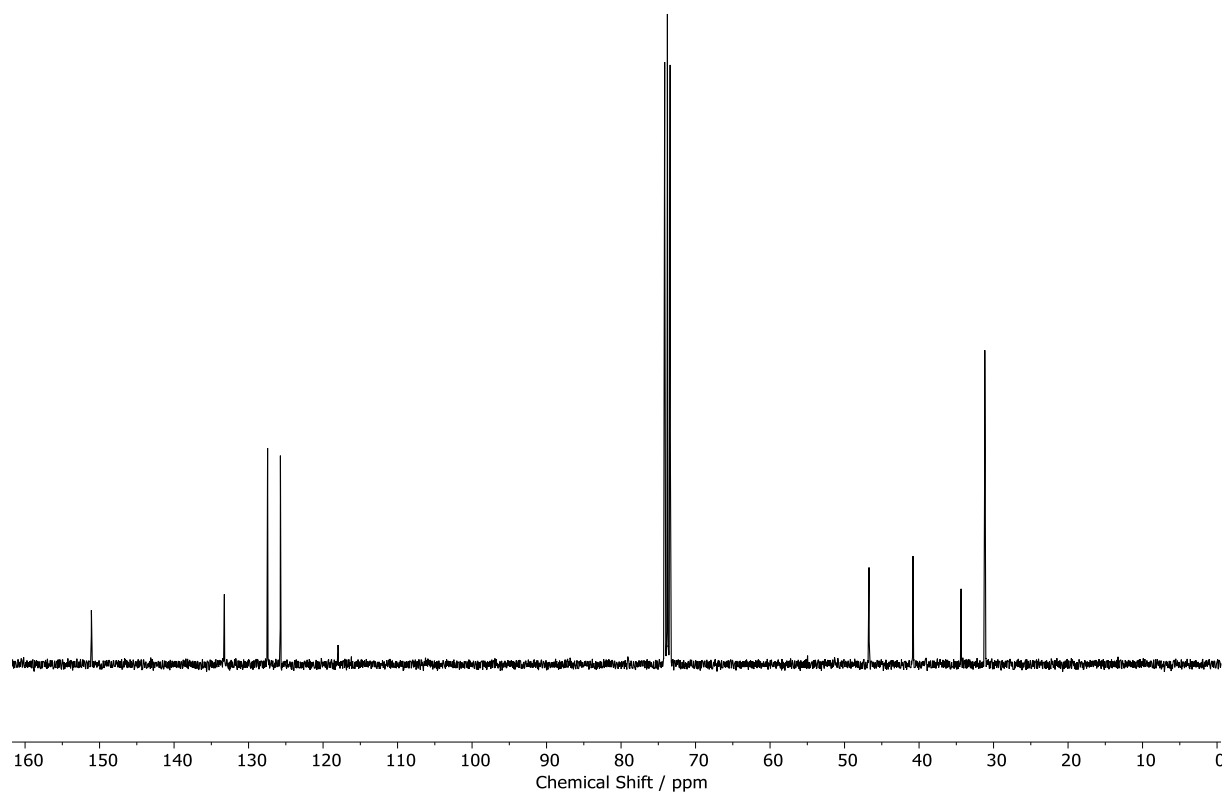
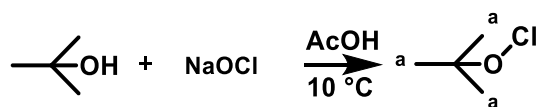


Figure 58: ¹³C NMR (300 MHz, tetrachloroethane-*d*₂) of (b-BnNHMs)

Tert-butyl hypochlorite³⁵



Scheme 36: Synthesis of Tert-butyl hypochlorite.

The synthesis was carried out under the absence of light. In an Erlenmeyer flask a sodium hypochlorite solution (372 g, 699.64 mmol, 14%) was cooled to -10°C. Under heavy stirring a mixture of *tert*-butanol (65.65 ml, 699.64 mmol) and acetic acid (40 ml, 699.64 mmol) were added slowly to the flask. After five minutes of stirring the organic phase was separated, washed with 10 % NaHCO₃ and brine, yielding the product, which was used without further purification.

Yield: 44.95 g, 414.02 mmol, 59%

¹H NMR (300 MHz, Chloroform-*d*) δ 1.33 (s, 1H).

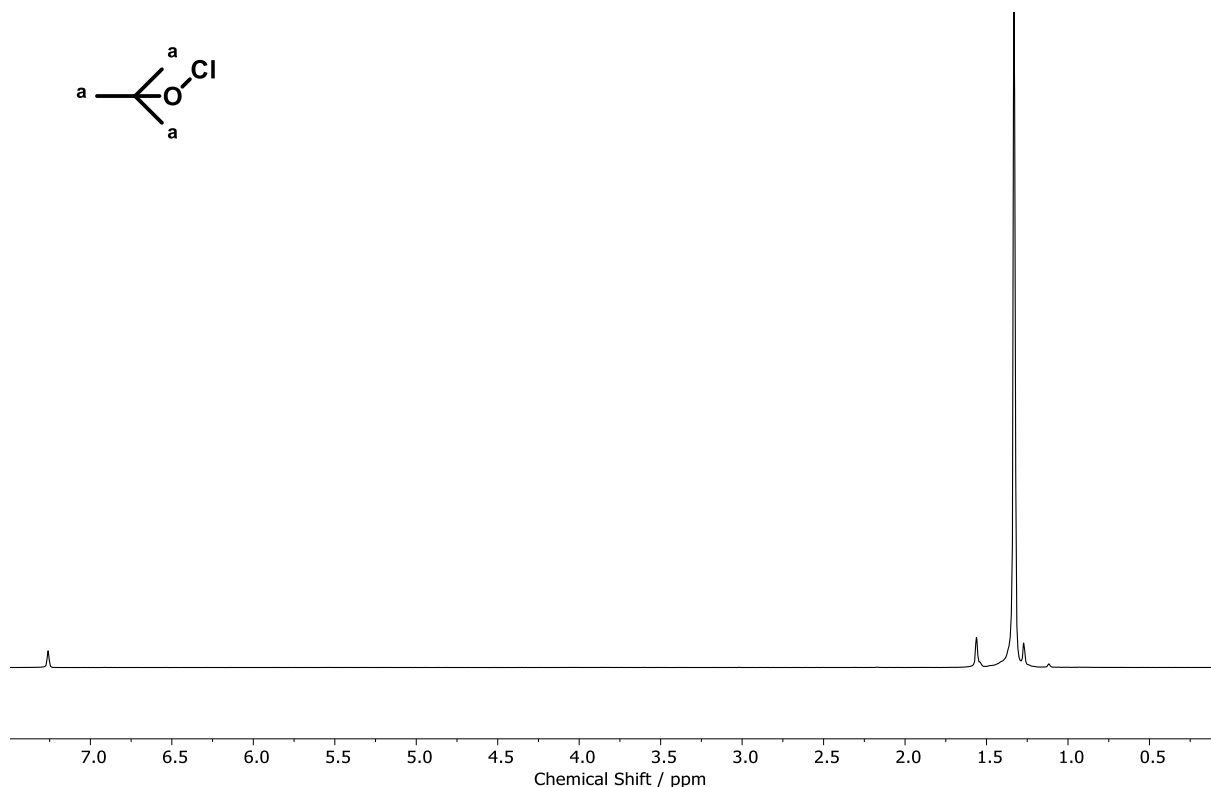
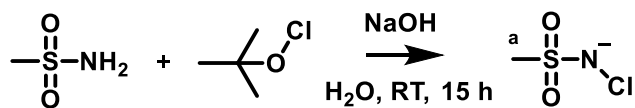


Figure 59: ¹H NMR (300 MHz, Chloroform-*d*) of *tert*-butyl hypochlorite.

Chloramine-M³⁵



Scheme 37: Synthesis of Chloramine-M.

Methylsulfonylamide (39.62 g, 414.0 mmol) was dissolved in 250 ml deionized water and sodium hydroxide (16.56 g, 414.0 mmol in 100 ml water) was added under ice cooling. Under stirring tert-butyl hypochlorite (44.95 g, 414 mmol) was added slowly, while the temperature was not allowed to rise over 40 °C. The solution was stirred for one day at room temperature. The solvent was evaporated, and the resulting solid was washed with acetone and dried under reduced pressure.

Yield: 36.58 g, 284.56 mmol 68%

¹H NMR (300 MHz, Deuterium Oxide) δ 2.96 (s, 1H).

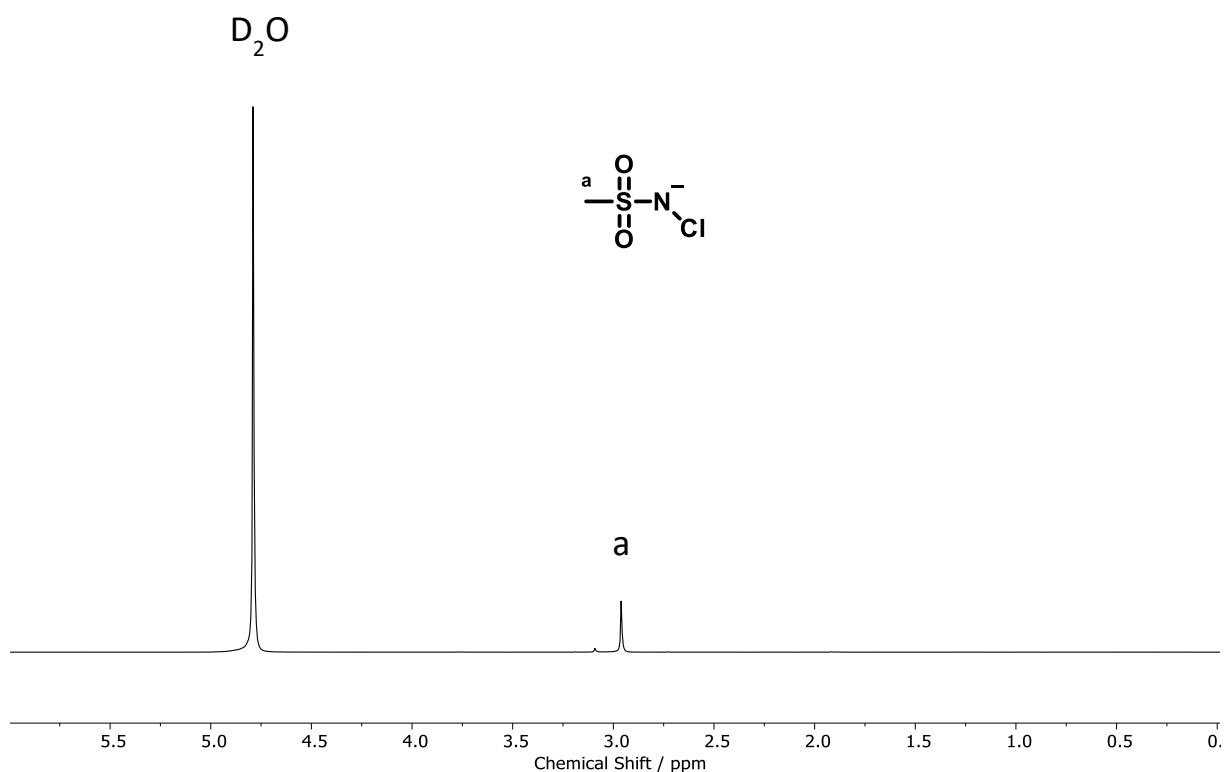
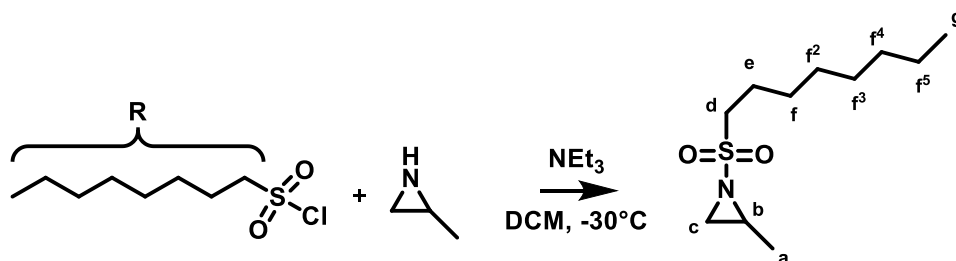


Figure 60: ¹H NMR (300 MHz, Deuterium Oxide) of Chloramine-M.

2-Methyl-N-Octasylaziridin (OsMAz)**Scheme 38:** Synthesis of 2-Methyl-N-Octasylaziridin (OsMAz)

In a flame dried flask 2-methylaziridin was dried over CaH_2 and cryo-transferred for purification. The purified 2-methylaziridin (1.85 ml, 25.85 mmol) was dissolved in dichloromethane and triethylamine (4.91 ml, 35.26 mmol). The solution was cooled to -30°C and octasylchloride (5.0 g, 23.5 mmol dissolved in DCM) was added dropwise to the solution. After stirring for two hours, the solution was allowed to reach room temperature and was washed with saturated NaHCO_3 and brine. The organic Phase was dried over MgSO_4 and reduced at a rotary evaporator, yielding the product. The product was purified *via* silica chromatography (Hexane/ethyl acetate: 8/1).

Yield: 4.26 g, 18.25 mmol 78%

A purification *via* silica chromatography is not necessary and can be neglect. Which increases the yield.

Yield: with 2-methylaziridin (2.95 ml, 51.71 mmol)

Octasylchloride (10.0 g, 47.01 mmol)

Product OsMAz (10.16 g, 43.54 mmol 93%)

^1H NMR (300 MHz, chloroform- d) δ 3.17 – 3.06 (m, 2H, d), 2.84 – 2.69 (m, 1H, b), 2.59 (d, J = 7.0 Hz, 1H, c), 2.03 (d, J = 4.6 Hz, 1H, c), 1.97 – 1.80 (m, 1H, e), 1.50 – 1.38 (m, 3 H, a), 1.37 – 1.22 (m, 10 H, f^{1-5}), 0.93 – 0.84 (m, 3H, g).

^{13}C NMR (700 MHz, benzene- d_6) δ 52.85, 34.59, 33.75, 32.21, 29.43, 29.43, 28.67, 23.65, 23.11, 16.89, 14.45.

IR (ν cm^{-1}): 2928, 2855, 1456, 1316, 1139, 857

Masse: m/z : 234.4 (M^+)

Experimental Part

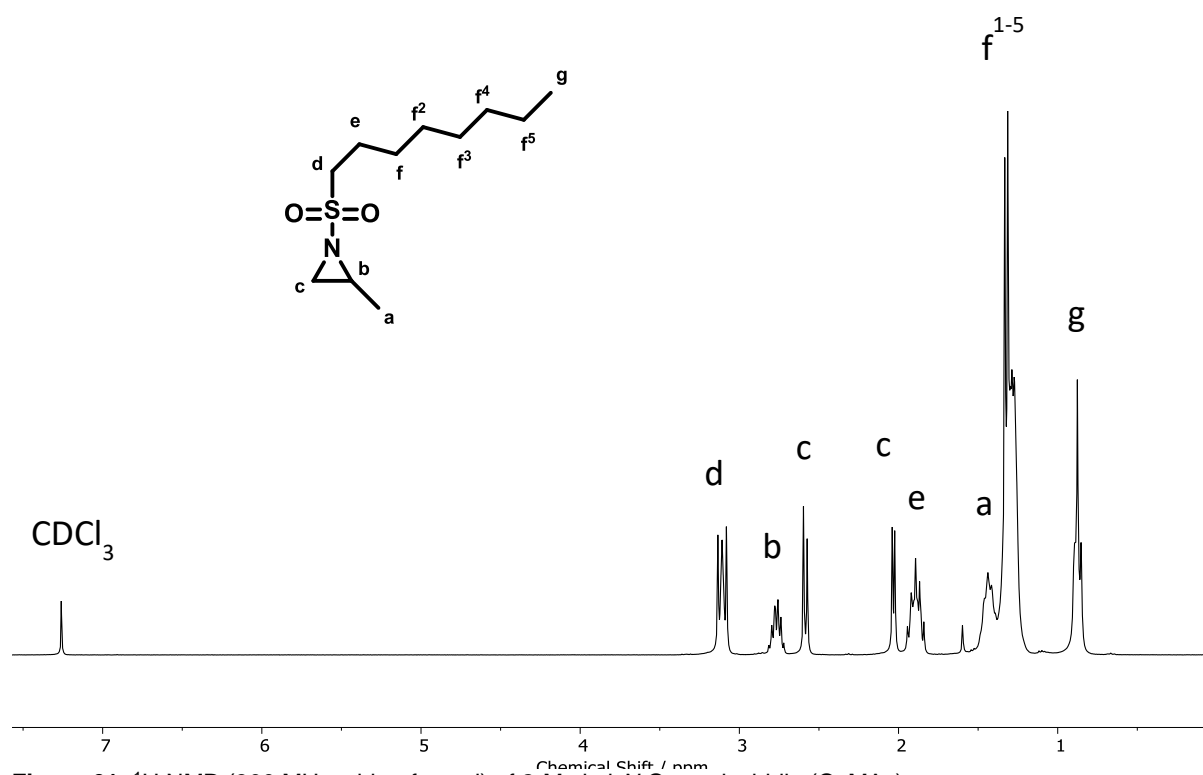


Figure 61: ^1H NMR (300 MHz, chloroform-d) of 2-Methyl-*N*-Octasylaziridin (OsMAz)

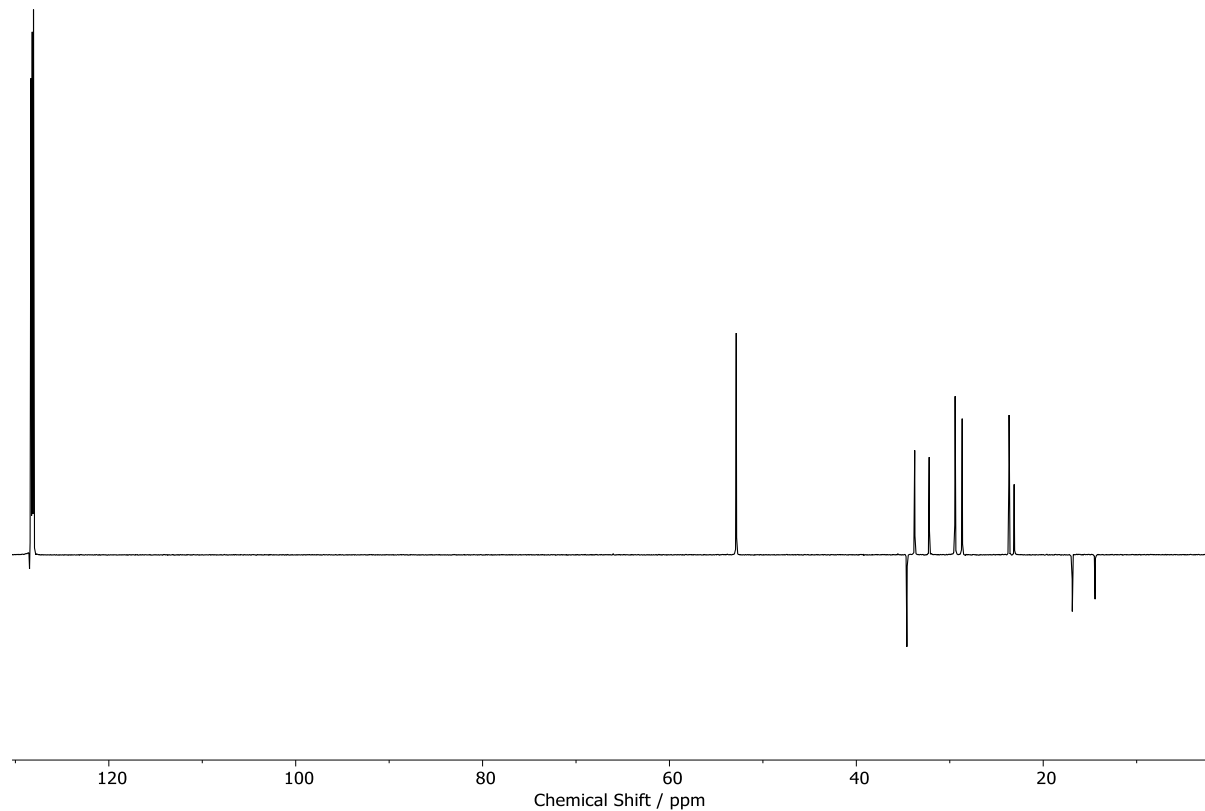


Figure 62: ^{13}C NMR (700 MHz, benzene- d_6) of 2-Methyl-*N*-Octasylaziridin (OsMAz)

Experimental Part

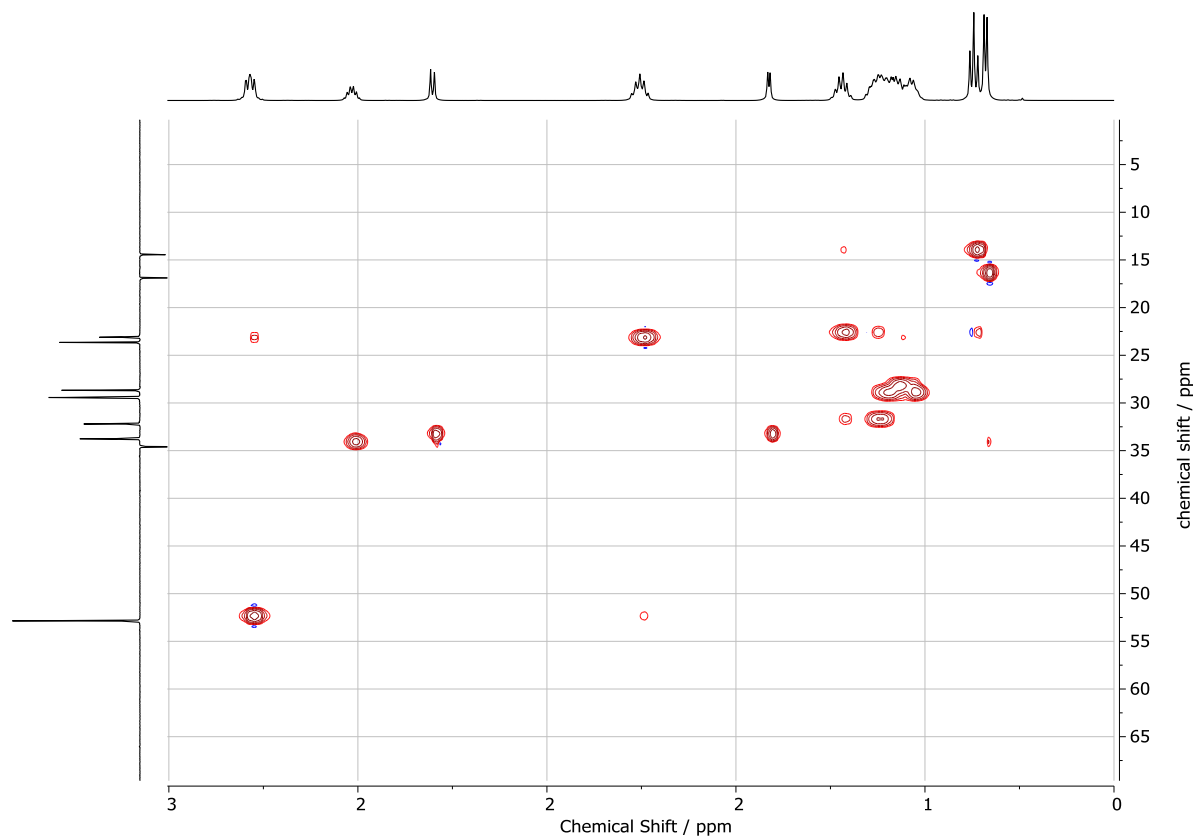


Figure 63: COSY-NMR (700 MHz, benzene- d_6) of 2-Methyl-*N*-Octasylaziridin (OsMAZ)

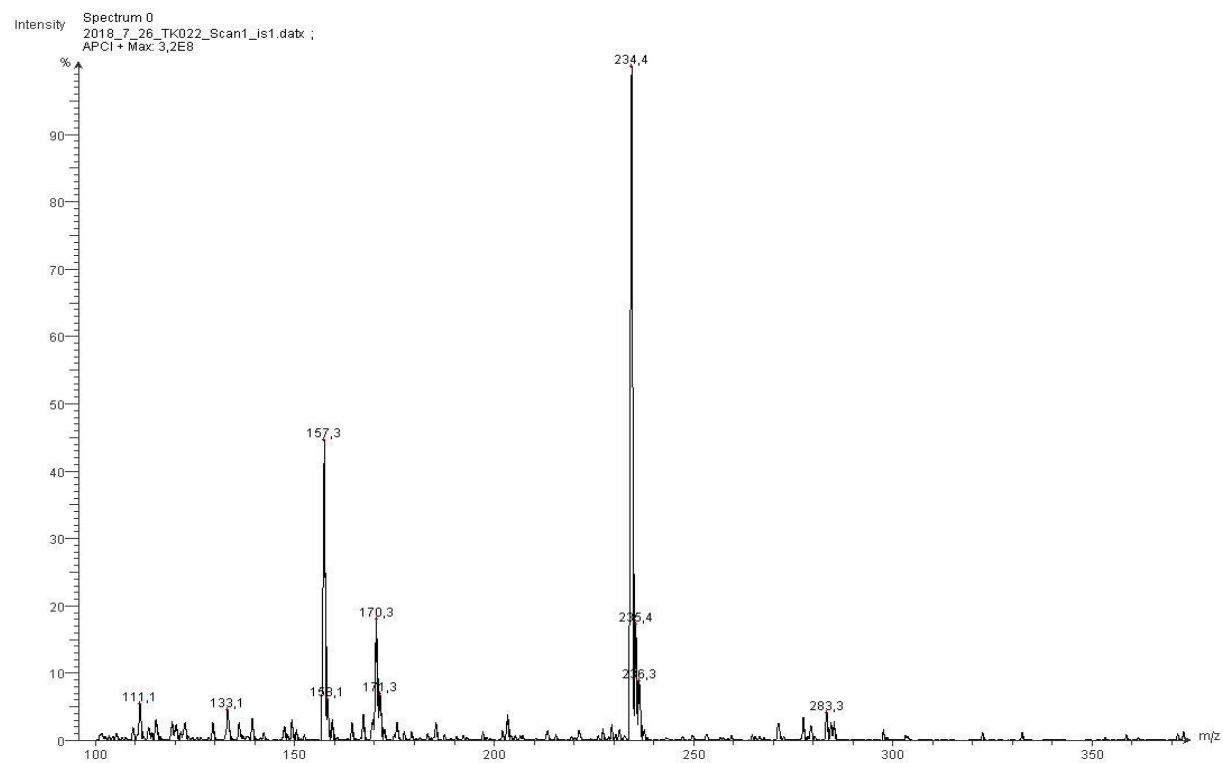


Figure 64: mass spectrum of 2-Methyl-*N*-Octasylaziridin

Experimental Part

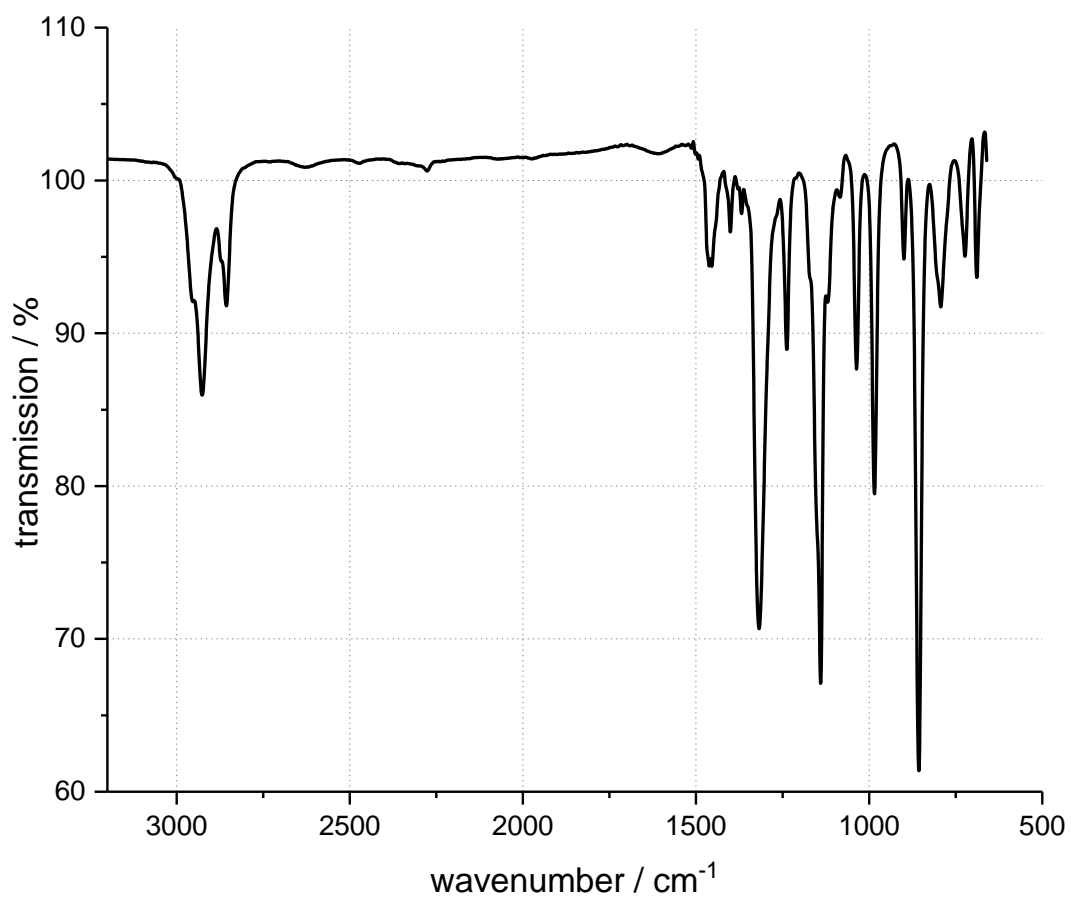
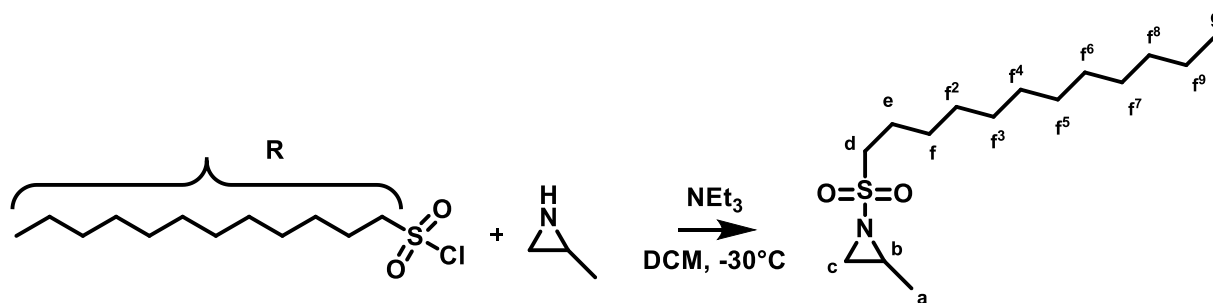


Figure 65: IR-spectrum of 2-Methyl-*N*-Octasylaziridin

2-Methyl-N-Dodesylaziridin (DDsMAz)



Scheme 39: Synthesis of 2-Methyl-N-Dodesylaziridin (DDsMAz)

In a flame dried flask 2-methylaziridin was dried over CaH_2 and cryo transferred for purification. The purified 2-methylaziridin (5.84 ml, 81.8 mmol) was dissolved in dichloromethane and triethylamine (15.5 ml, 111.6 mmol). The solution was cooled to -30°C and dodesylchloride (20 g, 74.4 mmol dissolved in DCM) was added dropwise to the solution. After stirring for 2 hours, the solution was allowed to reach room temperature and was washed with saturated NaHCO_3 and brine. The organic Phase was dried over MgSO_4 and reduced at a rotary evaporator, yielding the product. The product was purified *via* silica chromatography (DCM).

Rf: 100 % DCM: 0,43

Yield: 14.8 g, 51 mmol 69%

^1H NMR (300 MHz, Methylene Chloride- d_2) δ 3.16 – 2.99 (m, 2H), 2.81 – 2.62 (m, 1H), 2.53 (d, $J = 7.0$ Hz, 1H), 2.02 (d, $J = 4.6$ Hz, 1H), 1.93 – 1.75 (m, 2H), 1.48 – 1.12 (m, 20H), 0.88 (t, $J = 6.6$ Hz, 3H).

^{13}C NMR (300 MHz, benzene- d_6) δ 118.38, 53.28, 52.54, 34.32, 33.44, 32.16, 29.89, 29.89, 29.78, 29.63, 29.52, 29.21, 28.40, 23.34, 22.95, 16.58, 14.20.

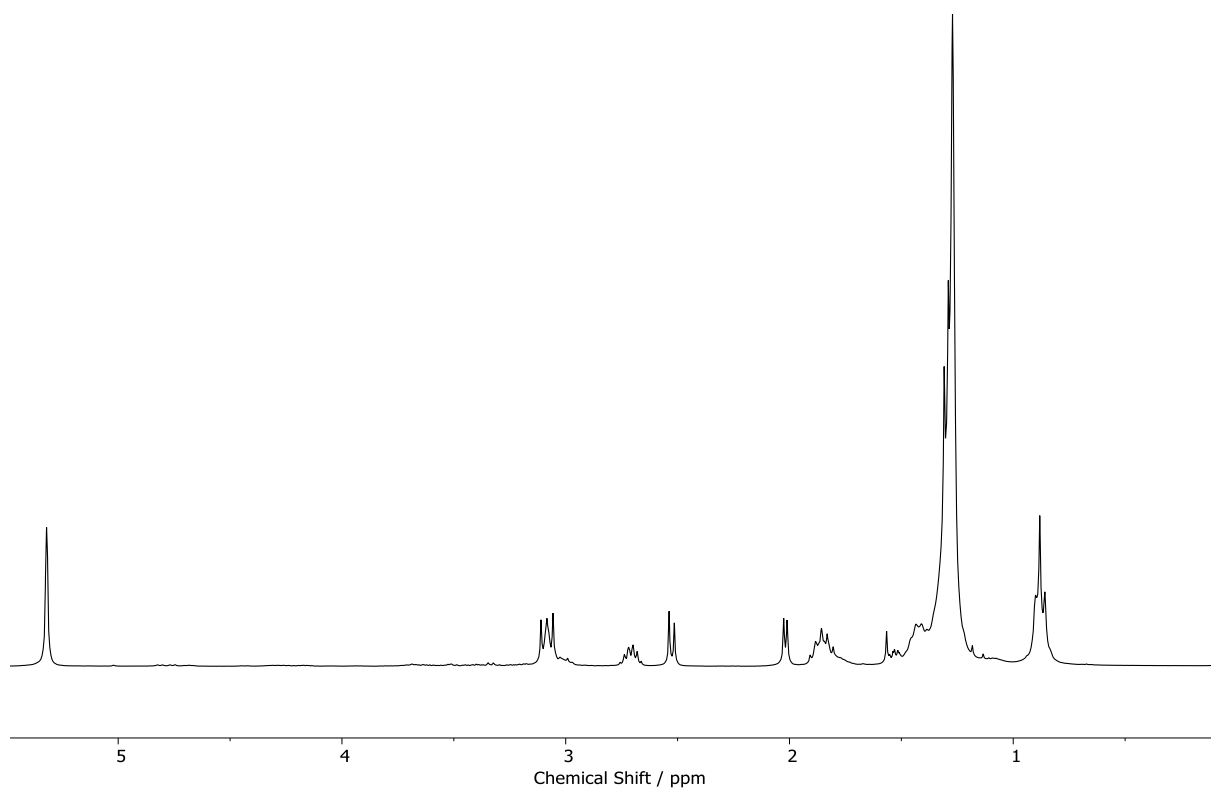


Figure 66: ¹H NMR (300 MHz, Methylene Chloride-*d*₂) of 2-Methyl-N-Dodesylaziridin (DDsMAz)

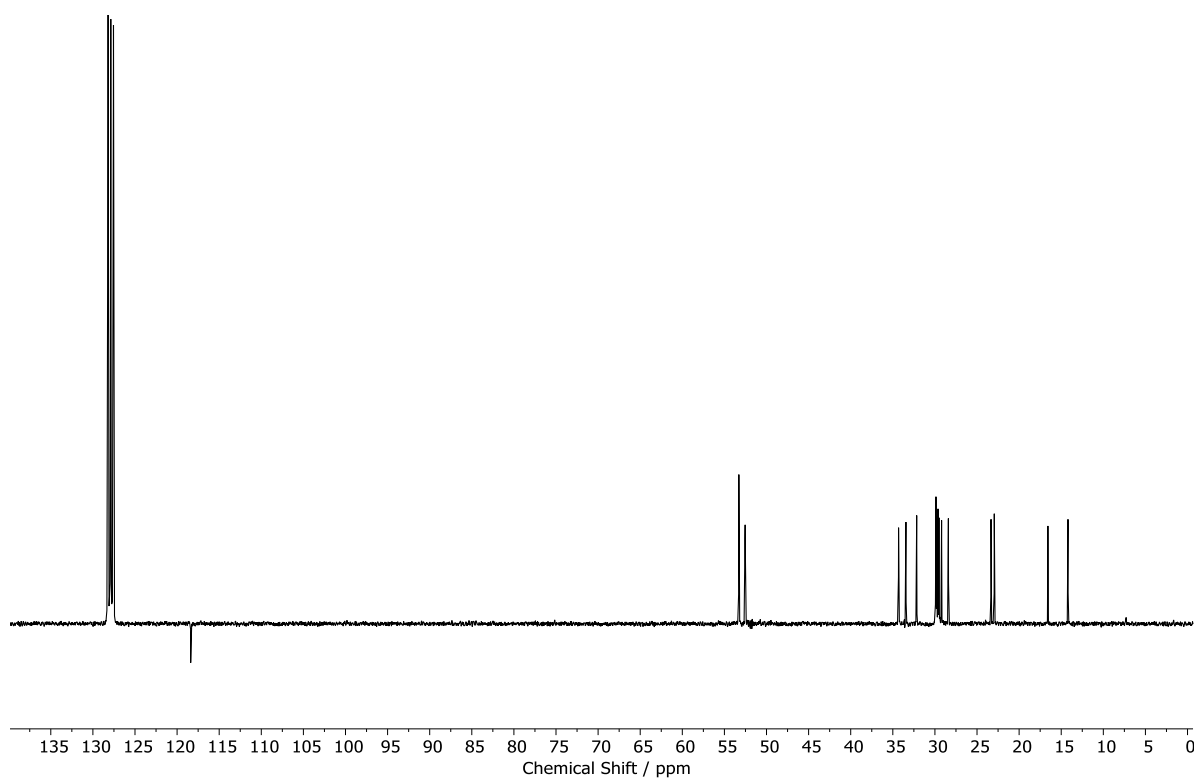
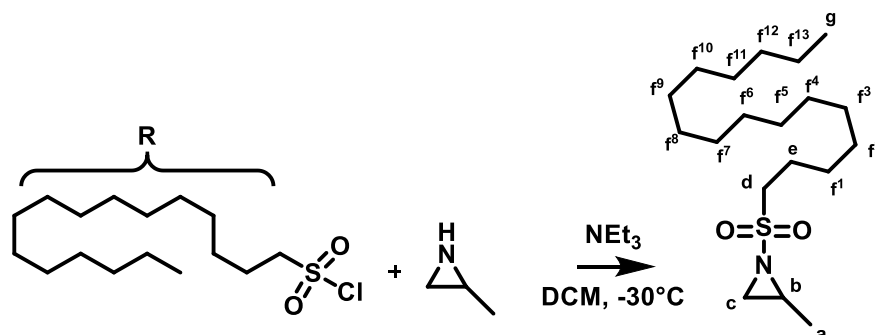


Figure 67: ¹³C NMR (300 MHz, benzene-*d*₆) of 2-Methyl-N-Dodesylaziridin (DDsMAz)

2-Methyl-*N*-Hexadesylaziridin (HDsMAz)**Figure 68:** Synthesis of 2-Methyl-*N*-Hexadesylaziridin (HDsMAz)

In a flame dried flask 2-methylaziridin was dried over CaH_2 and cryo transferred for purification. The purified 2-methylaziridin (6.57 ml, 92.32 mmol) was dissolved in dichloromethane and triethylamine (12.9 ml, 92.3 mmol). The solution was cooled to -30°C and hexadecacylchloride (20 g, 61.55 mmol dissolved in DCM) was added dropwise to the solution. After stirring for 2 hours, the solution was allowed to reach room temperature and was washed with saturated NaHCO_3 and brine. The organic Phase was dried over MgSO_4 and reduced at a rotary evaporator, yielding the product. The product was purified *via* silica chromatography (DCM).

Yield: 15.53 g, 44.9 mmol 73%

Rf: 100 % DCM 0,46

^1H NMR (300 MHz, tetrachloroethane- d_2) δ 3.08 – 2.93 (m, 2H), 2.70 – 2.56 (m, 1H), 2.47 (d, $J = 7.0$ Hz, 1H), 1.96 (d, $J = 4.7$ Hz, 1H), 1.87 – 1.68 (m, 2H), 1.41 – 1.28 (m, 1H), 1.30 – 1.05 (m, 2H), 0.79 (t, $J = 6.5$ Hz, 3H).

^{13}C NMR (300 MHz, tetrachloroethane- d_2) δ 52.33 (d), 35.11 (c), 33.75 (f^{12}), 31.80 (e), 29.83 – 29.08 (m, (f^1 - f^9)), 28.90 (f^{10}), 28.20 (f^{11}), 22.87 (f^{12}), 22.60 (f^{13}), 16.77 (a), 14.11 (g).

Experimental Part

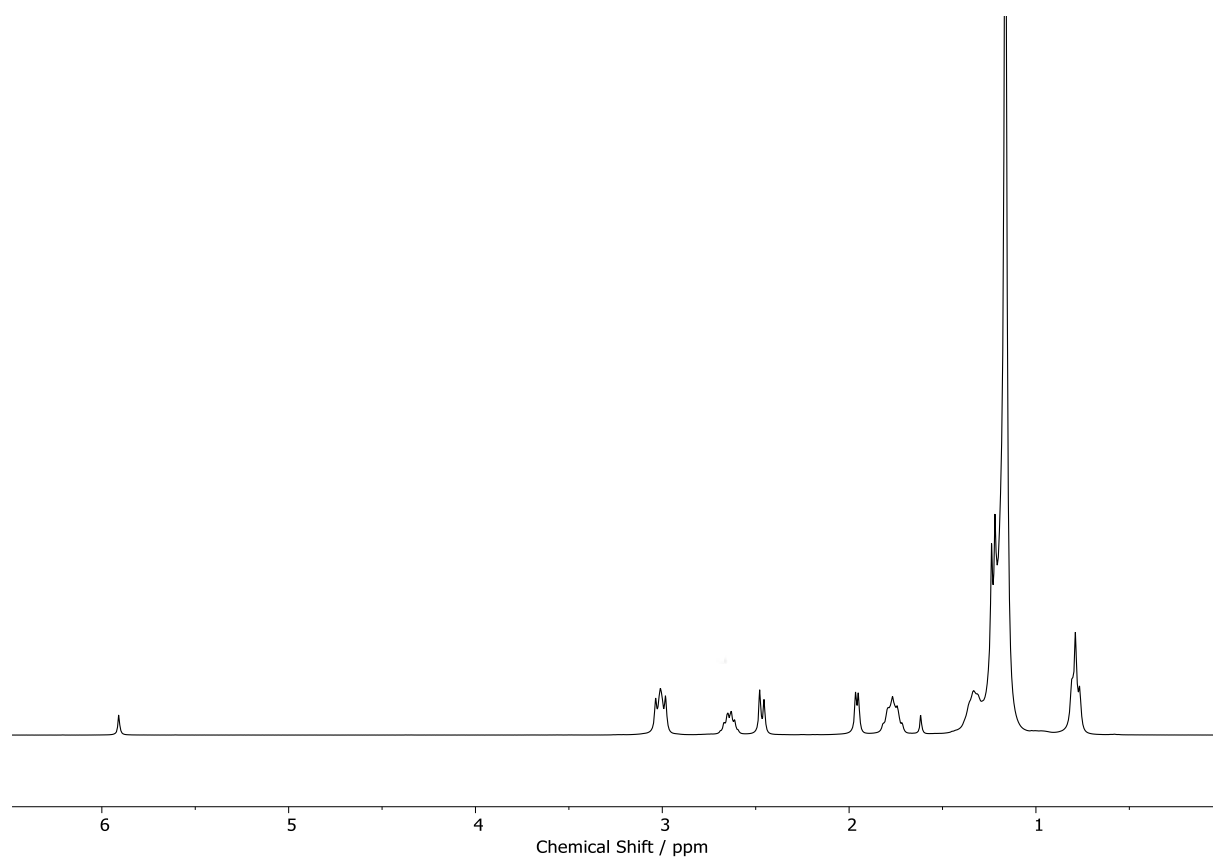


Figure 69: ^1H NMR (300 MHz, $\text{tetrachloroethane-}d_2$) of 2-Methyl-*N*-Hexadesylaziridin (HDsMAz).

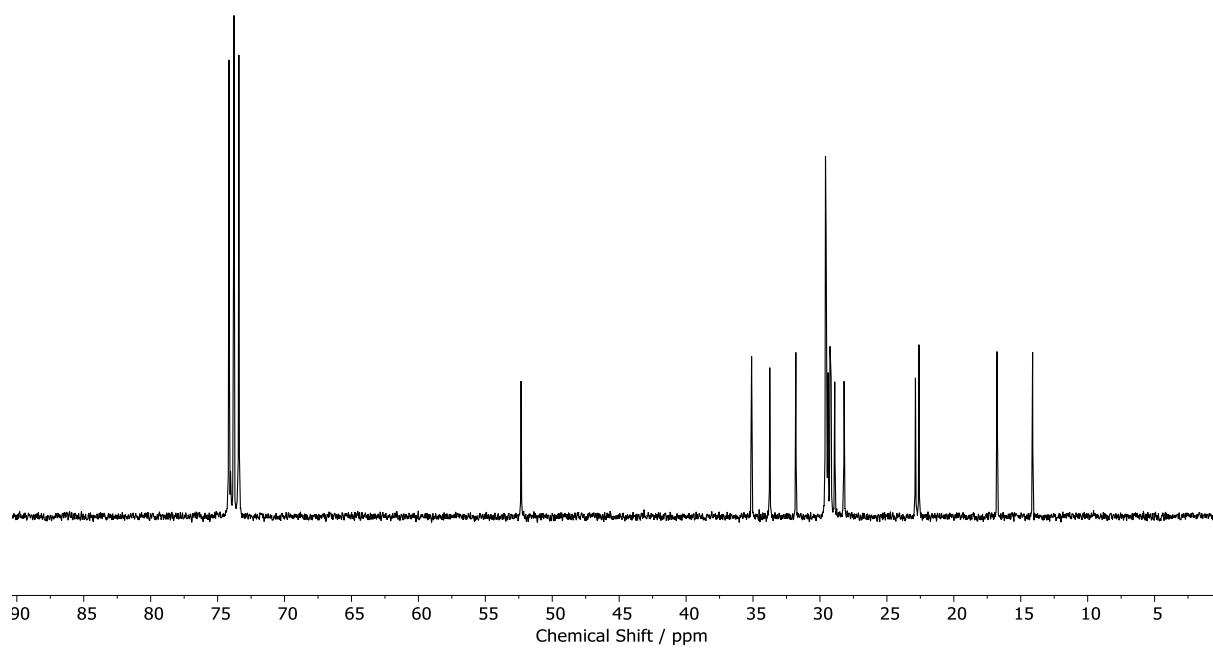
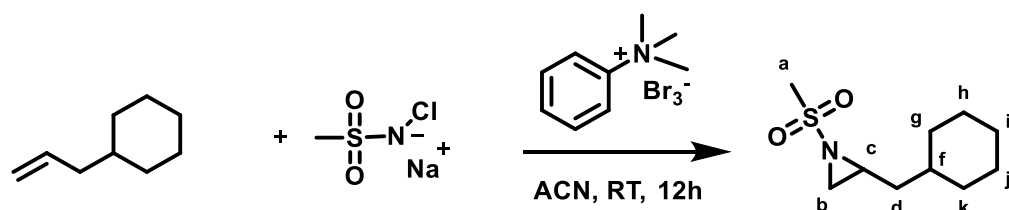


Figure 70: ^{13}C NMR (300 MHz, $\text{tetrachloroethane-}d_2$) of 2-Methyl-*N*-Hexadesylaziridin (HDsMAz).

2-(Cyclohexylmethyl)-N-Mesylaziridin (MsCyhexAz)**Scheme 40:** Synthesis of 2-(Cyclohexylmethyl)-N-Mesylaziridin (MsCyhexAz)

Chloramine-M (6.78 g 44.72 mmol) and allylcyclohexane (5.00 g 40.25 mmol) were dissolved in dry acetonitrile (200 ml) and trimethylphenylammonium tribromide (1.53 g, 4.06 mmol) was added. The solution was stirred for 48 h by room temperature and ethyl acetate (40 ml) and deionized water (40 ml) were added. The organic phase was separated, washed with brine and dried over MgSO_4 . The solvent was evaporated under reduced pressure and the obtained product purified through silica chromatography (EtAc: CyHex 2:8, Rf: 0.33) .

Yield: 4,2g, 19.3 mmol 48%

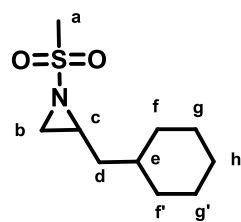
^1H NMR (700 MHz, benzene- d_6) δ 2.63 – 2.56 (m, 1H, c), 2.55 – 2.42 (m, 3H, a), 2.29 (d, J = 7.0 Hz, 1H, b), 1.63 – 1.49 (m, 6H, b,f,f',g,g',h (eq)), 1.27 – 1.19 (m, 1H, e), 1.18 – 1.07 (m, 3H, f, f, h), 1.07 – 0.96 (m, 2H, g, g'), 0.81 – 0.65 (m, 2H, d).

^{13}C NMR (700 MHz, benzene- d_6) δ 39.31, 39.20, 37.49, 36.30, 33.55, 32.80, 26.67, 26.44, 26.37.

Masse: m/z: 218.3 (M^+)

IR (ν cm^{-1}): 2924, 2852, 1450, 1311, 1150

Experimental Part



benzene

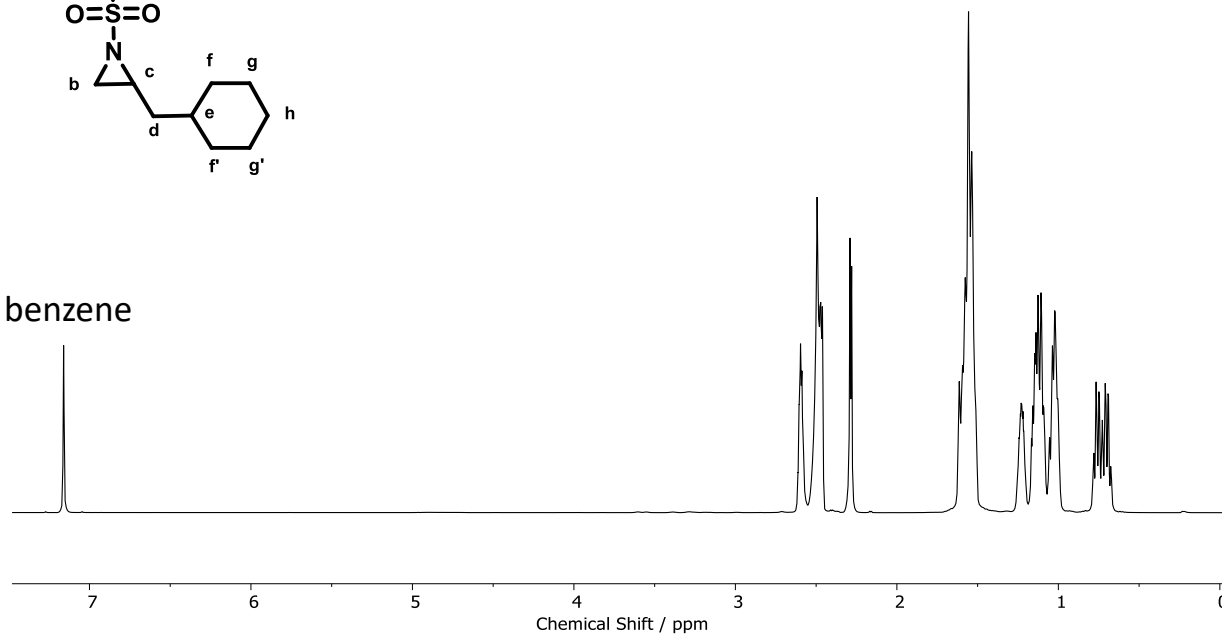


Figure 71: ¹H NMR (700 MHz, Benzene-d₆) of (MsCyhexAz).

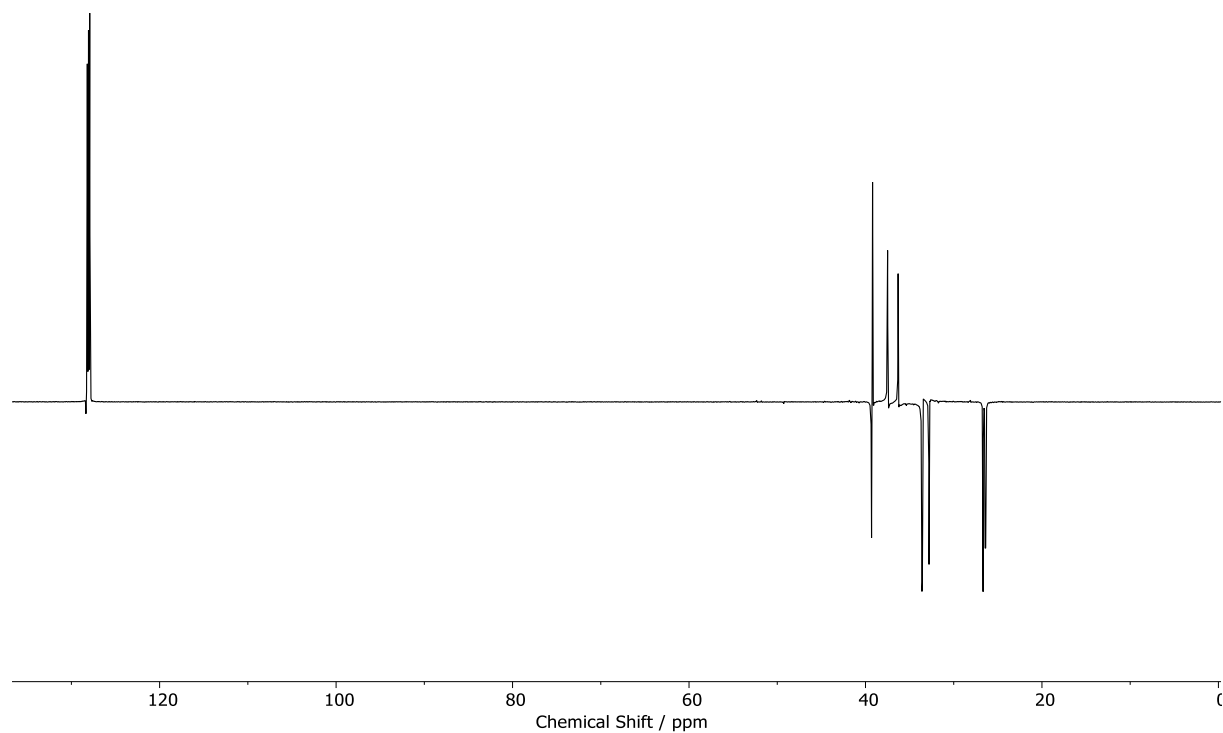


Figure 72: ¹³C NMR (700 MHz, benzene-d₆) of (MsCyhexAz).

Experimental Part

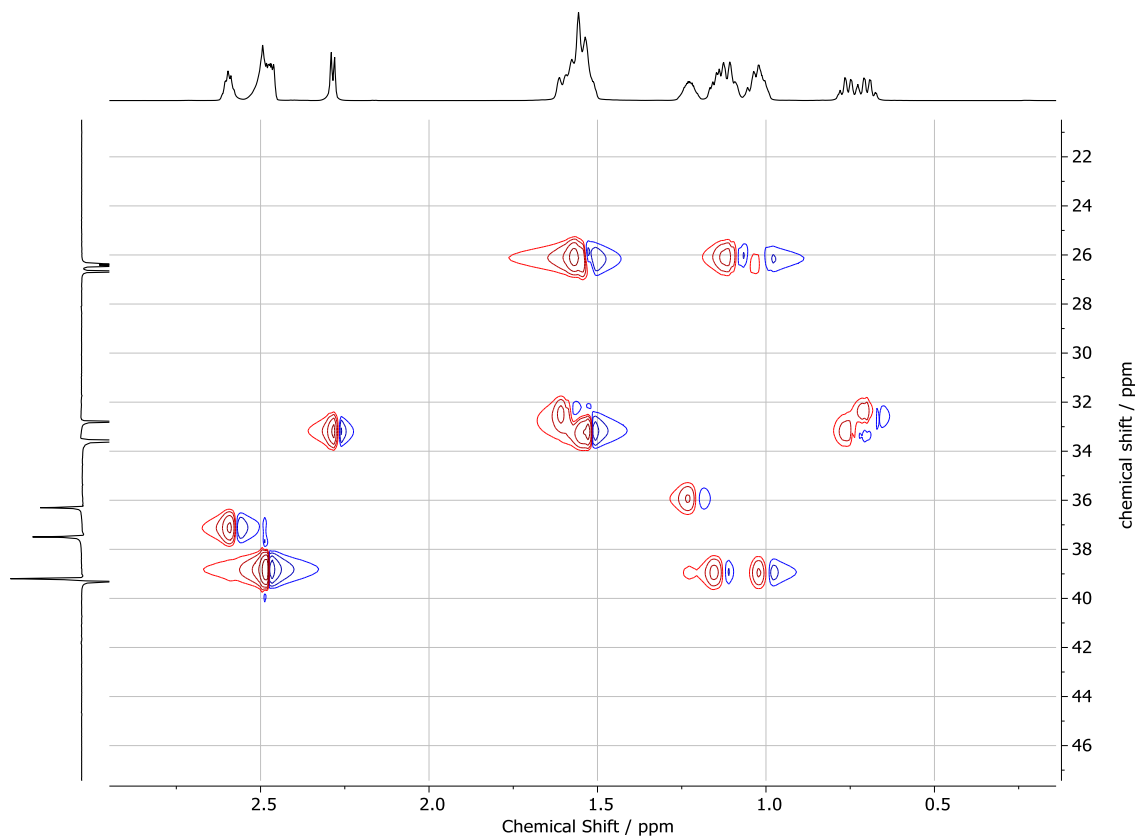


Figure 73: COSY NMR (700 MHz, benzene-d₆) of (MsCyhexAz).

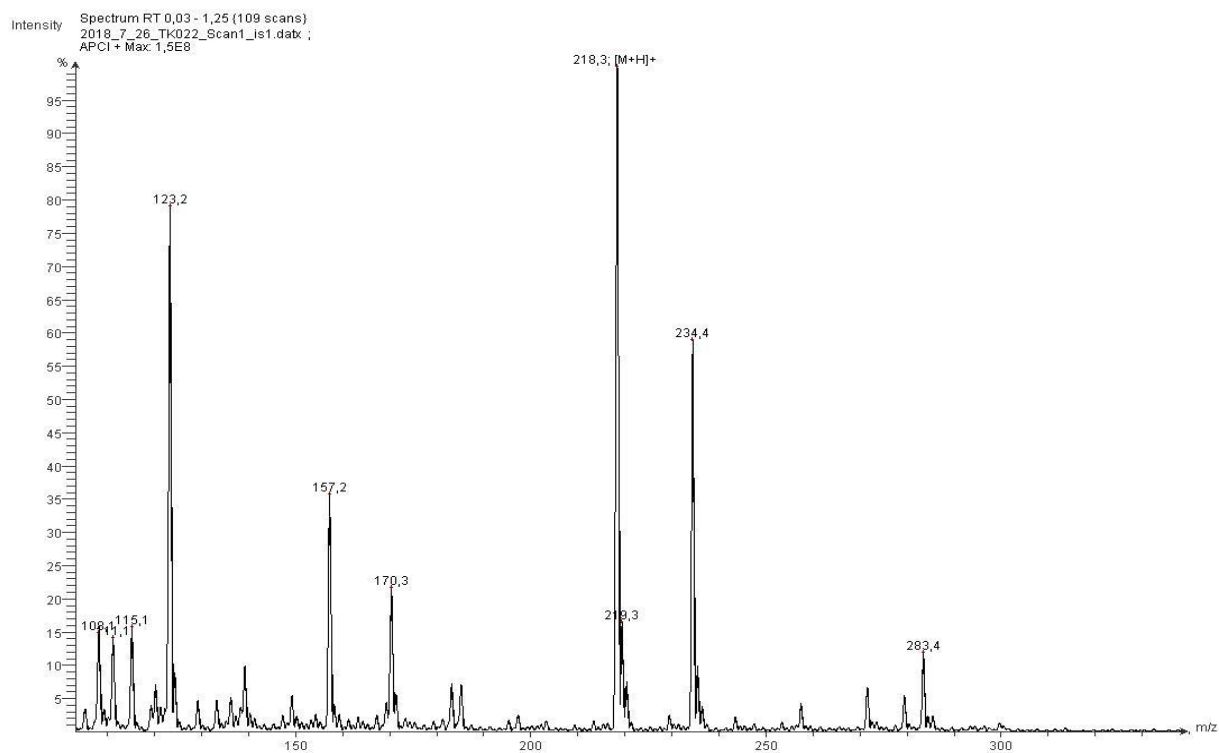


Figure 74: mass spectrum of (MsCyhexAz).

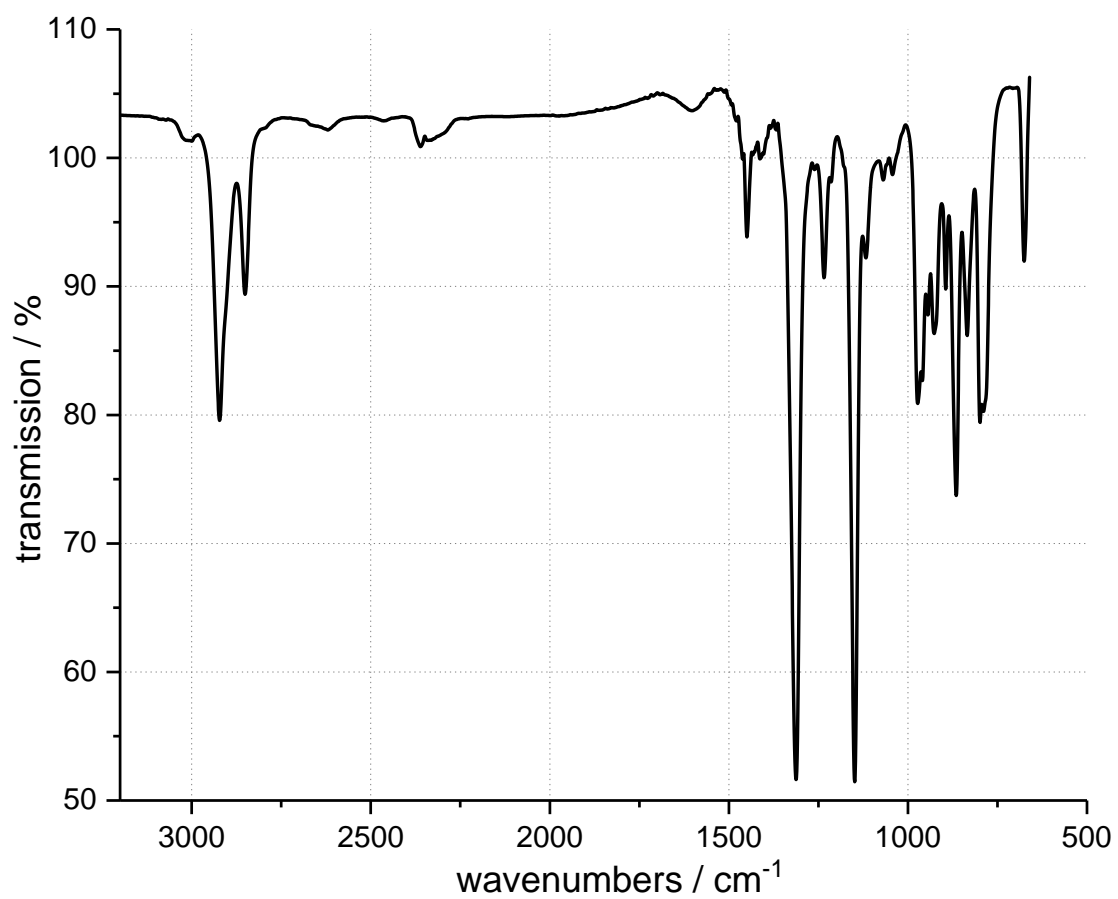
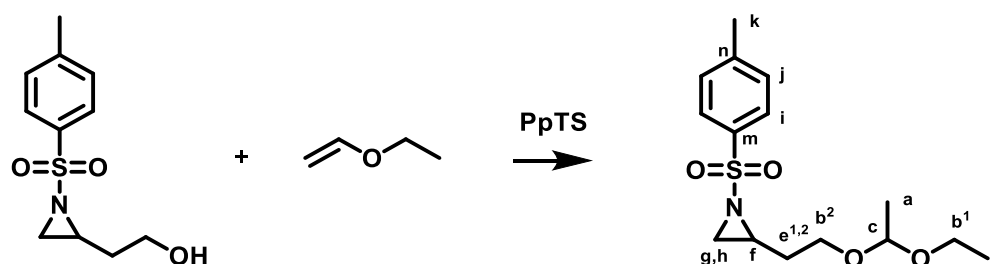


Figure 75: IR-spectrum of (MsCyhexAz).

2-((1-Ethylethoxy)ethyl)-*N*-Tosylaziridine (TsEtOHAz)²¹**Scheme 41:** Synthesis of 2-((1-Ethylethoxy)ethyl)-*N*-Tosylaziridine.

In a flame dried flask ethyl vinyl ether (30 ml, 310.8 mmol) was cryo-transferred for purification. 2-Ethanol-*N*-Tosylaziridin (5 g, 20.7 mmol) and pyridinium *p*-toluenesulfonate (0.02 eq. 104 mg, 414 μ mol) were added and stirred by -10 °C. The solution was stirred over night while reaching room temperature. After neutralizing with K_2CO_3 the solvent was removed on a rotary evaporator and the crude product purified through column chromatography.

Yield: 5.52 g, 17.6 mmol 85%

Rf: (EtAc:PE 1:3 0.5)

1H NMR (300 MHz, DCM- d_2) δ 7.79 (d, J = 8.2 Hz, 2H, i), 7.36 (d, J = 8.0 Hz, 2H, j), 4.58 (q, J = 5.3 Hz, 1H, c), 4.47 (q, J = 5.3 Hz, 1H, c'), 3.63 – 3.20 (m, 4H, b^{1,2}), 2.86 – 2.74 (m, 1H, f), 2.60 (dd, J = 7.1, 5.4 Hz, 1H, g), 2.44 (s, 3H), 2.11 (t, J = 4.4 Hz, 1H, h), 1.88 – 1.72 (m, 1H, e¹), 1.63 – 1.44 (m, 1H, e²), 1.25 – 1.09 (m, 6H, a)

^{13}C NMR (300 MHz, DCM- d_2) δ 145.25 (s, m), 135.61 (s, n), 130.22 (d, j), 128.45 (d, i), 100.28 (d, c), 62.82 (d, b), 61.50 (d, b), 38.50 (d, e), 34.01 (g/h), 32.43 (f), 21.90 (k), 20.18 (a), 15.69 (a).

Experimental Part

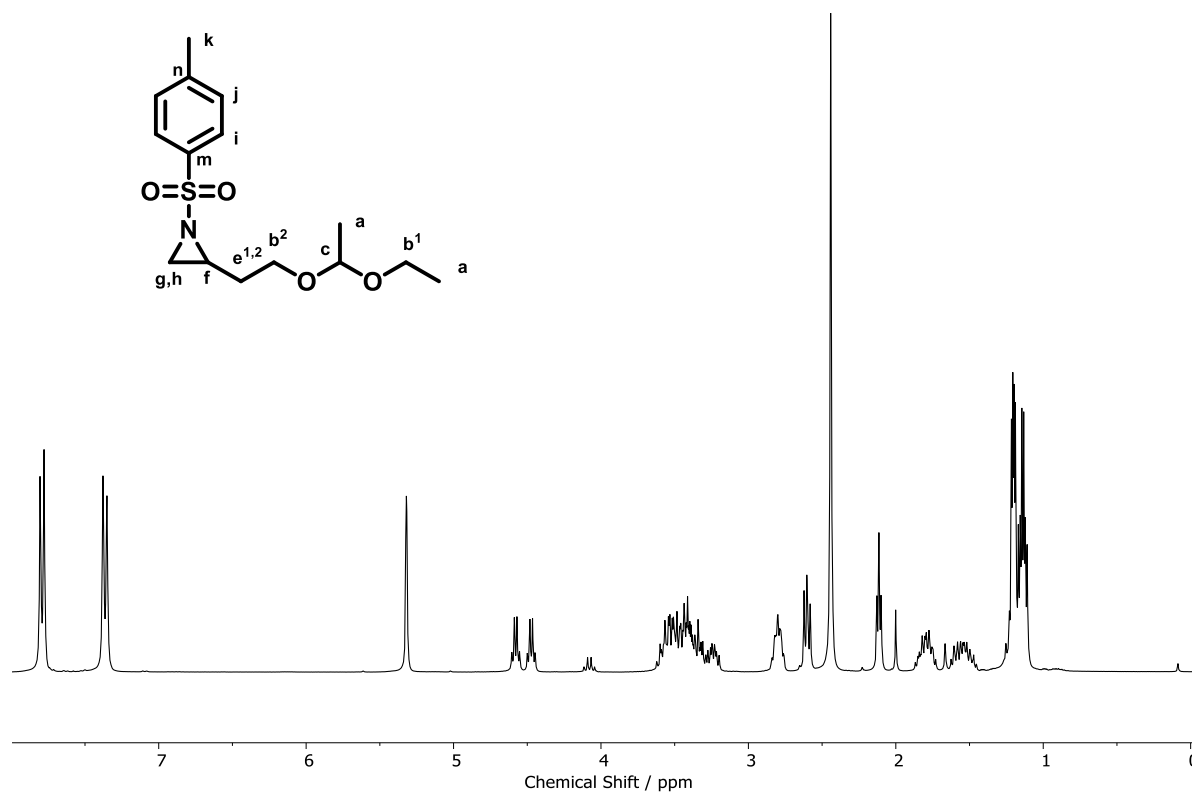


Figure 76: ^1H NMR (300 MHz, DCM-d_2) of 2-((1-Ethylethoxy)ethyl)-N-Tosylaziridine.

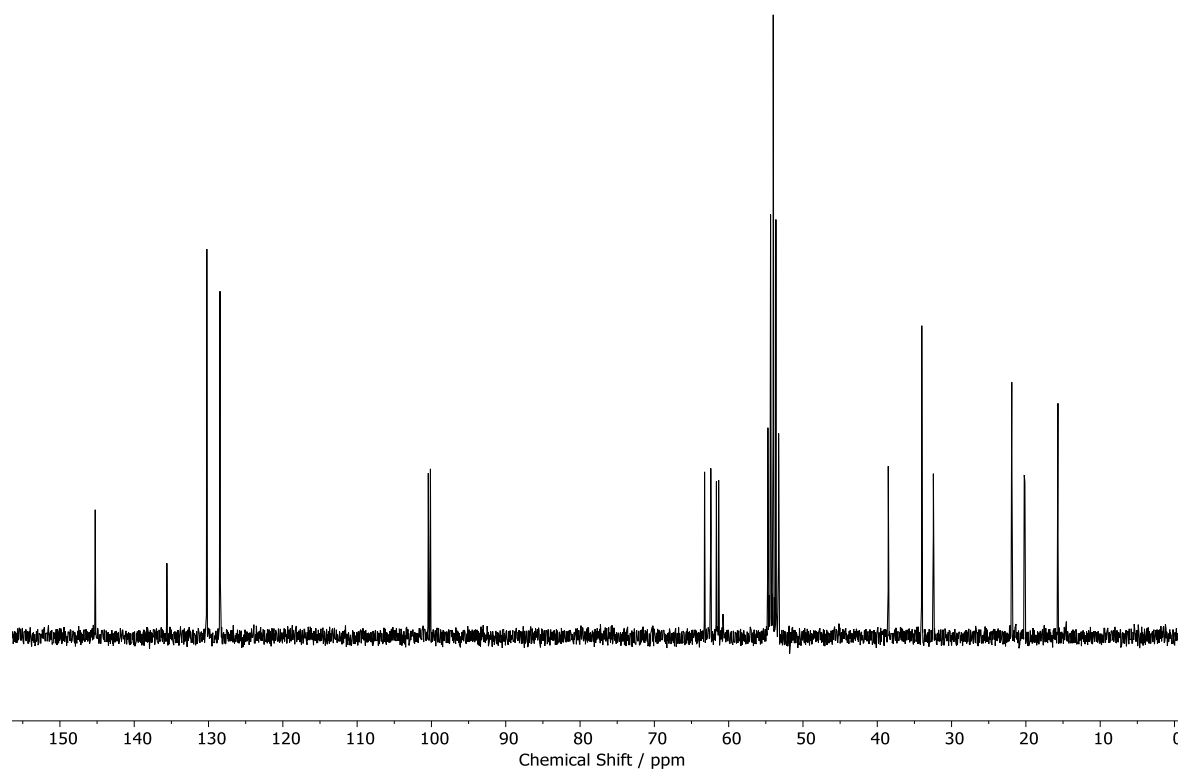
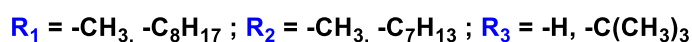
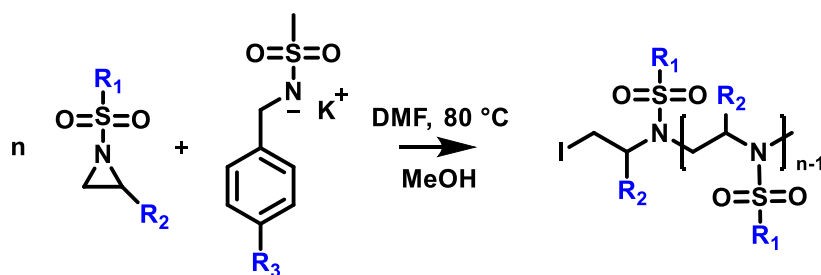
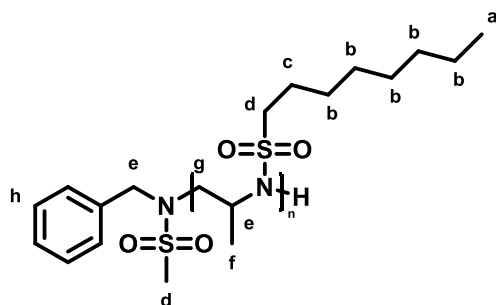


Figure 77: ^{13}C NMR (300 MHz, DCM-d_2) of 2-((1-Ethylethoxy)ethyl)-N-Tosylaziridine.

9.3 Polymer synthesis

Scheme 42: general polymer synthesis.

Reactions were carried out in flame-dried Schlenk tubes, while all educts were dried with benzene under reduced pressure (only exception potassium bis(trimethylsilyl)amide (KHMDs) which was dried overnight under reduced pressure). The dried monomers were dissolved in dry *N,N*-dimethylformamide (DMF) while the Initiator (BnNHMS) was dissolved in DMF (1 ml) and added to the solid KHMDs. After 1 minute, the activated Initiator was transferred into the monomer solution, which was stirred in a preheated oil bath (60-80 °C) for 12-24 h. Following a ¹H NMR analysis that showed the total conversion of the monomer the polymer was precipitated in Methanol or deionized water (30-40 ml), centrifuged and dried *in vacuo*.

9.3.1 Poly(2-Methyl-*N*-octasylaziridin) (Poly(OsMAz))

sample	X_n	Initiator	M_n (NMR) g/mol	M_n (GPC) g/mol	\bar{D}
P(OsMAz)	14	BnNHMs	3400	1600	1.24
P(OsMAz)	31	BnNHMs	7400	3200	1.15
P(OsMAz)	32	BnNHMs	7600	6900*	1.14
P(OsMAz)	58	BnNHMs	13700	5500	1.16
P(OsMAz)	116	BnNHMs	27100	8500	1.21

Poly(OsMAz)₁₄

starting material: OsMAz (12.5 g, 64.28 mmol), BnNHMs (1.00 g, 5.40 mmol),
KHMDS (969.57 mg, 4.86 mmol)

¹H NMR (300 MHz, methylene chloride-*d*₂) δ 7.50 – 7.30 (m, h), 4.09 – 3.67 (m, e),
3.50 – 3.20 (m, g), 3.16 – 2.92 (m, d), 1.96 – 1.63 (m, c), 1.52 – 1.11 (m, b, f), 1.03 –
0.77 (m, a).

Poly(OsMAz)₃₁

starting material: OsMAz (500.0 mg, 2.14 mmol), BnNHMs (15.88 mg, 85.70 μ mol),
KHMDS (15.39 mg, 77.15 μ mol)

¹H NMR (300 MHz, methylene chloride-*d*₂) δ 7.52 – 7.28 (m, h), 4.06 – 3.68 (m, e),
3.56 – 3.16 (m, g), 3.15 – 2.91 (m, d), 1.94 – 1.69 (m, c), 1.63 – 1.49 (m, f), 1.49 – 1.23
(m, b), 0.98 – 0.80 (m, a).

Experimental Part

Poly(OsMAz)₃₂

starting material: OsMAz (12.5 g, 64.28 mmol), BnNHMs (1.00 g, 5.40 mmol),
KHMDs (969.57 mg, 4.86 mmol)

¹H NMR (300 MHz, methylene chloride-*d*₂) δ 7.50 – 7.30 (m, h), 4.09 – 3.67 (m, e),
3.50 – 3.20 (m, g), 3.16 – 2.92 (m, d), 1.96 – 1.63 (m, c), 1.52 – 1.11 (m, b, f), 1.03 –
0.77 (m, a).

Poly(OsMAz)₅₈

starting material: OsMAz (500.0 mg, 2.14 mmol), BnNHMs (7.94 mg, 42.85 μmol),
KHMDs (7.70 mg, 38.58 μmol)

¹H NMR (300 MHz, Tetrachloroethane-*d*₂) δ 7.40 – 7.21 (m, h), 4.05 – 3.54 (m, e), 3.46
– 3.08 (m, g), 3.05 – 2.84 (m, d), 1.84 – 1.55 (m, c, f), 1.46 – 0.98 (m, b), 0.93 – 0.69
(m, a).

Poly(OsMAz)₁₁₆

starting material: OsMAz (500.0 mg, 2.14 mmol), BnNHMs (7.94 mg, 42.85 μmol),
KHMDs (7.70 mg, 38.58 μmol)

¹H NMR (300 MHz, tetrachloroethane-*d*₂) δ 7.47 – 7.21 (m, h), 4.24 – 3.60 (m, e), 3.51
– 3.05 (m, g), 3.17 – 2.82 (m, d), 1.92 – 1.58 (m, c, f), 1.50 – 1.12 (m, b), 0.98 – 0.71
(m, a).

T_g: 42 °C

T_m: 137 °C

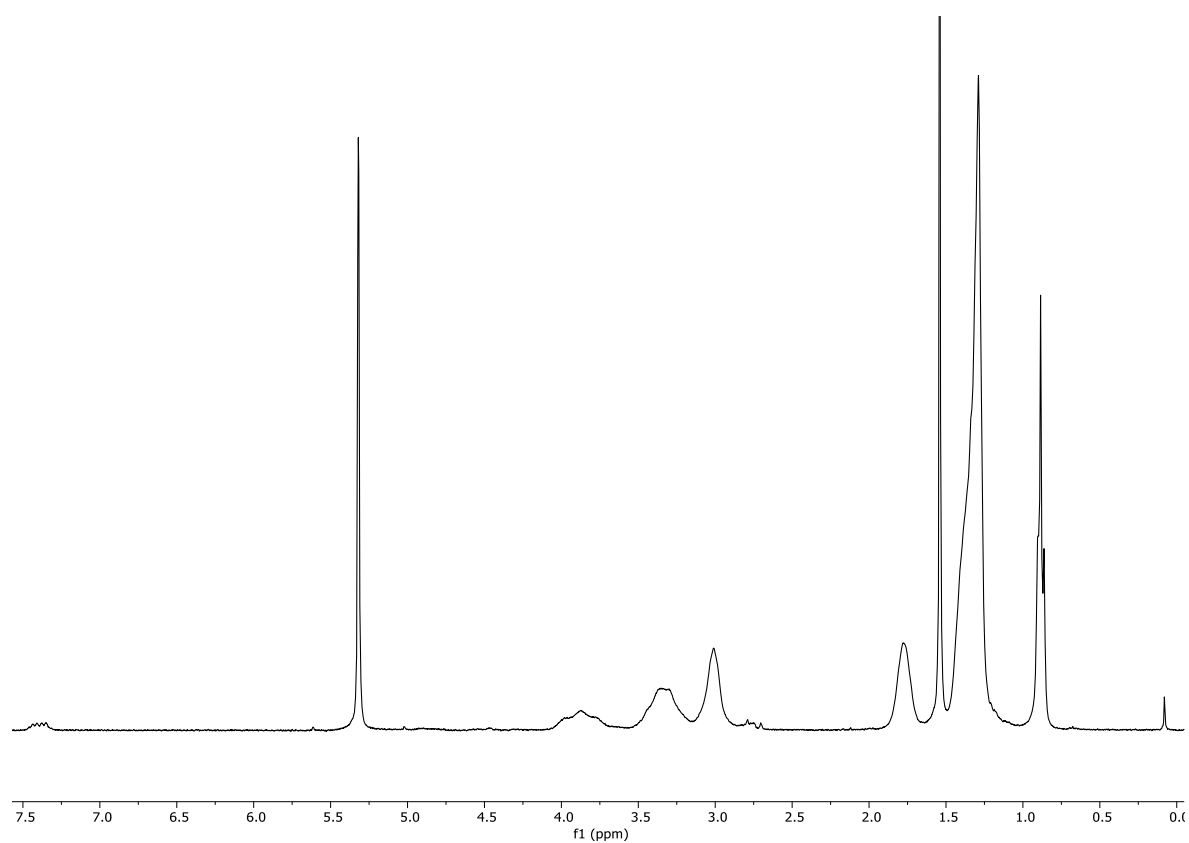


Figure 78: ¹H NMR (300 MHz, methylene chloride-*d*₂) of Poly(2-Methyl-*N*-octasylaziridin).

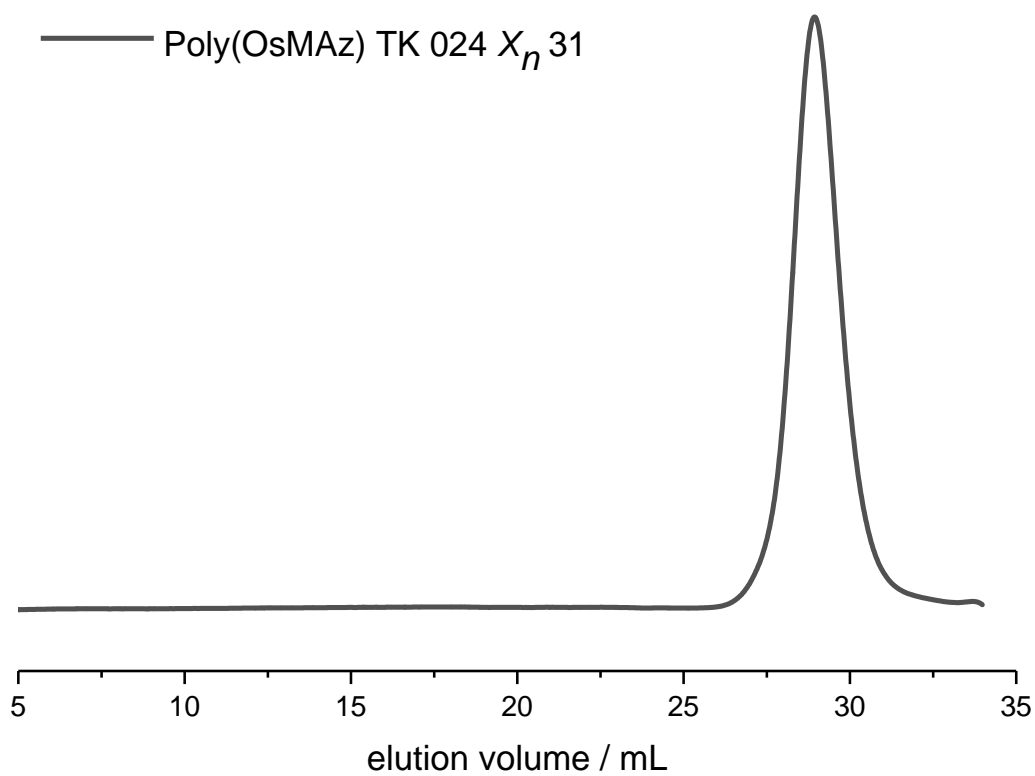


Figure 79: GPC-traces (RI-detection) of Poly(OsMAz) in DMF/PEG standard

Experimental Part

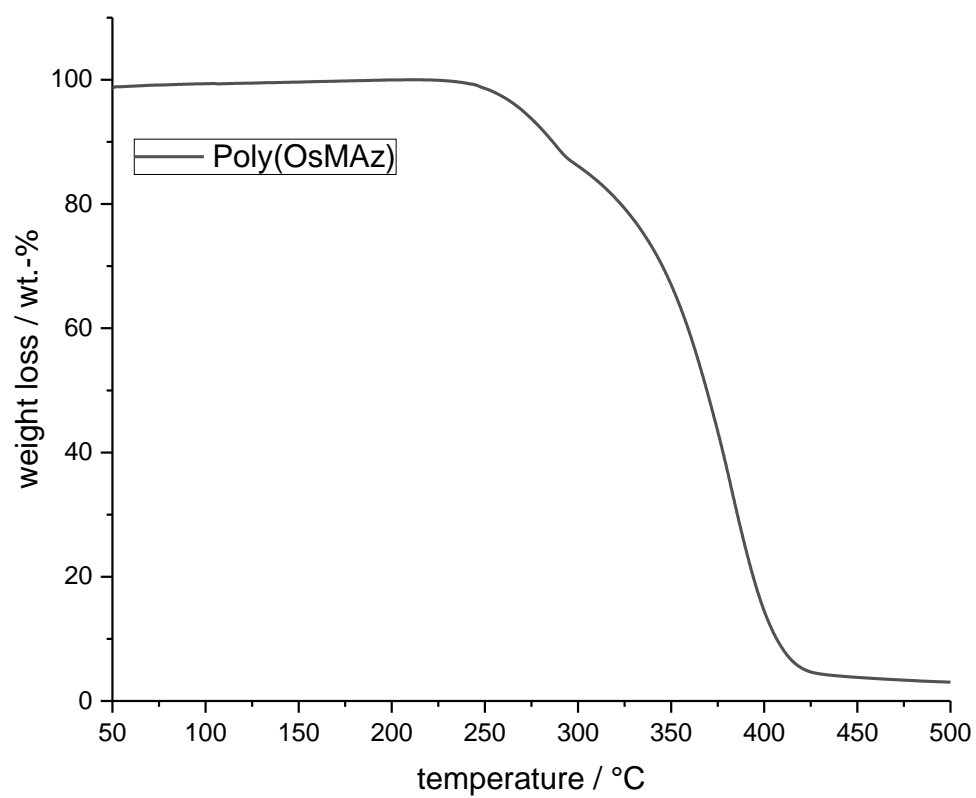


Figure 80: TGA of Poly(OsMAz).

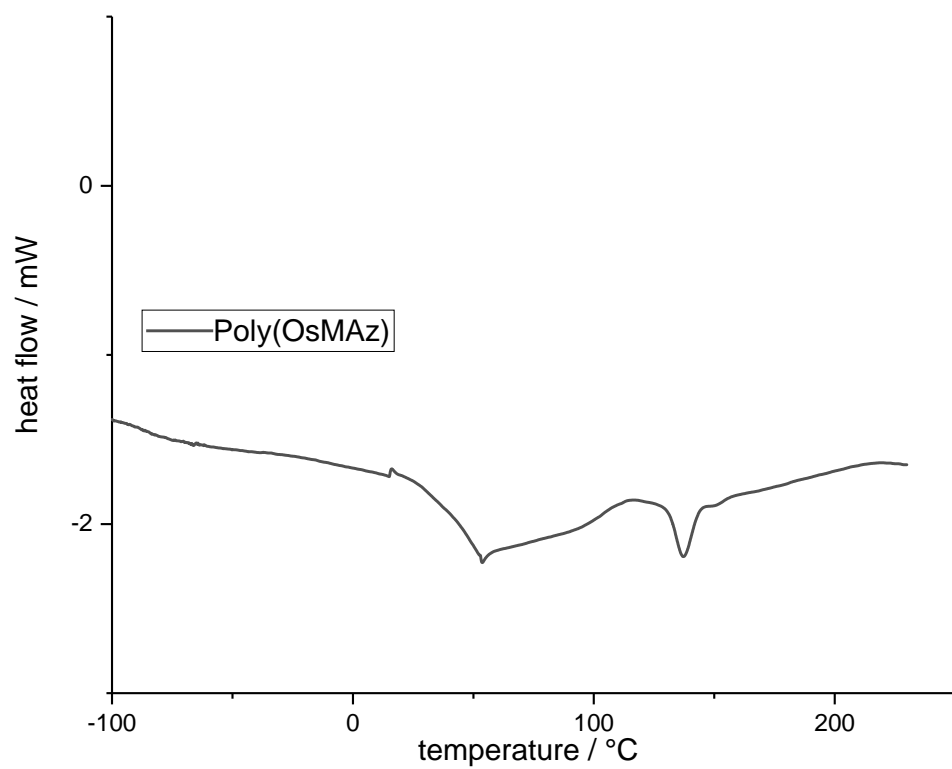
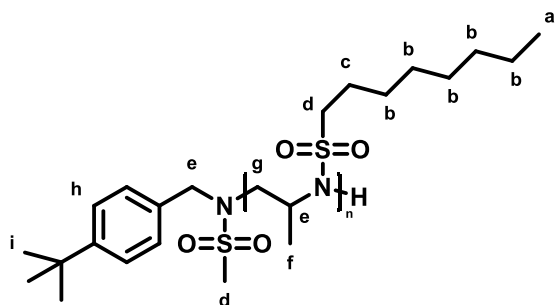


Figure 81: DSC of Poly(OsMAz)

9.3.2 Poly-2-Methyl-N-octasylaziridin (Poly(OsMAz))

sample	X_n	Initiator	M_n (NMR) g/mol	M_n (GPC) g/mol	\bar{D}
Poly(OsMAz)	12	4- ^t b-BnNHMs	3000	1600	1,22
Poly(OsMAz)	13	4- ^t b-BnNHMs	3500	1600	1.21

Poly(OsMAz)₁₃

starting material: OsMAz (500 mg, 2.14 mmol), BnNHMs (51.7 mg, 214 μ mol),
KHMDS (38.5 mg, 193 μ mol)

^1H NMR (300 MHz, methylene chloride- d_2) δ 7.54 – 7.27 (m, h), 4.13 – 3.63 (m, e),
3.49 – 3.16 (m, g), 3.13 – 2.92 (m, d), 1.88 – 1.68 (m, c), 1.65 – 1.13 (m, b, f), 0.93 –
0.84 (m, a, i).

Experimental Part

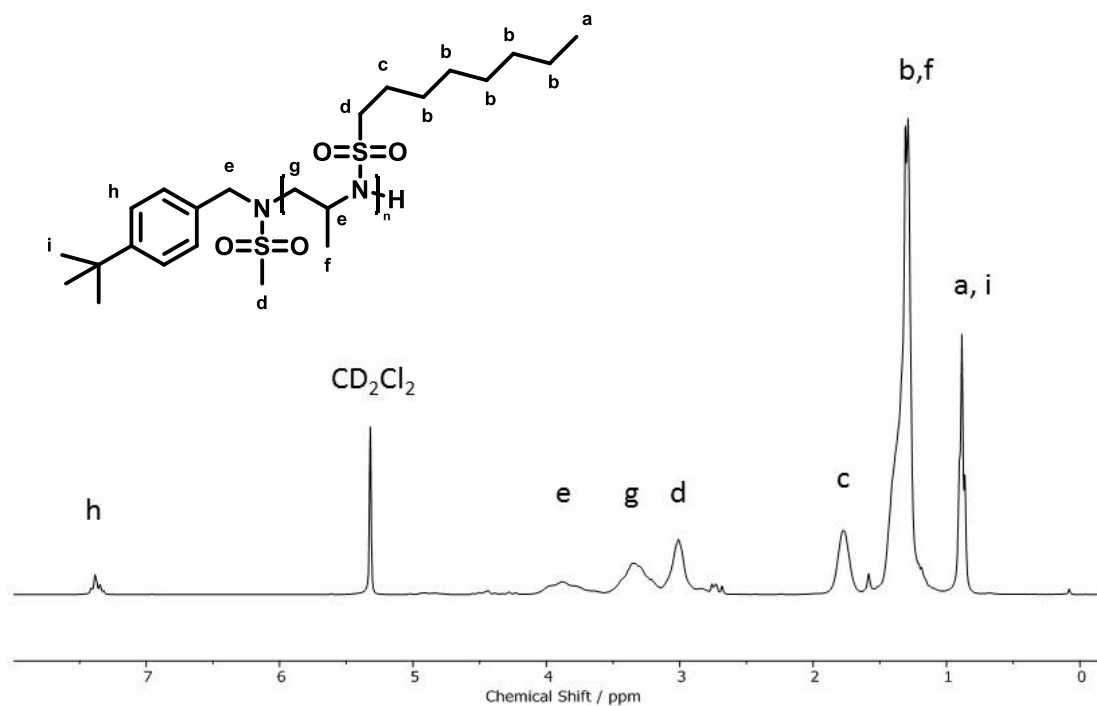


Figure 82: ¹H NMR (300 MHz, Methylene Chloride-*d*₂) of Poly(OsMAz) with 'b-BnNHMs initiator

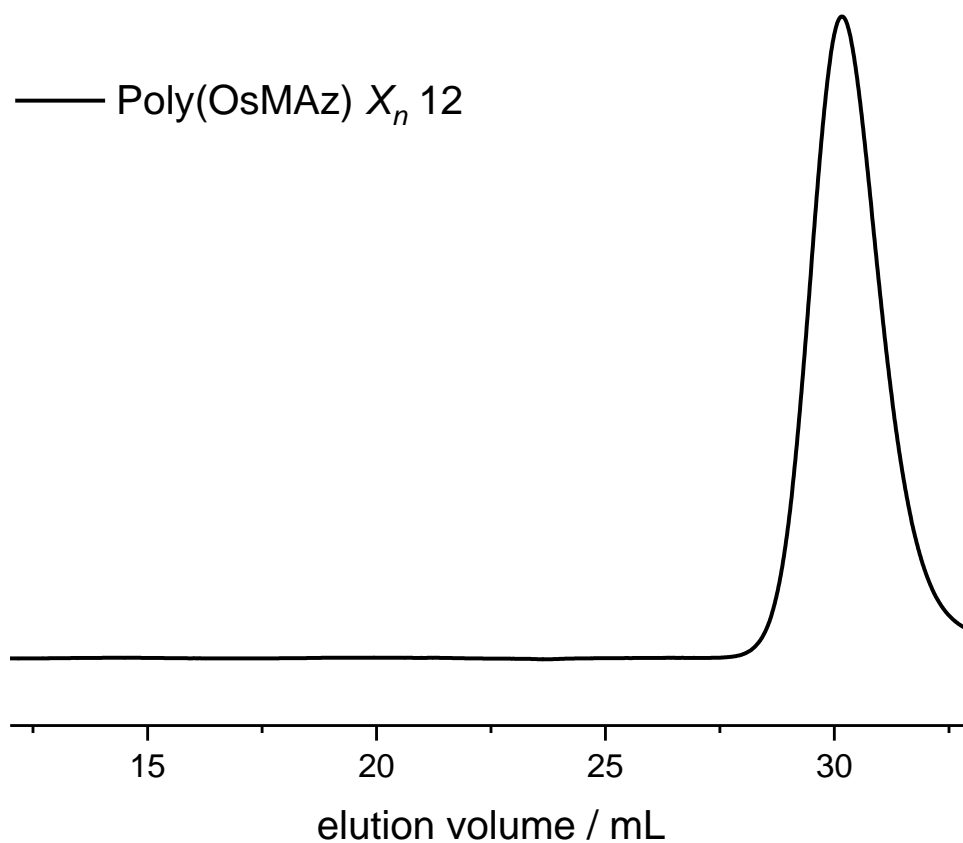
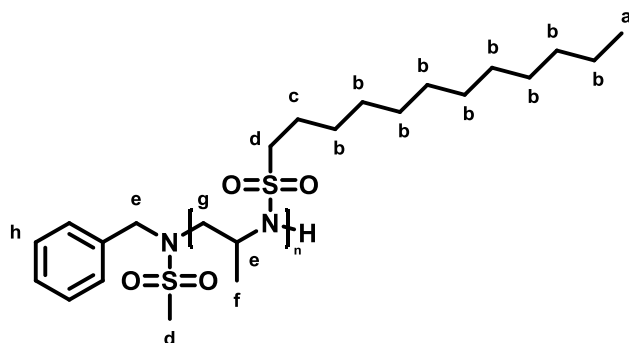


Figure 83: GPC-traces (RI-detection) of Poly(OsMAz) in DMF/ PEG standard

9.3.3 Poly-2-Methyl-N-dodesylaziridin (Poly(DDsMAz))**Table 21:** Overview of successful homo-polymerized Poly(DDsMAz)

sample	X_n	Initiator	M_n (NMR) g/mol	M_n (GPC) g/mol	\bar{D}
Poly(DDsMAz)	48	BnNHMs	14000	8600	1.10
Poly(DDsMAz)	102	BnNHMs	29700	14400	1.12

Poly(DDsMAz)₄₈

starting material: DDsMAz (250 mg, 863.6 μ mol), BnNHMs (5.3 mg, 29 μ mol),
KHMDS (5.2 mg, 26 μ mol)

^1H NMR (300 MHz, Tetrachloroethane- d_2) δ 7.40 – 7.21 (m, h), 4.03 – 3.53 (m, e), 3.52 – 3.06 (m, g), 3.06 – 2.78 (m, d), 1.84 – 1.58 (m, c), 1.47 – 1.02 (m, b,f), 0.90 – 0.67 (m, a).

Poly(DDsMAz)₁₀₂

starting material: DDsMAz (250 mg, 863.6 μ mol), BnNHMs (2.7 mg, 14 μ mol),
KHMDS (2.6 mg, 13 μ mol)

^1H NMR (300 MHz, tetrachloroethane- d_2) δ 7.42 – 7.23 (m, h), 4.09 – 3.58 (m, e), 3.54 – 3.09 (m, g), 3.07 – 2.71 (m, d), 1.86 – 1.58 (m, c), 1.47 – 1.01 (m, b,f), 0.89 – 0.69 (m, a).

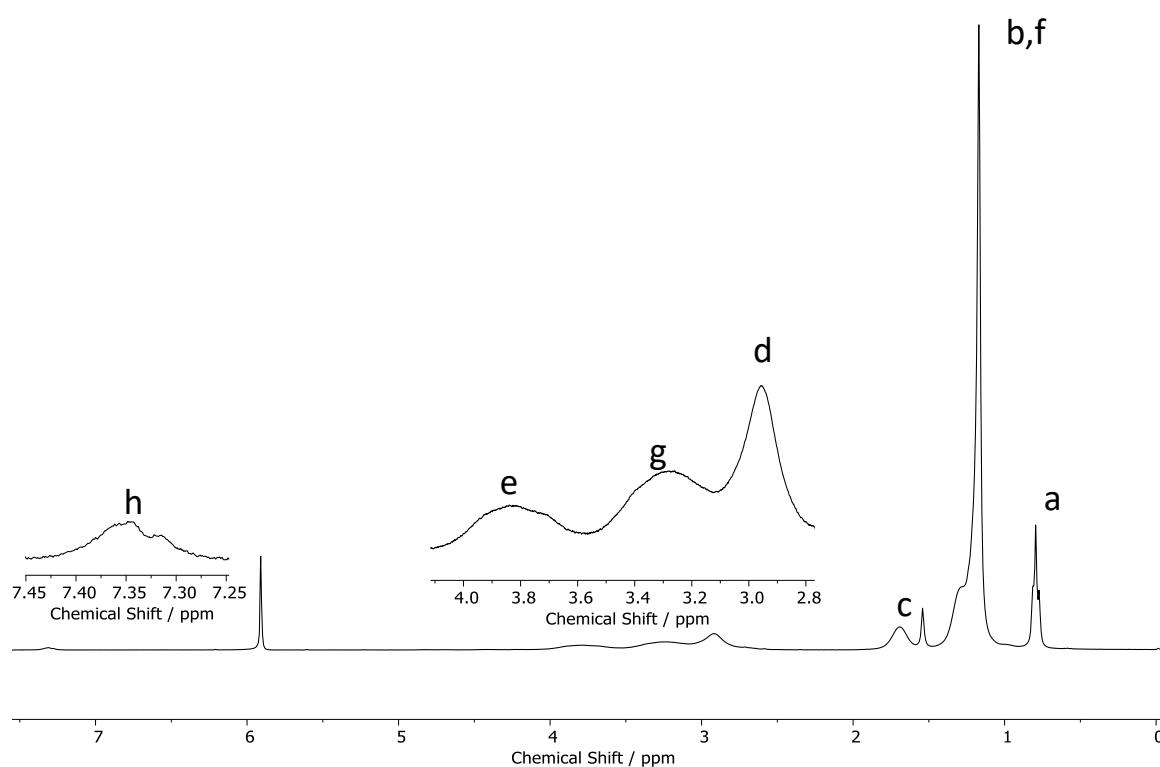


Figure 84: ^1H NMR (300 MHz, $\text{tetrachloroethane-}d_2$) of Poly(2-methyl-*N*-dodesylaziridine) Poly(DDsMAz).

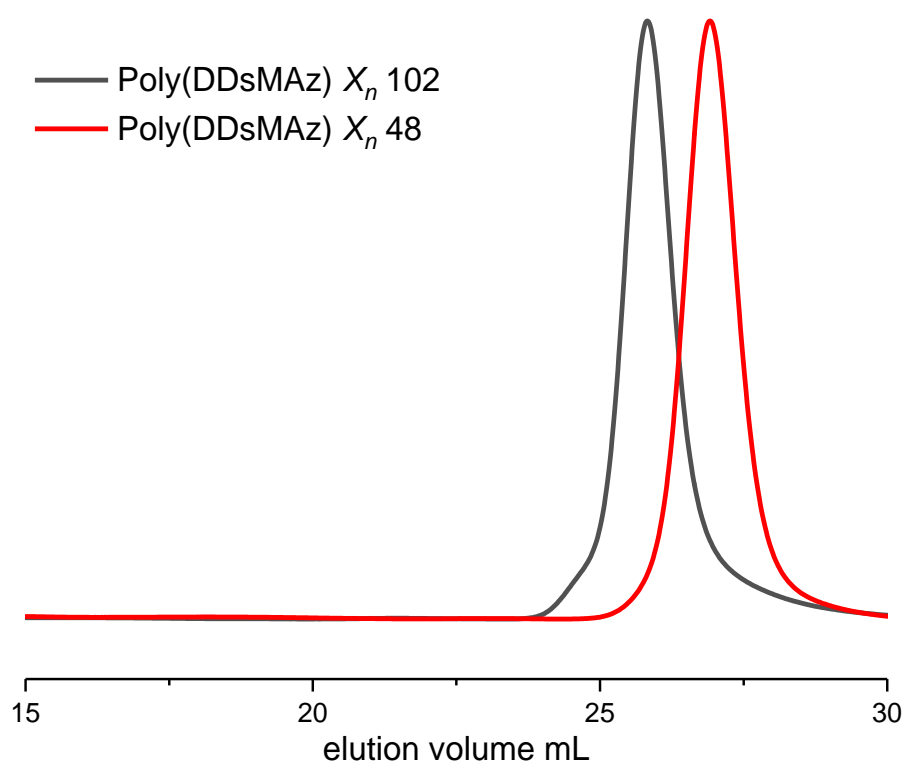


Figure 85: GPC traces of *homo*-polymerized Poly(DDsMAz) in THF.

Experimental Part

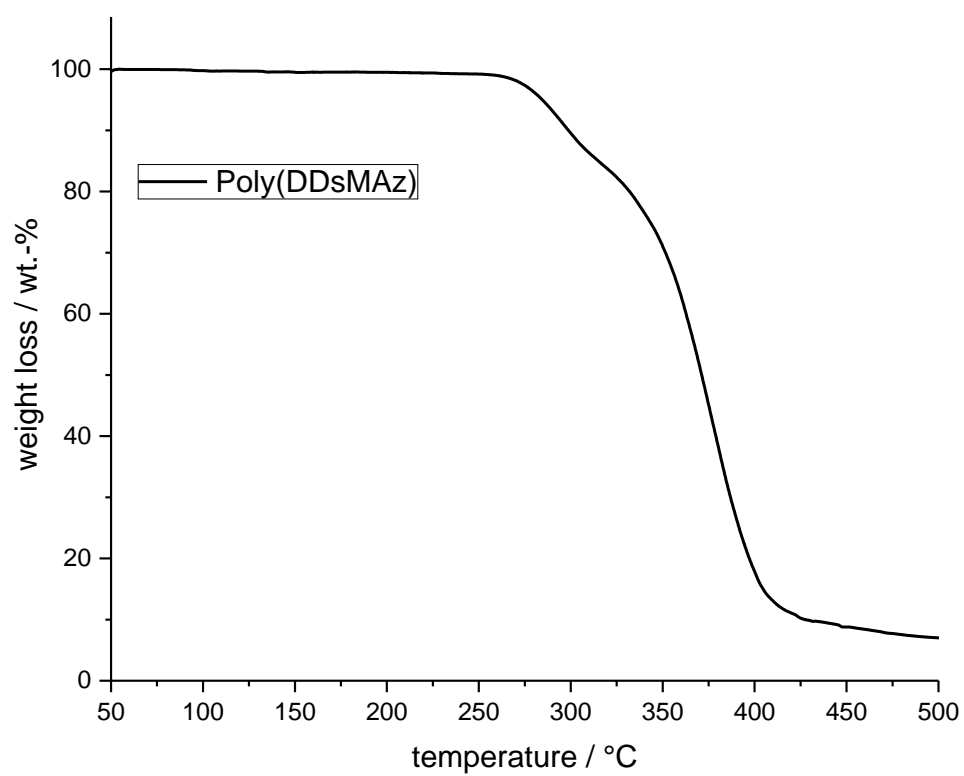


Figure 86: TGA of Poly(DDsMAz).

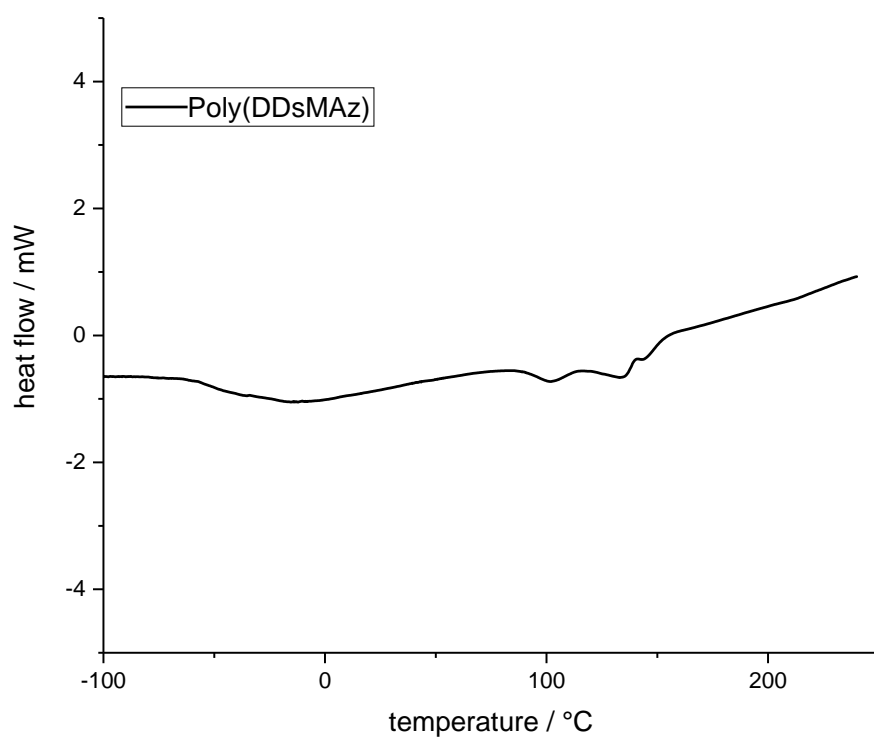
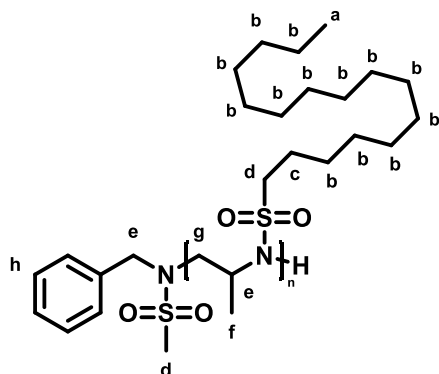


Figure 87: DSC of Poly(DDsMAz).

9.3.4 Poly(2-Methyl-N-hexadecasylaziridin) (Poly(HDsMAz))



sample	X_n	Initiator	M_n (NMR) g/mol	M_n (GPC) g/mol	\bar{D}
Poly(HDsMAz)	12	BnNHMs	4300	3800	1,15
Poly(HDsMAz)	15	BnNHMs	5400	4600	1.15
Poly(HDsMAz)	32	BnNHMs	11200	7500	1,26
Poly(HDsMAz)	35	BnNHMs	12300	-	-

Poly(HDsMAz)₃₂

starting material: HDsMAz (250 mg, 725 μ mol), BnNHMs (8.93 mg, 36.15 μ mol), KHMDS (6.5 mg, 33 μ mol)

^1H NMR (300 MHz, tetrachloroethane- d_2) δ 7.45 – 7.16 (m), 4.07 – 3.55 (m), 3.49 – 3.08 (m), 3.12 – 2.75 (m), 1.83 – 1.58 (m), 1.47 – 0.99 (m), 0.91 – 0.68 (m).

Poly(HDsMAz)₁₂

starting material: HDsMAz (100 mg, 289 μ mol), BnNHMs (5.36 mg, 29 μ mol), KHMDS (5.2 mg, 26 μ mol)

^1H NMR (250 MHz, methylene chloride- d_2) δ 7.44 – 7.23 (m, 1H), 4.03 – 3.62 (m, 3H), 3.43 – 3.17 (m, 2H), 1.85 – 1.57 (m, 5H), 1.52 – 1.01 (m, 61H), 0.91 – 0.74 (m, 9H).

Poly(HDsMAz)₃₂

starting material: HDsMAz (12.55 g, 36.3 mmol), BnNHMs (672.7 mg, 3.6 mmol), KHMDS (652 mg, 3.27 μ mol)

Experimental Part

^1H NMR (300 MHz, methylene chloride- d_2) δ 7.53 – 7.26 (m), 4.11 – 3.60 (m), 3.56 – 3.15 (m), 3.15 – 2.90 (m), 1.93 – 1.64 (m), 1.50 – 1.14 (m), 1.01 – 0.78 (m).

Poly(HDsMAz)₃₅

starting material: HDsMAz (10.34 g, 29.9 mmol), BnNHMs (184.8 mg, 1.0 mmol), KHMDS (179.1 mg, 898 μmol)

^1H NMR (300 MHz, Methylene Chloride- d_2) δ 7.40 – 7.22 (m), 3.98 – 3.62 (m), 3.48 – 3.08 (m), 3.07 – 2.80 (m), 1.84 – 1.57 (m), 1.42 – 1.05 (m), 0.93 – 0.71 (m).

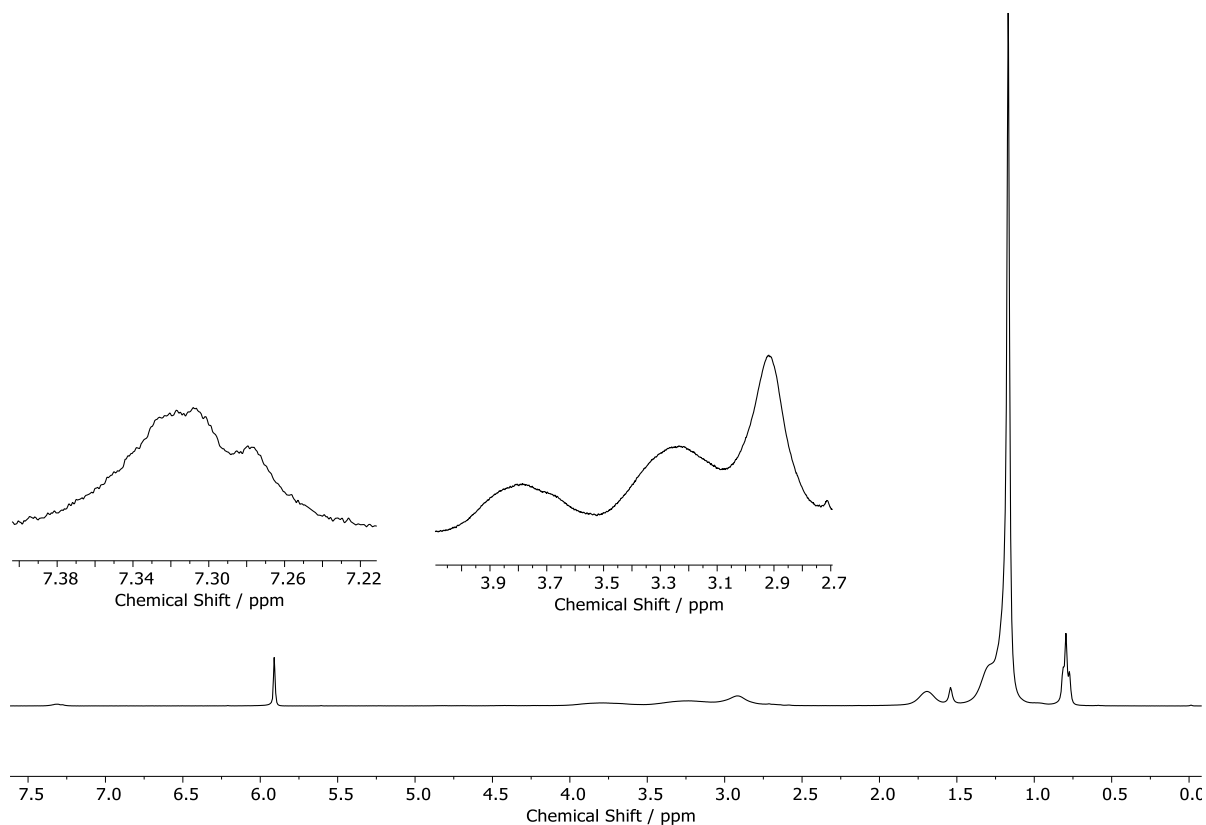


Figure 88: ^1H NMR (300 MHz, $\text{tetrachloroethane-}d_2$) of Poly(2-methyl-N-hexadecasylaziridine).

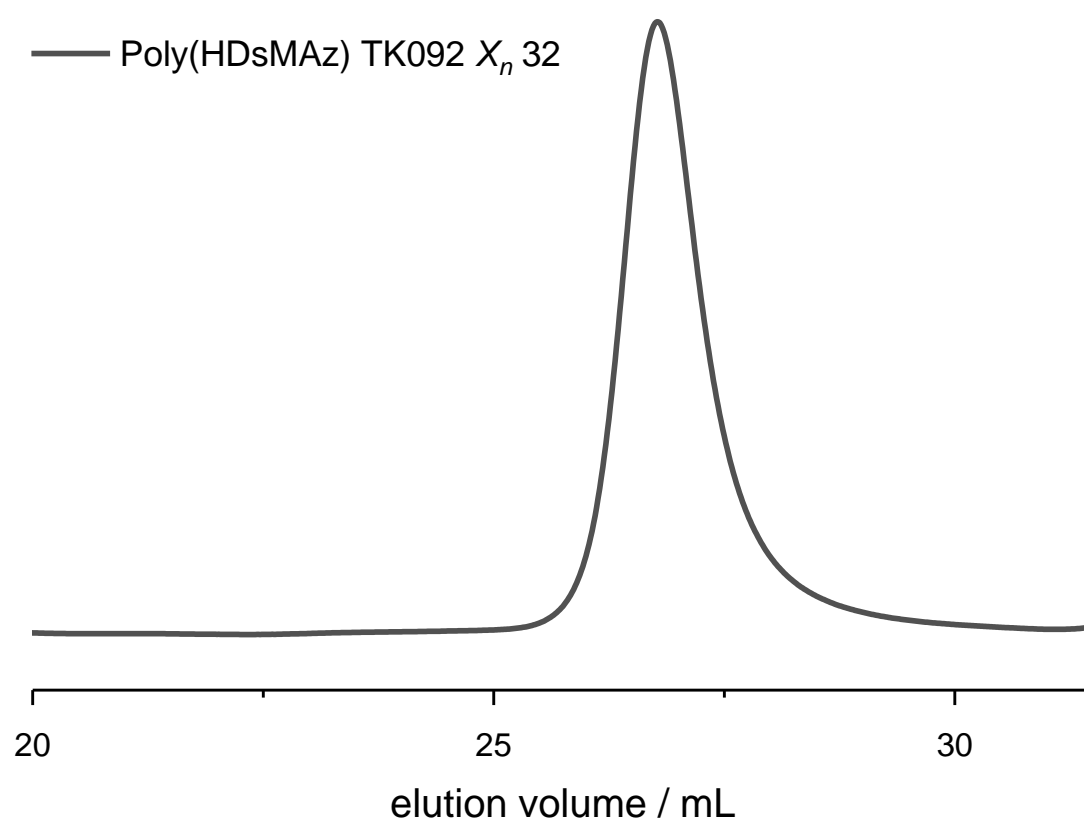


Figure 89: GPC traces (RI detection) of Poly(HDsMAz) in THF.

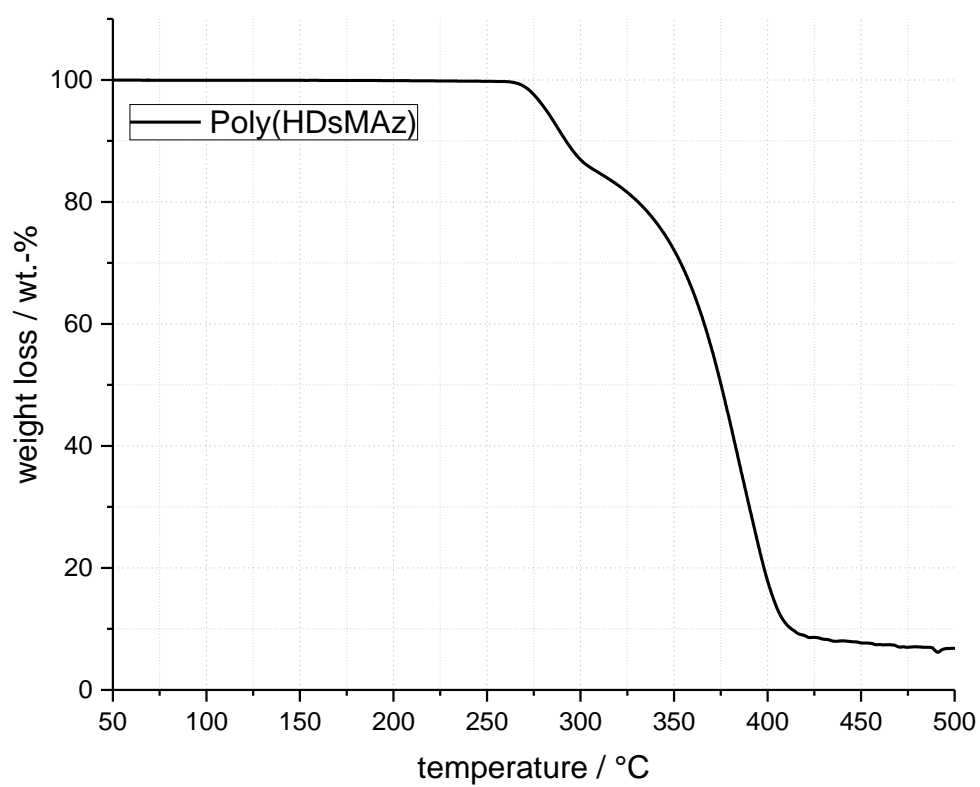


Figure 90: TGA of Poly(HDsMAz).

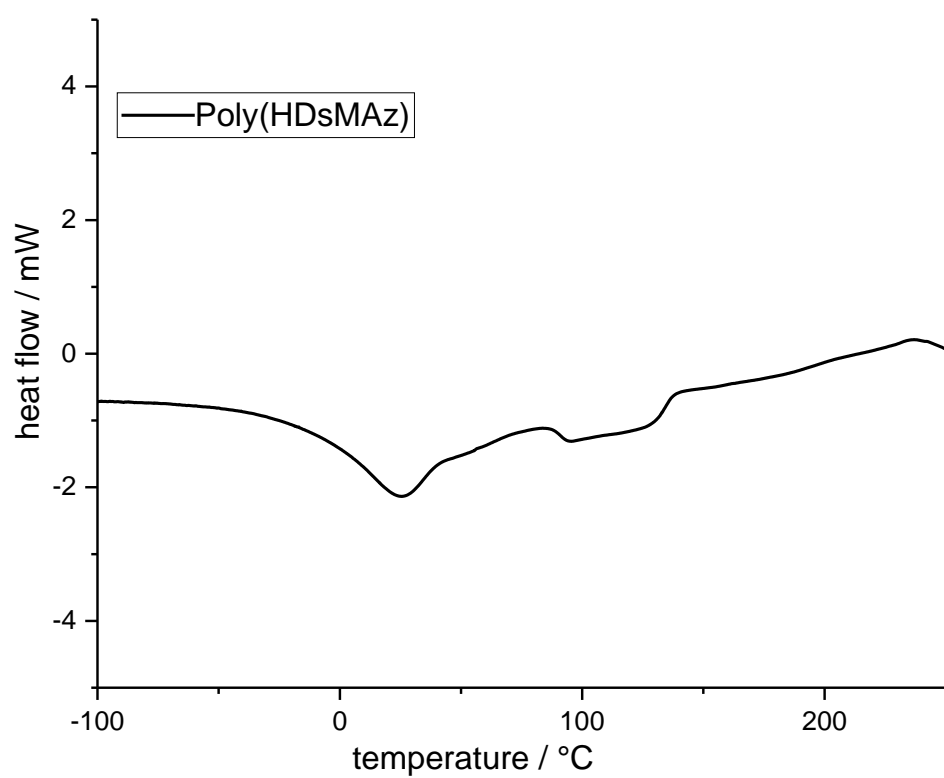
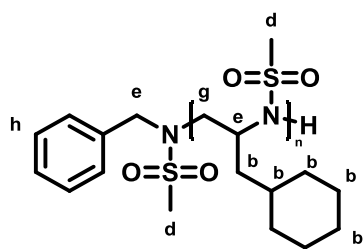


Figure 91: DSC of Poly(HDsMAz).

9.3.5 Poly(2-Cyclohexanemethyl-*N*-Mesylaziridin) (Poly(MsCyhexAz))

Sample	X_n	TG / °C	M_n (NMR) g/mol	M_n (GPC) g/mol	\bar{D}
P(MsCyhexAz)	26	130	5800	1800	1.15

starting material: MsCyHexAz (500 mg, 2.3 mmol), BnNHMs (17.1 mg, 92 μ mol),
 ^1H NMR (300 MHz, methylene chloride- d_2) δ 7.51 – 7.26 (m, h), 4.32 – 3.61 (m, e),
 3.58 – 3.09 (m, g), 3.07 – 2.66 (m, d), 2.12 – 0.63 (m, b).

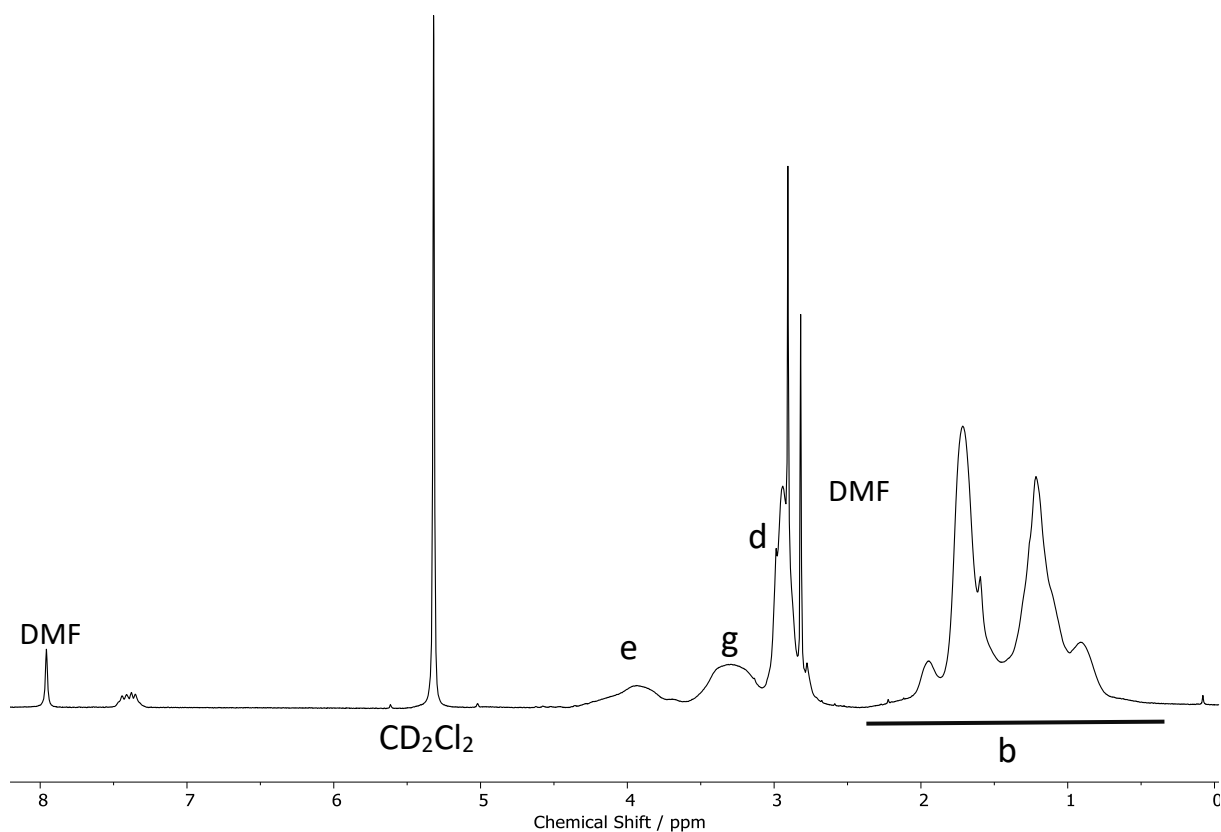


Figure 92: ^1H NMR (300 MHz, Methylene Chloride- d_2) of Poly(2-Cyclohexanemethyl-*N*-Mesylaziridin).

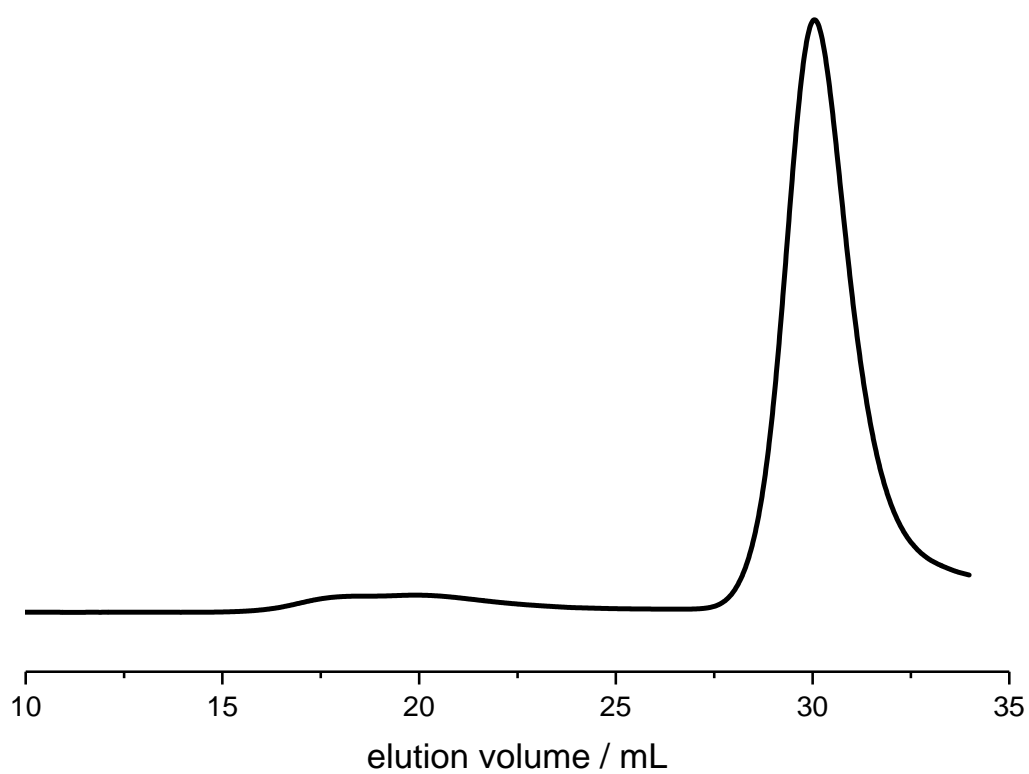


Figure 93: GPC traces (RI-detection) of polymerized Poly(MsCyhexAz) in DMF.

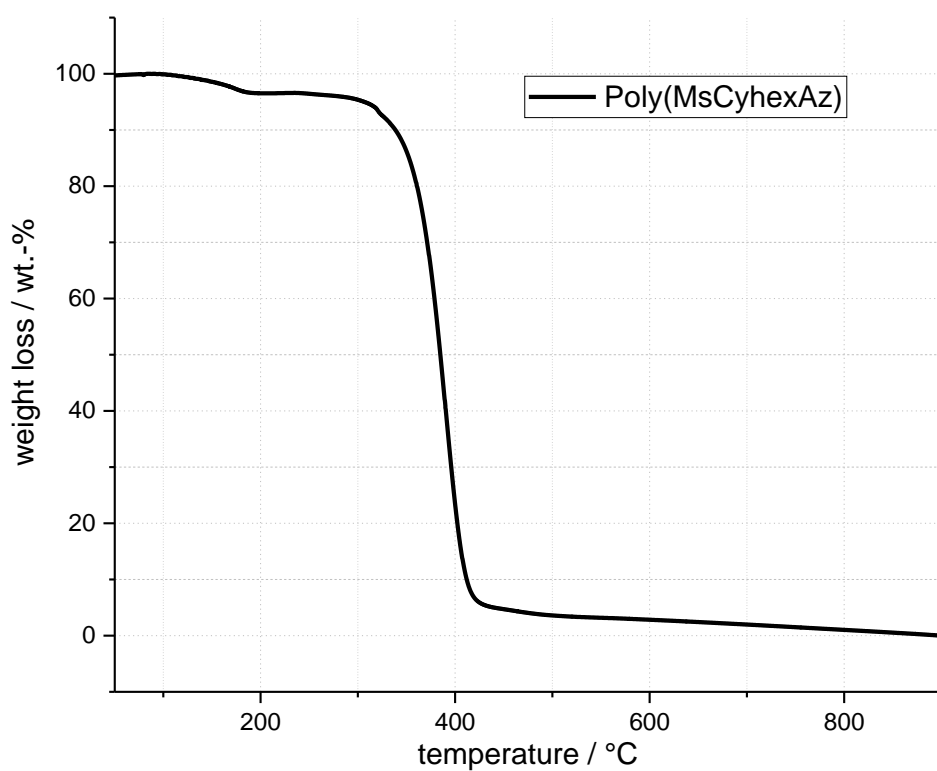


Figure 94: TGA of Poly(MsCyhexAz)

Experimental Part

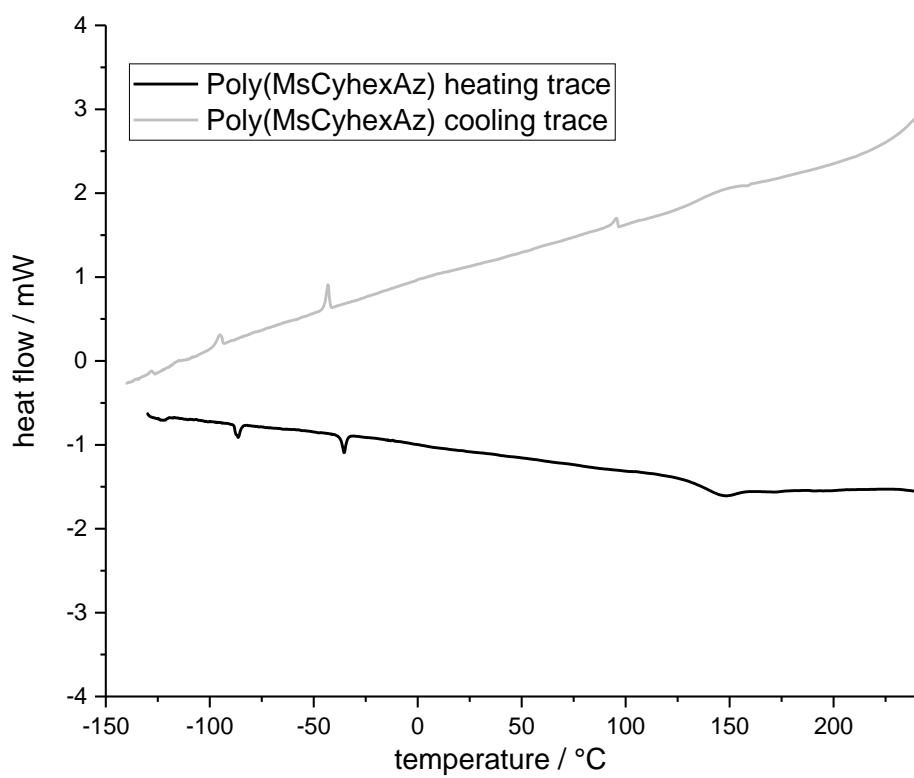
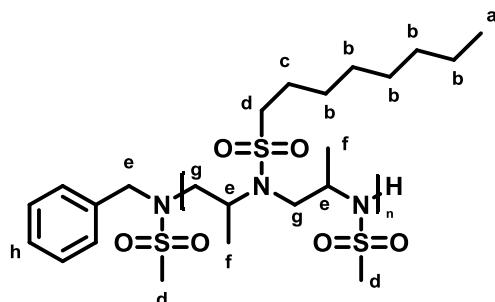


Figure 95: DSC of Poly(MsCyhexAz)

9.4 Copolymers

9.4.1 Poly(OsMAz)-co-(MsMAz)



Sample	ratio	X_n	$TG / ^\circ C$	M_n (NMR) g/mol	M_n (GPC) g/mol	\bar{D}
Poly(OsMAz-co-MsMAz)	1:1	30	55	5700	3000	1.15
Poly(OsMAz-co-MsMAz)	3:1	33	31	7100	3800	1.11
Poly(OsMAz-co-MsMAz)	1:3	20	58	3500	2000	1.14

Poly(OsMAz)-co-(MsMAz) (1:1)

starting material: OsMAz (250 mg, 1.07 mmol), MsMAz (145 mg, 1.07 mmol), BnNHMs (15.88 mg, 85.7 μ mol), KHMDS (15.39 mg, 77.15 μ mol),

1H NMR (300 MHz, methylene chloride- d_2) δ 7.52 – 7.26 (m,), 4.15 – 3.68 (m,), 3.60 – 3.14 (m,), 3.11 – 2.85 (m,), 1.90 – 1.67 (m,), 1.52 – 1.14 (m,), 1.01 – 0.76 (m,).

Poly(OsMAz)-co-(MsMAz) (3:1)

starting material: OsMAz (250 mg, 1.07 mmol), MsMAz (48.27 mg, 357 μ mol), BnNHMs (10.58 mg, 57.13 μ mol), KHMDS (10.25 mg, 51.40 μ mol),

1H NMR (300 MHz, Methylene Chloride- d_2) δ 7.55 – 7.23 (m, h), 4.20 – 3.65 (m, e), 3.54 – 3.19 (m, g), 3.13 – 2.86 (m, d), 1.90 – 1.65 (m, c), 1.64 – 1.14 (m, b, f), 1.04 – 0.77 (m, a).

Poly(OsMAz)-co-(MsMAz) (1:3)

starting material: OsMAz (250 mg, 1.07 mmol), MsMAz (48.27 mg, 357 μ mol), BnNHMs (10.58 mg, 57.13 μ mol), KHMDS (10.25 mg, 51.40 μ mol),

^1H NMR (300 MHz, Methylene Chloride- d_2) δ 7.57 – 7.26 (m, h), 4.16 – 3.76 (m, e), 3.57 – 3.19 (m, g), 3.20 – 2.83 (m, d), 1.93 – 1.72 (m, c), 1.71 – 1.59 (m, f), 1.57 – 1.11 (m, b), 1.03 – 0.81 (m, a).

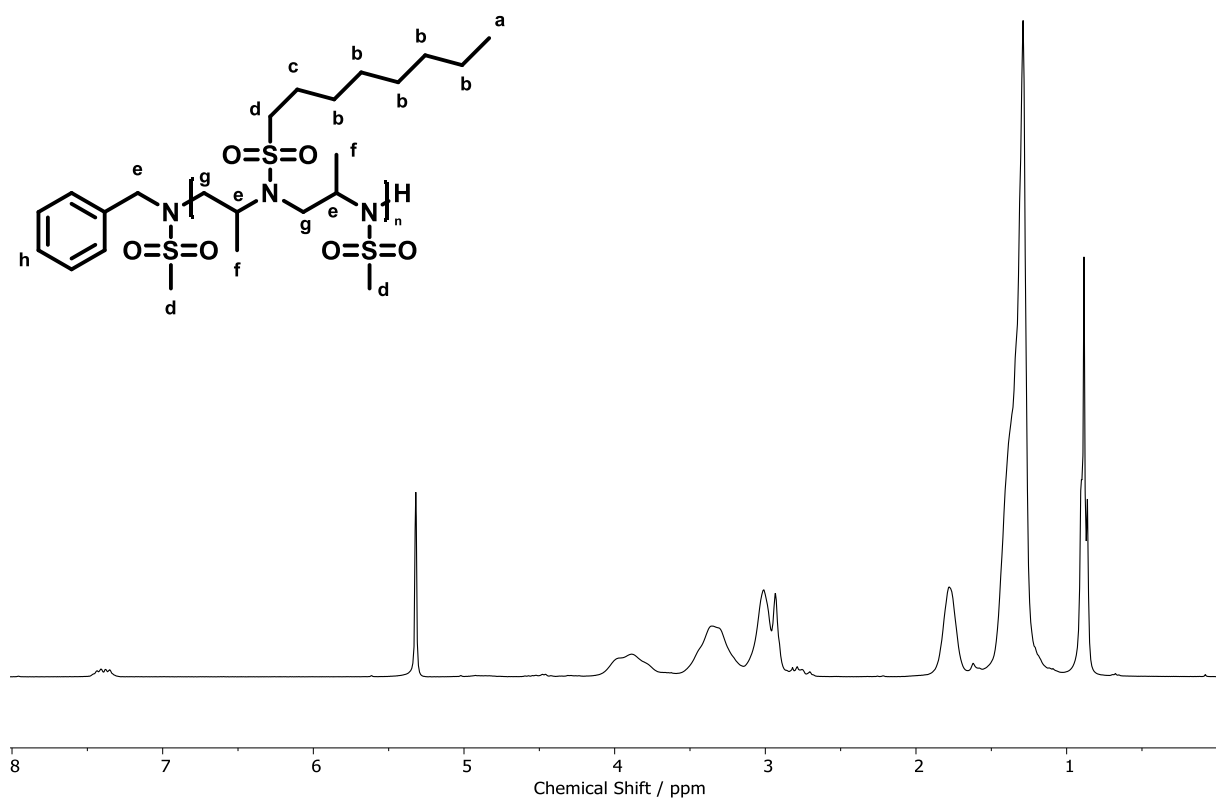


Figure 96: ^1H NMR (300 MHz, DCM- d_2) of Poly(OsMAz)-co-(MsMAz) (1:1)

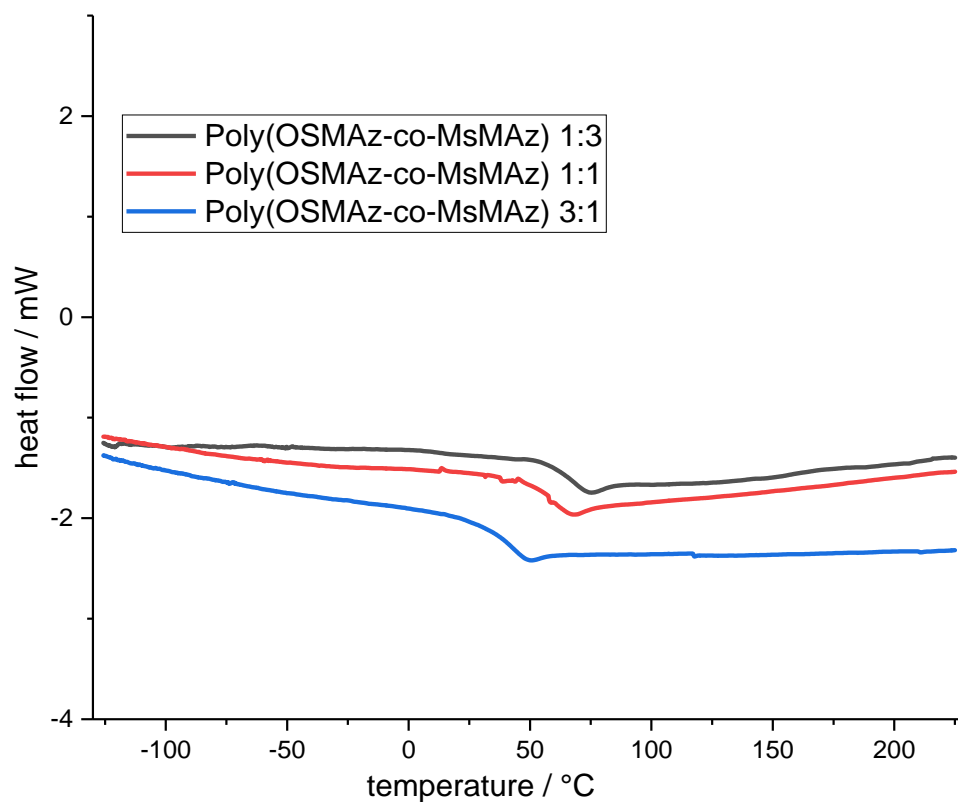


Figure 97: DSC of Poly(OSMAz)-co-(MsMAz) with different ratios

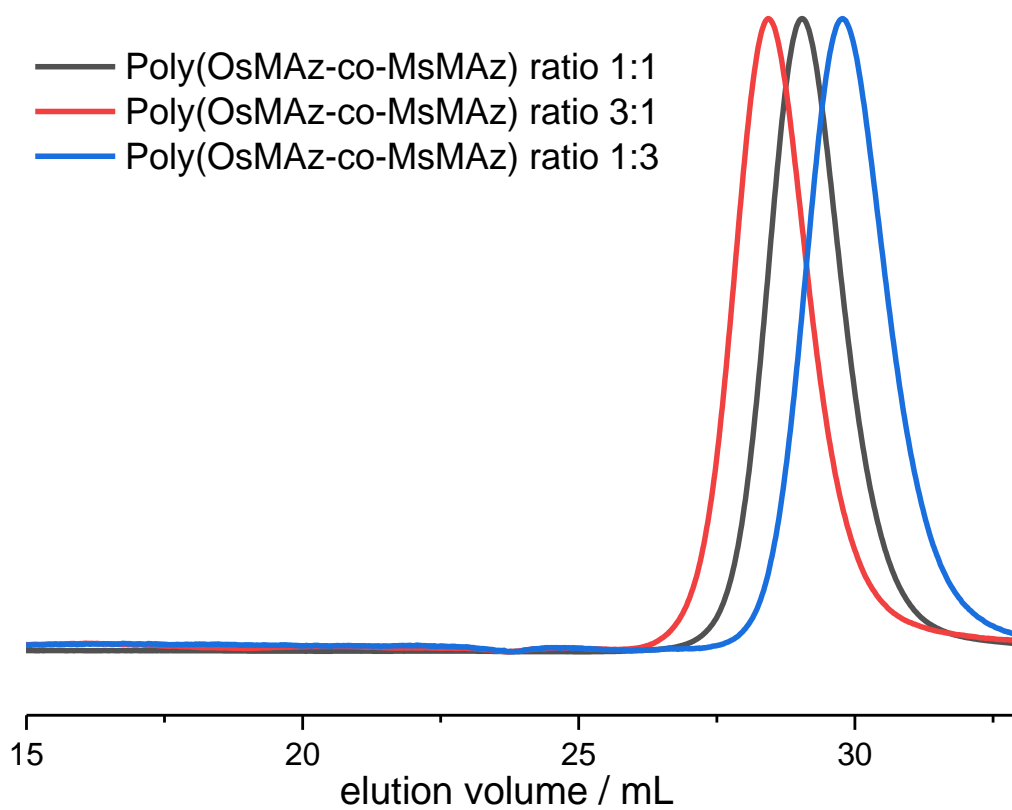
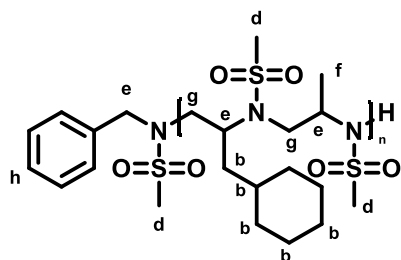


Figure 98: GPC-traces (RI-detection) of Poly(OSMAz-co-MsMAz) of different ratios in DMF

9.4.1 Poly(MsCyhexAz)-co-(MsMAz)

sample	ratio	X_n	$TG / ^\circ C$	M_n (NMR) g/mol	M_n (GPC) g/mol	\bar{D}
P(MsCyhexAz-co-MsMAz)	1:1	25	120	4600	2100	1.22

starting material: MsCyHexAz (250 mg, 1.15 mmol), MsMAz (155.5 mg, 1.15 mmol)

BnNHMs (17.1 mg, 92 μ mol), KHMDS (16.5 mg, 83 μ mol),

1H NMR (300 MHz, DCM- d_2) δ 7.44 – 7.18 (m, h), 4.21 – 3.56 (m, e), 3.52 – 3.05 (m, g),

3.01 – 2.64 (m, d), 1.98 – 1.40 (m, b), 1.40 – 0.72 (m, b, f).

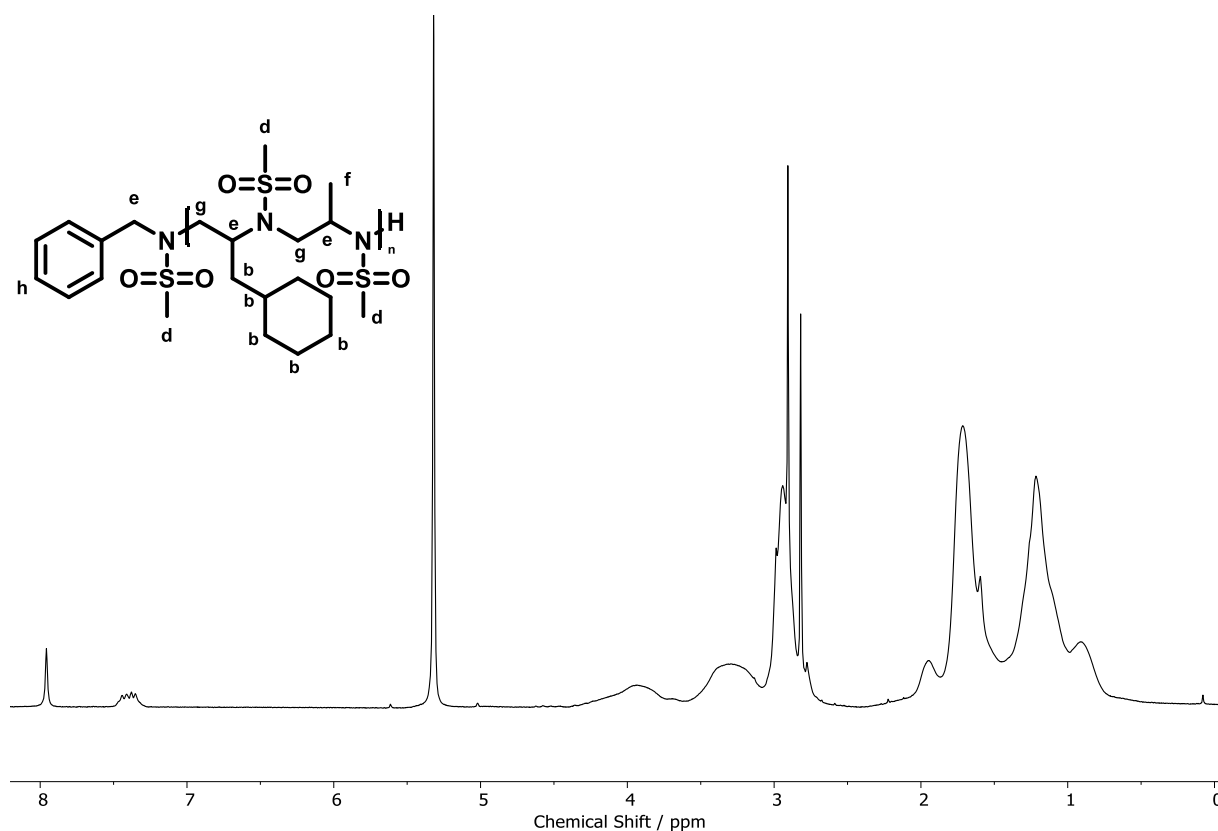


Figure 99: 1H NMR (300 MHz, DCM- d_2) of Poly(MsCyhexAz)-co-(MsMAz)

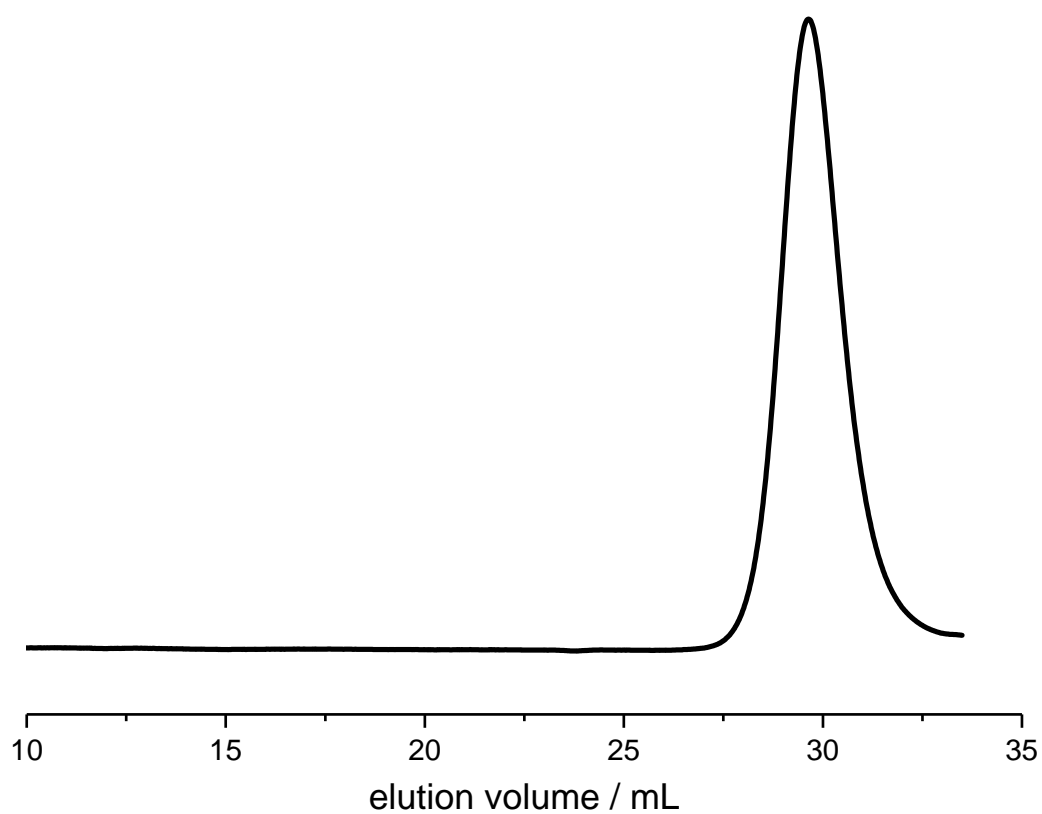


Figure 100: GPC-traces (RI-detection) of Poly(MsCyhexAz-co-MsMAz).

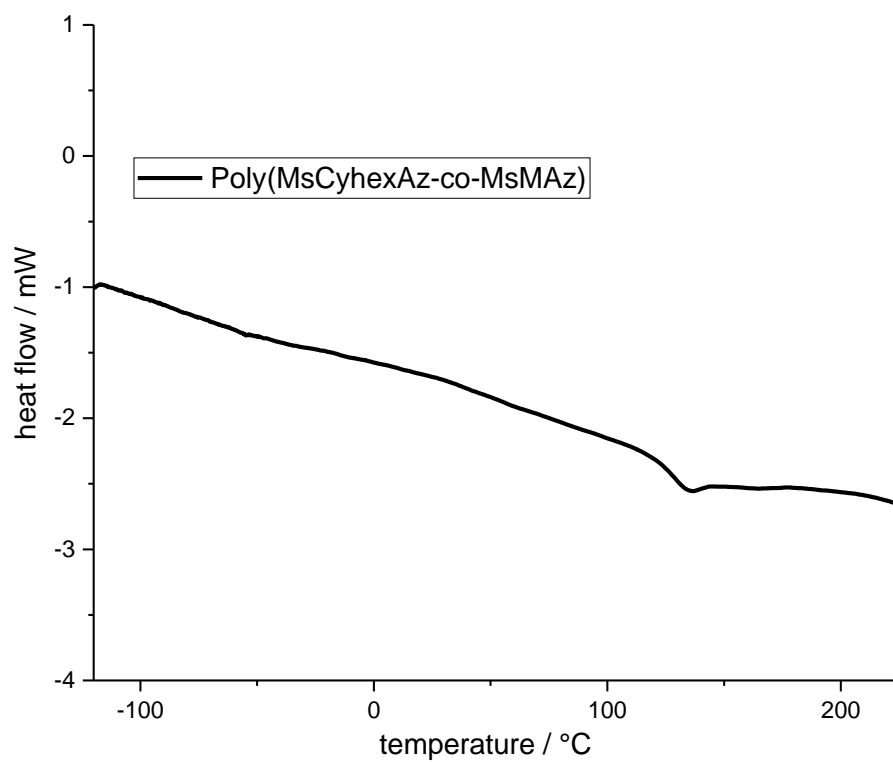


Figure 101: DSC of Poly(MsCyhexAz-co-MsMAz).

9.5 Project 2: Synthesis of Poly(TsEtOHaz)-*graft*-PEG

9.5.1 Poly{2-(2-Ethylethoxy)-Ethanol-*N*-Tosylaziridine}

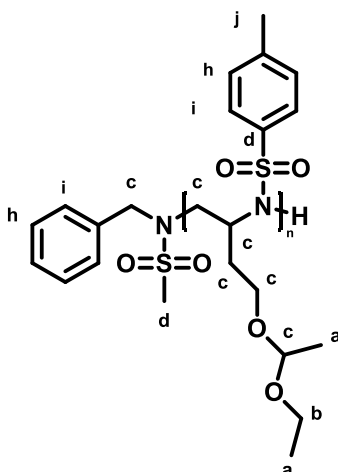


Table 22 Overview of synthesized Polymers

sample	X_n	M_n (GPC) g/mol	\bar{D}
Poly(TsEEEEAz)	50	3800	1,2
Poly(TsEEEEAz)	50	4800	1,19

Poly(TsEEEEAz)₅₀

starting material: TsEtOHaz (500 mg, 1.6 mmol), BnNHMs (5.9 mg, 32 μ mol), KHMDS (5.73 mg, 29 μ mol),

Poly(TsEEEEAz)₅₀

starting material: TsEtOHaz (2 g, 6.4 mmol), BnNHMs (23.64 mg, 127.6 μ mol), KHMDS (22.9 mg, 115 μ mol),

^1H NMR (300 MHz, DCM- d_2) δ 8.20 – 7.51 (m, i), 7.53 – 6.98 (m, h), 4.73 – 2.50 (m, c), 2.44 – 2.22 (m, d), 2.21 – 1.53 (m, b), 1.27 – 0.81 (m, a).

Experimental Part

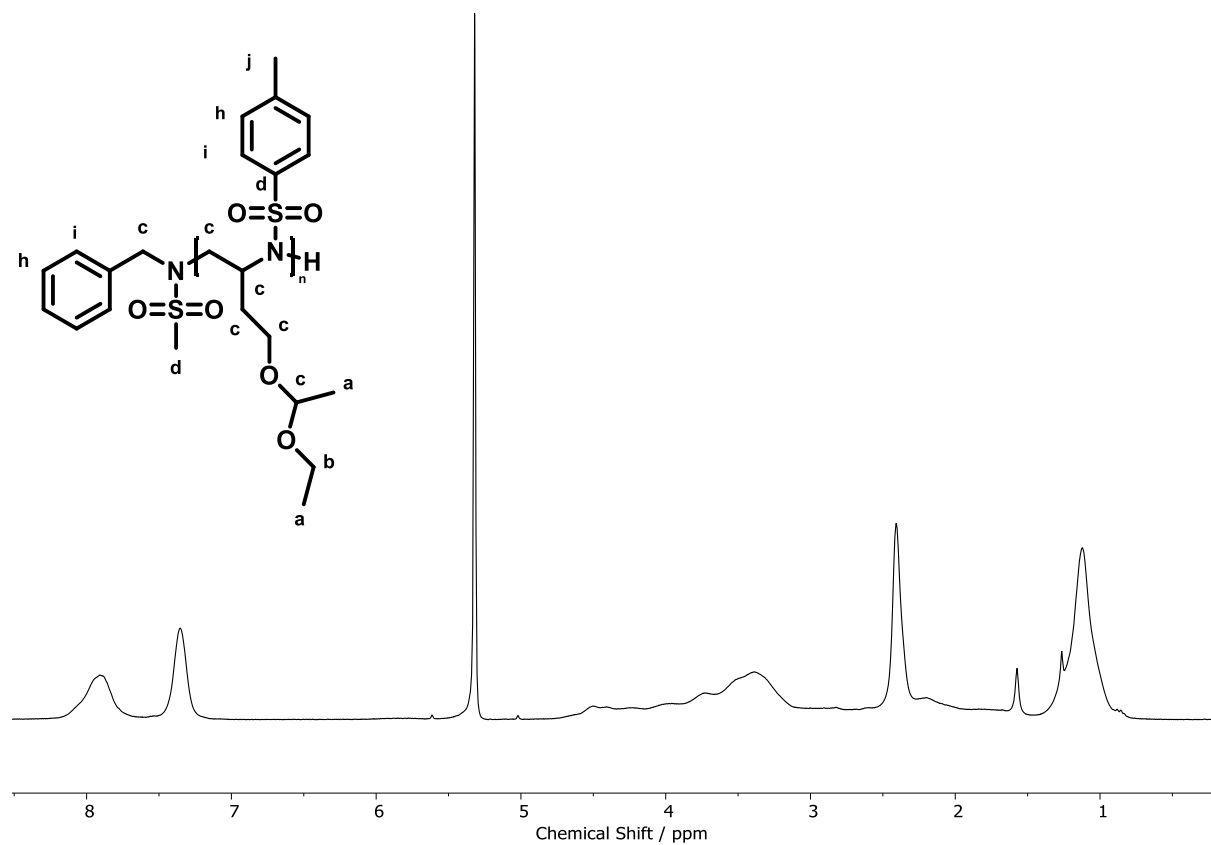


Figure 102 ^1H NMR (300 MHz, $\text{DCM}-d_2$) Poly{2-(2-Ethylethoxy)-Ethanol-N-Tosylaziridine}

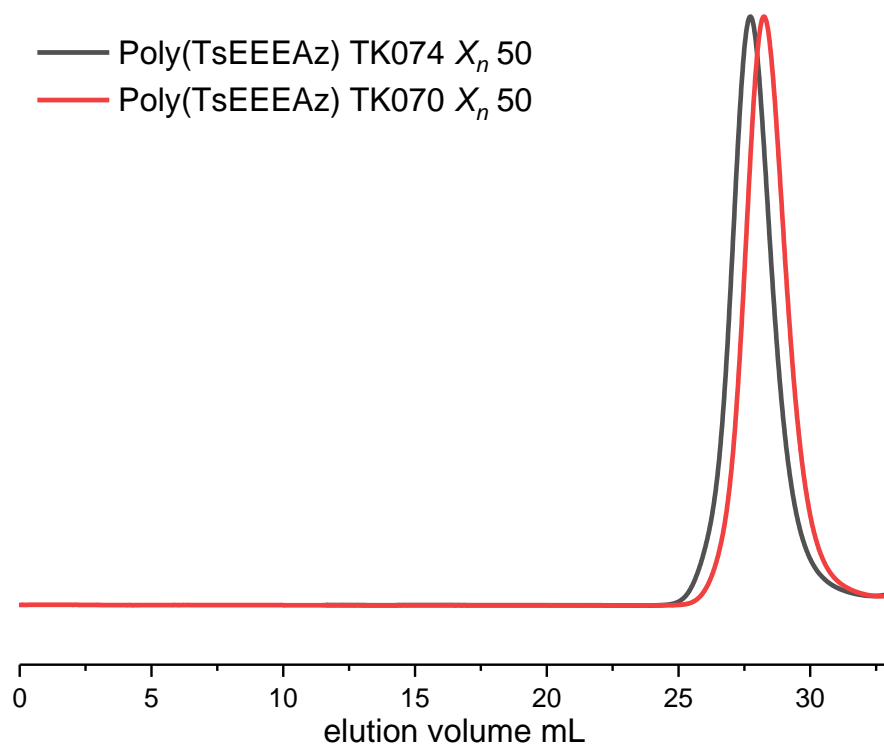
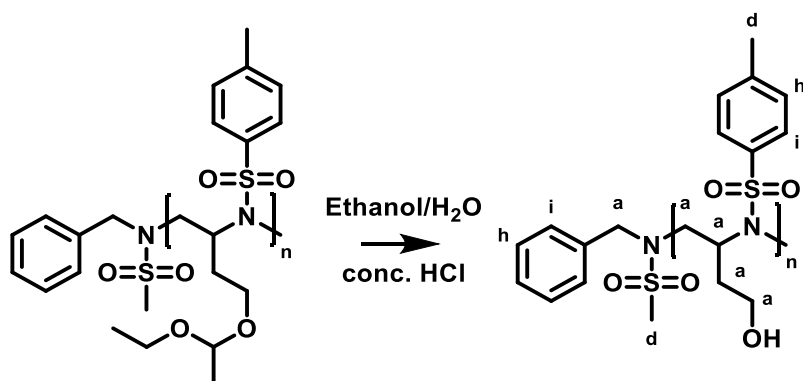


Figure 103 : GPC traces (RI-detection) of Poly(TsEEEEAz)

9.5.1 Poly(2-Ethanol-*N*-Tosylaziridine)**Scheme 43:** Hydrolysis of acetal groups

Poly(TsEEEEAz) (2 g, M_n 4600 g/mol) was dissolved in ethanol (40 mL) and water (2 mL). To the solution, HCl (20 mL, 37%) was added and then stirred at 70 °C overnight. The turbidity solution became transparent overnight and was reduced at the rotary evaporator. Yielding a brown solid. The product was purified through dialysis in THF. (2000 g/mol, regenerated cellulose)

sample	Sample name	X_n	M_n (GPC) g/mol	\bar{D}
P(TsEtOHAz)	TK072	50	3500	1.37
P(TsEtOHAz)	TK078	50	4600	1.13

Poly(TsEtOHAz)₅₀

starting material: Poly(TsEEEEAz) (250 mg), HCl (2.5 ml, 37%), Ethanol (5 ml),
 ^1H NMR (300 MHz, $\text{DMF-}d_7$) δ 8.38 – 7.78 (m, i), 7.72 – 7.28 (m, h), 4.67 – 3.01 (m, a), 2.60 – 2.28 (m, d), 2.28 – 1.80 (m, b).

Poly(TsEtOHAz)₅₀

starting material: Poly(TsEEEEAz) (2 g), HCl (20 ml, 37%), Ethanol (40 ml),
 ^1H NMR (300 MHz, $\text{DMF-}d_7$) δ 8.24 – 7.81 (m), 7.66 – 7.23 (m), 4.66 – 3.56 (m), 3.55 – 3.42 (m), 3.43 – 3.03 (m), 2.68 – 2.27 (m), 2.26 – 1.82 (m).

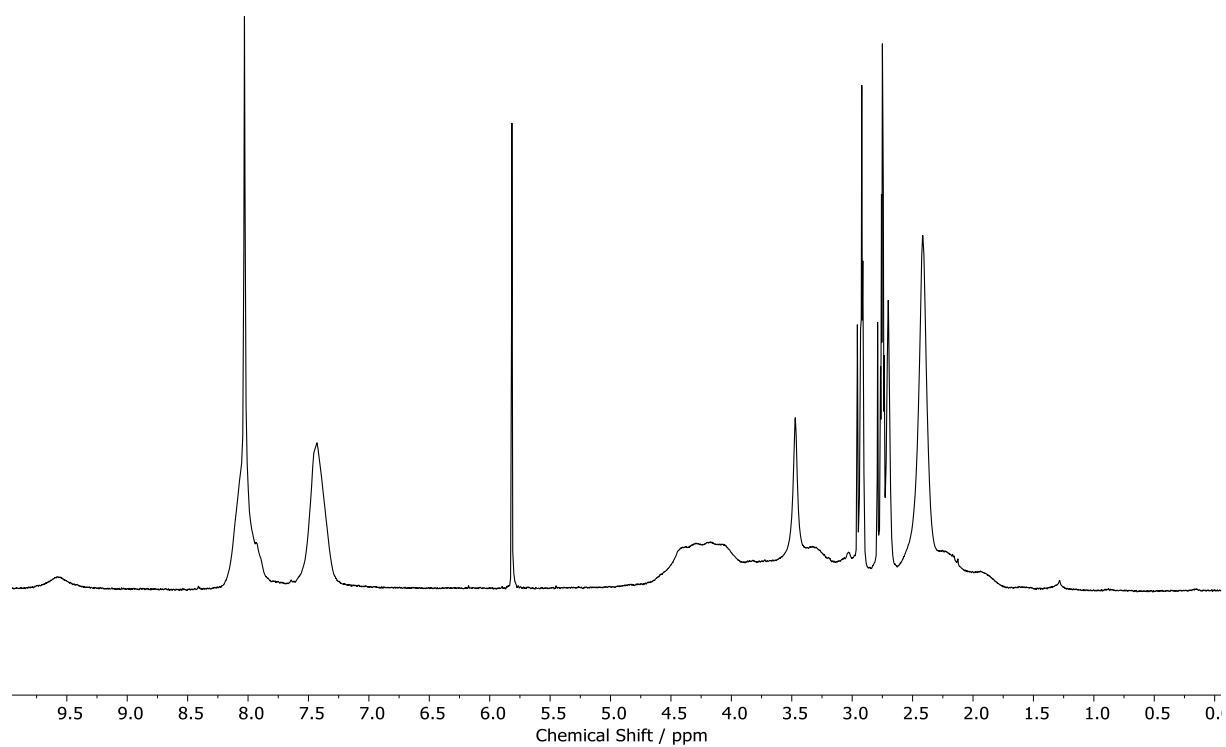


Figure 104: ^1H NMR (300 MHz, DMF-d_7) of Poly(2-Ethanol-*N*-Tosylaziridine)

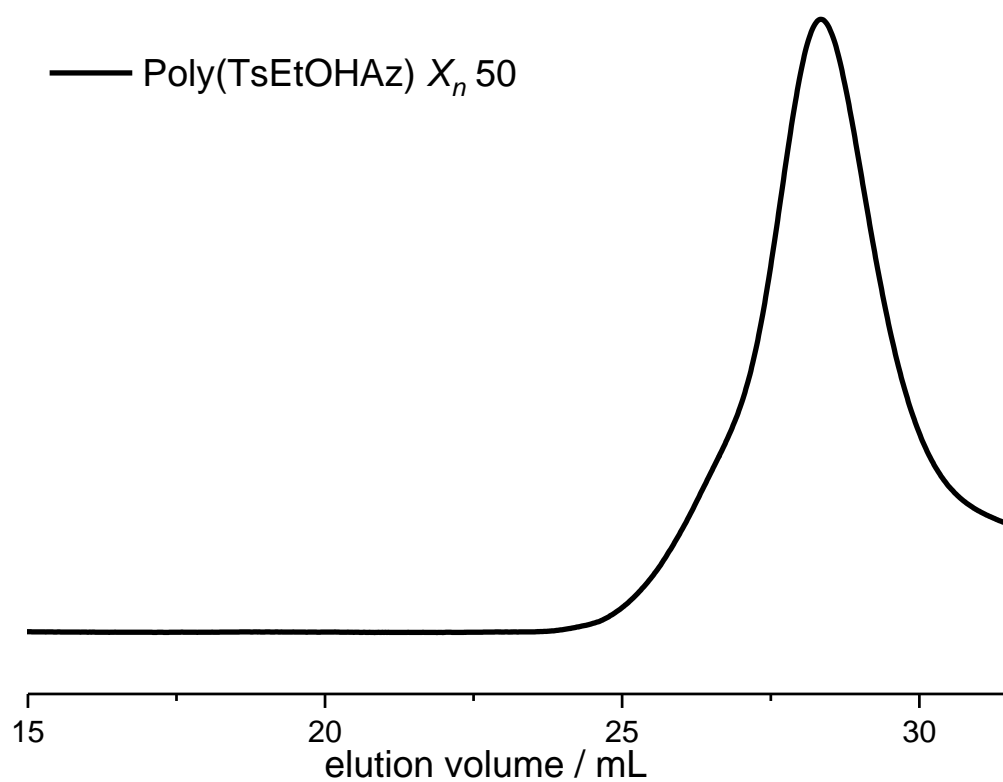
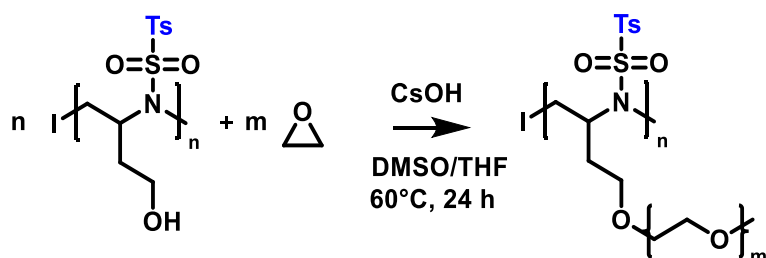


Figure 105: GPC traces of Poly(TsEtOHaz)

9.5.1 Poly(TsEtOHAz)-graft-PEO**Scheme 44:** Graft-from synthesis of Poly(TsEtOHAz)-graft-PEG.

The reaction was carried out in a flame-dried Schlenk flask under Argon atmosphere. Poly(TsEtOHAz) (12250 g/mol, 250 mg, 0.02 mmol) was transferred into the Schlenk flask, CsOH·H₂O (0.5 eq. 85.6 mg, 509 μmol) was added, heated in benzene (60°C) for at least 3 h and dried under reduced pressure.

The deprotonated starting material was dissolved in dry THF (2 ml) and DMSO (1 ml), and frozen with liquid N₂. Ethylene oxide (1 ml, 20.02 mmol) was cryo-transferred and transferred into the flask. The frozen the frozen educts were heated in an oil bath (60°C) for 12 h. Subsequently the polymer was precipitated in DEE (30-40 ml), centrifuged and dried *in vacuo*.

For Dialysis the product was dissolved in deionized water and placed in a freshly prepared regenerated cellulose membrane (3.5 kDA and 6-8 kDA). The membrane was placed in 1 L of deionized water and stirred. The water was changed after 12 h, 12 h and 24 h.

sample	M_n (GPC) g/mol	M_w (GPC) g/mol	\bar{D}
P(TsEtOHAz) -graft-PEO	5600	13100	2.3

¹H NMR (500 MHz, DMSO-*d*₆) δ 7.99 – 7.57 (m, i), 7.53 – 7.26 (m, h), 4.63 – 4.51 (m, e), 3.57 – 3.42 (m, a), 2.44 – 2.32 (m, d).

Experimental Part

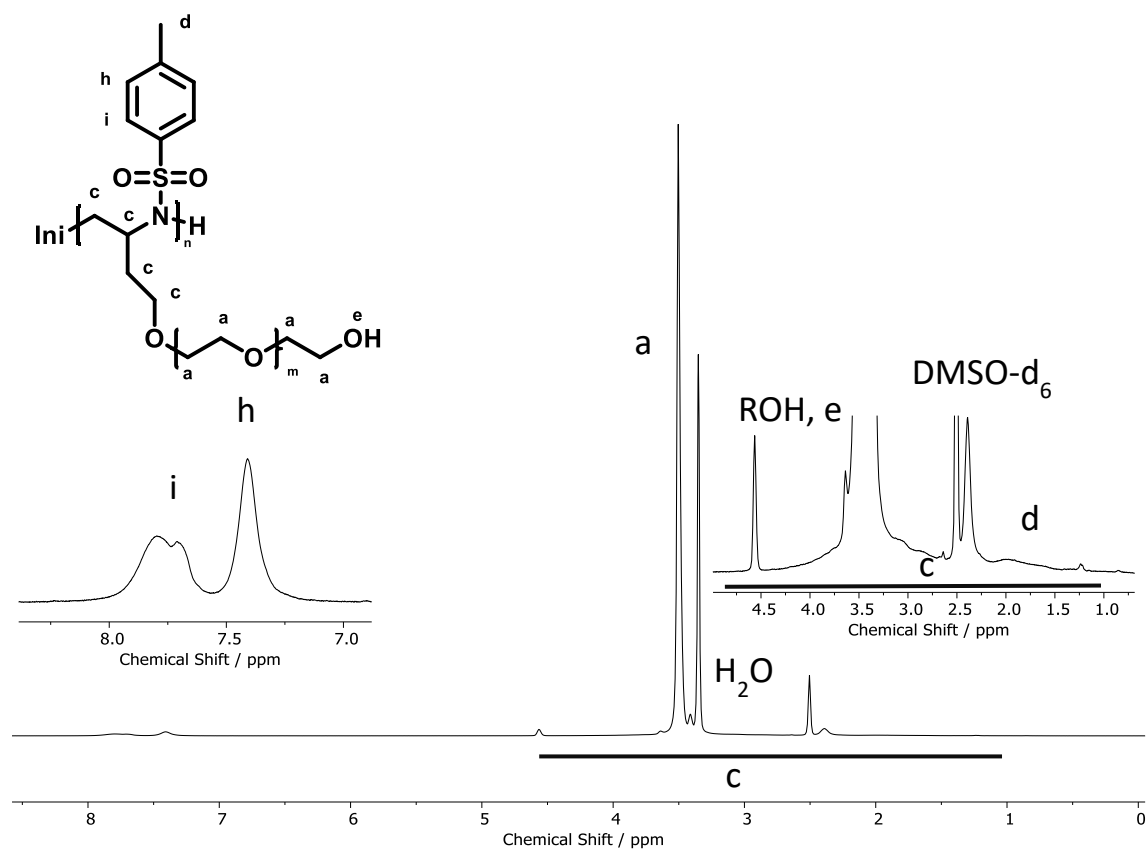


Figure 106: ^1H NMR (500 MHz, $\text{DMSO}-d_6$) of Poly(TsEtOHaz)-graft-PEG.

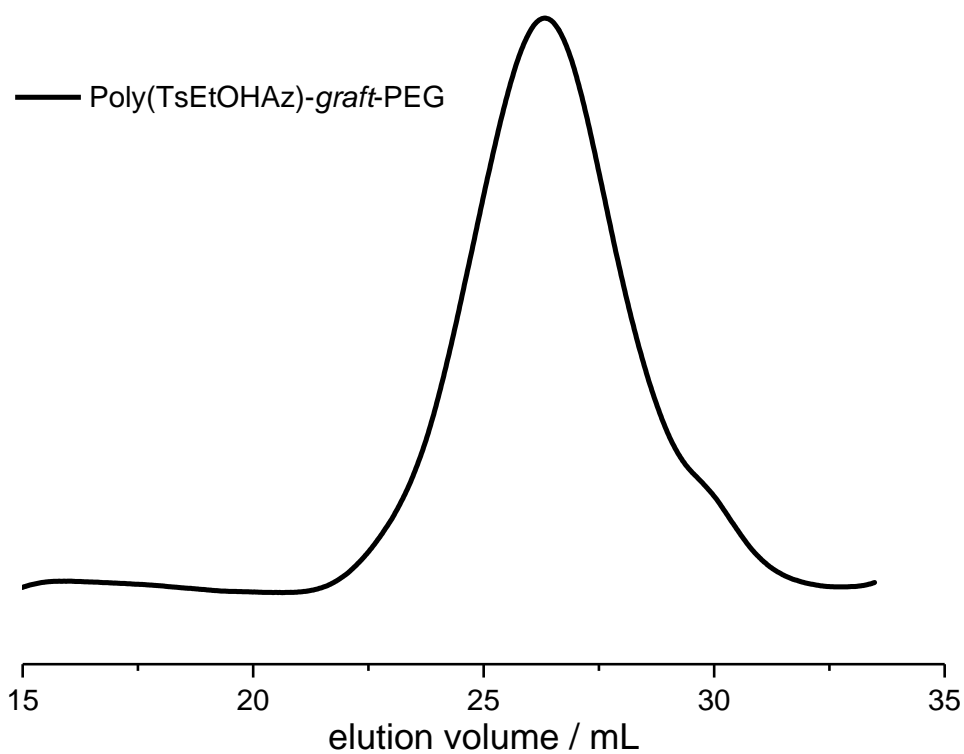
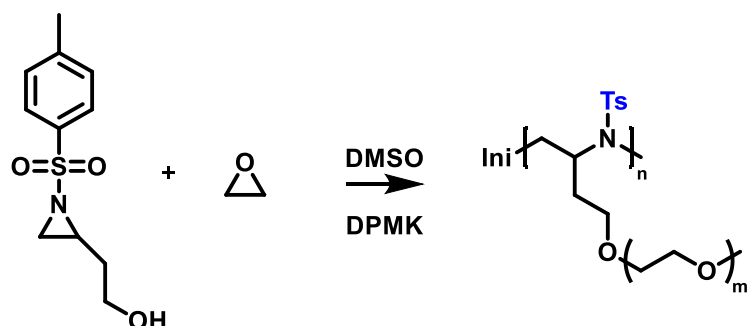


Figure 107: GPC (RI-detection) of Poly(TsEtOHaz)-graft-PEG.

9.5.1 Poly(TsEtOHAz)-graft-PEO**Scheme 45:** One-pot synthesis of Poly(TsEtOHAz)-graft-PEG

The reaction was carried out in a flame-dried Schlenk flask under Argon atmosphere. TsEtOHAz (250 mg, 1.04 mmol 10 eq.) was transferred into the Schlenk flask and dried with benzene. The starting material was dissolved in dried THF and DMSO and frozen with liquid N₂. Ethylene oxide (1 ml, 20.02 mmol) was cryo-distilled and transferred into the flask. The frozen the frozen educts were deprotonated with DPMK (0.1 eq. 94 μ L, 1.1 M in THF) and heated in an oil bath (60°C) for 12 h. Subsequently the polymer was precipitated in DEE (30-40 ml), centrifuged and dried *in vacuo*.

sample	number	M_n (GPC) g/mol	M_w (GPC) g/mol	\bar{D}
P(TsEtOHAz)-graft-PEG	TK132	2200	4200	1.87

¹H NMR (500 MHz, DMSO-*d*₆) δ 7.93 – 7.56 (m), 7.54 – 7.21 (m), 4.69 – 4.43 (m), 3.55 – 3.37 (m), 2.45 – 2.32 (m).

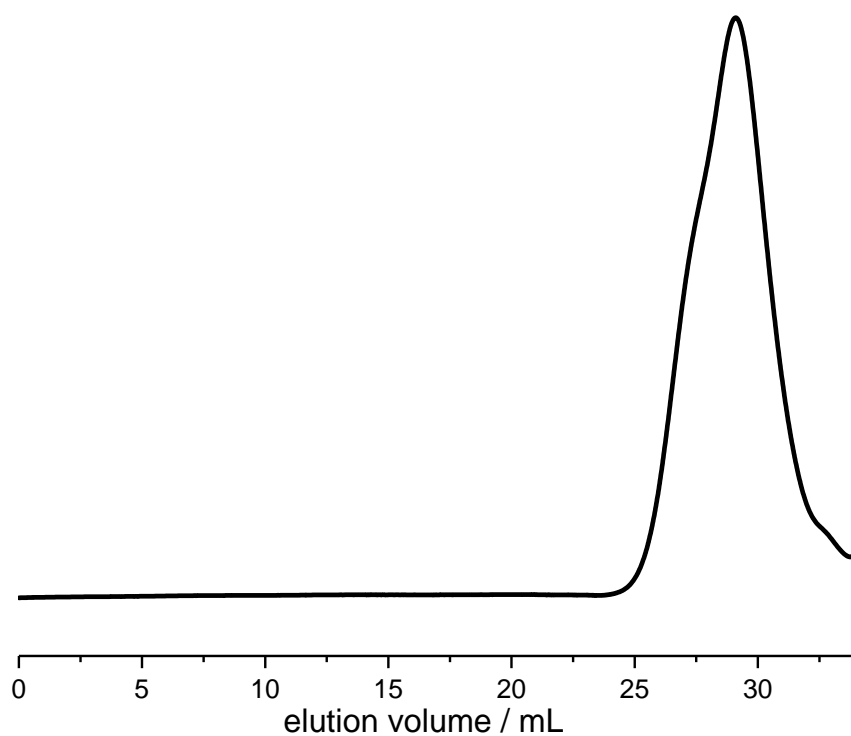


Figure 108: GPC trace (RI-detection) of Poly(TsEtOHaz)-*graft*-PEO one-pot synthesis

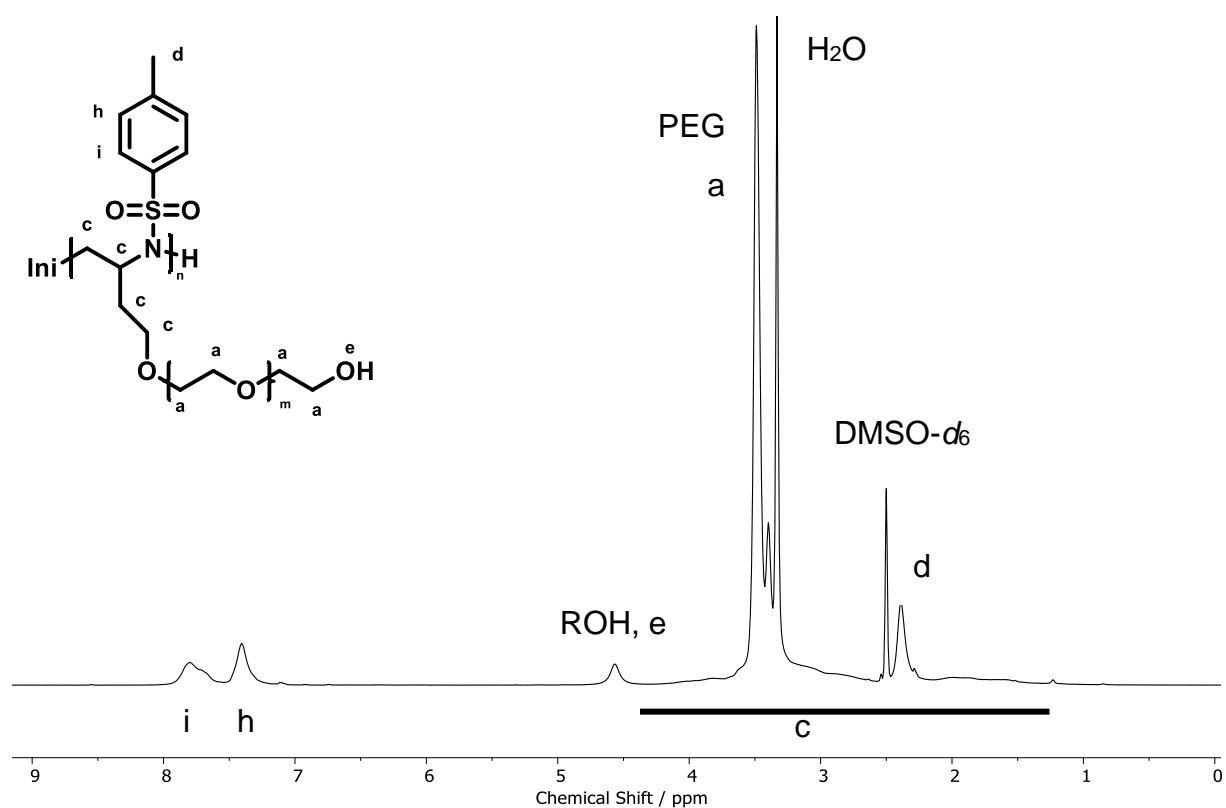


Figure 109: ^1H NMR (500 MHz, $\text{DMSO}-d_6$) of Poly(TsEtOHaz)-*graft*-PEG

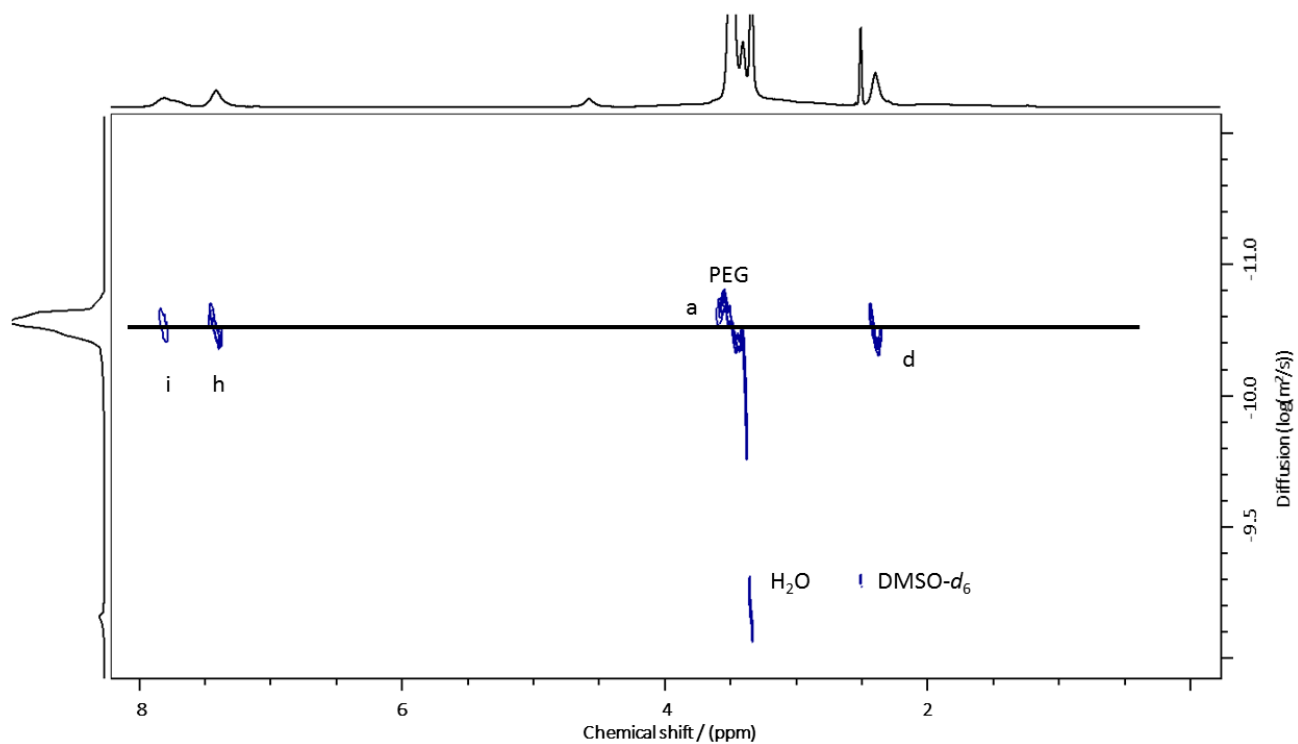


Figure 110: ¹H DOSY (DMSO-*d*₆, 500MHz, 298 K) of Poly(TsEtOHAz)-*graft*-PEG one-pot synthesis

10. Index

10.1 Scheme index

Scheme 1: Cationic ring opening polymerization of aziridines leads to hyperbranched (hbPEI).	13
Scheme 2: Anionic ring opening polymerization of activated N-sulfonylaziridines... ..	14
Scheme 3: Different synthesized hydrophobic monomers	15
Scheme 4: Synthesis of PEI-graft-PEG-polymers.....	17
Scheme 5: Anionic ring opening polymerization explained on the example of ethylene oxide derivatives	19
Scheme 6: Chain transfer to propylene oxide monomer due to deprotonation at the methyl group.....	20
Scheme 7: Influence of solvent polarity on chain end/ counter ion interactions.	21
Scheme 8: Mechanism of cationic ring opening polymerization of aziridines.....	23
Scheme 9: Possible reactions by substituting the N-H bound.....	23
Scheme 10: Mechanism of aza-anionic ring opening polymerization (AAROP) of activated N-sulfonylaziridines.	25
Scheme 11: Indication of substituent influence on the rate of propagation. Through increasing –I-effect the reactivity of the monomer is increased drastically, while the influence on the chain end is insignificant in comparison. (compare Fig. 2)	28
Scheme 12: 4-Styrenesulfonyl-(2-methyl)-aziridine can be used as a bivalent monomer and either be polymerized through radical or anionic polymerization.	29
Scheme 13: First synthesis of PAz with a functionalized hydroxide side chain. ³⁴	29
Scheme 14: highlighted reaction schema for assignment of classic ¹ H-NMR patterns	31
Scheme 15: Synthesized lipophilic monomers, Polymers and Copolymers.....	40
Scheme 16: Synthesis routes of activated N-sulfonylaziridines after Sharpless{Jeong, 1998 #100} and through amidation of sulfonyl chlorides	41
Scheme 17: bromine-catalyzed aziridination after Sharpless of a terminal olefin through trimethylphenylammonium tribromide	42
Scheme 18: Preparation of chloramine-M under exclusion of light	42

Scheme 19: synthesis 2-(cyclohexylmethyl)- <i>N</i> -mesylaziridine <i>via</i> Sharpless.	43
Scheme 20: Synthesis of activated N-sulfonylaziridines after Stewart.{Stewart, 2005 #45}	44
Scheme 21: Yield of synthesized <i>N</i> -sulfonylaziridines with lipophilic activation group before and after purification.	45
Scheme 22: Initiators for the anionic ROP of sulfonyl aziridines.	49
Scheme 23: Synthesis of BnNHMS and 4- ^t b-BnNHMS.	49
Scheme 24: Homopolymerization.	51
Scheme 25: Synthesized Copolymers.	60
Scheme 26: Synthesis overview of both conducted synthesis routes.	82
Scheme 27: Protection of TsEtOHaz through ethyl vinyl ether.	83
Scheme 28: Homopolymerization of TsEEEEaz.	85
Scheme 29: Deprotection of Poly(TsEEEEaz) through hydrolysis of the acetal group.	87
Scheme 30: Synthesis scheme of Poly(TsEtOHaz)-graft-PEG synthesis route one.	89
Scheme 31: One-pot synthesis of Poly(TsEtOHaz)-graft-PEG.	92
Scheme 32: Polymerization of a tri-block-copolymer.	96
Scheme 33:	101
Scheme 34: Synthesis of (^t b-BnNHMs).	103
Scheme 35: Synthesis of Tert-butyl hypochlorite.	105
Scheme 36: Synthesis of Chloramine-M.	106
Scheme 37: Synthesis of 2-Methyl-N-Octasylaziridin (OsMAz)	107
Scheme 38: Synthesis of 2-Methyl-N-Dodesylaziridin (DDsMAz)	111
Scheme 39: Synthesis of 2-(Cyclohexylmethyl)-N-Mesylaziridin (MsCyhexAz)	115
Scheme 40: Synthesis of 2-{{(1-Ethylethoxy)ethyl}-N-Tosylaziridine.	119
Scheme 41: general polymer synthesis.	121
Scheme 42: Hydrolysis of acetal groups.	145
Scheme 43: Graft-from synthesis of Poly(TsEtOHaz)-graft-PEG.	148
Scheme 44: One-pot synthesis of Poly(TsEtOHaz)-graft-PEG.	150

10.2 Table index

Table 1: Comparison of ethylene oxide and ethylene imine derivatives.....	22
Table 2: Investigated activation group for aza-anionic ring opening polymerization by Stewart: diphenylphosphinyl-, acetyl- and ethylcarbamoyl-. ¹²	24
Table 3	33
Table 4: Overview of Poly(OsMAz). M_n (NMR) given by eq. (8); M_n (GPC) and \bar{D} in DMF/PEG-standard	52
Table 5: Overview of successful polymerized Poly(2-methyl-N-dodesylaziridine) (DDsMAz). M_n (NMR) given by eq. (8); M_n (GPC) and \bar{D} in THF/PS-standard	54
Table 6: Overview of successful polymerized Poly(2-methyl-N-hexadecasyaziridine) Poly(HDsMAz). M_n (NMR) given by eq. (8); M_n (GPC) and \bar{D} in THF/PS-standard ..	55
Table 7: Overview of successful polymerized Poly(2-(cyclohexylmethyl)-N-mesyaziridine) Poly(MsCyhexAz). M_n (NMR) given by eq. (8); M_n (GPC) and \bar{D} in DMF/PEG-standard	58
Table 8: Overview of all synthesized copolymers and their ratios. M_n (NMR) given by eq. (8); M_n (GPC) and \bar{D} in DMF/PEG-standard	61
Table 10: Calculated r-parameter for the copolymerization of Poly(OsMAz-co-TsMAz).	68
Table 11: calculated r-parameter for the co-polymerization of poly-(MsCyhexAz-co-MsMAz).	70
Table 12: Solubility assay of synthesized Polymers with (10mg/mL)	71
Table 13: Overview over used polymer solutions in DCM for spin coating.	73
Table 14: Average values and standard deviation for left and right contact angle as well as layer thickness in dependence to the concentration.	75
Table 15: Average values and standard deviation for left and right contact angle as well as layer thickness in dependence to the side chain length.....	77
Table 16: average values and standard deviation for left and right contact angle as well as layer thickness in dependence to the degree of polymerization.	78
Table 17: average interface tension for a 1wt.% polymer cyclohexane solution.	81
Table 18 Overview of synthesized Polymers. M_n (GPC) and \bar{D} in DMF/PEG-standard	85

Table 19 Overview of synthesized Poly(TsEtOHaz); M_n (GPC) and \bar{D} in DMF/PEG-standard.....	87
Table 20: Overview of one-pot synthesis of Poly(TsEtOHaz)-graft-PEG,,; M_n (GPC) and \bar{D} in DMF/PEG-standard.....	93
Table 21: Overview over used polymer solutions in DCM for spin coating	99
Table 22: Overview of successful homo-polymerized Poly(DDsMAz).....	128
Table 23 Overview of synthesized Polymers.....	143

10.3 Figure index

Figure 1: Left; propagation rate of MsMAz by 50 °C and potassium as counter ion in different solvents to visualize the influence of solvent polarity on the propagation rate. Right; propagation rate of TsMAz by 50 °C in DMF with different counter ions. By Riegler et al. ³⁴	27
Figure 2: HOMO/LUMO Diagram in eV. Right: Influence of different substitutes on the LUMO of aziridine. Left: Influence of different substitutes on the HOMO of the active chain end compared to alkoxides By Gleede et al. ²⁰	28
Figure 3: ¹ H NMR spectra of 2-methylaziridine, substituted 2methyl-N-octasyaziridine and poly-(OsMAz). Highlighted areas show the classic patterns of aziridines and its polymers	32
Figure 4: Left: depiction model of a size exclusion chromatography. Molecules of different hydrodynamic radius (pictured through colored shapes) are fractionated through different retention times. Right: depiction of a GPC diagram by plotting elution volume against the signal intensity. Blue line indicates high and low exclusion limited through calibration standard.	35
Figure 5: intrinsic forces affecting molecules of a liquid.....	36
Figure 6: Depiction of a spinning drop measurement. The second phase (deep blue) deforms (light blue) through centrifugal force.	37
Figure 7: Depicture of the measurement process. A 100 µL syringe is used to create 5 µL droplets on the	37
Figure 8: Definition of the contact angle after Thomas Young	38
Figure 9: ¹ H NMR (700 MHz, benzene- <i>d</i> ₆) of 2-(Cyclohexylmethyl)- <i>N</i> -mesylaziridin (MsCyhexAz).	43
Figure 10: ¹ H NMR (300 MHz, Chloroform- <i>d</i>) of 2-Methyl- <i>N</i> -Octasyaziridin (OsMAz).	46
Figure 11: ¹ H NMR (300 MHz, Methylene Chloride- <i>d</i> ₂) of 2-Methyl- <i>N</i> -Dodesylaziridin (DDsMAz).	47
Figure 12: ¹ H NMR (300 MHz, Tetrachloroethane- <i>d</i> ₂) of 2-methyl- <i>N</i> -hexadecasyaziridine (HDsMAz).	48
Figure 13: ¹ H NMR (300 MHz, Chloroform- <i>d</i>) of <i>N</i> -benzylmesylsulfonamide (BnNHMs).	50

Figure 14: ^1H NMR (300 MHz, tetrachloroethane- d_2) of 4- ^tb -BnNHMs.	50
Figure 15: ^1H NMR (300 MHz, tetrachloroethane- d_2) of Poly(2-methyl- <i>N</i> -octasylaziridine).....	53
Figure 16: GPC traces (RI detection) of Poly(2-methyl- <i>N</i> -octasylaziridine) in DMF.	53
Figure 17: ^1H NMR (300 MHz, tetrachloroethane- d_2) of Poly(2-methyl- <i>N</i> -dodesylaziridine) Poly(DDsMAz).	56
Figure 18: ^1H NMR (300 MHz, Methylene Chloride- d_2) of Poly(2-methyl- <i>N</i> -hexadecasyaziridine) Poly(HDsMAz).....	56
Figure 19: GPC traces (RI detection) of Poly(2-methyl- <i>N</i> -dodesylaziridine) (Poly(DDsMAz)) in THF.	57
Figure 20: GPC traces (RI detection) of Poly(2-methyl- <i>N</i> -hexadecasyaziridine) (Poly(HDsMAz)) in THF.	57
The ^1H NMR of Poly(MsCyhexAz) shows an increased backbone ratio to 1:2:3 due to the CH_3 -mesyl group (multiplets e,g,d). Furthermore, the sterically demanding cyclohexylmethyl-group peaks overlap between 1.34–0.69 ppm (multiplet, b). (Figure 22) The polymerization itself was conducted over 4 days as a first ^1H NMR indicated a not completed conversion.	58
Figure 22: ^1H NMR (300 MHz, Methylene Chloride- d_2) Poly(2-(Cyclohexylmethyl)- <i>N</i> -mesylaziridine) Poly(MsCyhexAz).	58
Figure 23: GPC traces (RI detection) of Poly(2-(cyclohexylmethyl)- <i>N</i> -mesylaziridine) Poly(MsCyhexAz) in DMF.....	59
Figure 24 ^1H NMR (300 MHz, Methylene Chloride- d_2) of Poly(OsMAz-co-MsMAz).	62
Figure 25: GPC-traces (RI detection) of Poly(OsMAz-co-MsMAz) in different ratios in DMF.....	62
Figure 26: ^1H NMR (300 MHz, DCM- d_2) of Poly(Cyhex-co-MsMAz).....	63
Figure 27: GPC-traces (RI-detection) of Poly(MsCyhexAz-co-MsMAz).....	64
Figure 28 ^1H NMR (700 MHz, DMF- d_7) of Poly(OsMAz-co-TsMAz).	Fehler!
Textmarke nicht definiert.	
Figure 29: Monomer conversion of OsMAz (orange) and TsMAz (green) vs the total conversion.	67
Figure 30: mole fraction of the incorporated TsMAz (orange) vs the total conversion.	67

Figure 31: Copolymerization diagram of Poly(OsMAz-co-TsMAz).....	68
Figure 32: Monomer conversion of MsMAz and MsCyhexAz vs the total conversion.	69
Figure 33: mol-fraction of the incorporated MsMAz vs the total conversion.....	70
Figure 34: Copolymerization diagram of Poly(MsCyhexAz-co-MsMAz).....	70
Figure 36: Contact angle of a water droplet on a coated microscopy slide.....	72
Figure 35: Contact angle of water on an uncoated microscopy slide.....	72
Figure 37: illustration of a layer thickness measurement through a cantilever.....	73
Figure 38: coated microscope slides on white paper. Black line for location purpose under the microscope.	73
Figure 39: Obtained surface profile of a spin coated microscopy slide. Sharp peak is cause by the removal of the polymer layer Poly(HDsMAz) X_n 60 measurement 2. ..	74
Figure 40: Contact angles for coated glass slides vs polymer concentration.....	75
Figure 41: Contact angle of various polymers with different side chain lengths.....	77
Figure 42: Contact angle of Poly(HDsMAz) with X_n 15, 30, 60	79
Figure 43: average interfacial tension for a 1wt.% polymer cyclohexane solution. ...	80
Figure 44: ^1H NMR (300 MHz, DCM- d_2) 2-((1-Ethylethoxy)ethyl)- <i>N</i> -Tosylaziridine.	84
Figure 45: ^1H NMR (300 MHz, DCM- d_2) of Poly(TsEEEEAz).....	86
Figure 46: GPC traces (RI-detection) of Poly(TsEEEEAz).....	86
Figure 47: Stacked ^1H NMR of starting material Poly(TsEEEEAz) (blue) and product Poly(TsEtOHAz) (red).....	88
Figure 48: GPC traces (RI-detection) of Poly(TsEtOHAz).	88
Figure 49: GPC traces (RI detection) of Poly(TsEtOHAz)-graft-PEG.	90
Figure 50: ^1H NMR (500 MHz, DMSO- d_6) of Poly(TsEtOHAz)- <i>graft</i> -PEG.	91
Figure 51: ^1H DOSY (DMSO- d_6 , 700MHz, 298 K) of Poly(TsEtOHAz)- <i>graft</i> -PEG...	91
Figure 52: GPC trace (RI detection) of Poly(TsEtOHAz)- <i>graft</i> -PEG one-pot synthesis.	94
Figure 53: ^1H NMR (500 MHz, DMSO- d_6) of Poly(TsEtOHAz)- <i>graft</i> -PEG one-pot synthesis.....	95
Figure 54: ^1H DOSY (DMSO- d_6 , 700MHz, 298 K) of Poly(TsEtOHAz)- <i>graft</i> -PEG one- pot synthesis.....	95
Figure 55: ^1H NMR (300 MHz, Chloroform- d) of benzyl- <i>N</i> -methylsulfonamide	102

Figure 56: ^{13}C NMR (300 MHz, Chloroform-d) of benzyl-N-methylsulfonamide.....	102
Figure 57: ^1H NMR (300 MHz, tetrachloroethane- d_2) of (^tb -BnNHMs)	104
Figure 58: ^{13}C NMR (300 MHz, tetrachloroethane- d_2) of (^tb -BnNHMs).....	104
Figure 59: ^1H NMR (300 MHz, Chloroform-d) of tert.-butyl hypochlorite.....	105
Figure 60: ^1H NMR (300 MHz, Deuterium Oxide) of Chloramine-M.....	106
Figure 61: ^1H NMR (300 MHz, chloroform-d) of 2-Methyl-N-Octasylaziridin (OsMAz)	108
Figure 62: ^{13}C NMR (700 MHz, benzene- d_6) of 2-Methyl-N-Octasylaziridin (OsMAz)	108
Figure 63: COSY-NMR (700 MHz, benzene- d_6) of 2-Methyl-N-Octasylaziridin (OsMAz)	109
Figure 64: mass spectrum of 2-Methyl-N-Octasylaziridin	109
Figure 65: IR-spectrum of 2-Methyl-N-Octasylaziridin	110
Figure 66: ^1H NMR (300 MHz, Methylene Chloride- d_2) of 2-Methyl-N-Dodesylaziridin (DDsMAz)	112
Figure 67: ^{13}C NMR (300 MHz, benzene- d_6) of 2-Methyl-N-Dodesylaziridin (DDsMAz)	112
Figure 68: Synthesis of 2-Methyl-N-Hexadesylaziridin (HDsMAz).....	113
Figure 69: ^1H NMR (300 MHz, tetrachloroethane- d_2) of 2-Methyl-N-Hexadesylaziridin (HDsMAz).	114
Figure 70: ^{13}C NMR (300 MHz, tetrachloroethane- d_2) of 2-Methyl-N-Hexadesylaziridin (HDsMAz).	114
Figure 71: ^1H NMR (700 MHz, Benzene- d_6) of (MsCyhexAz).	116
Figure 72: ^{13}C NMR (700 MHz, benzene- d_6) of (MsCyhexAz).	116
Figure 73: COSY NMR (700 MHz, benzene- d_6) of (MsCyhexAz).	117
Figure 74: mass spectrum of (MsCyhexAz).	117
Figure 75: IR-spectrum of (MsCyhexAz).	118
Figure 76: ^1H NMR (300 MHz, DCM- d_2) of 2- $\{(1\text{-Ethylethoxy})\text{ethyl}\}$ -N-Tosylaziridine.	120
Figure 77: ^{13}C NMR (300 MHz, DCM- d_2) of 2- $\{(1\text{-Ethylethoxy})\text{ethyl}\}$ -N-Tosylaziridine.	120

Figure 78: ^1H NMR (300 MHz, methylene chloride- d_2) of Poly(2-Methyl-N-octasylaziridin).....	124
Figure 79: GPC-traces (RI-detection) of Poly(OsMAz) in DMF/PEG standard	124
Figure 80: TGA of Poly(OsMAz).....	125
Figure 81: DSC of Poly(OsMAz).....	125
Figure 82: ^1H NMR (300 MHz, Methylene Chloride- d_2) of Poly(OsMAz) with t -BnNHMs initiator.....	127
Figure 83: GPC-traces (RI-detection) of Poly(OsMAz) in DMF/ PEG standard	127
Figure 84: ^1H NMR (300 MHz tetrachloroethane- d_2) of Poly(2-methyl-N-dodesylaziridine) Poly(DDsMAz).....	129
Figure 85: GPC traces of homo-polymerized Poly(DDsMAz) in THF.	129
Figure 86: TGA of Poly(DDsMAz).....	130
Figure 87: DSC of Poly(DDsMAz).....	130
Figure 88: ^1H NMR (300 MHz, tetrachloroethane- d_2) of Poly(2-methyl-N-hexadecasyaziridine).....	132
Figure 89: GPC traces (RI detection) of Poly(HDsMAz) in THF.	133
Figure 90: TGA of Poly(HDsMAz).....	134
Figure 91: DSC of Poly(HDsMAz).....	134
Figure 92: ^1H NMR (300 MHz, Methylene Chloride- d_2) of Poly(2-Cyclohexanemethyl-N-Mesylaziridin).....	135
Figure 93: GPC traces (RI-detection) of polymerized Poly(MsCyhexAz) in DMF. .	136
Figure 94: TGA of Poly(MsCyhexAz).....	136
Figure 95: DSC of Poly(MsCyhexAz).....	137
Figure 96: ^1H NMR (300 MHz, DCM- d_2) of Poly(OsMAz)-co-(MsMAz) (1:1)	139
Figure 97: DSC of Poly(OsMAz)-co-(MsMAz) with different ratios	140
Figure 98: GPC-traces (RI-detection) of Poly(OsMAz-co-MsMAz) of different ratios in DMF	140
Figure 99: ^1H NMR (300 MHz, DCM- d_2) of Poly(MsCyhexAz)-co-(MsMAz)	141
Figure 100: GPC-traces (RI-detection) of Poly(MsCyhexAz-co-MsMAz).....	142
Figure 101: DSC of Poly(MsCyhexAz-co-MsMAz).....	142
Figure 102 ^1H NMR (300 MHz, DCM- d_2) Poly{2-(2-Ethylethoxy)-Ethanol-N-Tosylaziridine}	144

Figure 103 : GPC traces (RI-detection) of Poly(TsEEEEAz).....	144
Figure 104: ^1H NMR (300 MHz, DMF- d_7) of Poly(2-Ethanol- <i>N</i> -Tosylaziridine)	146
Figure 105: GPC traces of Poly(TsEtOHAz).....	147
Figure 106: ^1H NMR (500 MHz, DMSO- d_6) of Poly(TsEtOHAz)-graft-PEG.	149
Figure 107: GPC (RI-detection) of Poly(TsEtOHAz)-graft-PEG.....	149
Figure 108: GPC trace (RI-detection) of Poly(TsEtOHAz)-graft-PEO one-pot synthesis	151
Figure 109: ^1H NMR (500 MHz, DMSO- d_6) of Poly(TsEtOHAz)-graft-PEG	151
Figure 110: ^1H DOSY (DMSO- d_6 , 500MHz, 298 K) of Poly(TsEtOHAz)-graft-PEG one- pot synthesis.....	152
Figure 111: Poly(HDsMAz) X_n 10 measurement 1.....	174
Figure 112: Poly(HDsMAz) X_n 10 measurement 2.....	175
Figure 113: Poly(HDsMAz) X_n 10 measurement 3.....	176
Figure 114: Poly(HDsMAz) X_n 10 measurement 4.....	177
Figure 115: Poly(HDsMAz) X_n 60 measurement 1.....	178
Figure 116: Poly(HDsMAz) X_n 60 measurement 2.....	179
Figure 117: Poly(HDsMAz) X_n 60 measurement 3.....	180
Figure 118: Poly(DDsMAz) X_n 30 measurement 1.....	181
Figure 119: Poly(DDsMAz) X_n 30 measurement 2.....	182
Figure 120: Poly(DDsMAz) X_n 30 measurement 3.....	183
Figure 121: Poly(OsMAz) X_n 30 measurement 1	184
Figure 122: Poly(OsMAz) X_n 30 measurement 2	185
Figure 123: Poly(OsMAz) X_n 30 measurement 3	186
Figure 124: Poly(HDsMAz) 2.0 wt. % X_n 30 measurement 2.....	187
Figure 125: Poly(HDsMAz) 2.0 wt. % X_n 30 measurement 3.....	188
Figure 126: Poly(HDsMAz) 2.0 wt. % X_n 30 measurement 1	189
Figure 127: Poly(HDsMAz) 1.0 wt. % X_n 30 measurement 1	190
Figure 128: Poly(HDsMAz) 1.0 wt. % X_n 30 measurement 2.....	191
Figure 129: Poly(HDsMAz) 1.0 wt. % X_n 30 measurement 3.....	192
Figure 130: Poly(HDsMAz) 0.5 wt. % X_n 30 measurement 1	193
Figure 131: Poly(HDsMAz) 0.5 wt. % X_n 30 measurement 2.....	194
Figure 132: Poly(HDsMAz) 0.5 wt. % X_n 30 measurement 3.....	195

Figure 133: Poly(HDsMAz) 0.5 wt. % X_n 30 measurement 4.....	196
Figure 134: Poly(MsMAz) X_n 30 measurement 1.....	197
Figure 135: Poly(MsMAz) X_n 30 measurement 2.....	198
Figure 136: Poly(MsMAz) X_n 30 measurement 3.....	199
Figure 137: ^1H NMR Kinetic 700 MHz DMF- d_7 of MsMAz and MsCyhexAz	207
Figure 138: ^1H NMR Kinetic 700 MHz DMF- d_7 of OsMAz and MsMAz	207
Figure 139: ^1H NMR Kinetic 700 MHz DMF- d_7 of OsMAz and TsMAz.....	208
Figure 140: Jaacks fit of ^1H NMR kinetic data of MsCyhexAz and MsMAz.....	209
Figure 141: Jaacks fit of ^1H NMR kinetic data of OsMAz and TsMAz.....	209
Figure 142: Meyer-Lowry fit of ^1H NMR kinetic data of MsCyhexAz and MsMAz ..	210
Figure 143: Meyer-Lowry fit of ^1H NMR kinetic data of OsMAz and TsMAz	210

11. References

1. Gabriel, S., Ueber Vinylamin. *Berichte der deutschen Chemie Gesellschaft* **1888**, 21 (1), 1049-1057.
2. W.P.Coker US 3326895. 1967.
3. Steuerle, U.; Feuerhake, R., Aziridines. *Ullmann's Encyclopedia of Industrial Chemistry* **2001**.
4. Jones, G. D.; Langsjoen, A.; Neumann, S. M. M. C.; Zomlefer, J., The Polymerization of ethyleneimine. *The Journal of Organic Chemistry* **1944**, 09 (2), 125-147.
5. Stewart, I. C.; Lee, C. C.; Bergman, R. G.; Toste, F. D., Living Ring-Opening Polymerization of N-Sulfonylaziridines: Synthesis of High Molecular Weight Linear Polyamines. *Journal of the American Chemical Society* **2005**, 127 (50), 17616-17617.
6. Boussif, O.; Lezoualc'h, F.; Zanta, M. A.; Mergny, M. D.; Scherman, D.; Demeneix, B.; Behr, J. P., A versatile vector for gene and oligonucleotide transfer into cells in culture and in vivo: polyethylenimine. *Proceedings of the National Academy of Sciences of the United States of America* **1995**, 92 (16), 7297-7301.
7. Jäger, M.; Schubert, S.; Ochrimenko, S.; Fischer, D.; Schubert, U. S., Branched and linear Poly(ethylene imine)-based conjugates: synthetic modification, characterization, and application. *Chemical Society Reviews* **2012**, 41 (13), 4755-4767.
8. Drese, J. H.; Choi, S.; Lively, R. P.; Koros, W. J.; Fauth, D. J.; Gray, M. L.; Jones, C. W., Synthesis–Structure–Property Relationships for Hyperbranched Aminosilica CO₂ Adsorbents. **2009**, 19 (23), 3821-3832.
9. Bolto, B. A., Soluble polymers in water purification. *Progress in Polymer Science* **1995**, 20 (6), 987-1041.
10. von Zelewsky, A.; Barbosa, L.; Schläpfer, C. W., Poly(ethylenimines) as Brønsted bases and as ligands for metal ions. *Coordination Chemistry Reviews* **1993**, 123 (1), 229-246.
11. Khansarizadeh, M.; Mokhtarzadeh, A.; Rashedinia, M.; Taghdisi, S.; Lari, P.; Abnous, K.; Ramezani, M., Identification of possible cytotoxicity mechanism of polyethylenimine by proteomics analysis. *Human & Experimental Toxicology*, **2016**, 35 (4), 377-387.
12. Mintzer, M. A.; Simanek, E. E., Nonviral Vectors for Gene Delivery. *Chemical Reviews* **2009**, 109 (2), 259-302.
13. Herold D., K. K. Oxidation of polyethylene glycols by alcohol dehydrogenase *Biochemical Pharmacology* **1989**, 38 (1), 73-76.
14. Finch, C. A., Poly(ethylene glycol) chemistry: Biotechnical and biomedical applications. Edited by J. Milton Harris. Plenum Publishing, New York, 1992. ISBN 0-306-44078-4. **1994**, 33 (1), 115-115.

11. References

15. Smyth, H. F.; Carpenter, C. P.; Weil, C. S., The Toxicology of the Polyethylene Glycols*. *Journal of the American Pharmaceutical Association (Scientific ed.)* **1950**, 39 (6), 349-354.
16. Gaziova, Z.; Baumann, V.; Winkler, A.-M.; Winkler, J., Chemically defined polyethylene glycol siRNA conjugates with enhanced gene silencing effect. *Bioorganic & Medicinal Chemistry* **2014**, 22 (7), 2320-2326.
17. Shokrzadeh, N.; Winkler, A.-M.; Dirin, M.; Winkler, J., Oligonucleotides conjugated with short chemically defined polyethylene glycol chains are efficient antisense agents. *Bioorganic & Medicinal Chemistry Letters* **2014**, 24 (24), 5758-5761.
18. Gordon J. Lutz, S. R. S., Jason H. Williams, *Production and In Vivo Applications of Gene Transfer Vectors* 3ed.; Humana Press: Totowa, 2008; Vol. 1, p 141-150.
19. Gleede, T.; Rieger, E.; Blankenburg, J.; Klein, K.; Wurm, F. R., Fast Access to Amphiphilic Multiblock Architectures by the Anionic Copolymerization of Aziridines and Ethylene Oxide. *Journal of the American Chemical Society* **2018**, 140 (41), 13407-13412.
20. Gleede, T.; Rieger, E.; Liu, L.; Bakkali-Hassani, C.; Wagner, M.; Carlotti, S.; Taton, D.; Andrienko, D.; Wurm, F. R., Alcohol- and Water-Tolerant Living Anionic Polymerization of Aziridines. *Macromolecules* **2018**, 51 (15), 5713-5719.
21. Rieger, E.; Manhart, A.; Wurm, F. R., Multihydroxy Polyamines by Living Anionic Polymerization of Aziridines. *ACS Macro Letters* **2016**, 5 (2), 195-198.
22. Szwarc, M.; Levy, M.; Milkovich, R., POLYMERIZATION INITIATED BY ELECTRON TRANSFER TO MONOMER. A NEW METHOD OF FORMATION OF BLOCK POLYMERS¹. *Journal of the American Chemical Society* **1956**, 78 (11), 2656-2657.
23. Hirao, A.; Goseki, R.; Ishizone, T., Advances in Living Anionic Polymerization: From Functional Monomers, Polymerization Systems, to Macromolecular Architectures. *Macromolecules* **2014**, 47 (6), 1883-1905.
24. Frey, H.; Ishizone, T., Living Anionic Polymerization – Part II: Further Expanding the Synthetic Versatility for Novel Polymer Architectures. **2018**, 219 (1), 1700567.
25. Tieke, B., *Makromolekulare Chemie: Eine Einführung*. John Wiley & Sons, Inc: 2014; Vol. 3. ISBN: 978-3-527-33216-8
26. Herzberger, J.; Niederer, K.; Pohlitz, H.; Seiwert, J.; Worm, M.; Wurm, F. R.; Frey, H., Polymerization of Ethylene Oxide, Propylene Oxide, and Other Alkylene Oxides: Synthesis, Novel Polymer Architectures, and Bioconjugation. *Chem Rev* **2016**, 116 (4), 2170-243.
27. Nikos Hadjichristidis, A. H., *Anionic Polymerization Principles, Practice, Strength, Consequences and Applications*. Springer Japan: Tokyo, 2015.

11. References

28. Henry Hsieh, R. P. Q., *Anionic Polymerization Principles and Practical Applications*. 1 ed.; CRC Press Boca Raton, 1996; Vol. 1.
29. Pearson, R. G., Hard and Soft Acids and Bases. *Journal of the American Chemical Society* **1963**, 85 (22), 3533-3539.
30. Pearson, R. G. Chemical hardness and density functional theory. *J. Chem. Sci.* **2005**, 117 (5), 369-377.
31. Sweeney, J. B., Aziridines: epoxides' ugly cousins? *Chemical Society Reviews* **2002**, 31 (5), 247-258.
32. Ham, G. E., Activated Aziridines. I. Reaction of Anilines with O-Ethyl-N,N-Ethyleneurethane. Mechanism and Hammett ρ -Constant. *The Journal of Organic Chemistry* **1964**, 29 (10), 3052-3055.
33. Rieger, E.; Gleede, T.; Manhart, A.; Lamla, M.; Wurm, F. R., Microwave-Assisted Desulfonylation of Polysulfonamides toward Polypropylenimine. *ACS Macro Letters* **2018**, 7 (6), 598-603.
34. Rieger, E.; Gleede, T.; Weber, K.; Manhart, A.; Wagner, M.; Wurm, F. R., The living anionic polymerization of activated aziridines: a systematic study of reaction conditions and kinetics. *Polymer Chemistry* **2017**, 8 (18), 2824-2832.
35. Rieger, E.; Alkan, A.; Manhart, A.; Wagner, M.; Wurm, F. R., Sequence-Controlled Polymers via Simultaneous Living Anionic Copolymerization of Competing Monomers. *Macromolecular rapid communications* **2016**, 37 (10), 833-839.
36. Mbarushimana, P. C.; Liang, Q.; Allred, J. M.; Rupar, P. A., Polymerizations of Nitrophenylsulfonyl-Activated Aziridines. *Macromolecules* **2018**, 51 (3), 977-983.
37. Thomi, L.; Wurm, F. R. In *Living Anionic Polymerization of Functional Aziridines*, Macromolecular Symposia, Wiley Online Library: **2015**; pp 51-56.
38. Gleede, T.; Rieger, E.; Homann-Müller, T.; Wurm, F. R., 4-Styrenesulfonyl-(2-methyl)aziridine: The First Bivalent Aziridine-Monomer for Anionic and Radical Polymerization. *Macromolecular Chemistry and Physics* **2018**, 219 (1).
39. Overberger, C. G.; Tobkes, M., Polymerization behavior of aziridines with 1,2-epoxides. *Journal of Polymer Science Part A: General Papers* **1964**, 2 (5), 2481-2487.
40. Meyer, V. E.; Lowry, G. G., Integral and differential binary copolymerization equations. *Journal of Polymer Science Part A: General Papers* **1965**, 3 (8), 2843-2851.
41. Jaacks, V., A novel method of determination of reactivity ratios in binary and ternary copolymerizations. *Macromolecular Chemistry and Physics* **1972**, 161 (1), 161-172.
42. Jeong, J. U.; Tao, B.; Sagasser, I.; Henniges, H.; Sharpless, K. B., Bromine-Catalyzed Aziridination of Olefins. A Rare Example of Atom-Transfer Redox Catalysis by a Main Group Element. *Journal of the American Chemical Society* **1998**, 120 (27), 6844-6845.

11. References

43. Burlingham, B. T.; Widlanski, T. S., Synthesis and Reactivity of Polydisulfonimides. *Journal of the American Chemical Society* **2001**, 123 (13), 2937-2945.
44. Vonnegut, B., Rotating Bubble Method for the Determination of Surface and Interfacial Tensions. *Review of Scientific Instruments* **1942**, 13 (1), 6-9.

12. Appendix

12.1 Contact angle measurement

Measurement	HDsMAz <i>Xn</i> 15 left angle	HDsMAz <i>Xn</i> 15 right angle
1	106.1	105.8
2	101.5	101.4
3	101.8	101.7
4	101.1	101.2
5	103.9	103.9
average mean	102.88	102.8
standard deviation	1.88	1.79

Measurement	HDsMAz <i>Xn</i> 60 left angle	HDsMAz <i>Xn</i> 60 right angle
1	69.5	80.0
2	49.0	56.0
3	77.8	81.1
4	87.6	89.2
5	76.2	75.2
6	58.4	69.6
7	67.5	71.1
average mean	69.4	74.6
standard deviation	11.89	9.77

Measurement	DDsMAz left angle	DDsMAz right angle
1	102.1	101.9
2	101.6	101.4
3	102.5	102.4
4	100.9	100.9
5	102.0	101.9
6	103.0	102.8
average mean	102.0	101.9
standard deviation	0.66	0.62

12. Appendix

Measurement	OsMAz left angle	OsMAz right angle
1	98.8	98.7
2	97.8	97.7
3	96.8	96.8
4	98.2	98.1
5	96.2	96
6	98.5	98.6
average mean	97.7	97.7
standard deviation	0.93	0.97

Measurement	HDsMAz 0.5 wt.% left angle	HDsMAz 0.5 wt% right angle
1	96.0	95.9
2	100.3	100.2
3	99.0	98.9
4	99.8	99.6
5	99.9	99.6
average mean	99.0	98.8
standard deviation	1.56	1.53

Measurement	HDsMAz left angle	HDsMAz right angle
1	103.5	103.4
2	104.0	103.4
3	104.0	103.9
4	105.1	105.0
5	102.3	102.0
6	104.4	104.3
average mean	103.9	103.7
standard deviation	0.86	0.93

12. Appendix

Measurement	HDsMAz 2 wt% left angle	HDsMAz 2 wt% right angle
1	104.7	104.7
2	106.4	106.2
3	105.3	105.6
4	104.7	104.4
average mean	105.3	105.2
standard deviation	0.69	0.72

Measurement	MsMAz left angle	MsMAz right angle
1	60.2	60.0
2	68.0	67.7
3	60.4	60.8
4	59.2	59.7
5	65.7	65.5
6	69.7	70.2
7	62.4	62.3
8	62.0	62.3
average mean	63.5	63.6
standard deviation	3.64	3.59

12.2 Layer thickness measurement

Platte 1 measurement	HDsMAz X_n 10 / Å	nm
1	769	
2	768	
3	783	
average value	773	77
standard deviation	7	1

Platte 2 measurement	HDsMAz X_n 60 / Å	nm
1	1000	
2	1010	
3	943	
average value	984	98
standard deviation	29	3

Platte 3	DDsMAz / Å	nm
1	1000	
2	1010	
3	943	
average value	1060	106
standard deviation	51	5

Platte 4	OsMAz / Å	nm
1		
2	1000	
3	1106	
average value	1053	105
standard deviation	53	5

Platte 9	HDsMAz 2.0 wt. % / Å	nm
1	2690	
2	2506	
3	2352	
average value	2516	252
standard deviation	138	14

12. Appendix

Platte 10	HDsMAz X_n 30 1.0 wt.% / Å	nm
1	1300	
2	1270	
3	1255	
average value	1275	127
standard deviation	19	2

Platte 11	HDsMAz X_n 30 0.5 wt.% / Å	nm
1	374	
2	378	
3	418	
average value	390	39
standard deviation	20	2

Platte 11	MsMAz X_n 30/ Å	nm
1	1144	
2	1223	
3	1181	
average value	1183	118
standard deviation	32	3

Level: CYS
 Mass: 800A
 600A
 400A
 200A
 0A
 -200A
 -400A
 -600A
 -800A
 -1000A
 -1200A

Height

Scan Length (μm)

Normal

Scan Length (μm)	Current (A)
25	-400
100	400
175	-400
250	400

174

12. Appendix

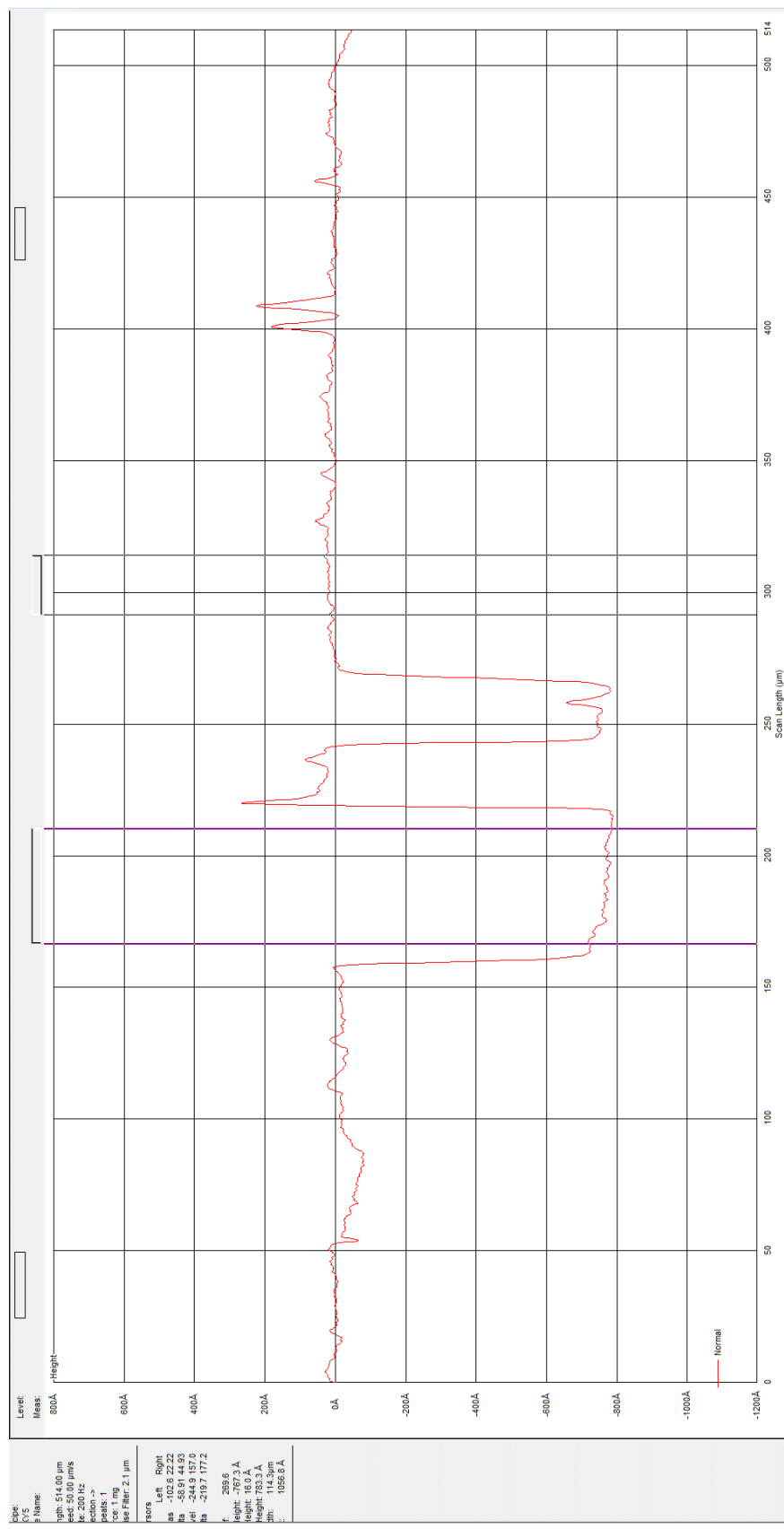


Figure 112: Poly(HDsMAz) X_n 10 measurement 2

12. Appendix

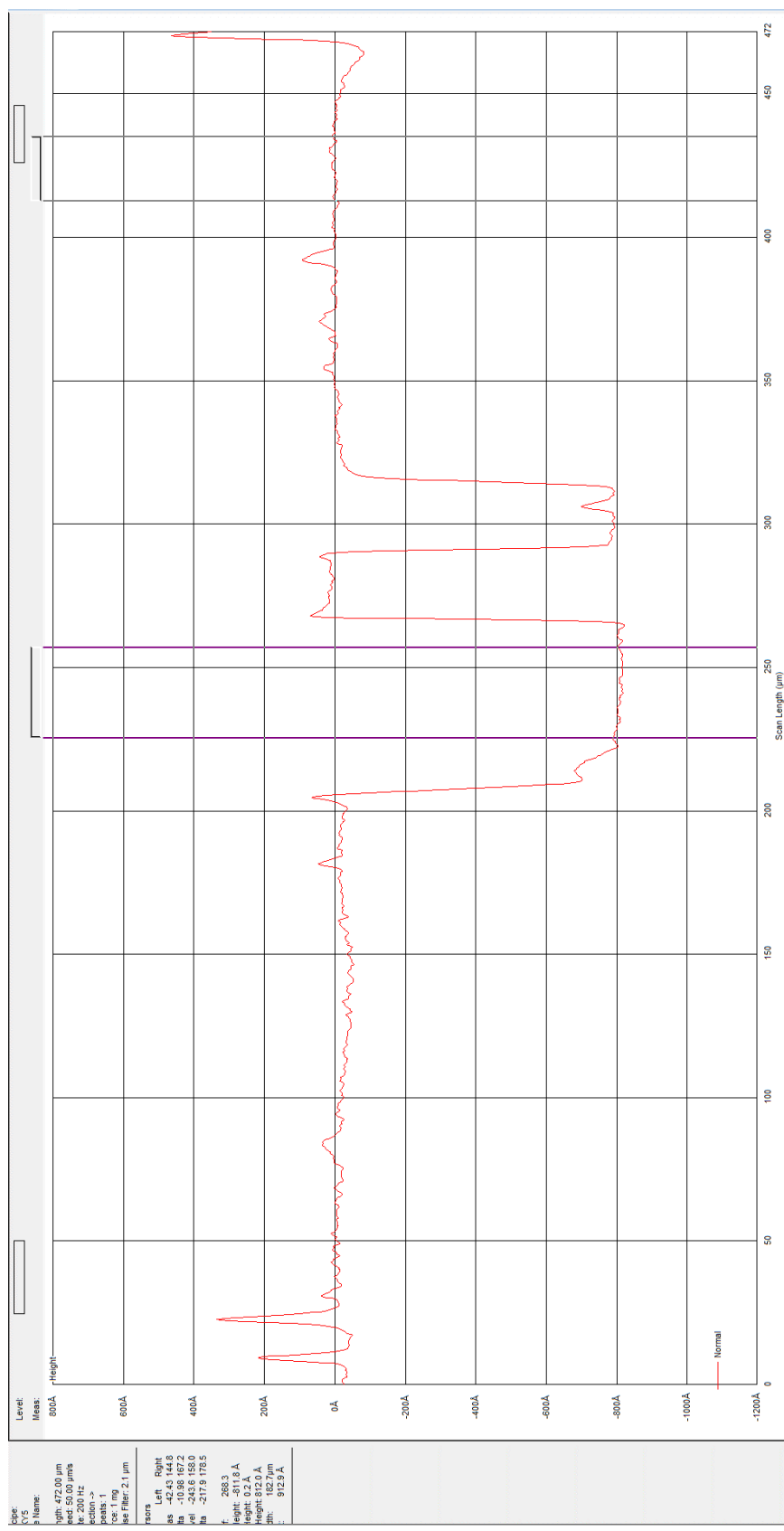


Figure 113: Poly(HDsMAz) X_n 10 measurement 3

12. Appendix

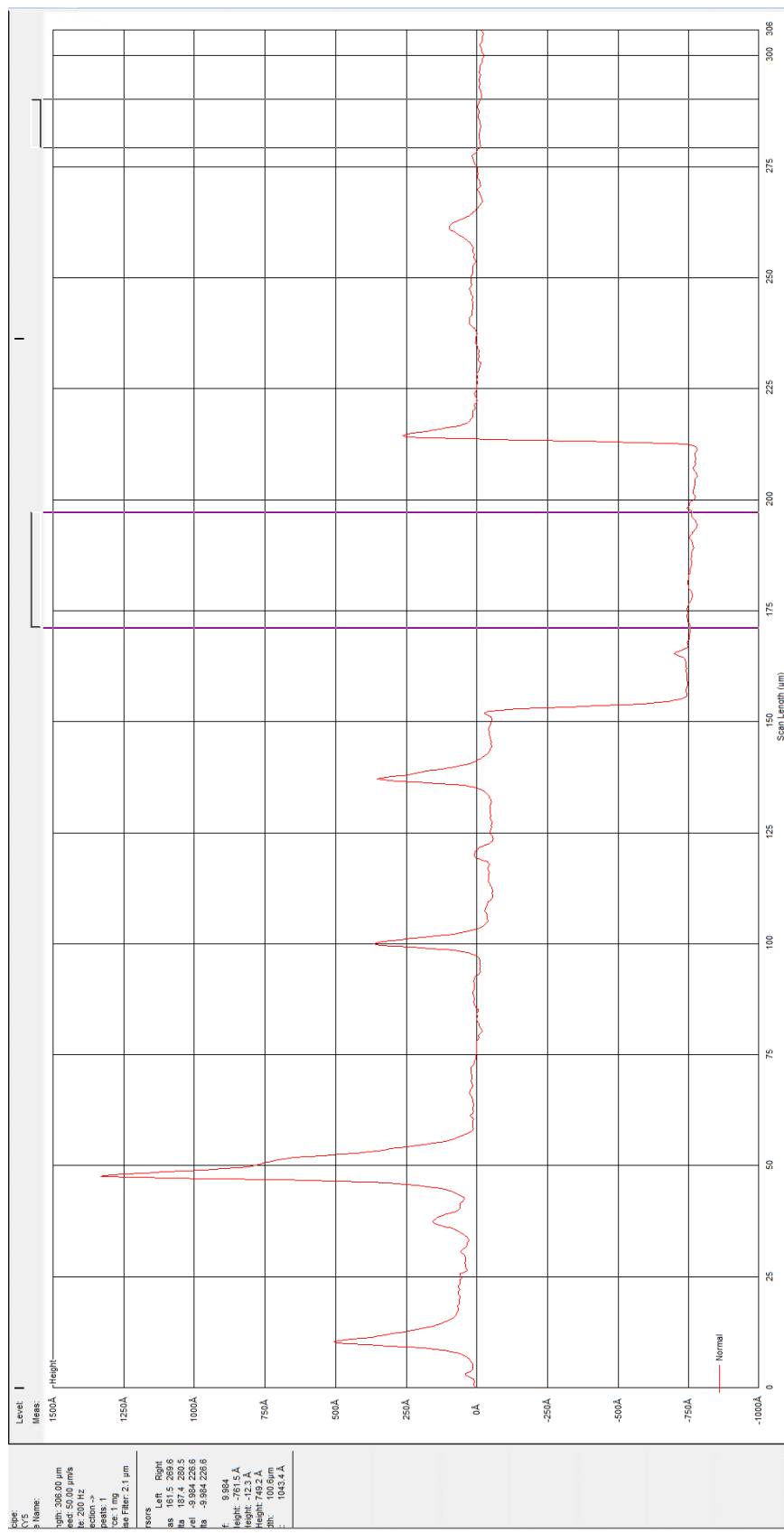


Figure 114: Poly(HDsMAz) X_n 10 measurement 4

178

12. Appendix

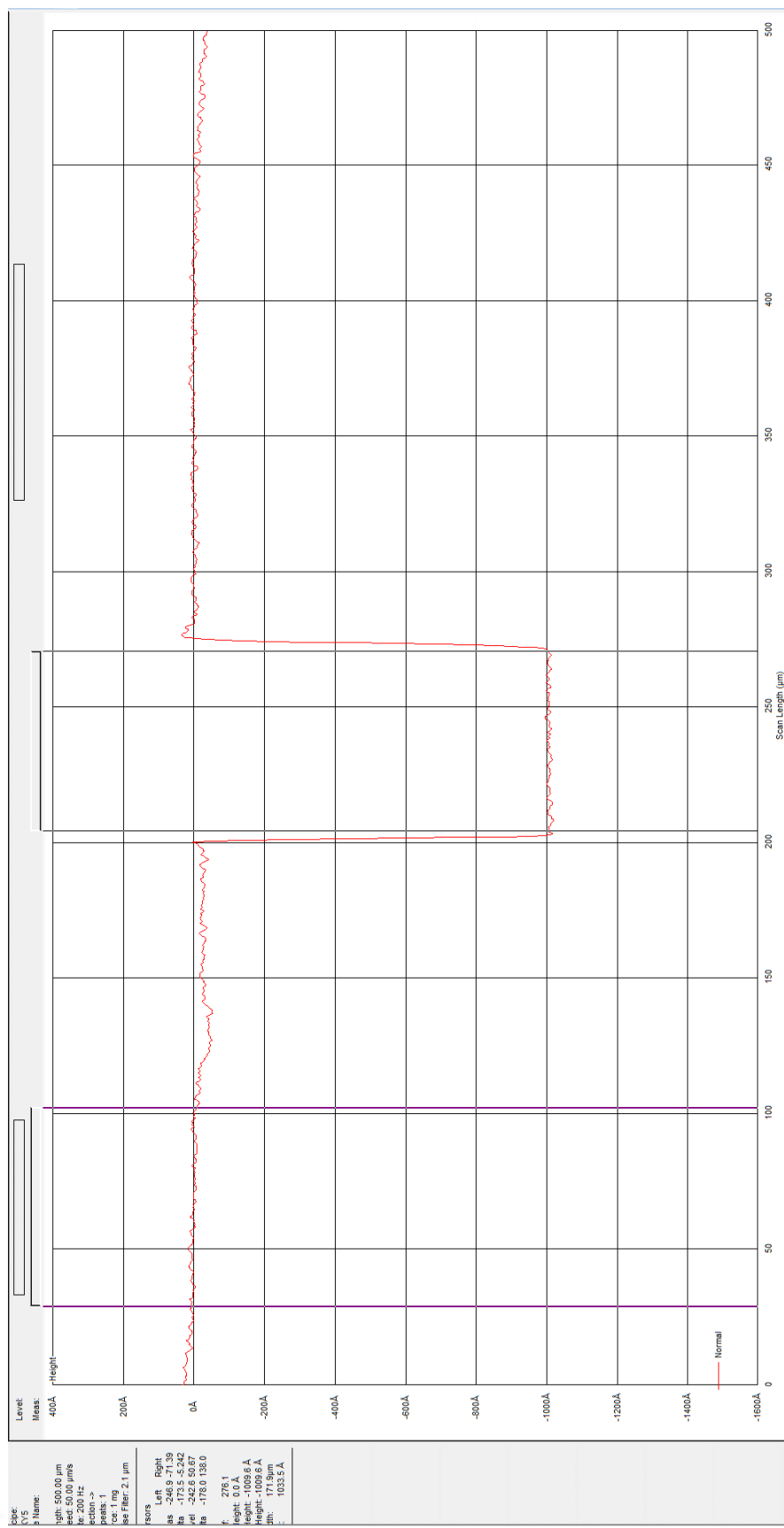


Figure 116: Poly(HDsMAz) X_n 60 measurement 2

12. Appendix

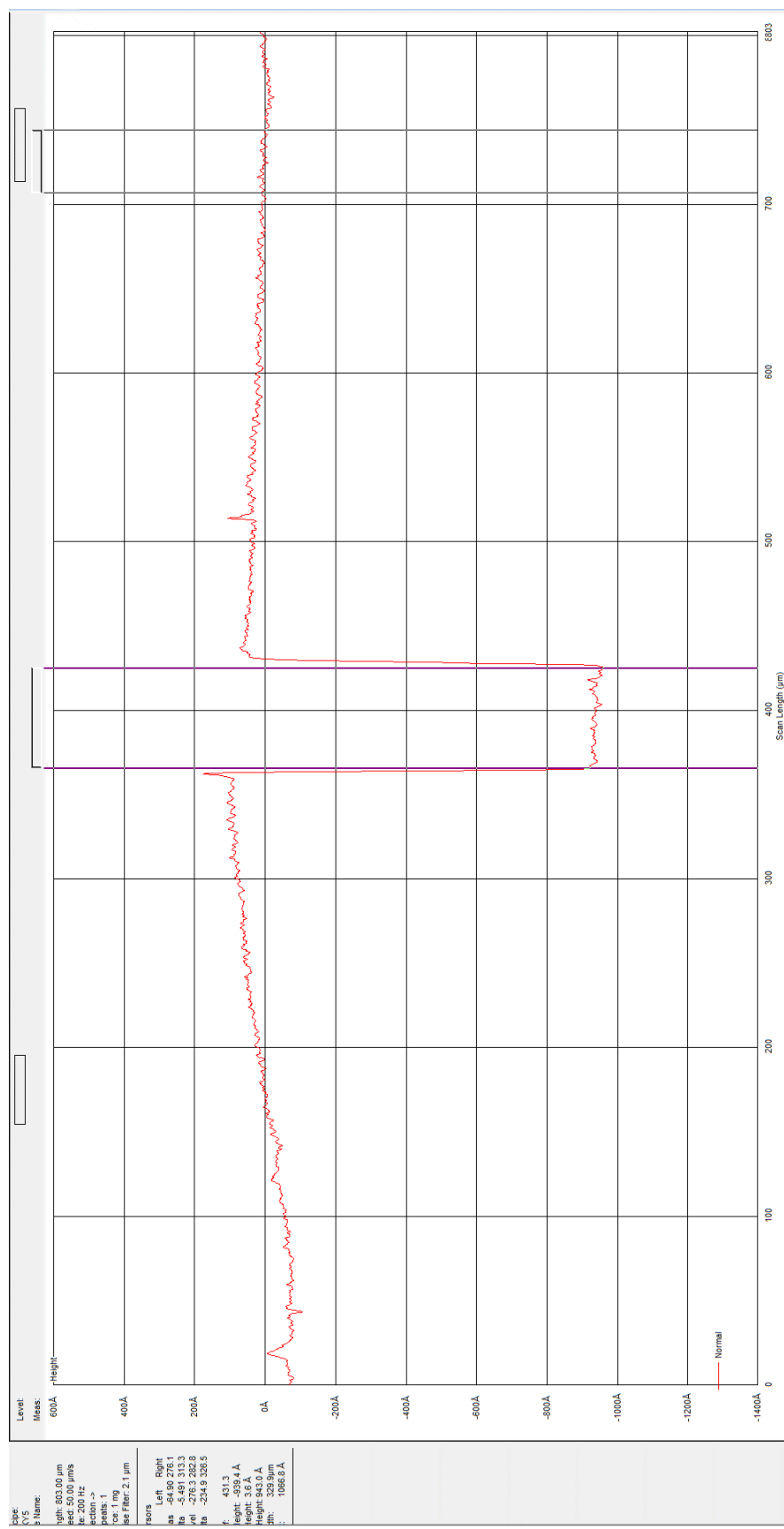


Figure 117: Poly(HDsMAz) X_n 60 measurement 3

12. Appendix

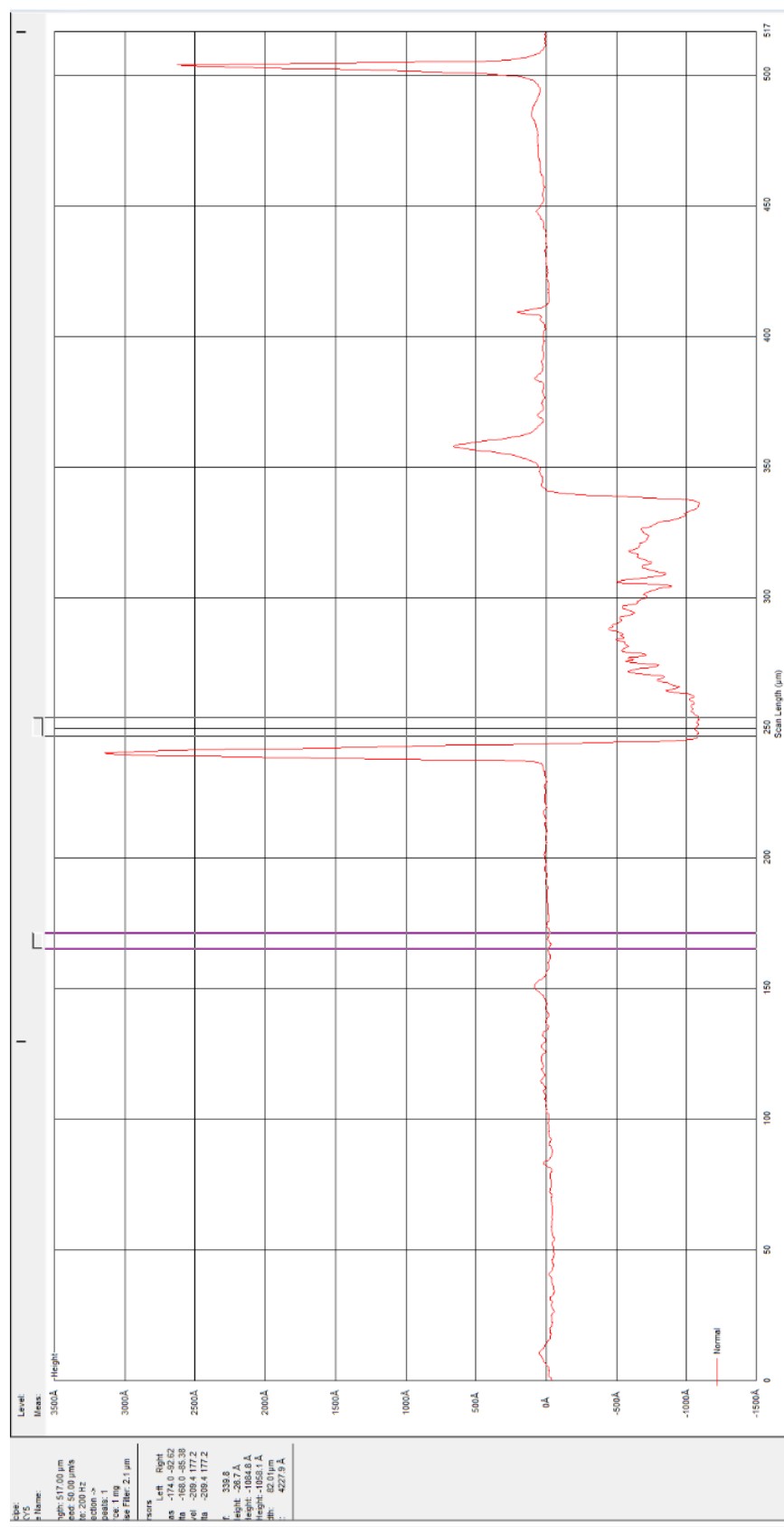


Figure 118: Poly(DDsMAz) X_n 30 measurement 1

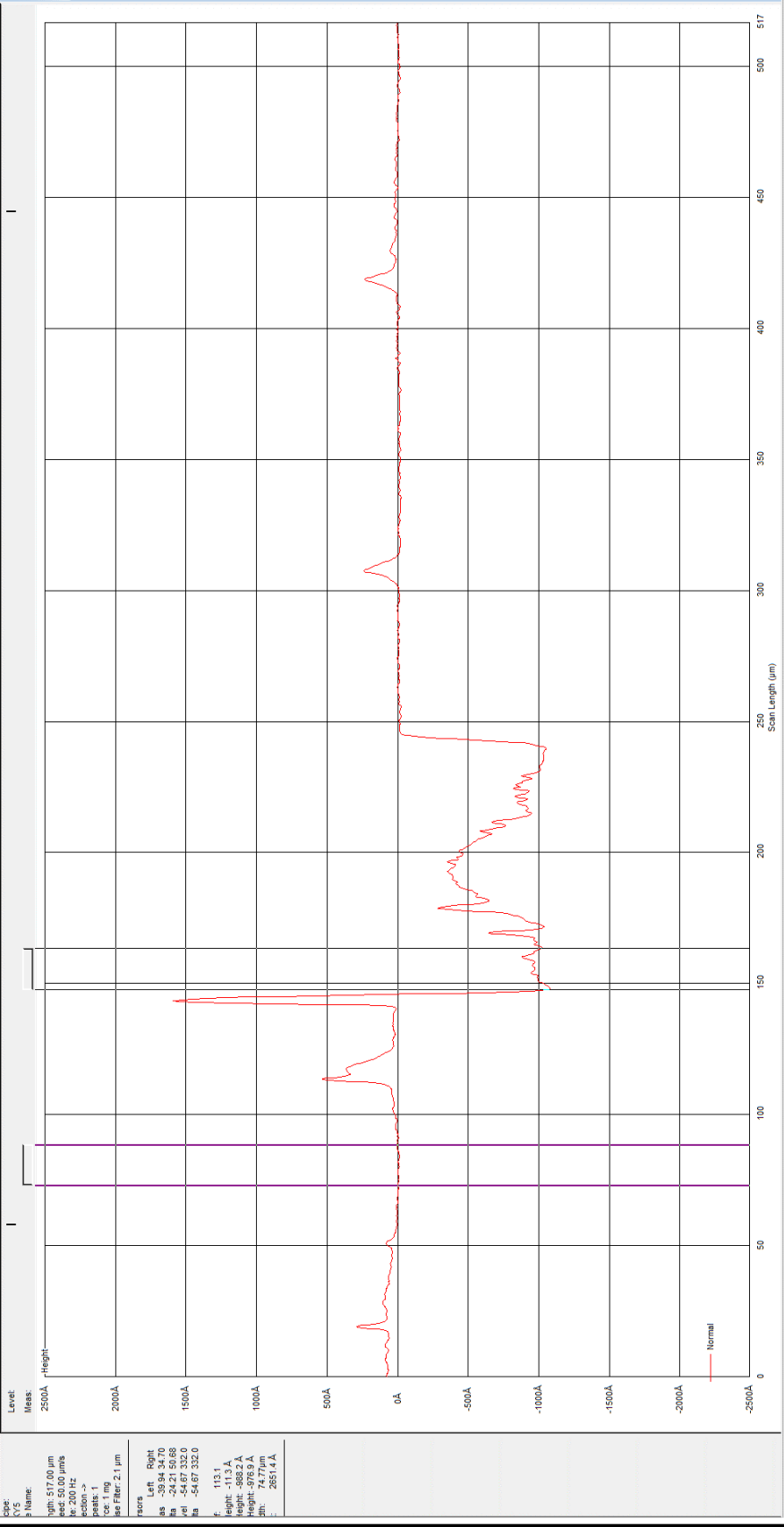


Figure 119: Poly(DDsMAz) Xn 30 measurement 2

12. Appendix

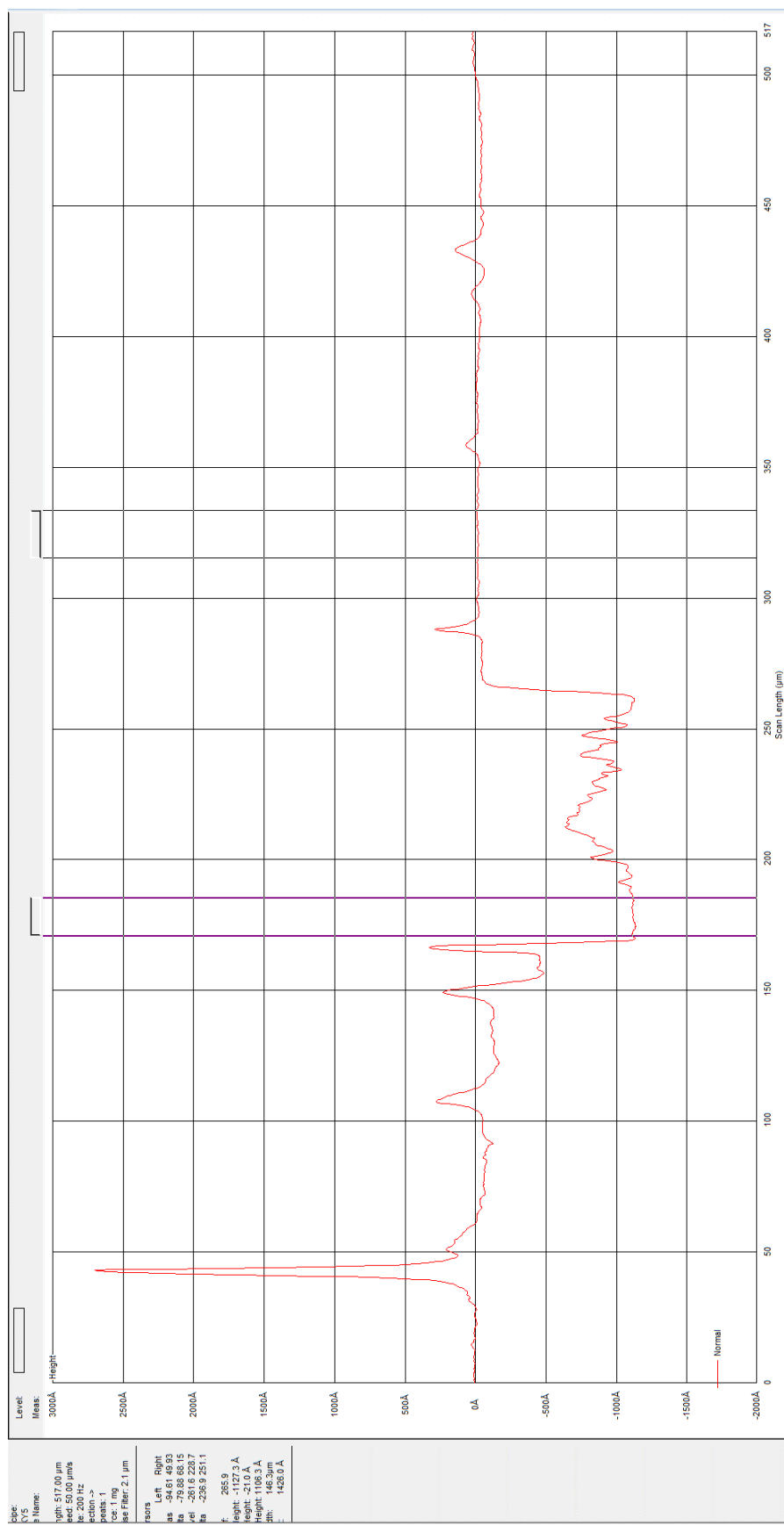


Figure 120: Poly(DDsMAz) X_n 30 measurement 3

12. Appendix

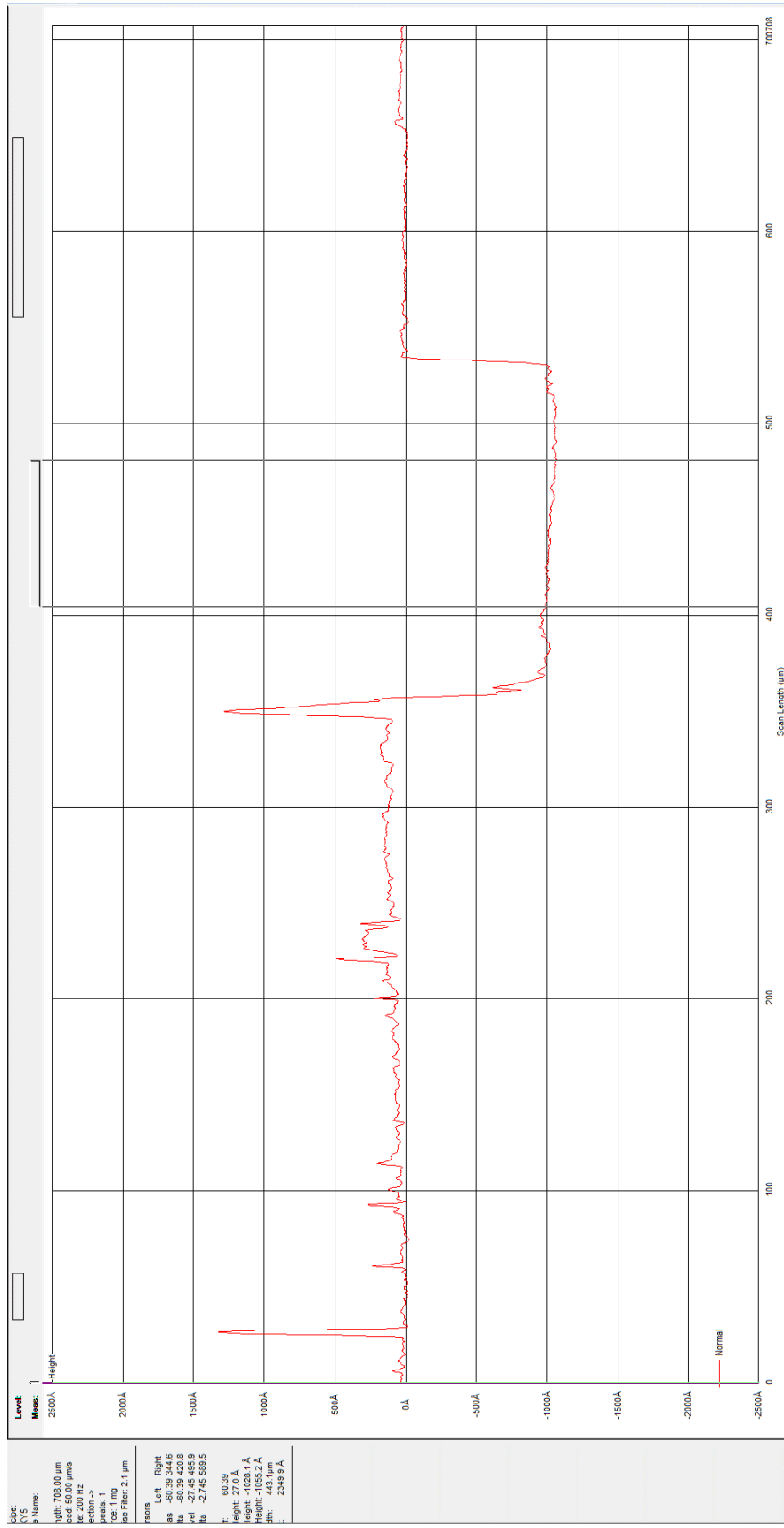


Figure 121: Poly(OsMAz) X_n 30 measurement 1

12. Appendix

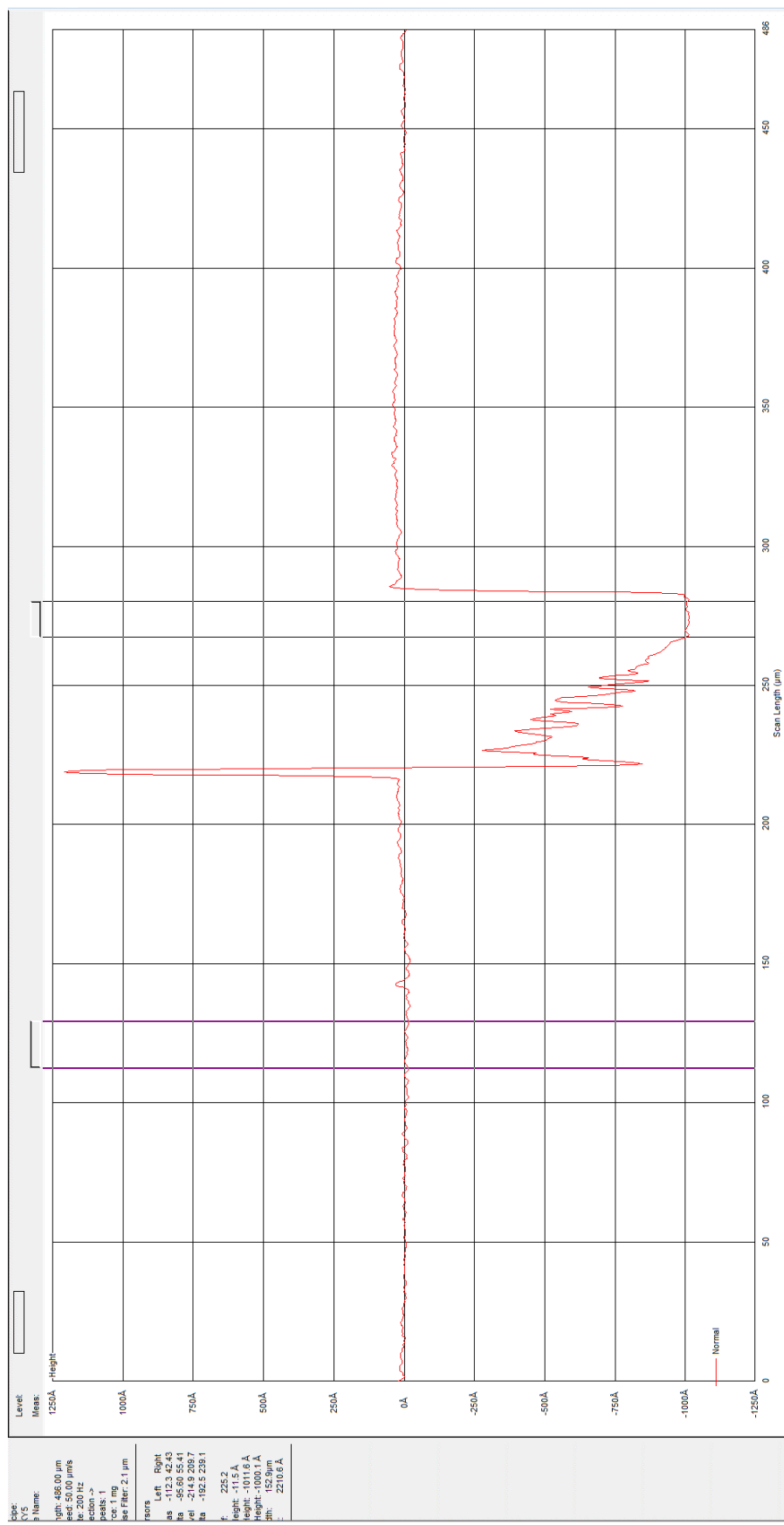


Figure 122: Poly(OsMAz) X_n 30 measurement 2

12. Appendix

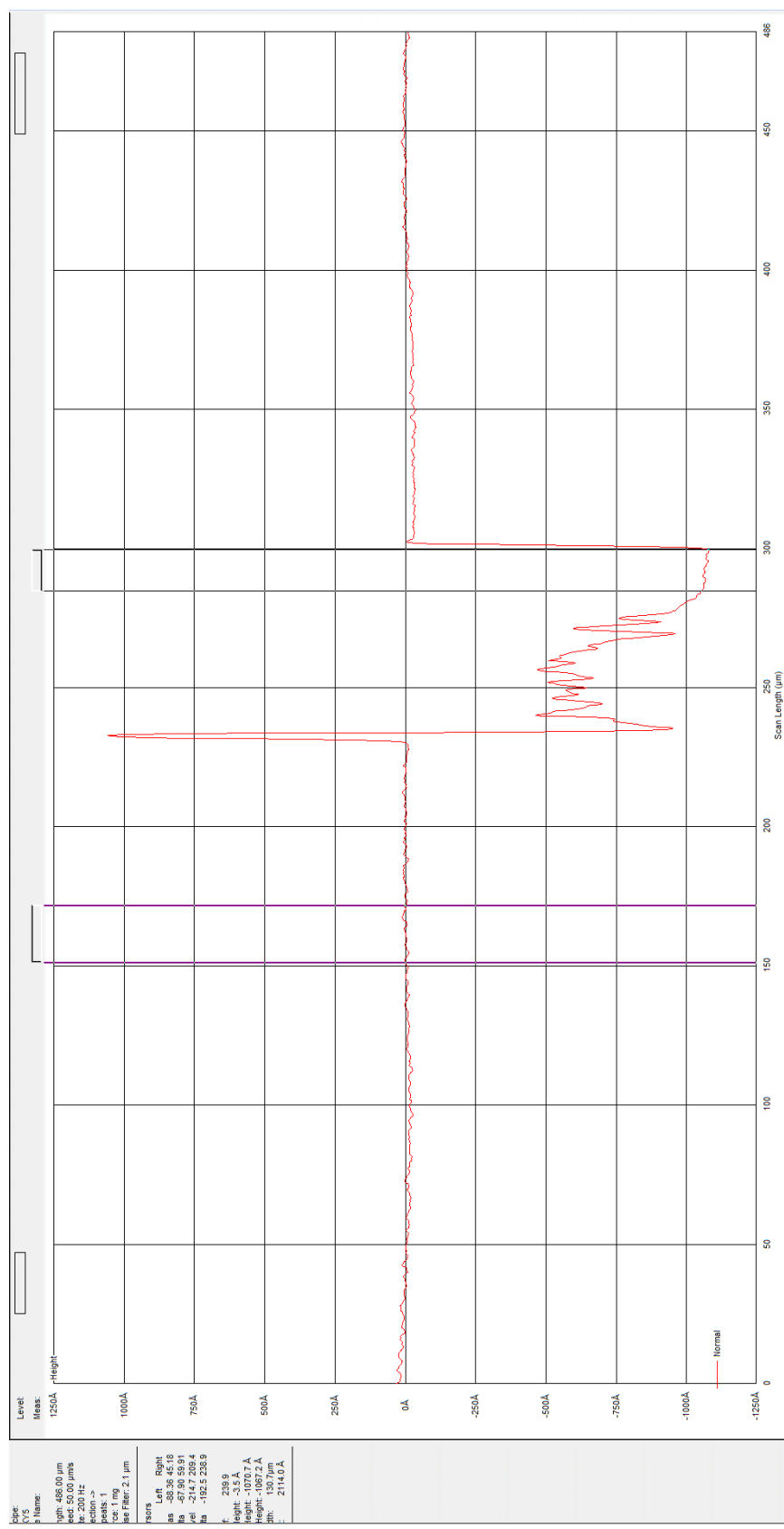


Figure 123: Poly(OsMAz) X_n 30 measurement 3

12. Appendix

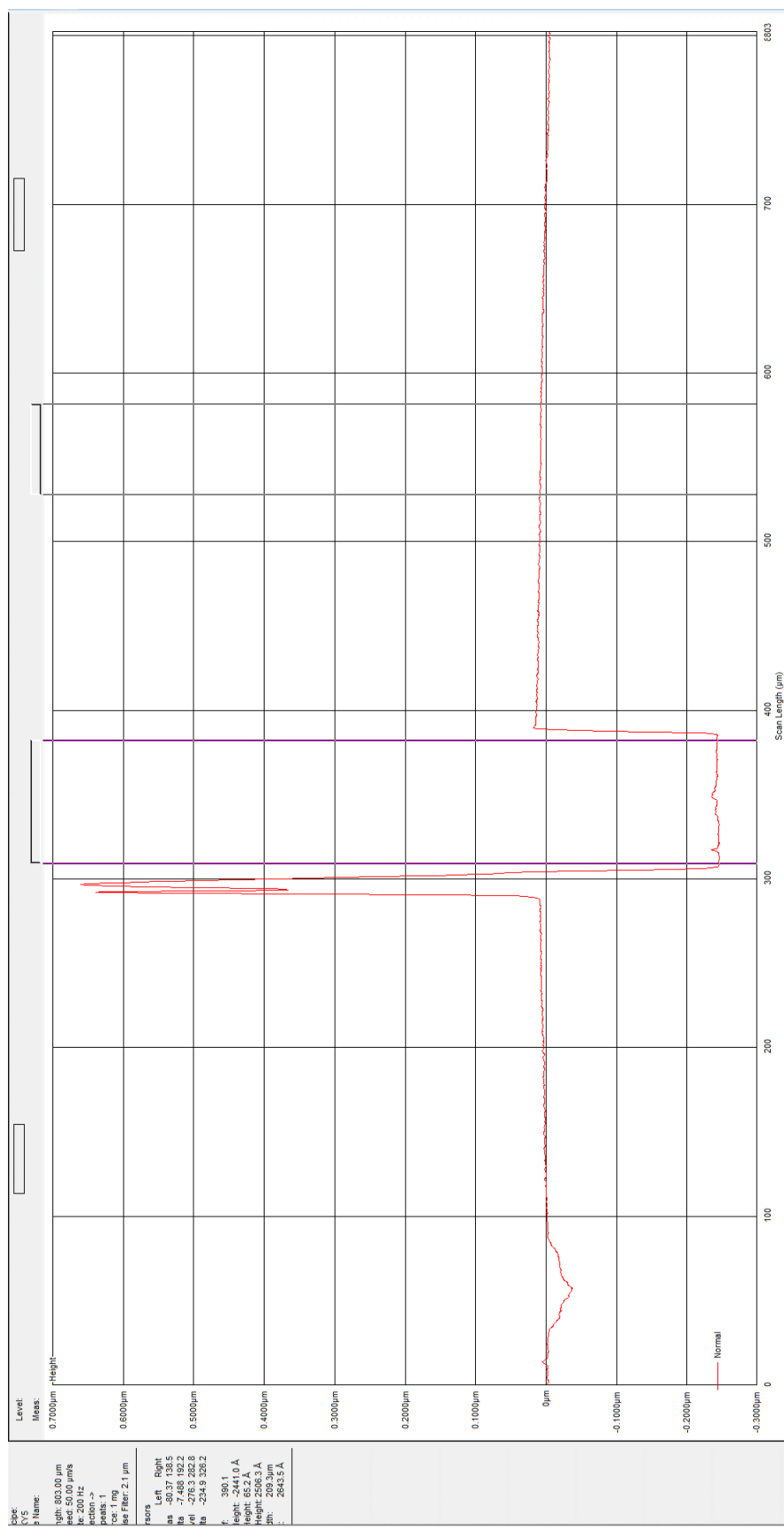


Figure 124: Poly(HDsMAz) 2.0 wt. % X_n 30 measurement 2

12. Appendix

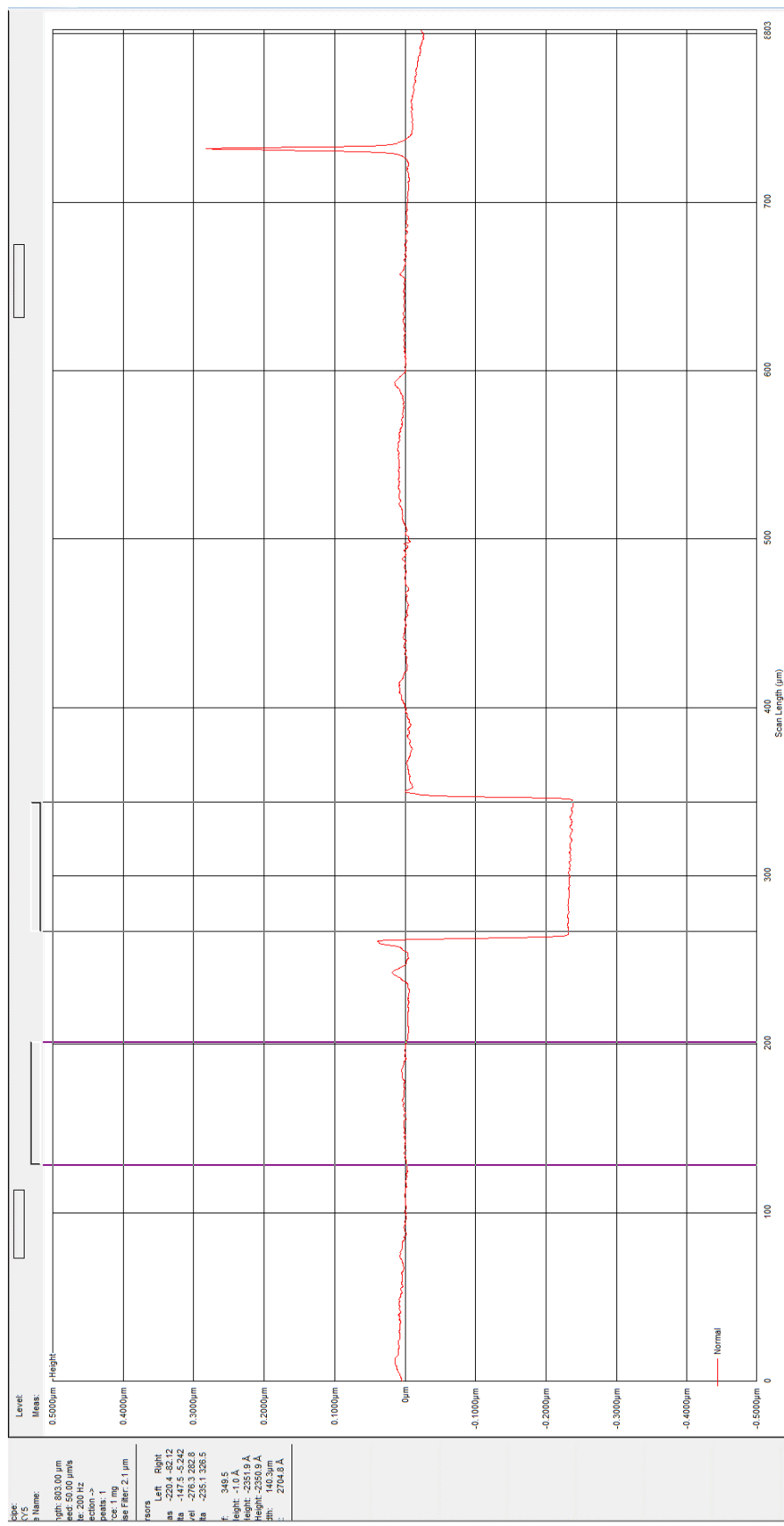


Figure 125: Poly(HDsMAz) 2.0 wt. % Xn 30 measurement 3

12. Appendix

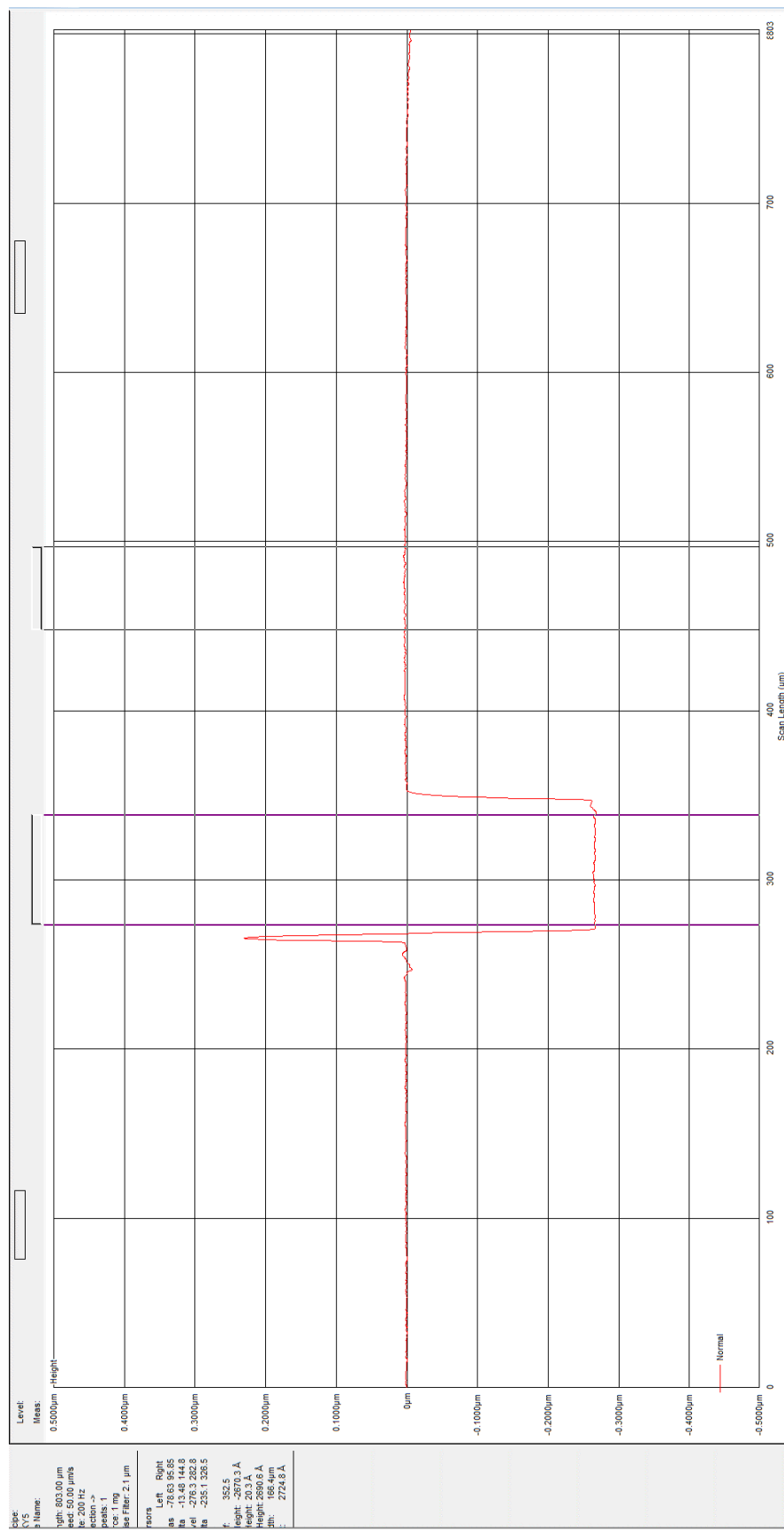


Figure 126: Poly(HDsMAz) 2.0 wt. % X_n 30 measurement 1

12. Appendix

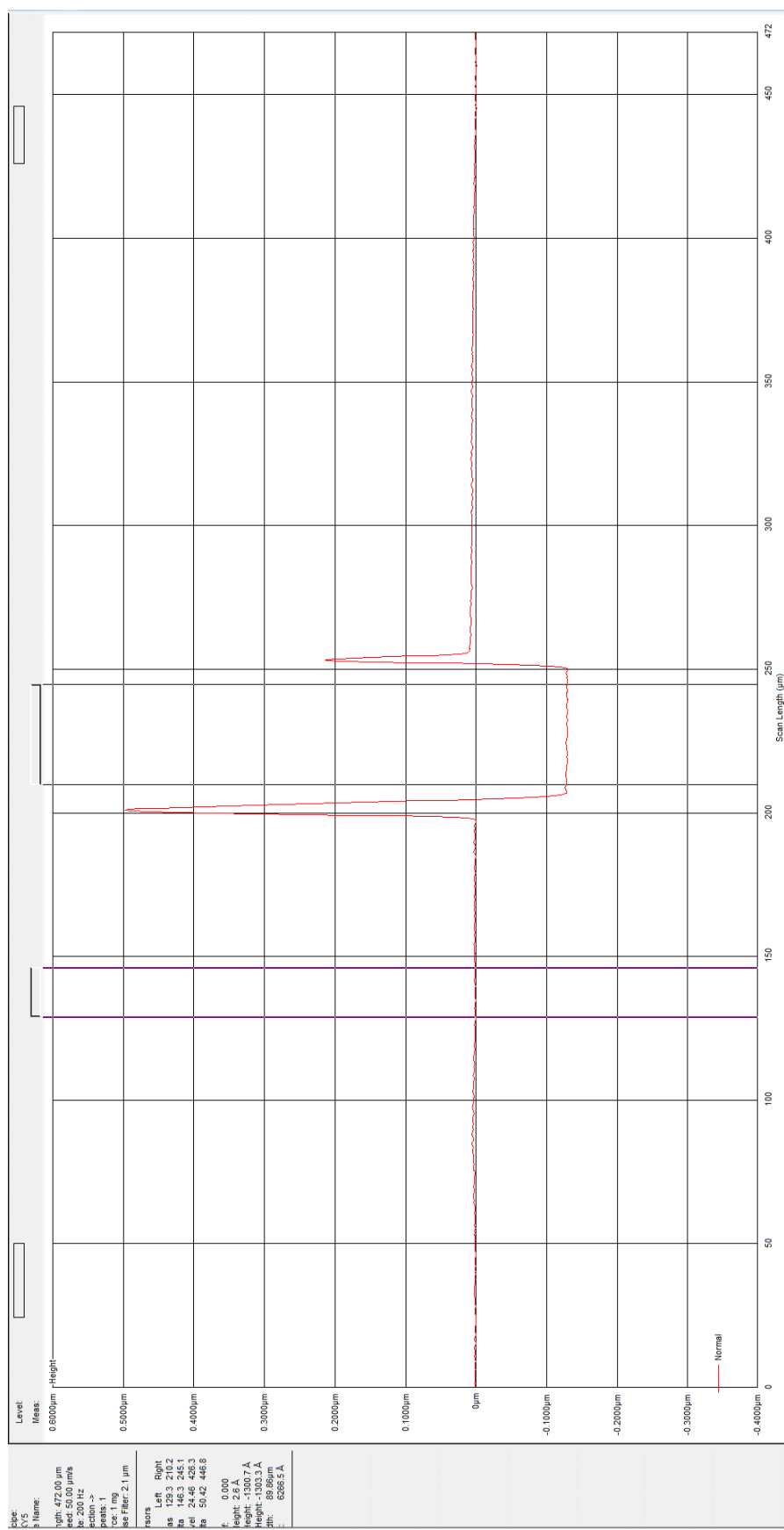


Figure 127: Poly(HDsMAz) 1.0 wt. % X_n 30 measurement 1

12. Appendix

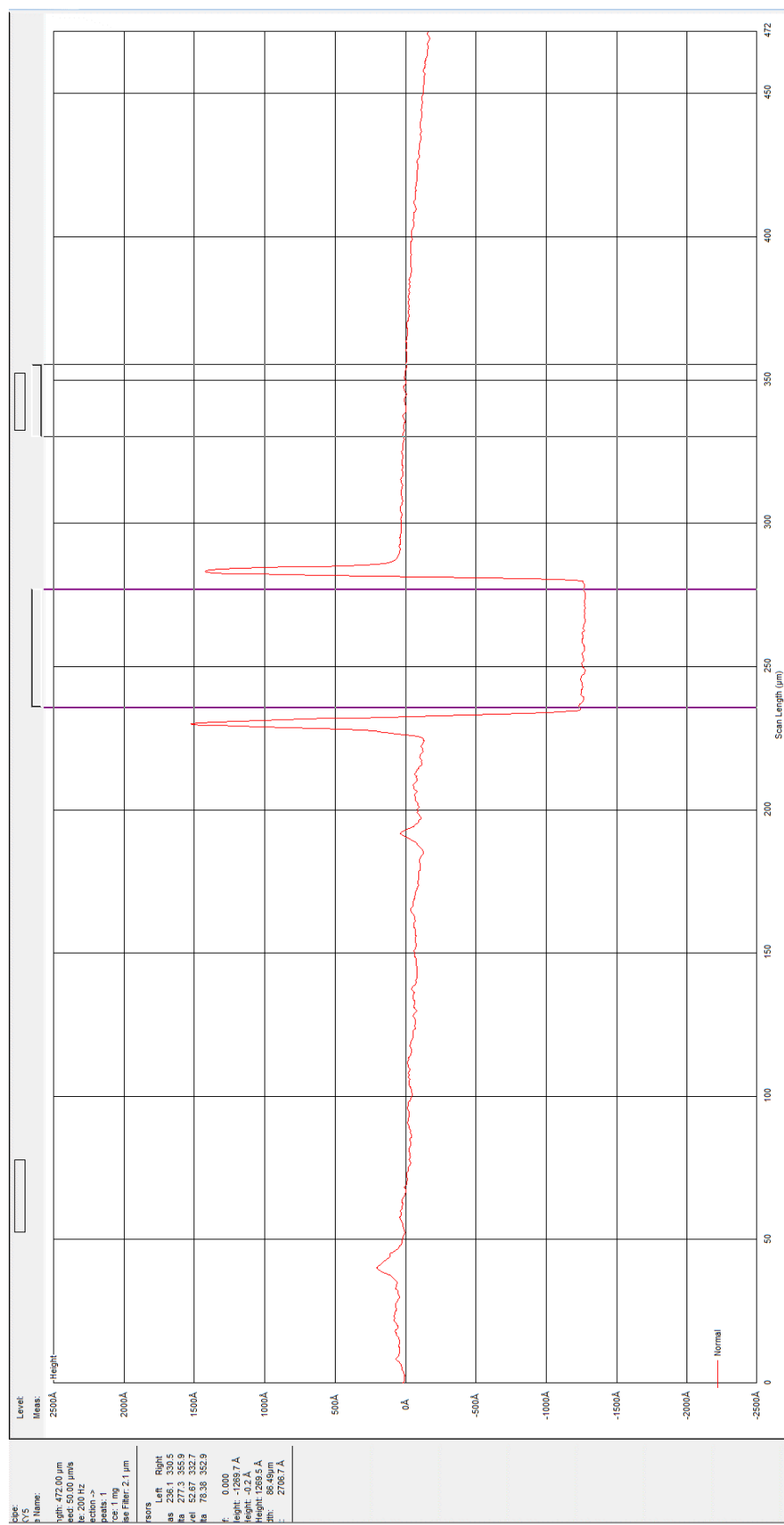


Figure 128: Poly(HDsMAz) 1.0 wt. % X_n 30 measurement 2

12. Appendix

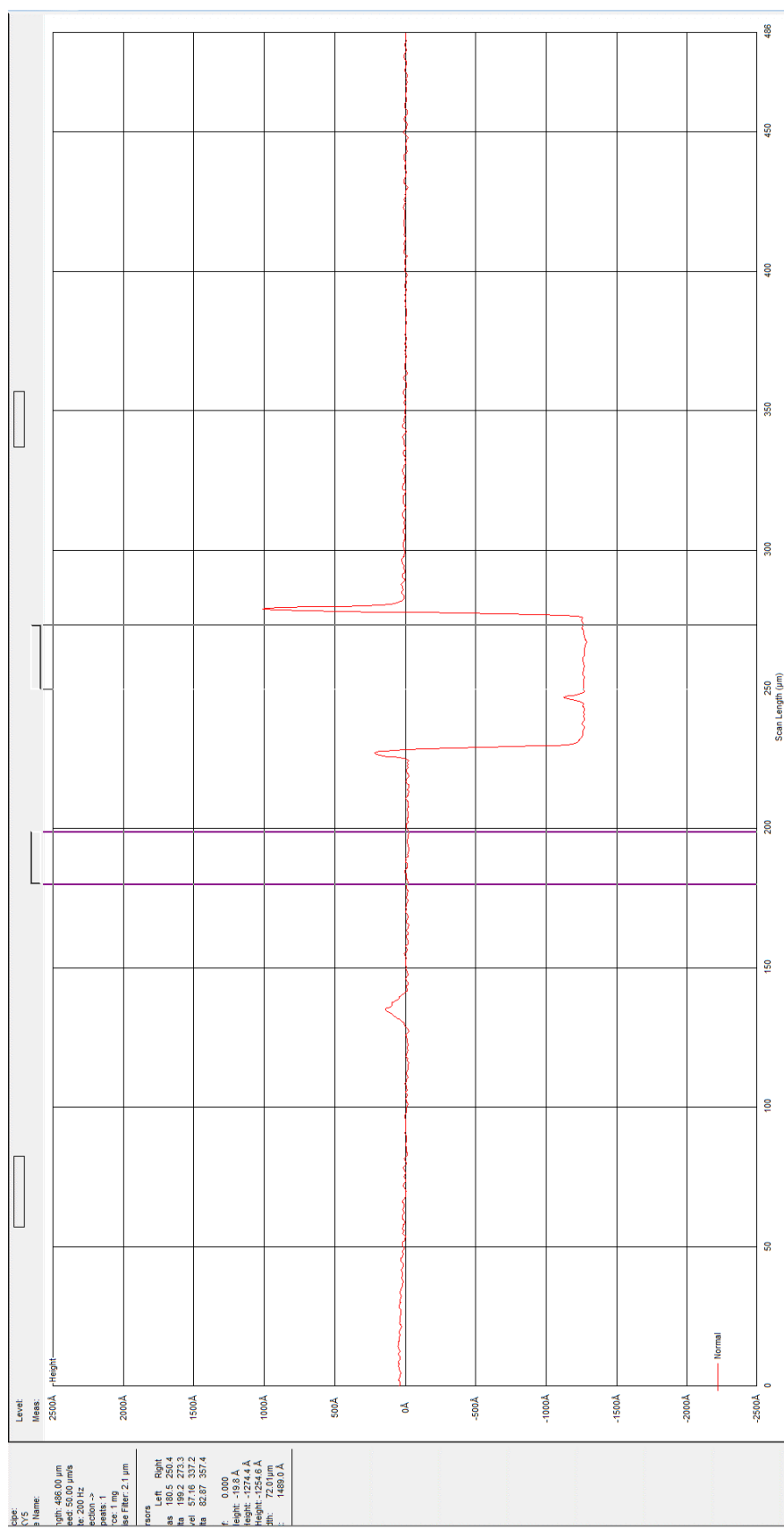


Figure 129: Poly(HDsMAz) 1.0 wt. % X_n 30 measurement 3

12. Appendix

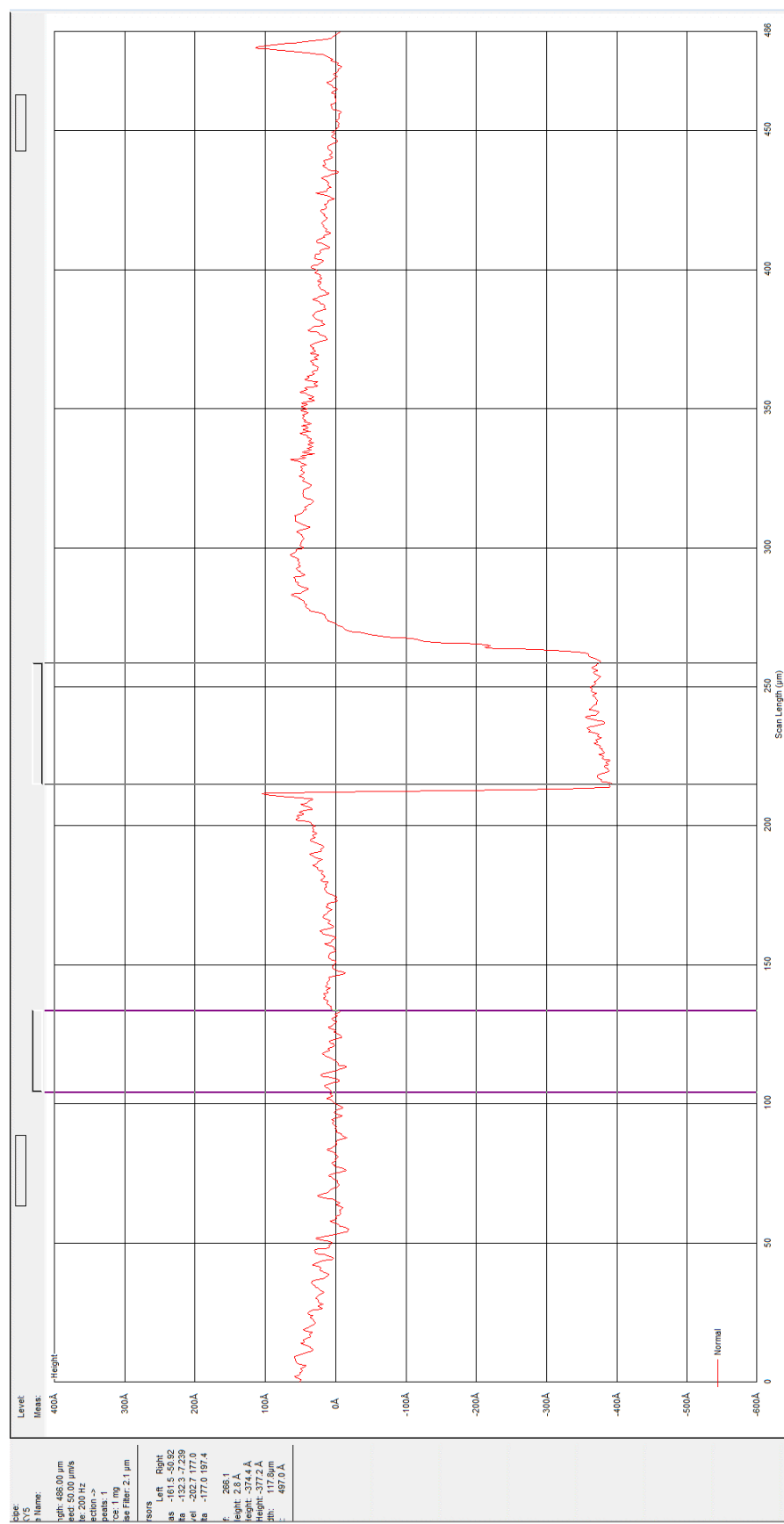


Figure 130: Poly(HDsMAz) 0.5 wt. % X_n 30 measurement 1

12. Appendix

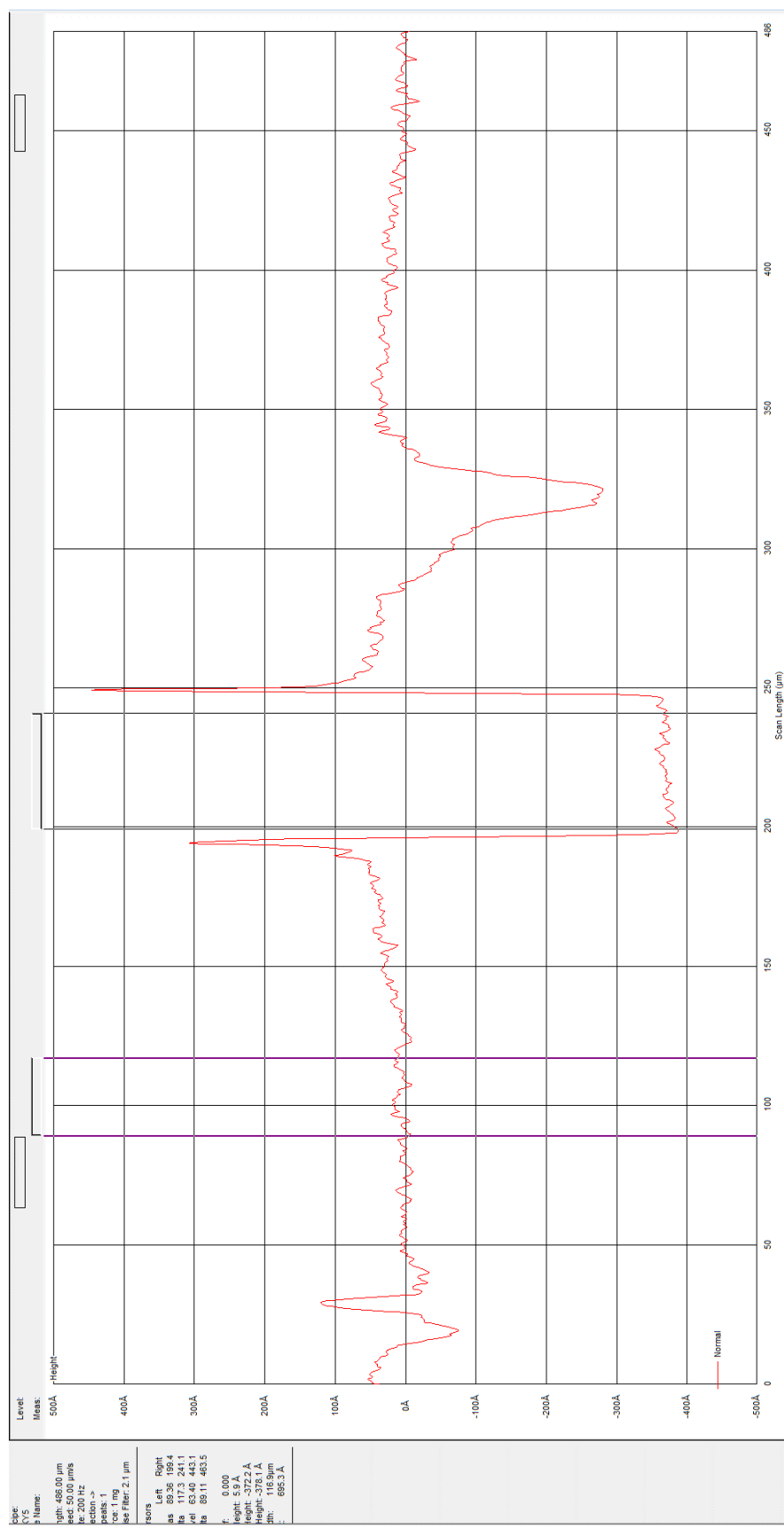


Figure 131: Poly(HDsMAz) 0.5 wt. % X_n 30 measurement 2

12. Appendix

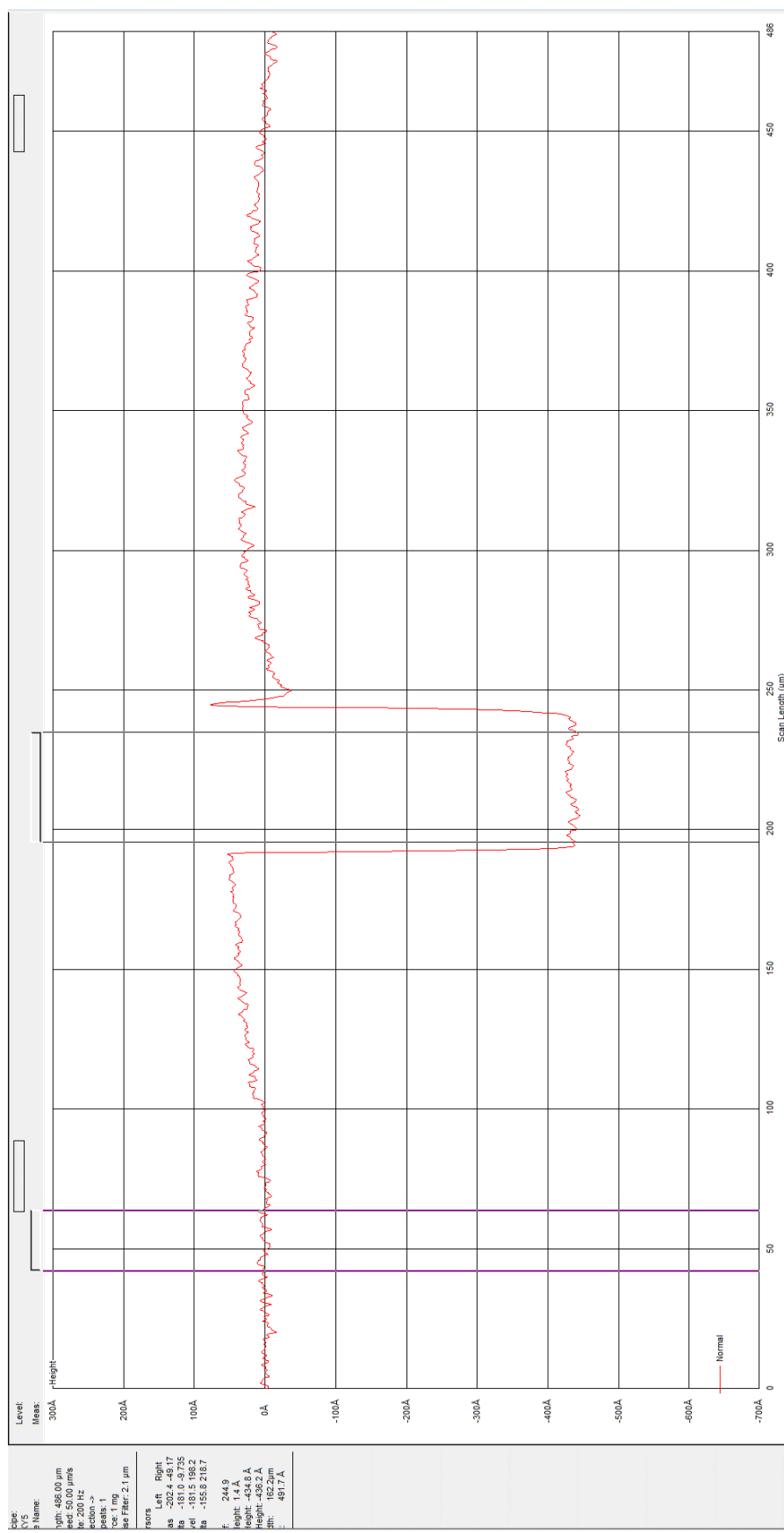


Figure 132: Poly(HDsMAz) 0.5 wt. % X_n 30 measurement 3

12. Appendix

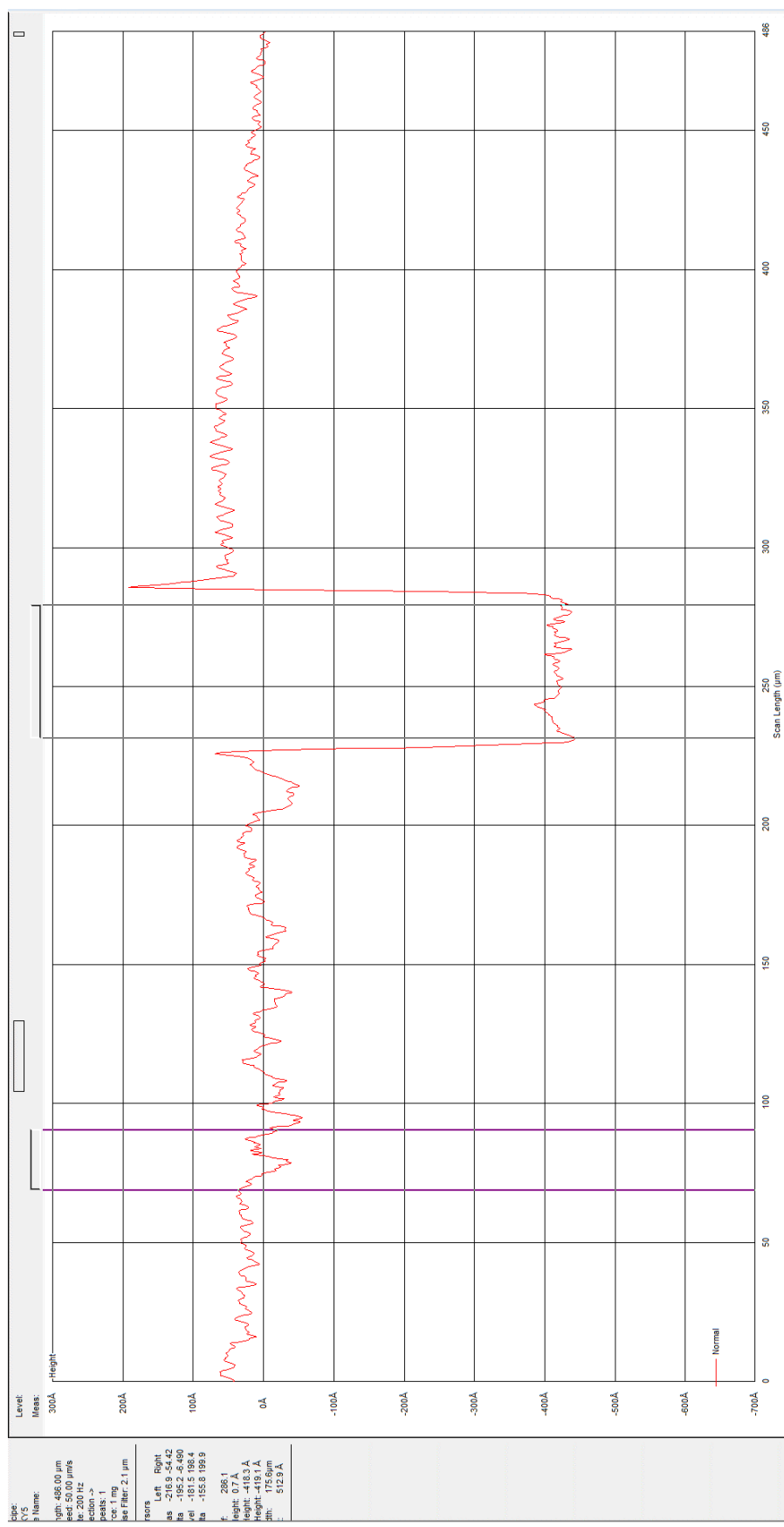


Figure 133: Poly(HDsMAz) 0.5 wt. % X_n 30 measurement 4

12. Appendix

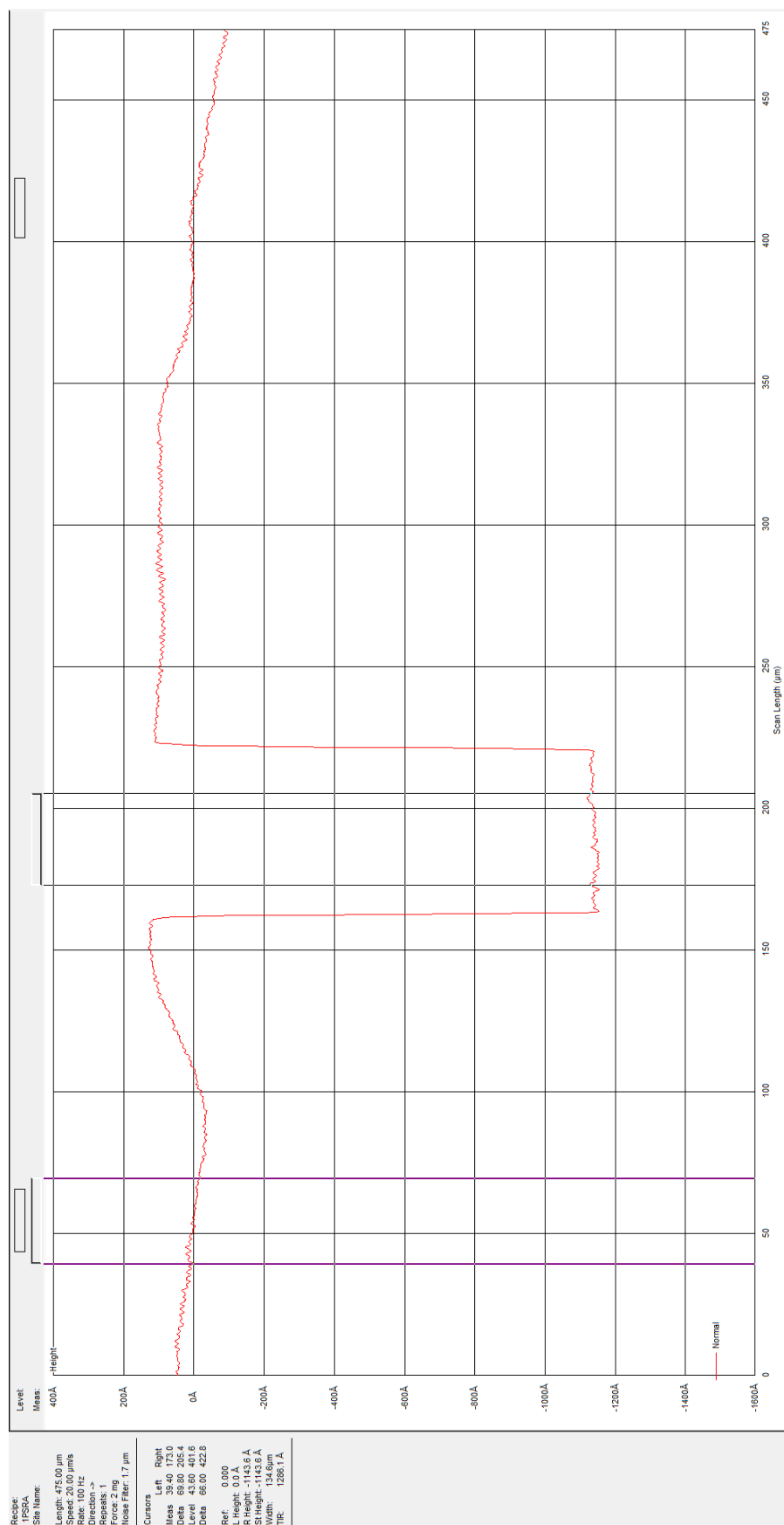


Figure 134: Poly(MsMAz) X_n 30 measurement 1

12. Appendix

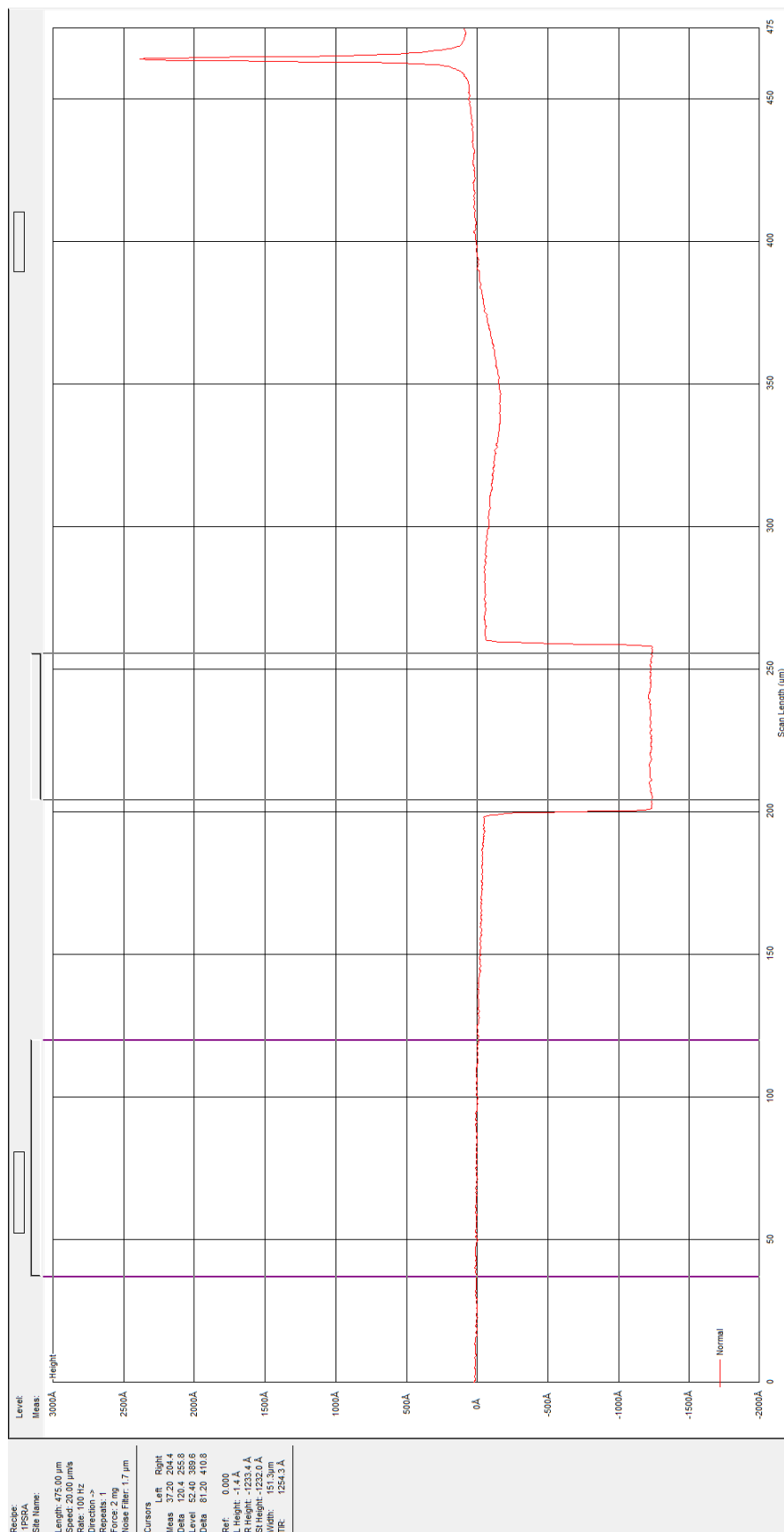


Figure 135: Poly(MsMAz) X_n 30 measurement 2

12. Appendix

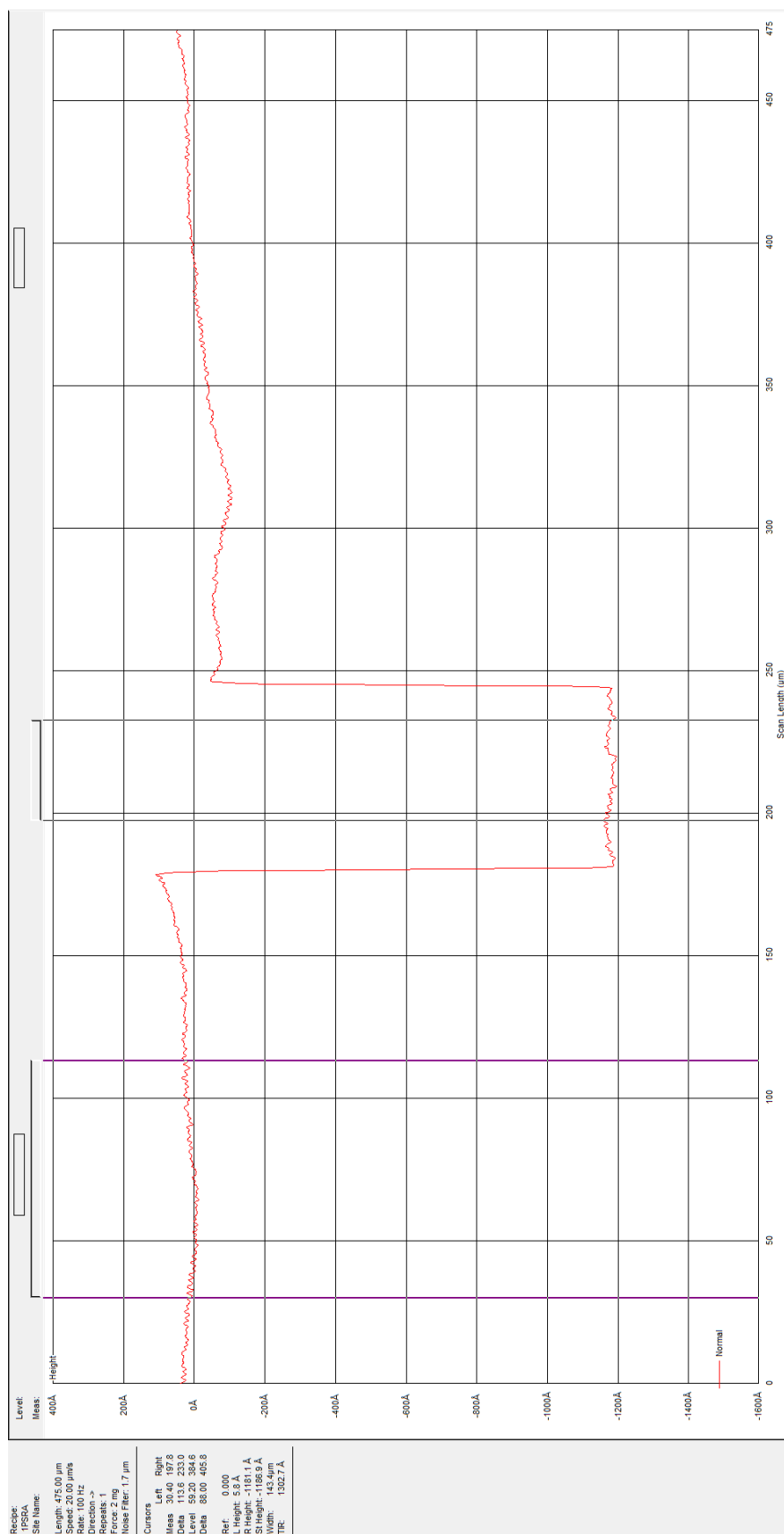


Figure 136: Poly(MsMAz) X_n 30 measurement 3

12.4 Spinning drop measurement

	Cyclohexane		Poly(OsMAz)	
measurement	1	2	1	2
run number	Interfacial Tension [mN/m]		Interfacial Tension[mN/m]	
1	39.0	39.0	28.3	28.3
2	39.0	39.0	28.7	28.3
3	39.0	39.0	28.3	28.3
4	39.0	39.0	28.3	28.3
5	39.0	39.0	28.7	28.3
6	39.0	39.0	28.3	28.3
7	39.0	39.0	28.7	28.3
8	39.0	39.0	28.3	28.3
9	39.0	39.0	28.3	28.3
10	39.0	39.0	28.2	28.3
11	39.0	39.0	28.7	28.3
12	39.0	39.0	28.3	28.3
13	39.0	39.0	28.3	28.3
14	39.0	39.0	28.3	28.3
15	39.0	39.0	28.7	28.3
16	39.0	39.0	28.2	28.3
17	39.0	39.0	28.2	28.3
18	39.0	39.0	28.2	28.3
19	39.0	39.0	28.7	28.3
20	39.0	39.0	28.3	28.3
21	39.0	39.0	28.3	28.3
22	39.0	39.0	28.3	28.3
23	39.0	39.0	28.3	28.3
24	39.0	39.0	28.3	28.3
25	39.0	39.0	28.3	28.3
26	39.0	39.0	28.3	28.3
27	39.0	39.0	28.3	28.3
28	39.0	39.0	28.3	28.3
29	39.0	39.0	28.3	28.3
30	39.0	39.0	28.3	28.3
31	39.0	39.0	28.2	28.3
32	39.0	39.0	28.3	28.3
33	39.0	39.0	28.3	28.3
34	39.0	39.0	28.3	28.3
35	39.0	39.0	28.2	28.3
36	39.0	39.0	28.2	28.3

12. Appendix

	Cyclohexane		Poly(OsMAz)	
measurement	1	2	1	2
run number	Interfacial Tension [mN/m]		Interfacial Tension [mN/m]	
37	39.0	39.0	28.3	28.3
38	39.0	39.0	28.3	28.3
39	39.0	39.0	28.3	28.3
40	39.0	39.0	28.3	28.3
41	39.0	39.0	28.2	28.3
42	39.0	39.0	28.3	27.8
43	39.0	39.0	28.2	27.8
44	39.0	39.0	28.7	27.8
45	39.0	39.0	28.7	27.4
46	39.0	39.0	28.7	27.4
47	39.0	39.0	28.7	27.4
48	39.0	39.0	28.7	27.4
49	39.0	39.0	28.3	27.4
50	39.0	39.0	28.7	27.4
51	39.0	39.0	28.7	27.4
52	39.0	39.0	28.7	27.4
53	39.0	39.0	28.7	27.4
54	39.0	39.0	28.3	27.4
55	39.0	39.0	28.2	27.4
56	39.0	39.0	28.7	27.0
57	39.0	39.0	28.2	26.5
58	39.0	39.0	28.3	26.5
59	39.0	39.0	28.2	26.5
60	39.0	39.0	28.2	28.3
61	39.0	39.0	28.3	28.3
62	39.0	39.0	28.3	28.3
63	39.0	39.0	28.3	27.8
64	39.0	39.0	28.3	28.3
65	39.0	39.0	28.3	27.8
66	39.0	39.0	28.3	28.3
67	39.0	39.0	28.2	28.3
68	38.5	38.5	28.2	28.3
69	38.5	38.5	28.3	27.8
70	37.9	37.9	28.3	27.8
71	37.9	37.9	28.3	28.3
72	38.5	38.5	28.3	27.8
73	38.5	38.5	28.2	28.3
74	38.5	38.5	28.3	27.8
75	37.9	37.9	28.3	28.3

12. Appendix

	Cyclohexane		Poly(OsMAz)	
measurement	1	2	1	2
run number	Interfacial Tension [mN/m]		Interfacial Tension [mN/m]	
76	37.9	37.9	28.2	28.3
77	37.9	37.9	28.3	28.3
78	37.9	37.9	28.3	28.3
79	37.9	37.9	28.2	28.3
80	37.9	37.9	28.2	28.3
81	37.9	37.9	28.3	28.3
82	37.9	37.9	28.3	28.3
83	39.0	39.0	28.7	28.3
84	39.0	39.0	28.7	28.3
85	39.0	39.0	28.7	28.3
86	39.0	39.0	28.7	28.3
87	39.0	39.0	28.7	27.8
88	39.0	39.0	28.7	28.3
89	39.0	39.0	28.7	28.3
90	39.0	39.0	28.7	28.3
91	39.0	39.0	28.7	28.3
92	39.0	39.0	28.7	28.3
93	39.0	39.0	28.7	28.3
94	38.5	38.5	28.7	28.3
95	39.0	39.0	28.7	28.3
96	38.5	38.5	28.7	28.3
97	38.5	38.5	28.7	27.8
98	38.5	38.5	28.7	28.3
99	37.9	37.9	28.7	28.3
100	37.9	37.9	28.7	28.3

12. Appendix

	Poly(DDsMAz)		Poly(HDsMAz)	
measurement	1	2	1	2
run number	Interfacial Tension VG[mN/m]		Interfacial Tension VG[mN/m]	
1	29.9	30.5	33.2	33.2
2	29.9	30.5	33.2	33.2
3	30.4	30.0	32.7	33.2
4	29.9	30.5	33.2	33.2
5	29.9	30.0	32.7	33.2
6	29.9	30.5	32.7	33.2
7	29.9	30.0	33.2	33.2
8	29.9	30.0	32.7	33.2
9	29.9	30.0	33.2	33.2
10	29.9	30.0	33.2	33.2
11	29.9	30.0	33.2	33.2
12	29.9	30.0	33.2	33.2
13	29.9	30.0	33.2	33.2
14	29.9	30.0	33.2	33.2
15	29.9	30.0	33.2	33.2
16	29.9	30.0	32.7	33.2
17	29.9	30.0	32.7	33.2
18	29.9	30.0	33.2	33.2
19	29.9	30.0	33.2	33.2
20	29.9	30.0	32.7	33.2
21	29.9	30.0	33.2	33.2
22	29.9	30.0	32.7	33.2
23	29.9	30.0	33.2	33.2
24	29.9	30.0	33.2	33.2
25	29.9	30.0	33.2	33.2
26	29.9	30.0	32.7	33.2
27	29.9	30.0	33.2	33.2
28	29.9	30.0	33.2	33.2
29	29.9	30.0	33.2	33.2
30	29.9	30.0	33.2	33.2
31	29.9	30.0	33.2	33.2
32	29.9	30.0	33.2	33.2
33	29.9	30.0	33.2	33.2
34	29.9	30.0	33.2	33.2
35	29.9	30.0	33.2	33.2
36	29.9	30.0	33.2	33.2
37	29.9	30.0	33.2	33.2
38	29.9	30.0	33.2	33.2
39	29.9	30.0	33.2	33.2

12. Appendix

	Poly(DDsMAz)		Poly(HDsMAz)	
measurement	1	2	1	2
run number	Interfacial Tension VG[mN/m]		Interfacial Tension VG[mN/m]	
40	29.9	30.0	33.2	33.2
41	29.9	30.0	33.2	33.2
42	29.9	30.0	33.2	33.2
43	29.9	30.0	33.2	33.2
44	29.9	30.0	32.7	33.2
45	29.9	30.0	33.2	33.2
46	29.9	30.0	33.2	33.2
47	29.9	30.0	33.2	33.2
48	29.9	30.0	33.2	33.2
49	29.9	30.0	32.7	33.2
50	29.9	30.0	33.2	33.2
51	29.9	30.0	33.2	33.2
52	29.9	30.0	33.2	33.2
53	29.9	30.0	33.2	33.2
54	29.9	30.0	33.2	33.2
55	29.9	30.0	32.7	33.2
56	29.9	30.0	32.7	33.2
57	29.9	30.0	33.2	33.2
58	29.9	30.0	33.2	33.2
59	29.9	30.0	33.2	33.2
60	29.9	30.0	33.2	33.2
61	29.9	30.0	33.2	33.2
62	29.9	30.0	32.7	33.2
63	29.9	30.0	32.7	33.2
64	29.9	30.0	33.2	33.2
65	29.9	30.0	33.2	33.2
66	29.9	30.0	33.2	33.2
67	29.9	30.0	32.7	33.2
68	29.9	30.0	33.2	33.2
69	29.9	30.0	33.2	33.2
70	29.9	30.0	32.7	33.2
71	29.9	30.0	32.7	33.2
72	29.9	30.0	33.2	33.2
73	29.9	30.0	33.2	33.2
74	29.9	30.0	32.7	33.2
75	29.9	30.0	32.7	33.2
76	29.9	30.0	32.7	33.2
77	29.9	30.0	32.7	33.2
78	29.9	30.0	32.7	33.2
79	29.9	30.0	32.7	33.2

12. Appendix

	Poly(DDsMAz)		Poly(HDsMAz)	
measurement	1	2	1	2
run number	Interfacial Tension VG[mN/m]		Interfacial Tension VG[mN/m]	
80	29.9	30.0	32.7	33.2
81	29.9	30.0	32.7	33.2
82	29.9	30.0	32.7	33.2
83	29.9	30.0	33.2	33.2
84	29.9	30.0	32.7	33.2
85	29.9	30.0	32.7	33.2
86	29.9	30.0	32.7	33.2
87	29.9	30.0	32.7	33.2
88	29.9	30.0	32.7	33.2
89	29.9	30.0	32.7	33.2
90	29.9	30.0	32.7	33.2
91	29.9	30.0	32.7	33.2
92	29.9	30.0	32.7	33.2
93	29.9	30.0	32.7	33.2
94	29.9	30.0	32.7	33.2
95	29.9	30.0	32.7	33.2
96	29.9	30.0	32.7	33.2
97	29.9	30.0	32.7	33.2
98	29.9	30.0	32.7	33.2
99	29.9	30.0	32.7	33.2
100	29.9	30.0	32.7	33.2

12.5 ^1H NMR-Kinetic

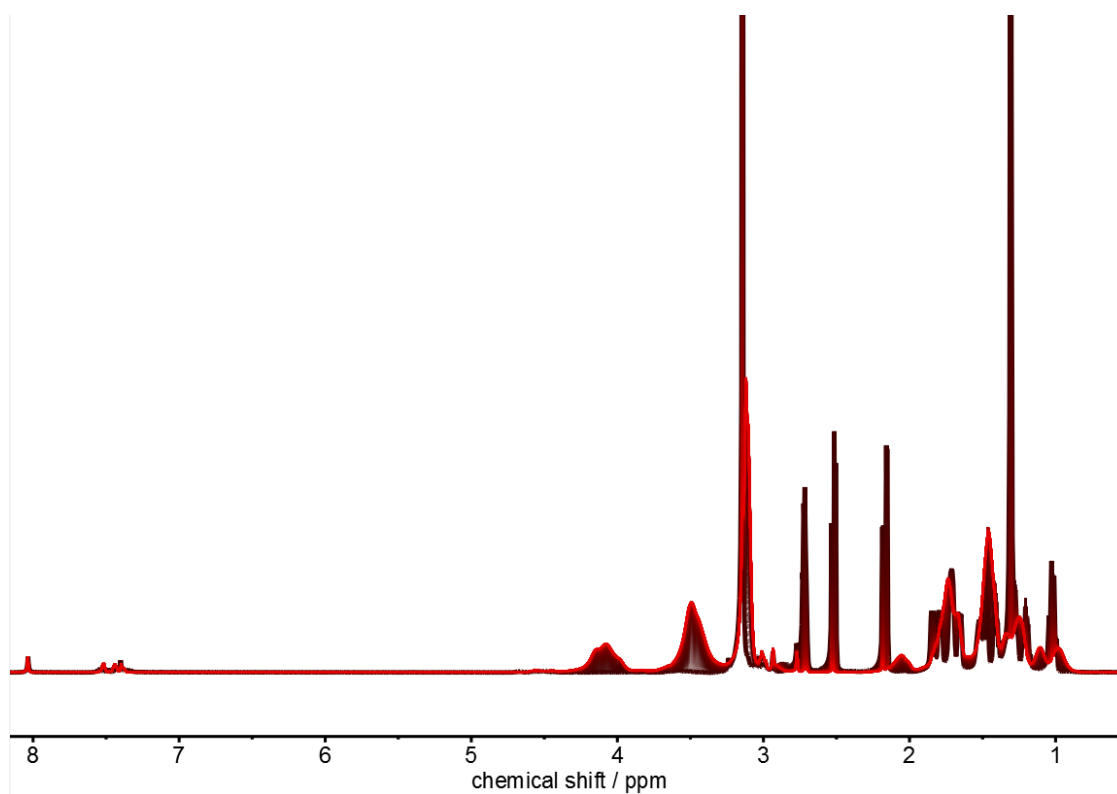


Figure 137: ^1H NMR Kinetic 700 MHz $\text{DMF-}d_7$ of MsMAz and MsCyhexAz

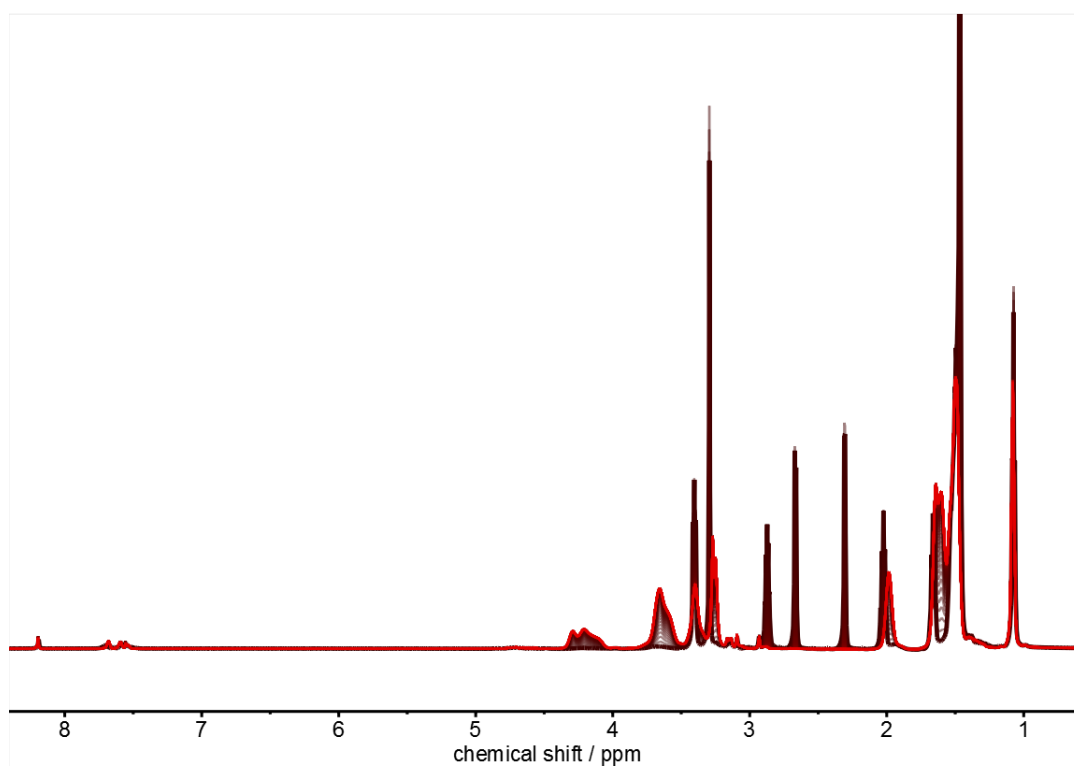


Figure 138: ^1H NMR Kinetic 700 MHz $\text{DMF-}d_7$ of OsMAz and MsMAz

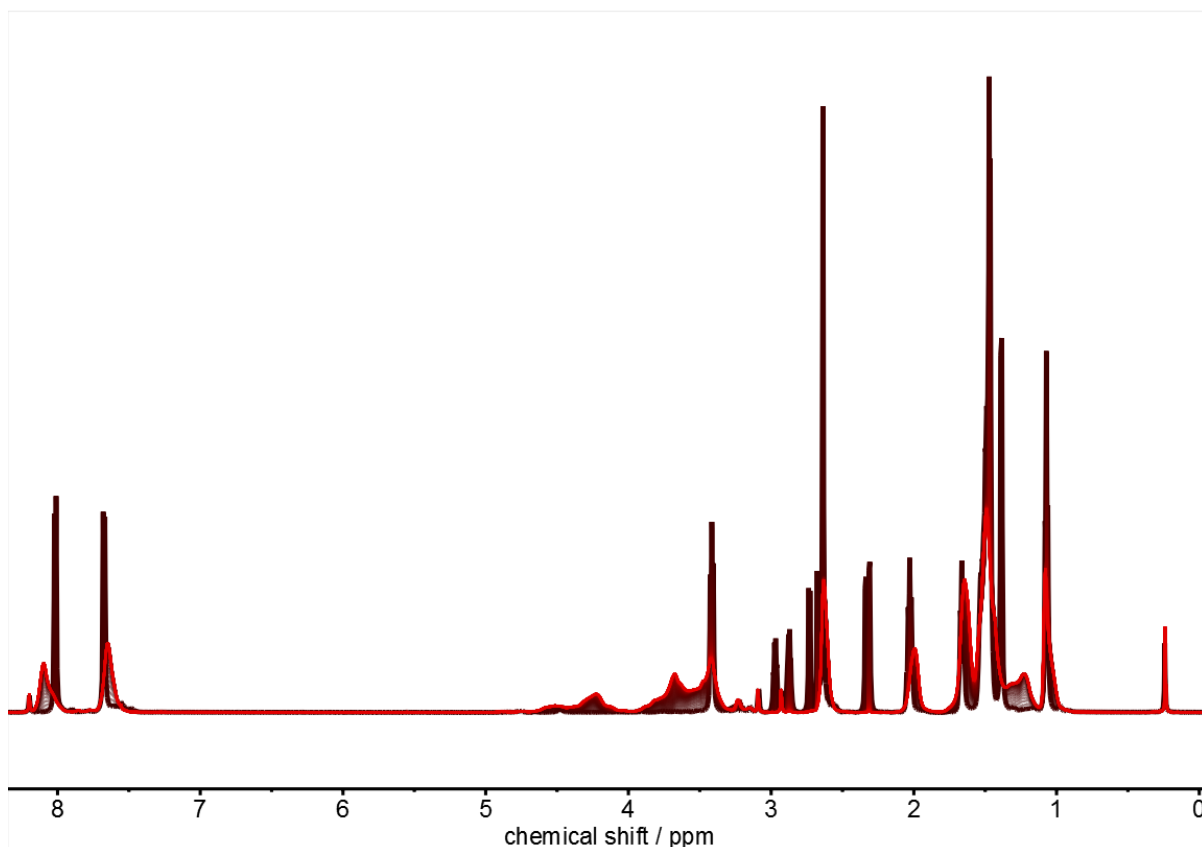


Figure 139: ^1H NMR Kinetic 700 MHz $\text{DMF-}d_7$ of OsMAz and TsMAz

Evaluation after Jaacks

For the evaluation after Jaacks⁴¹ an ideal copolymerization with $r_1 \cdot r_2 = 1$ was assumed. Following the assumption the copolymerization equation simplifies (eq.) Using the ^1H NMR kinetic data and calculating a fit following eq() the r-parameters were calculated.

$$\frac{\partial[M_A]}{\partial[M_B]} = r_1 \frac{[M_A]}{[M_B]} \quad (\text{X})$$

$$\frac{\partial[M_A]}{\partial[M_{A,0}]} = \left(\frac{[M_B]}{[M_{B,0}]} \right)^{r_1} \quad (\text{X})$$

$$\log([M_A]) = r_1 \log([M_B]) + \log\left(\frac{[M_{A,0}]}{[M_{B,0}]}\right) \quad (\text{y})$$

$$r_2 = \frac{1}{r_1} \quad \text{Y}$$

12. Appendix

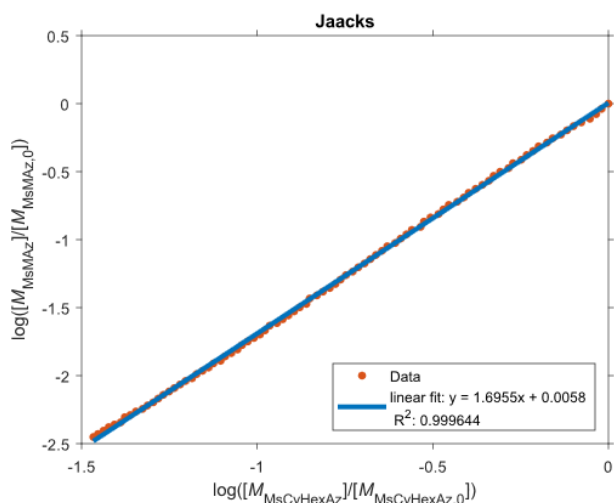


Figure 140: Jaacks fit of ^1H NMR kinetic data of MsCyHexAz and MsMAz

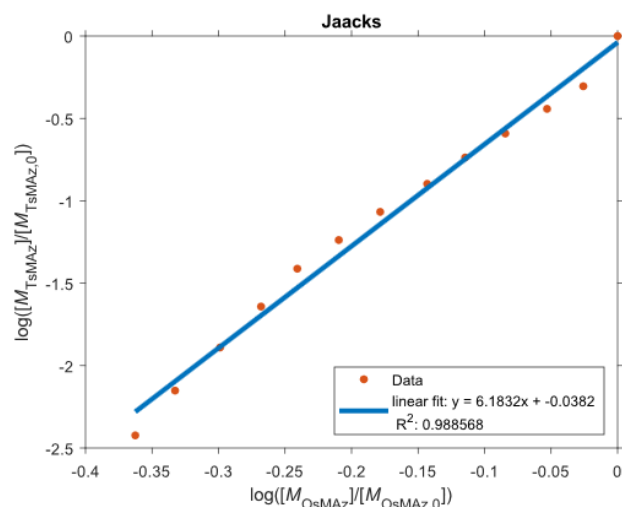


Figure 141: Jaacks fit of ^1H NMR kinetic data of OsMAz and TsMAz

Evaluation after Meyer-Lowry

Integration of the copolymerization equation after Meyer-Lowry⁴⁰ was used to determine the r -parameter and depict the Copolymerization diagrams. Using the ^1H NMR kinetic data the reactivity ratios were calculated.

$$X = 1 - \left(\frac{f_A}{f_{A,0}} \right)^\alpha \left(\frac{1 - f_A}{1 - f_{A,0}} \right)^\beta \left(\frac{f_A - \delta}{f_{A,0} - \delta} \right)^\gamma \quad (\text{a})$$

$$\alpha = \frac{r_2}{1 - r_2}; \beta = \frac{r_1}{1 - r_1}; \gamma = \frac{1 - r_1 r_2}{(1 - r_1)(1 - r_2)}; \delta = \frac{1 - r_2}{2 - r_1 - r_2} \quad (\text{b})$$

$$X = 1 - \frac{[M_A] + [M_B]}{[M_{A,0}] + [M_{B,0}]}; f_A = \frac{[M_A]}{[M_A] + [M_B]} \quad (\text{b})$$

12. Appendix

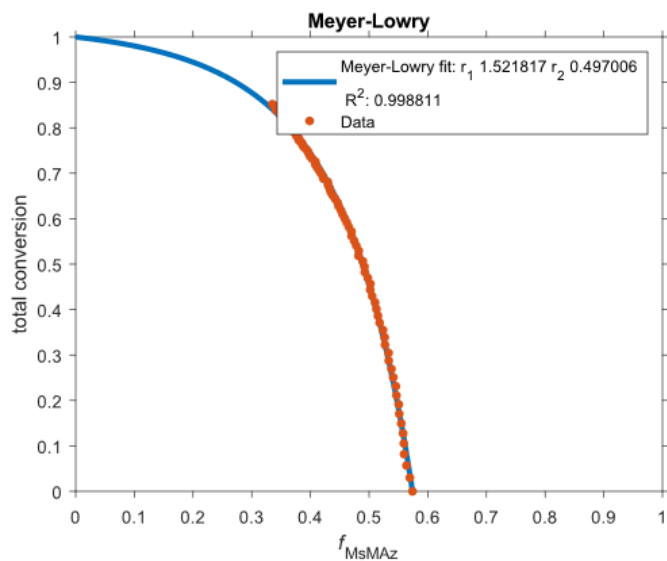


Figure 142: Meyer-Lowry fit of ^1H NMR kinetic data of MsCyhexAz and MsMAz

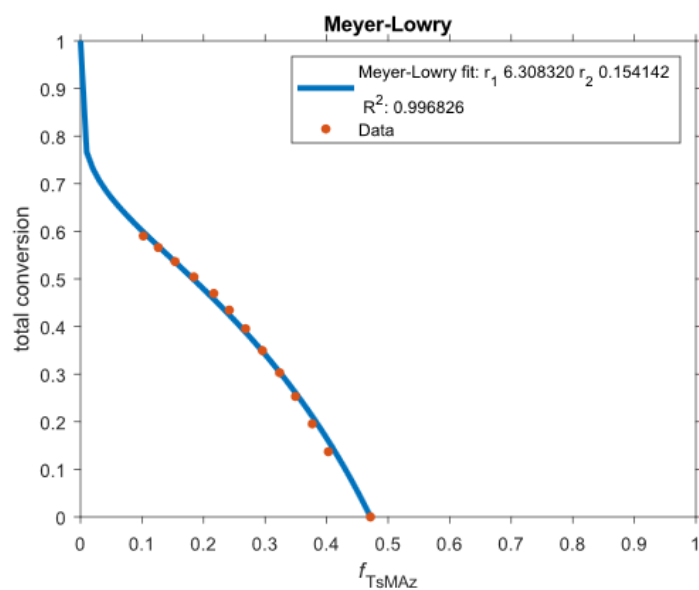


Figure 143: Meyer-Lowry fit of ^1H NMR kinetic data of OsMAz and TsMAz